Università degli Studi di Parma

Dipartimento di Ingegneria Civile, dell'Ambiente, del Territorio e Architettura

Dottorato di Ricerca in Ingegneria Civile – XXVII Ciclo
Curriculum: Infrastrutture (ICAR/04)

Dario Pecchini

Evaluating Safety Performances of Rural Roundabouts via Conflict Opportunities Technique

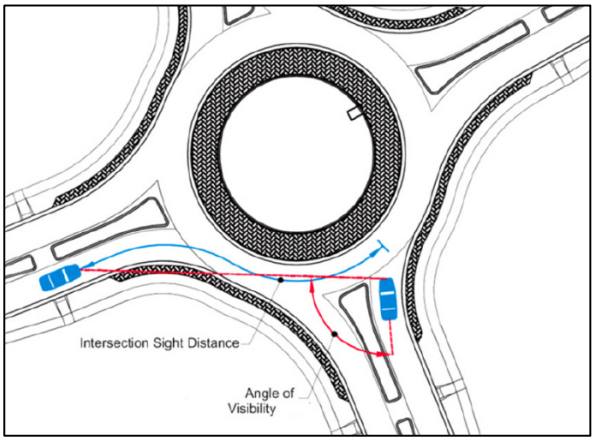

Coordinatore del Dottorato: Chiar.mo Prof. Gianfranco Forlani

Tutor: Chiar.mo Prof. Felice Giuliani

Parma, Gennaio 2015

Università degli Studi di Parma

Dipartimento di Ingegneria Civile, dell'Ambiente, del Territorio e Architettura

Dottorato di Ricerca in Ingegneria Civile – XXVII Ciclo
Curriculum: Infrastrutture (ICAR/04)

Dario Pecchini

Evaluating Safety Performances of Rural Roundabouts via Conflict Opportunities Technique

Coordinatore del Dottorato: Chiar.mo Prof. Gianfranco Forlani
Tutor: Chiar.mo Prof. Felice Giuliani

Parma, Gennaio 2015

“What makes something special is not just what you have to gain,
but what you feel there is to lose.”
Andre Agassi

“Insanity: doing the same thing over and over again and expecting
different results.”
Albert Einstein

Abstract

Roundabouts, when properly designed, can provide substantial safety benefits as compared with traditional intersections. Geometric design plays a key role in inducing drivers to reduce their speed when approaching and guiding through roundabouts. Safety Performance Functions and Traffic Conflicts analyses are the most diffused approaches for identifying parameters actually conditioning safety performances of roundabouts. In this study, an alternative model is proposed, based on estimation of potentially hazardous collisions, i.e. Conflict Opportunities, via probabilistic theory, rather than analyses of video recordings.

Calculation of Conflict Opportunities directly takes into account daily changes of traffic flows and differences among free traffic flows periods and situations where both entering and conflicting traffic flows are high.

Forty-three rural roundabouts were sampled, and, for each leg, 21 geometrical features, selected from technical literature, were collected. For the most frequent types of vehicle crashes, Conflict Opportunity rates were converted into estimated crash rates by means of calibration functions, where independent variables are the geometric features found to be correlated with crash rates. In this regard, exploratory data analyses were particularly useful. They allow maximizing insight into the data set and uncovering underlying structures difficult to capture. Among the various applied techniques, Discriminant Analyses and Multiple regressions with different hypotheses about distribution of residuals proved to be very proficient in identifying a restricted number of significant geometric variables. The model seems to perform well for the considered types of motor vehicle crashes, expect for circulating exiting crashes, probably affected by too few data in the collected sample.

Summary

As claimed by World Health Organisation, motor vehicle crashes are projected to become the third most common cause of death by 2020. The tremendous social impact of crashes has attracted attention of scientist, health officials, legislators and policy makers.

Road safety research is needed to increase the understanding of how crashes occur, since they represent the principal manifestation of road safety itself: where there is smoke, there is fire. Therefore, analytical tools able to predict crash rates are fundamental for identifying the most hazardous sites and preventing injuries and deaths. From this perspective, road intersections are of primary importance: they constitute only a small part of the overall highway system, but they are the locations of a significant portion of total crashes. Numerous road junctions have been converted into roundabouts in the last decades, and new or upgraded intersections are still more likely to be roundabouts than other types of at-grade intersections. Their worldwide diffusion is because roundabouts, when properly designed, can provide substantial safety benefits as compared with traditional intersections. In addition to reducing crashes, roundabouts can improve traffic flow, reduce fuel consumption and increase vehicle capacity. However, various critical issues concerning both safety and capacity are internationally recognised.

As a result, research is particularly active in trying to enhance safety at roundabouts by improving their design. The problem is that there is not an agreed-upon understanding of how a roundabout should work, that is whether roundabouts should privilege functional performances or safety ones. For instance, from a safety perspective, it seems that Countries where roundabouts have been regarded as high capacity intersections experienced more crash rates than other Countries which have placed emphasis on speed-reducing capability of roundabouts. These statistics prove the importance of geometric design, which plays a key role in reaching a well-balanced trade-off between functional requirements and safety issues.

The latter are always the combined outcome of poor roadway design and undesired driver's behaviour, but properly designed roundabouts induce drivers to adopt careful conducts. After all, differently from signalised intersections, where traffic stream movements are rigidly regulated, traffic operations at roundabouts strictly rely on complex mutual interactions between multiple vehicular flows. Geometric features must correctly guide these reciprocal actions. The question arises of individuating parameters actually relevant for safety issues.

To date, there are fundamentally two main approaches for pursuing these goals. One of them consists in developing multivariate models called Safety Performance Functions, where the expected crash rate is estimated as function of traits peculiar to the analysed road location.

Traffic volumes are expressed in terms of Annual Average Daily Traffic (AADT), i.e. the average number of vehicles that pass through a road section during a 24-hour period in a certain year. However, in this way, relevant daily changes of traffic operational condition cannot be taken into account. For example, at roundabouts, free traffic flows conditions are completely different from situations where both entering and conflicting vehicle volumes are high. In the latter case, rear end collision and failure to yield crashes would be more likely to occur as compared to time periods characterised by low traffic flows, where, instead, single vehicle run off crash rates are expected to show an increase.

The other procedure is based on the quantification of the so-called traffic conflicts, i.e. events where road users must take evasive manoeuvres, such as breaking or swerving, for avoiding collisions. The assumption is that rates of dangerous situations increase in proportion to crash rates. Screening of traffic conflict is performed by checking video recordings of investigated road sites. Identification of Traffic Conflict events relies on the subjective judgment of observers, with inevitable inter-observer variability that can distort the true situation. The multifaceted interaction between cofounding variables involving human behaviour, vehicle and environmental factors could mislead the ascertainment of a potential critical situation. For example, a breaking action performed by an observed driver for causes not related to the need for prevent near crashes could be erroneously interpreted as an evasive manoeuvre.

Safety Performance Functions and Traffic Conflicts analyses are the most diffused approaches in road safety research. Indeed, there is a third, little-known method. It derives by attempts to overcome the limits and cost-and time-savings operations required by Traffic Conflict analyses. Potentially hazardous collisions, here defined as “Conflict Opportunities”, are analytically derived by recurring to probabilistic theory. To estimate them, it is necessary not only to assess the probability that a vehicle conducts a certain manoeuver, but also the probability that other drivers follow simultaneously conflicting trajectories.

For example, a vehicle that is about to turn left during the green light at a signalised intersection may collide with those in the opposite flow. Calculation of COs directly takes into account daily changes of traffic flows; this allows achieving safety estimations related to actual traffic conditions appearing during the analysis.

The estimation of the crash rate code based on the CO concept maintains a common structure: for each crash typology, crash rates are estimated by multiplying the associated number of COs for specific coefficients. The primary assumption of the CO technique is:

$$\text{Expected crash rates} = (\text{number of COs}) \times (\text{crash to conflict ratio})$$

Once the number of COs for a specific manoeuvre is evaluated via analytical formulas, crash rates can be derived by multiplying each value by its relative crash to conflict ratio. These coefficients represent the ratio between real crashes and estimated number of COs occurred in the same time period.

Despite their potential advantages, current models based on CO estimation and specifically designed for roundabouts do not implement geometrical features; they only show relationships between traffic flows and assessments of crash rates.

Safety consequences of geometric configuration choices cannot be ascertained. Therefore, they can be applied for safety evaluations of existing roundabouts only.

The aim of this study is to investigate the feasibility of developing crash rate models based on COs, expressly devoted to roundabouts and sensible to geometric features. The pursued approach for achieving this aim consisted in searching for correlations between the crash to conflict ratios and geometrical factors supposed to be decisive for road safety, but not involved in CO calculations. After having obtained these calibration functions, by knowing the value of geometrical parameter, associated coefficients would be directly determined, allowing for converting CO rates into crash rates.

Rural roundabouts out of Non-Motorised Users (NMUs) itineraries were considered. This choice was dictated by the fact that, in urban contexts, road geometry is less important than road environment in influencing drivers' behaviour. They have to simultaneously perform a great number of tasks when driving in urban streets, and increased rates of workload induce drivers to decrease their speed. There is another reason behind the decision of not considering urban roundabouts and road vulnerable users. More variables should have been taken into account, with more intricate patterns to analyse. After all, this study aims to verify the feasibility of applying a novel method. Before treating complex situations, preliminary results must be obtained for straightforward situations in order to understand whether the taken path is promising or not.

As a first step, a database was collected of crashes associated with injuries or deaths occurred at rural roundabouts sited in the Province of Mantua, Lombardia Region, North Italy. Police crash reports were used for reconstructing investigated vehicular collisions. Each of them was then assigned to a specific crash typology. In particular, the five most frequent ones were considered,

- Collision due to failure to yield starting from a stopped position;
- Collision due to a failure to yield without stopping;
- Single vehicle run off at the entry, the circulatory roadway, the exit;
- Rear end collision at the entry;
- Circulating exiting collision; only possible at multilane roadway circulatory roundabouts.

These crash types cover by themselves almost 80% of the entire number of crashes accordingly to numerous international inquiries.

Traffic flows were acquired by specifying the travel demands between the origin and destination legs of analysed roundabouts. The statistical unit here considered is not the roundabout as a whole, but the leg the vehicles involved in a crash came from. Its geometric features were gathered and, eventually, 43 rural roundabouts and 151 legs were sampled. Eighty-seven legs were the location of one or more crashes. For each leg, crash rates were calculated along with twenty-one geometrical features recognised to be the most important ones by scientific literature and practical experience of different Countries.

The problem arises of managing all of these information before making inferences from data and developing analytical models. Exploratory data analyses were particularly useful in suggesting the factors which revealed to be most likely to influence safety performance of roundabouts for each crash typology. They

allow maximizing insight into a data set and uncovering underlying structures difficult to capture. In particular, Discriminant Analyses and Multiple regressions with different hypotheses about distribution of residuals proved to be very proficient in identifying a restricted number of significant geometric variables.

Starting from numerous covariates, only the vehicle trajectory deflection, the entry path radius and visibility measures revealed to significantly condition crash rates. The output of explorative data analyses seems reasonable and consistent with other studies, except for circulating exiting crashes, for which the only important parameter is the inscribed circle diameter. No regard for vehicle path radii of roundabouts and differences in speed between circulating and exiting flows, which instead are established as decisive factors for this kind of crash.

Drastic reduction of variables to take into account greatly simplified implementation of geometrical design in the proposed crash prediction models based on COs. Correlations were researched between crash to conflict ratios and geometrical factors found to be significant for safety issues. Calibration functions were then obtained for coefficients (i.e. crash to conflict ratio) of the model. Overall, well-defined trends have been obtained, with better results for legs with high traffic flows. Negative results instead characterised circulating exiting crashes.

These controversial results are probably due to the few available data for this kind of crash. More extended records would probably allow achieving better results. These considerations may be extended to the other four typologies of vehicle collisions, although, in these cases, results appear to be more reliable.

Table of Contents

Chapter 1

Evaluating Safety Performances of Roundabouts

Roundabouts are a common form of intersection used throughout the world. Their diffusion derives from improvements of safety and traffic flow they can ensure when properly designed. The main benefits potentially achieved by converting traditional at-grade intersections to roundabouts consist in reducing conflict points, decreasing the vehicle speed and, consequently, the crash severity (Kennedy, 2005; Highway Agency, 2007; AASHTO, 2010; NCHRP, 2010; Montella, 2011; Elvik, et al., 2009; Guichet, 1993). The reduction of traffic flow congestion, experienced by numerous case studies, is equally relevant (Elvik, 2003; Daniels, et al., 2010).

However, various critical issues concerning both safety and capacity are internationally recognised. For example, roundabouts would be avoided if significant spread exists between traffic volumes affecting the main direction and secondary roads: there would not be adequate gaps for minor vehicle flows. Roundabouts constructed inside built-up areas have a negative effect on bike safety, as do roundabouts that replaced previously signalized intersections. Accommodation of large goods vehicle and prevention of overturns pose additional challenges to the designers because of wider space necessary for performing successfully turning manoeuvre into the ring (NCHRP, 2003; Arnold, et al., 2010).

As a result, the choice of using a roundabout should be a case-by-case decision, and the design process would require a considerable amount of iteration among geometric layout, operational analysis and safety evaluation (Isebrands, et al., 2008).

1.1 How do roundabouts work

Differently from signalised intersections, where traffic stream movements are rigidly regulated, traffic operations at roundabouts strictly rely on a complex mutual

interaction between multiple vehicular flows approaching to the ring simultaneously (NCHRP, 2010). Road users entering a roundabout are required to give way to those already in the ring, no matter which road they are coming from. As a result, drivers are induced to observe movements of other vehicles in a careful way. However, drivers have to check for traffic coming from only one direction, and thus wrong evaluation of gaps when trying to enter the ring are less likely to occur at roundabouts than at other intersections. In addition, geometric configuration of roundabouts, as compared to two-way stop control and signalized intersections, promotes the reduction of conflict points, which decrease from thirty-two and eliminates those occurring when paths of two traffic streams intersect, the so-called *Crossing Conflict* (Elvik, et al., 2009). These are the most severe of all conflicts and the most likely to involve injuries or fatalities.

There are other reasons behind superior safety performances of roundabouts in relation to other at-grade intersections. Deviation of vehicle trajectories imposed by the central island forces drivers to slow down when approaching to the ring (Spacek, 2004; Kennedy, 2007). Therefore, they travel through the intersection at similar low speeds, and this guarantee more time for reacting to potential conflicts and help to reduce crash severity and the probability of injuries and deaths.

The human factor has its importance too. Delays are generally shorter at roundabouts as compared to signalised intersections, and this moderates the frustration and aggressiveness of drivers, who, at the same time, do not have the incentive to speed up for "beating the light" of signalised intersections (Walden, 2008). Furthermore, the absence of an exchange of the right-of-way priority by the traffic signal increases the risk perception of drivers and, consequently, their caution when approaching and crossing the intersection.

1.2 An overview of roundabout safety performances

Numerous researches have been conducted in order to assess safety performances of roundabouts and safety potential benefit achievable by converting existing traditional at-grade intersections into roundabouts.

A large study was conducted in Victoria, Australia on 73 roundabouts before and after their installation (AUSTROADS, 1993). A 74 percent reduction was recorded in the casualty crash rate after installation of roundabouts. Property damage only (PDO) crashes decreased by 32 percent, although the authors pointed out that not all property damage accidents were reported so it is difficult to quantify the effects of the roundabouts on these types of accidents.

Giaever reported that the use of roundabouts in Norway increased from only 15 in 1980 to more than 500 in 1992 (Giaver, 1992). He also compared 59 roundabouts to 124 signalised intersections and recognised that crash rates per million vehicles crossing roundabouts were lower in relation to the other typology of road junction. Conversely, negative outputs were found for cyclists, given that 36 percent of crashes reported for roundabouts involved two-wheeled vehicles, as compared to only 23 percent at signalized intersections.

Schoon and Van Minnen analysed 46 retro-fitted roundabouts and found that the casualty rate per year for the roundabouts reduced by 1.47 casualties/intersection/year. The casualty rate of cyclists also reduced by 0.52 casualties/intersection/year. Most of these crashes occurred when cyclist had been riding along circulatory circle lanes. Consequently, suggestions were provided to avoid bike lanes within the circulating roadways (Schoon & Van Minnen, 1994)

Guichet carried out an extensive scientific investigation in France and revealed that roundabouts performed better in terms of safety as compared to signalised intersection in both rural and urban areas. In particular, under similar traffic flows, the latter had accident frequencies four times higher than roundabouts (Guichet, 1997).

In Nederland, Ourston investigated the effect of conversion of nine traffic signals to roundabouts. He found a 27 percent reduction in total crashes and a 33 percent reduction in casualties (Ourston, 1996).

Brilon analysed in depth the changes in crash rates experienced by a sample of traditional at-grade intersections sited in Germany and converted into roundabouts (Brilon, et al., 1997). The majority of these were single-lane compact roundabouts. New interventions reduced the total number of crashes by 40 percent, with the greatest benefit for roundabouts located outside urban areas. As for the previously mentioned Dutch study (Schoon & Van Minnen, 1994), circulatory cycle lanes proved not to be safer for cyclists. Recommendation were given to design single-lane roundabouts with inscribed circle diameter of 30 m.

Conventional intersections located in the United Sates were compared with roundabouts built in United Kingdom. The latter showed remarkable safety outcomes for low traffic volumes. For total entering volumes of 20,000 vehicles per day, crash rates were 33 percent lower for roundabouts than for signalized intersections in urban and suburban areas and 56 percent lower in rural areas. The safety performances of roundabouts and signalized intersections were substantially similar for high traffic flows (ITE, 1999).

An American study focused on estimation of safety benefits achieved by converting traditional intersections into roundabouts was carried out by taking into account 23 retro-fitted roundabouts, of which 19 were previously stop-controlled, and four were signalised intersections. For the latter, estimates indicated a decrease of 74 percent for crashes associated with injuries and deaths (Persaud, et al., 2001). Another American report analysed 55 sites where traditional signalised intersections were converted to roundabouts (NCHRP, 2007). It was estimated a 60 percent reduction in severe injury crash rates at signalised intersections sited in urban areas, while for rural areas, a 87 percent decreases was estimated.

Isebrands and Hallmark examined 19 retro-fitted roundabouts built in a rural environment with high-speed approaches. They acquired an estimated 62 percent to 67 percent reduction in total crashes and a decrease of around 85 per cent in injury crashes (Isebrands, 2011).

Elvik undertook a meta-analysis of 28 studies reported outside the United States and focused on the effects of road safety induced by conversion of

traditional at-grade intersections into roundabouts. Outcomes showed that fatal crash rates was reduced by about 50 to 70 percent, while injury crash rates decreased by about 30 to 50 percent, depending on the previous type of the intersection and the number of legs. As for PDO crashes, the effect of roundabouts did not proved to be significant. Small roundabouts appeared to have lower crash rates than large ones (Elvik, 2003).

1.2.1 The Italian case

The Italian case deserves specific attention. Roundabouts started to appear in Italy with decades of delays, as compared to other Countries accustomed with this type of intersections. The first national standard on geometric design of roundabouts, which is quite rough and incomplete, was not established until 2006 (Ministero delle Infrastrutture e dei Trasporti, 2006). In few years, roundabouts were built at an aggressive pace with the belief that injury and death crashes could have been considerably prevented (LAGS, 2010). Currently, no researches has been conducted for a systematic ascertainment of safety advantages attained by installing roundabouts in place of existing traditional at-grade intersections. However, various studies and survey inspections suggested that Italian roundabouts provided poor safety benefits (Sacchi, et al., 2011). By analysing national crash records from 2003 to 2012, for death crashes per year occurred at roundabout, a marked rising trend can be noticed, while injury crashes per year have increased steadily. An intensification of roundabout crashes could be explained by the fact that the amount of these intersections has dramatically increased, but examination of additional data reveals outcomes worthy of further investigations. From 2003 to 2012, roundabout injury crashes increased by 78 percent, in opposition to the overall national trend (-5.1 %) and injury crashes occurred at the other kinds of intersection in the same period (-21.7%) (Figure 1.1, 1.2). The evolution of the social cost of road crashes is very similar. While social costs of roundabouts crashes increased by 75 percent, both overall national data (-9.5%) and those related to the other at-grade intersections (-10%) experienced a significant decrease (ISTAT, 2014). Table 1.1 show that reduction of crashes occurred at traditional at-grade intersections is only slightly higher than the overall case. Furthermore, the difference between injury crashes recorded for roundabout and those collected for other at-grade intersections shows a result less satisfactory than the evolution of injury crashes along all of the national road network. Same considerations regard the evolution of social costs affecting road crashes. These outcomes suggest that safety benefits reached by installation of roundabouts are quite limited.

Another clue is provided by the analysis of the gravity index, i.e. the number of casualties per 1,000 crashes. In the last decade, gravity index of roundabouts has not been significantly lower than one of other at-grade intersections and even exceeded it for three years. Roundabouts do not appear to have contributed to an

effective drop of crash severity as compared to other locations, for example the straight lines.

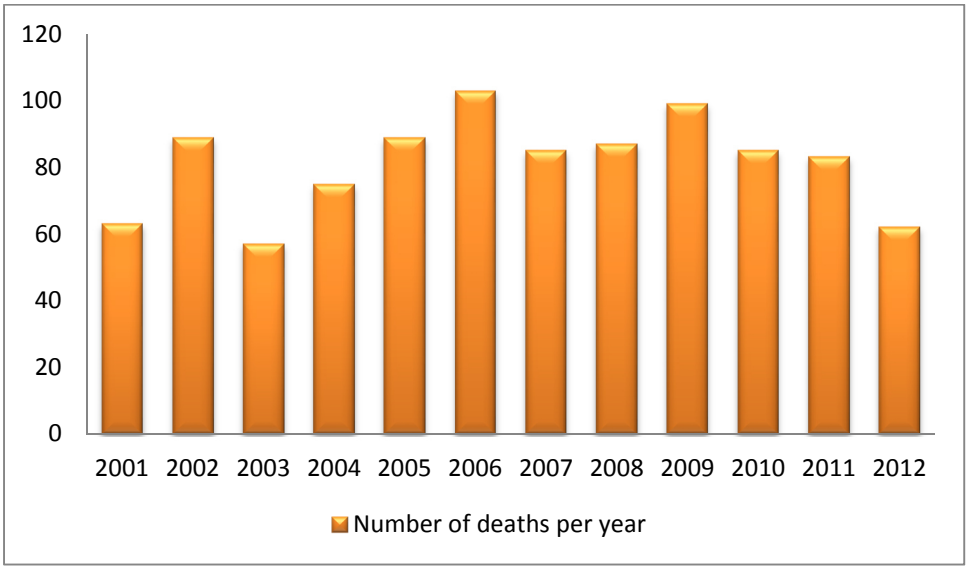

Figure 1.1 Number of deaths per year at roundabouts. ISTAT data

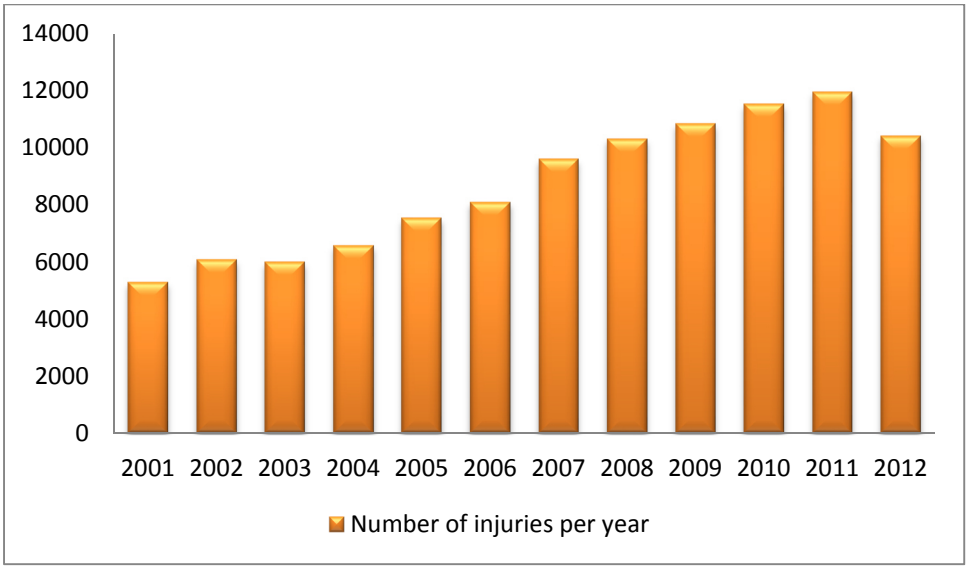

Figure 1.2 Number of injuries per year at roundabouts. ISTAT data

	Overall Road network	At-grade intersections (no roundabouts)	Roundabouts	All of the at-grade intersections	Straight lines
2003	18.2	10.6	9.6	10.6	22.6
2004	17.5	10.8	11.1	10.8	21
2005	17.1	10.5	11.6	10.6	20.5
2006	16.7	10.2	12.6	10.3	19.8
2007	15.5	9.8	8.8	9.7	18.2
2008	15	9.1	8.4	9	18.3
2009	13.6	8.3	9.1	8.3	16.5
2010	13.3	8.1	7.3	8.1	15.8
2011	13	8.2	6.9	8.1	15.2
2012	13.6	8	6.6	7.8	16

Table 1.1 Number of injuries per year at roundabouts. ISTAT data

No definitive conclusion can be drawn from these general data, given that number of roundabouts built every year is unknown, but the possibility cannot be excluded that part of the Italian roundabouts do not reach adequate safety outcomes (LAGS, 2010). This could be the reflection of the numerous inconsistencies affecting the Italian requirements for design of roundabouts, as well as an a priori belief that this kind of intersection is the best possible solution for all the situations (Sacchi, et al., 2011). There is a limited understanding of situations where roundabouts may be useless or even unsafe for road users. Practices and scientific inquiries of other Countries accustomed for decades with this kind of intersections can provide notions and principles with general validity regarding their installation in road network.

1.2.2 Criticalities posed by roundabouts

Roundabouts should be avoided when closely spaced to signalised intersections in order to avoid that queues may spill back into the roundabout itself. In this regard, it is internationally recognised that roundabouts do not operate well when affected by traffic platoon originated by signalised intersections sited in proximity (NCHRP, 2010). In fact, drivers coming from the other roads may not find adequate gaps for entering the ring, with consequent deterioration of both Level of Service (LOS) and safety, given that they could try to exploit too little gaps.

Roundabouts need for proper visibility; if unfavourable topography, steep grades or built environment do not allow meeting this requirement, other

intersections should be considered (Department of Transport and Main Roads, 2014).

Safety of road vulnerable users is another concern of primary importance. Both pedestrians and bicyclists needs for appropriate treatments and facilities, given that vehicle traffic is yield controlled, so it does not necessarily come to a full stop. As a matter of fact, roundabouts are not recommended for roads and streets characterised by high pedestrians and bicycle traffic flows (NCHRP, 1998).

Various studies enlightened the fact that injury crashes involving vulnerable road users, such as pedestrians and bicyclists, were found to increase AT retro-fitted roundabouts (De Brabander & Vereeck, 2006).

As regards pedestrians, they may hesitate when crossing the street near a roundabout because entering traffic does not necessarily stop, and these difficulties could be exacerbated by age and physical impairments. In particular, pedestrians with vision disabilities may have the most trouble establishing safe opportunities to cross. They may have difficulty in determining gap acceptance without the aid of audible signal due to the disruptive and possibly confusing sound of circulating traffic.

Safety of cyclists is even more critical. Daniels et al. noted an increased risk associated with injury crashes involving bicyclists at locations where roundabouts replaced traditional intersections. Roundabouts with bicycle lanes experienced poorer safety performances, and additional facilities, such as separate bicycle path and grade-separated bicycle path are necessary for securing cyclists (Daniels, et al., 2010).

Accommodation of large goods vehicles (LGV) and prevention of their overturns pose additional challenges to the designers because of wider space necessary for performing successful turning manoeuvre into the ring. Prevention of LGV overturning events is an essential concern too. Most of these crashes are not reported in statistical records because they are rarely serious, given that speed of involved vehicles is generally low. Nevertheless, these events have economic consequences due to road damage, lorries damage and subsequent traffic disruption (NCHRP, 2003).

An additional aspect that should not be neglected is the fact that roundabouts can be difficult to manoeuvre, because they demand special attention to surroundings. Before entering the ring, drivers have to observe traffic in the circle and watching out for pedestrian and bicyclists. As a matter of fact, a roundabout represents a more challenging orientation task for all road users than an ordinary junction because of the circular design (Hels & Orozova- Bekkevold, 2006). This may increase the probability of orientation failure and the risk of crashes.

To sum up, in light of beneficial aspects and potential concerns posed by roundabouts, their adoption should be a case-by-case decision (Isebrands, et al., 2008).

From this essential literary review, it transpires a quite heterogeneous framework about safety performances achieved by replacing traditional at-grade intersections with roundabouts. After all, driving culture, volumes of different kinds of road users, formal and informal rules differ considerably between countries.

There is not even an agreed-upon understanding of how roundabouts should work, that is whether they should privilege functional performances or safety ones (Kennedy, 2007). In most Countries, roundabouts are intended as a traffic calming measure aimed to reduce vehicle speed, while in United Kingdom and Australia capacity issues are privileged. These two perspectives inevitably imply different design standards. For instance, features such as entry flares and segregated right turn lanes used in UK for increasing capacity of roundabouts may represent flawed geometric design for other Countries. All of these considerations suggest the importance of adopting a critical approach when estimating safety achievements of roundabouts. Proper safety forecasts should derive by analyses taking into account all of the factors recognised as significant for crash occurrence. Geometric design is such a factor because it influences drivers' behaviour when approaching and crossing the roundabout. Indeed, it seems that Countries where roundabouts have been regarded as high capacity intersections have experienced more crash rates than other Countries that have placed emphasis on speed-reducing capability of roundabouts (Kennedy, 2007).

As for each road infrastructure, geometric design criteria are of primary importance for achieving the best performances of roundabouts in terms of both capacity and safety. A trade-off must be reached between operational performances and safety issues. As an example, an accentuated deflection imposed by geometrical layout of roundabouts to vehicle trajectories may force drivers to reduce their speed but travel delays would increase with consequent deterioration of traffic flow. Multilane roundabouts can benefit from an enhanced capacity, but experience clearly shows that they are affected by higher crash rates than roundabouts with single-lane entry at all legs and one circulatory lane (NCHRP, 2010). The occurrence probability of single crash typologies is influenced by geometry too (NCHRP, 1998). An entry that is almost perpendicular to the circulating vehicle path will make rear end and loss of control more likely because abrupt braking may be necessary (Highway Agency, 2007).

At the same time, safety performances of roundabout are strictly influenced by traffic flow variations. When high traffic volumes converge at a specific roundabout, rear end crashes and failure to yield would be more likely to occur as compared to temporal situations in which the same roundabout is affected by low traffic volumes, a situation in which single vehicle run off crashes are expected to increase.

Therefore, the design process should require a considerable amount of iterations among geometric layout, operational analyses and safety evaluations. In other words, the criteria for choosing the intersection layout should consider both functional and safety aspects. In the first case, the comparison is based on performance index, such as the delay experienced in crossing the intersections, mainly dependent on traffic flow entities.

As regards safety, the target is the estimation of crash rates because, conventionally, the principal manifestation of road safety are crashes. Since decades, road safety research has focused on analytical models able to evaluate crash rates as a function of roundabouts characteristics, such as traffic volumes

and geometric features. This could allow identifying the most benefit arrangement of the intersection in terms of road safety.

1.3 Basic Principles for Predicting the Expected Level of Safety for road entities

The safety of a road entity can be defined as the mean of crashes expected to occur on it, per unit of time, in a certain time period (Hauer, 1997). The word expect refers to a long-term average which would materialise if it were possible to keep constant traffic flow, driver demography, vehicle characteristics and all other relevant conditions of the period, as well as the traits and properties of the entity.

Therefore, analytical tools developed for evaluating safety of a road entity present output related to the number of crashes estimated to occur on it in a given time period. After having defined a reference population, such as, for example, intersections or road segments with similar geometric features and traffic flows, a sample must be randomly collected by selecting the entities from which estimating safety performances of investigated reference population. Collected crash data should be analysed and reviewed to identify locations with safety issues or locations with potential for future safety issues, and to select countermeasures to improve safety (AASHTO, 2010).

Unfortunately, detailed driving data such as, for example, acceleration, braking and steering information, as well as driver response to stimuli, are typically not available. As a result, researchers have framed their analytic approaches to study the factors that affect the number of crashes occurring in a specific road entity (i.e. a roadway segment or intersection) over a specified time period, typically years (Hauer, 2004).

Before describing the various methodologies for estimating road safety, a terminology clarification is required: crash frequency of a road location is different from its corresponding crash rate (FHWA, 2012). The former is defined as the number of crashes occurring within a specific reference population. Each crash occurred at sites belonging to the collected sample is added up. An average accident frequency is then calculated (Equation 1.1)

$$f_{rp} = \frac{\sum_j f_j}{n} \tag{1.1}$$

where:

- f_{rp} = estimated average crash frequency for the reference population;
- f_j = crash frequency at site j of the collected sample;
- n = number of sites;

The crash rate is expressed by the following expression (Equation 1.2)

$$R_{rp} = \frac{100{,}000{,}000 \times C}{365 \times N \times V} \quad (1.2)$$

where:

- R = Estimated crash rate for a reference populations of a particular typology of intersections expressed as accidents per million entering vehicles (MEV);
- C = Total number of crashes occurred at sites belonging to the collected sample in the study period;
- N = Number of years of data;
- V = Average annual daily traffic entering the intersections of the analysed sample.

An intuitive and immediate measure of safety performances characterising a road entity could be its historical data about traffic crashes. Attention should be addressed to locations affected by the highest crash frequencies. The tacit assumption is that the past apparent crash trend recorded for a sample representing a specific reference population can be a good forecast of its future safety performances.

However, this approach has proved not to be able to provide reliable results, as confirmed by empirical evidences. The essence of road safety itself can explain the shortcomings affecting this method. Crash frequency of a specific location is a random process, which changes with time.

Even if all conditions affecting safety of a given site could remain constant on time, the number of crashes occurring each year might fluctuate significantly. In particular, when a random deviation from mean occurs, the next event should be expected to return to the mean (Hauer, 1997). This implies that the count of crashes occurred in the past is a biased estimate of the number of crashes expected in a future period (i.e. "regression to the mean bias"). Therefore, if the analyst focuses his attention on already occurred crashes without any further treatment or analysis, he will be attracted by sites with the highest crash frequencies, the same sites which will probably experience a marked decrease of crashes in the following times (Figure 1.3).

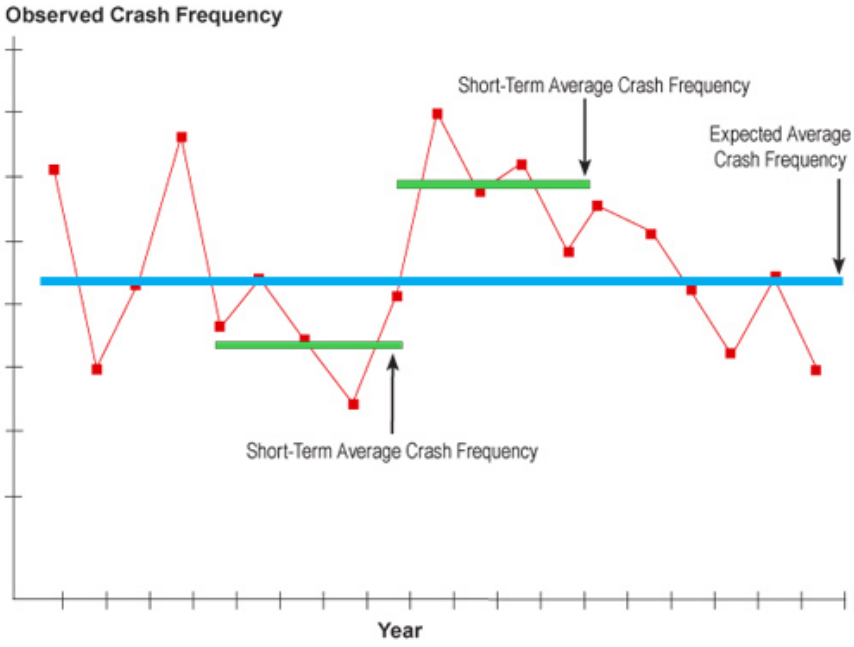

Figure 1.3 Graphical representation of the regression-to-the mean phenomenon

This approach is incorrect. If a location has experienced no crashes in the past years, thinking that it will never be the set of any crash in the future is obviously unrealistic. In other words, the approach focused on crash frequency neglect the random nature of crashes and produces estimates affected by "regression to the mean bias" (Cafiso, et al., 2013).

In addition, the entities considered in the analysis would not constitute a representative randomised sample, given the absence of locations with limited crash history, which instead will be more likely to be subjected to a future growth in crash frequency (Saunier, et al., 2010). In this regard, there is another source of error: crash frequencies do not take into account traffic flows, which deeply influence safety performances of road entities (Technical Committee 13 Road Safety, 2004). This last issue could apparently be overcome by considering the crash rate in place of frequency rate, but in this way, an unrealistic linear relationship between traffic volumes and crashes would be hypothesised. The shortage of available data is another recurrent concern for road safety studies. This is especially true for rural roadway sections and for the rural intersections where crashes may be very rare events. Various locations have no crashes at all, or just one crash over a period of numerous years. In practice, it may be impossible to estimate crash frequency of a reference population when a sufficient number of sites having similar characteristics cannot be found. The method of Sample

Moments would be completely useless in estimating the parameters of the reference population.

In such cases, development of crash prediction models (also called safety performance functions, SPF) may alleviate this problem.

1.4 Safety performance functions

They are essentially multivariate statistical equations aimed to predict the average number of crashes per year which are going to occur at investigated road entity, whose exposure rates and geometrical features represent the explanatory variables of crash prediction models (Hauer, 1997; AASHTO, 2010; FWHA, 2013).

An SPF is to be developed for each group of road entities with similar geometrical and functional features. For example, there should be SPFs conceived for three-leg intersections and other SPFs devoted to four-leg intersections, as well as roadway segments. Safety performances will generally vary among sites grouped in the same category (i.e. reference population); related SPF provide the expected value of crash frequency predicted to affect sites belonging to the analysed reference population.

For roadway segments, exposure measures can be the segment length and the traffic flow (expressed in terms of AADT) passing through the analysed section, while geometrical characteristics may be the number of lanes, traffic control, or median type. A sample SPF developed for roadway segments is given by Equation 1.3:

$$Y_i = exp[\alpha + \beta * \ln(AADT) + \gamma * ln(L)] = exp[\alpha] * AADT^{\beta} * L^{\gamma} \quad (1.3)$$

where:

- Y_i: predicted average crash frequency per year at site *i*;
- L: segment length;
- AADT: annual average daily traffic flows passing through the segment;
- α, β, γ: parameters to be calibrated.

For intersections, exposure measures are represented by the AADT on the major and minor intersecting roads as shown by the sample SPF in Equation 1.4.

$$Y_i = exp\left[\alpha + \beta_1 * \ln\left(AADT_{major}\right) + \beta_2 * \ln(AADT_{minor})\right] = \\ = exp[\alpha] * \left(AADT_{major}\right)^{\beta_1} * (AADT_{minor})^{\beta_2} \quad (1.4)$$

where:

- Y_i: predicted average crash frequency per year at site *i*;

- AADT: annual average daily traffic flows on the major road;
- AADT: annual average daily traffic flows on the minor road;
- α, β1, β2: parameters to be calibrated.

After the acquisition of crash data and roadway characteristics, the question arises of identifying the covariates to take into account and the functional form of the SPF. In this regard, authors proposed the Integrate-Differentiate (ID) method, which consists in creating an empirical integral function for each independent variable. Covariates are then separated into a series of bins in increasing order. By comparing graphs obtained with ID method with pre-established graphs of well-known functions, the proper relationships between dependent and independent variables may be revealed. Subsequently, stepwise regression approaches are applied for capturing the significant variables (Hauer & Bamfo, 1997; Bauer & Harwood, 2014). In short, database of crashes and roadway characteristics allow selecting the functional form best suited for the prediction model, whose parameters are then estimated by recurring to regression techniques.

Traditional least-squares regression assumes a normally distributed error structure and a constant variance. However, as explained in the followings, these assumptions are unrealistic for modelling crash counts.

Conversely, generalised linear models (GLM) can be applied for situations where (McCullagh & Nelder, 1989):

- dependent variable is not-normally distributed;
- the variance of dependent variable depends on the mean;
- dependent variable has a non-continuous distribution with restricted values;
- effect of the predictors on the dependent variable is not linear.

In GLM, the dependent variable values are predicted from a linear combination of predictor variables, which are connected to the dependent variable via a specific transformation defined by the so-called link functions. The general linear model for a single dependent variable can be considered a special case of the generalized linear model: here, the dependent variable values are expected to follow the normal distribution, and the link function is a simple identity function. In other words, the linear combination of values for the predictor variables is not transformed.

In the general linear model a response variable Y is linearly associated with values on the X variables, as shown in Equation 1.5.

$$Y = \beta_0 + \beta_1 X_1 + \cdots \beta_k X_k + \epsilon \tag{1.5}$$

where:

- β_k: coefficients to be estimated
- X_k: predictors;

- ε: error variability that cannot be accounted for by the predictors; the expected value of ε is assumed to be 0.

Instead, in GLM models, the relationship between dependent variable and predictors is expressed by Equation 1.6:

$$Y = g(\beta_0 + \beta_1 X_1 + \cdots + \beta_k X_k) + \epsilon \tag{1.6}$$

where the inverse function of g function is called the link function. It follows that (Equation 1.7):

$$f(E[Y]) = \beta_0 + \beta_1 X_1 + \cdots + \beta_k X_k \tag{1.7}$$

where:

- *f* function is the link function;
- *E[Y]*: expected value of dependent variable.

It is worth pointing out that a Δ_i increase of covariate X_i does not provoke a proportional growth of *E[Y]*, but instead a proportional increment of *f(E[Y])*. In symbols (Equation 1.8):

$$\begin{aligned} &\beta_0 + \beta_1 X_1 + \cdots + \beta_i (X_i + \Delta_i) + \cdots + \beta_k X_k = \\ &\qquad = \beta_0 + \beta_1 X_1 + \cdots + \beta_i X_i + \beta_i \Delta_i) + \cdots + \beta_k X_k \\ &\qquad = f(E[Y]) + \beta_i \Delta_i \end{aligned} \tag{1.8}$$

Various link functions can be chosen (McCullagh & Nelder, 1989), depending on the assumed distribution of the y variable values, such as, for example:

- Identity link function, $f(z) = z$;
- Log link function, $f(z) = log(z)$;
- Power link function, $f(z) = z^a$, for a given a;
- Logit link function (binomial distribution), $f(z)=log(z/(1-z))$.

Log link and Power link functions are frequently exploited in developing SPF.

Originally crash counts occurred at a given location were analytically interpreted as a Poisson random variable because they appeared to satisfy the three properties under which a certain process can be adequately described via a Poisson model. In fact, for a given location, crashes are random events which may happen at any time, while two or more crashes cannot occur precisely at the same time; for a particular location, the occurrence of a single crash in a particular time period does not affect the probability of an additional crash occurring in another time interval; for a specific location, the expected number of crashes during one period is the same as the expected number of crashes related to any other time interval of the same extension.

In accordance with Poisson distribution, the probability of site *i* having Y_i crashes per year is given by Equation 1.9:

$$P(Y_i) = \frac{e^{(-\lambda_i)} * \lambda_i^{Y_i}}{Y_i!} \quad (1.9)$$

where:

- λ_i: the Poisson parameter for site i, that is the expected number of crashes per year, E[Y].

With the aim of relating the expected number of crashes with the site characteristics, starting from Equation 1.9 a GLM log-linear model can be obtained (Equation 1.10):

$$\lambda_i = e^{(\beta X_i)} \quad (1.10)$$

Alternatively (Equation 1.11):

$$\ln(\lambda_i) = \beta X_i \quad (1.11)$$

where:

- β: vector of X_i coefficients.
- X_i: vector of explanatory variables.

It is worth noting that the log link function provides a linear combination of covariates (Equation 1.11). The GLM log-linear model is appreciated for predictions on crash counts because it ensures that the Poisson parameter λ_i (i.e. the expected number of crashes in a given time period) is always positive.

However, the Poisson distribution constrains the mean and the variance to be equal, while empirical evidence revealed that crash data are usually overdispersed, that is their variance exceed their mean (AASHTO, 2010). This peculiar overdispersion showed by crash counts is due to different factors prevalently related to the concerns affecting data acquisition, unaccounted temporal correlations and unobserved heterogeneity (Hauer, 2004). For each entity, certain traits are available and can be measured or estimated. The problem is that the degree of accuracy may significantly vary because measured traits are often averages over road section length or averages over time (e.g. traffic flows expressed in terms of AADT). There are also measurable traits that are not represented in the model, as well as unmeasurable traits which anyway influence safety performances of road. The same measured traits may be subjected to estimation error; for example, AADT is estimated on the basis of few days of traffic counting that may have been carried out in a previous year at a nearby but different location. In addition, the same average may represent very different distributions.

If a certain road section carries 100 vehicles at night and 900 during daytime while another one serves 500 vehicles at night and in daytime, the two sections will have the same AADT but different crash frequencies. Unrepresented traits could affect a wide, miscellaneous range of factors, such as whether, drivers' behaviour, demography, economic conditions and functional land use (i.e. territorial distribution of production commercial and consumption activities, as well as of residential areas).

For all of these reasons, crash frequency distribution among entities of the same reference population presents a typical accentuated dispersion. Estimating a common Poisson model for overdispersed crash counts can result in biased and inconsistent parameter estimates which in turn could lead to erroneous inferences regarding the factors that determine crash frequencies (AASHTO, 2010).

Poisson-Gamma regressions, where the rate parameter λ_i of the Poisson distribution is treated as a particular random variable, allow accommodating the peculiar overdispersion of crash counts. Poisson-Gamma regressions are an extension of the simple Poisson regressions and belong to the family of Negative Binomial (NB) models. They fundamentally assume the Poisson mean λ_i takes the following form (Equation 1.12):

$$\lambda_i = e^{(\beta_{i0}+\sum_j x_{ij}\beta_{ij})} e^{\varepsilon_i} \tag{1.12}$$

where:

- x_{ij}: *j-th* covariate;
- β_{ij}: coefficient of *j-th* covariate;
- β_{i0}: constant term capturing unknown and unobserved factors;
- ε_i: disturbance term introduced for taking into account unrepresented traits of the model.

The statistical error e^{ε_i} is an independent gamma distributed random variable with unit mean and variance equal to *k,* that is the overdispersion parameter, which represents the degree of overdispersion: the larger the value of *k*, the more the crash data are overdispersed. In fact, if *k* is zero, the negative regression model reduces to a Poisson regression model. A certain amount of studies prefer to adopt the reciprocal of the overdispersion parameter, that is $\varphi=1/k$ (FWHA, 2013).

The βs coefficients and *k* parameter must be estimated from experimental data. Let

$$\mu_i = e^{(\beta_{i0}+\sum_j x_{ij}\beta_{ij})} \tag{1.14}$$

and

$$\nu_i = e^{\varepsilon_i} \tag{1.15}$$

The Poisson mean with Gamma heterogeneity (Equation 1.12) can be written as (Equation 1.16):

$$\lambda_i = \mu_i \nu_i \tag{1.16}$$

With these assumptions (Hauer, 1997), it can be shown that variable Y_i follows a negative binomial distribution with mean μ_i and variance equal to (Equation 1.17):

$$VAR[Y_i] = E[Y_i] + kE[Y_i]^2 = E[Y_i] + \frac{(E[Y_i])^2}{\phi} = E[Y_i] * \left(1 + \frac{1}{\phi} * E[Y_i]\right) \tag{1.17}$$

where:

- *k*: overdispersion parameter;
- *φ*: reciprocal of the overdispersion parameter;

while its probability density function is given by Equation 1.18:

$$f_{Y_i} = \begin{pmatrix} Y_i + \frac{1}{\alpha} - 1 \\ \frac{1}{\alpha} - 1 \end{pmatrix} \left(\frac{1}{1 + \alpha\mu_i}\right)^{1/\alpha} \left(\frac{\alpha\mu_i}{1 + \alpha\mu_i}\right)^{y_i} \tag{1.18}$$

Probability density function is fundamental for calibration process. As in all GLM models, the regression coefficients are estimated by means of maximum likelihood, which consists of estimating a parameter vector that defines a distribution that is most likely to generate the observed data. In this way, the probability of observing the crash counts is expressed as a function of the only unknown parameter values, which are estimated in a way that the model equation fits the crash data as well as possible.

From Equation 1.14, it is clear that the mean of the negative binomial random variable Y_i follows a log-linear relationships with the covariates (Equation 1.19):

$$\ln(\mu_i) = \beta_{i0} + \sum_j x_{ij}\beta_{ij} \tag{1.19}$$

In shorts, the negative binomial model has been mathematically obtained by assuming that unobserved crash heterogeneity across sites with similar traits is gamma distributed, while crash counts recorded for a single sites are Poisson distributed (Hauer, 1997; AASHTO, 2010).

1.5 Empirical Bayes method observational before/after evaluation studies

As already specified, crash prediction models allow overcoming the difficulty posed by a restricted number of available crash data. They are derived from crash counts recorded for a range of sites having similar physical, geometrical and functional characteristics. However, all of the factors actually influencing safety performances of road sites cannot be taken into account. In fact, regression equations do not necessarily depict cause-and-effect relationships between crash frequencies and covariates (Sheskin, 2003). SPFs rely exclusively on traffic volume and segment length (in case of straight roads) for their strong correlation with expected crash frequency. For these reasons, the expected number of crashes for a specific site will generally differ from the mean value of its reference population. Probably, the safety of an entity could be best estimated by considering both the crash frequency recorded at the site of interest and crash frequencies pertaining to a range of sites with similar geometrical and functional characteristics. A specific SPF may predict the average crash frequency for this reference population. The theoretical framework for combining the information contained in crash counts of the analysed site with the source of knowledge achievable from safety performances of similar entities is the Empirical Bayesian (EB) method (Hauer, 1997). Given a specific time period, let *K* be the observed crash frequency for a specific site, and *P[k]* the predicted value of crash frequencies for a reference population formed by entities with similar traits. The idea is that the best estimate of expected crash frequency for the investigated entity is exactly the mean of a subpopulation related to reference sites having experienced the same *K* crash frequency (Figure 1.4).

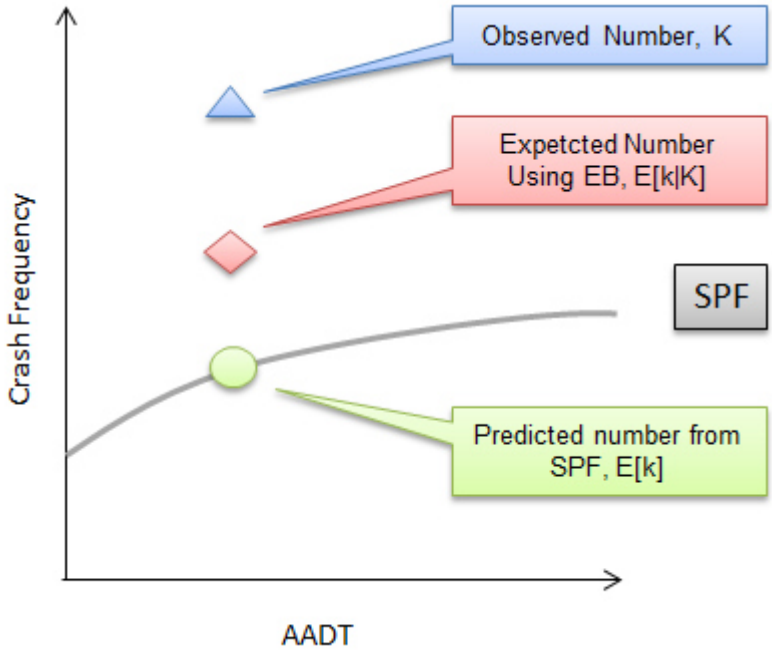

Figure 1.4 Graphical representation of the correction applied by Empirical Bayes method observational before-after studies on the SPFs predictions

In accordance with EB method, this estimate, indicated as *E[k|K]*, is calculated as a combination of the expected crash frequency estimated for the reference population and crash counts of the analysed site (Equation 1.20):

$$E[k|K] = \alpha P[k] + (1 - \alpha)K \tag{1.20}$$

Where:

- *E[k]*: the predicted value of crash frequency for the reference population, achievable from a Safety Performance Function;
- *K*: crash counts for the investigated entity;
- *E[k|K]*: expected crash frequency for the investigated entity.
- *α*: a weight coefficient.

In other words, EB method is used to estimate the expected long-term crash frequency, which is a weighted average of the observed crash frequency at the site of interest and crash frequency predicted by SPF.

The weight coefficient *α* of Equation 1.20 is a number between 0 and 1 that needs to be chosen. If *α* is near 1, then the expected crash frequency *E[k|K]* is

close to the mean of its reference population *P[k]*; conversely, a value of *α* close to zero states a strict dependence of *E[k|K]* on the crash count *K*. The coefficient *α* can be determined via Equation 1.21:

$$\alpha = \frac{1}{1 + \frac{VAR[k]}{P[k]}} \tag{1.21}$$

where:

- *P[k]*: the predicted value of crash frequency for the reference population;
- *VAR[k]*: the variance of crash frequency for the reference population.

The weight attached to the two combined terms depends only on the ratio *VAR[k]/P[k]*. In case that all the entities of the reference population would be known to have the same expected crash frequency, *VAR[k]* and *α* would be equal to 0 and 1, respectively. As a result, *P[k]* would be the estimate for the entity of interest, regardless of its crash counts. Conversely, if the expected crash frequencies in the reference population would dispersed to such an extent that *VAR[k] >> P[k]*, *α* would be negligible, and *E[k|K]* would be entirely determined by crash counts of the investigated site.

It is worth noting that the weight factor α is dependent on the overdispersion parameter k related to SPF adopted for calculating *P[k]* of the reference population. In case that the expected crash frequencies within the reference population were supposed to follow a gamma probability distribution, variance of crash frequency for the reference population would be equal to $P[Y_i] + kP[Y_i]^2 \approx kP[Y_i]^2$. The weight factor could be estimated as (Equation 1.22):

$$\alpha = \frac{1}{1 + kP[k]} \tag{1.22}$$

It turns out the importance of a proper calibration of the overdispersion parameter in order to achieve reliable safety estimates (Cafiso, et al., 2013). In this perspective, another fundamental aspect is certainly the proficiency of the EB method in mitigating the RTM bias. Equation 1.15 can be written as (Equation 1.23):

$$E[k|K] = \alpha P[k] + (1 - \alpha)K = K + \alpha(P[k] - K) \tag{1.23}$$

This expression (Equation 1.23) shows that expected crash frequency for the investigated entity is estimated as a sum of its recorded crash counts and a sort of correction term. As already explained, the essence of regression-to-the mean phenomenon lies in the fact that if crash counts occurred over a certain time period at a specific site experienced a downtrend, a return to the mean should be expected and vice versa. The characteristic fluctuation around the mean of crash frequency is directly implemented in EB method whereby the correction term of

Equation 1.23, which will be positive when K is less than *P[k]* and negative when K is higher than *P[k]*.

Another fundamental assumption of EB method pertains to changes over time of factors influencing safety and involved in the analytical form of SPFs adopted for the reference population. In the conventional application of GLMs to develop SPFs, it is desirable to estimate different coefficients for each year for which data is available, with the assumption that changes from year to year experienced by different factors are similar for all reference sites (Hauer, 1997). In this perspective, it is reasonable to assume that coefficients β_{ij} of covariates are constant over time, and it is therefore only necessary to estimate for each year the different constant term β_{i0}, introduced for capturing the unknown and unobserved factors (Equation 1.12). In the estimation of these β_{i0}, each annual crash count is an observation, with a certain amount of reciprocal correlation among them. Ignoring correlation in developing SPFs via application of GLMs could provoke an underestimation of variance related to the coefficients of the model, and this could impair selection of coefficients actually influencing safety of the entities. To overcome this difficulty, an alternative methodology was proposed for calibrating coefficients of the model. This is the generalised estimating equation (GEE) (Liang & Zeger, 1986; Lord & Persaud, 2000; Cafiso & D'Agostino, 2012). GEE is a semiparametric regression technique alternative to the likelihood-based GLM. Its semiparametric essence derives from the fact that estimations of coefficients only depend on the mean and the variance of dependent variable. The basic idea is to generalise the usual univariate likelihood equation of GLMs by introducing a new covariance matrix of vector of responses, that is the dependent variable. It is worth mentioning that there is not a diagonal variance matrix because observed measures are correlated to each other. Briefly, terms of traditional GLM likelihood equation are replaced by generalised linear models, which allow including correction terms in order to adjust for temporal correlations.

The most important reference source for implementation of EB method is the AASHTO Highway Safety Manual (AASHTO, 2010), which presents a variety of SPFs for quantitatively estimating crash frequency or severity at a variety of locations. Proposed crash prediction models can be used by jurisdictions to make better safety decisions. They can be the structural frame of a network screening aimed to identify sections that may have the best potential for safety improvements. Alternatively, they can be proficient in determining the safety impacts of design changes at the project level or the safety effects of engineering treatments because, as already explained, these beneficial measures are usually implemented at locations that have recorded higher than normal crash counts, with exposition to RTM bias. On the other hand, EB methods were primarily introduced for performing Observational Before-After studies focused on evaluation of the road safety effect achieved by the implementation of a specific engineering treatment. The before period ends when the treatment is applied.

EB approach employs SPFs for both the before and after period. In particular, for a given site where a treatment has been applied, after having estimated the average crash frequency in the Before period, it is necessary to predict the crash frequencies in the after period in the absence of the countermeasure. The before

estimates are then used for adjusting the other ones. Eventually, the safety effectiveness of the treatment for the investigated site can be quantified by comparing, in terms of odd ratio, the observed after crash frequency to the expected after crash frequency calculated with the hypothesis that the treatment was not applied. By considering representative samples of treated and untreated sites, it is possible to gather a general measure of the safety effectiveness of the treatment.

The use of the observed number of crashes experienced by the treatment sites in the before period along with EB expected crashes in the after period with and without the treatment, enables to estimate two fundamental indexes for the investigated treatment: the crash modification factor (CMF) and the crash reduction factor (CRF). CRF is the percentage crash reduction that might be expected after implementing a given countermeasure at a specific site. For example, if the installation of centreline rumble strips on a two-lane roadway has a CRF equal to 14, this means applying this countermeasure at a specific site will determine an expected average crash reduction of 14%. CMF is calculated as 1-(CRF/100); it is a multiplicative factor used to compute the expected number of crashes after implementing a given countermeasure at a specific site. For the example before, CMF will be 1 - (23/100) = 0.77. This value, if multiplied by predicted crash frequency related to the baseline condition (i.e. before the application of the countermeasure) and derived by a specific SPF, can provide the EB estimated crash frequency. The use of CMF is depicted by Equation 1.24:

$$N_{predicted} = N_{spf} * (CMF_{1i} * CMF_{2i} * \dots * CMF_{ni}) * C_i \quad (1.24)$$

where:

- $N_{predicted}$ = predicted average crash frequency for a specific year for site type *i*;
- N_{spf} = predicted average crash frequency determined for base conditions of the SPF developed for site type *i*;
- CMF_{ni} = crash modification factors specific to SPF for site type *i*;
- C_x = calibration factor for adjusting SPF for local conditions for site type *i*.

Practically, CMFs adjust the estimate for additional site specific conditions, that may be different from the base conditions. Schematically, the underlying essence behind CMF is depicted in Figure 1.5.

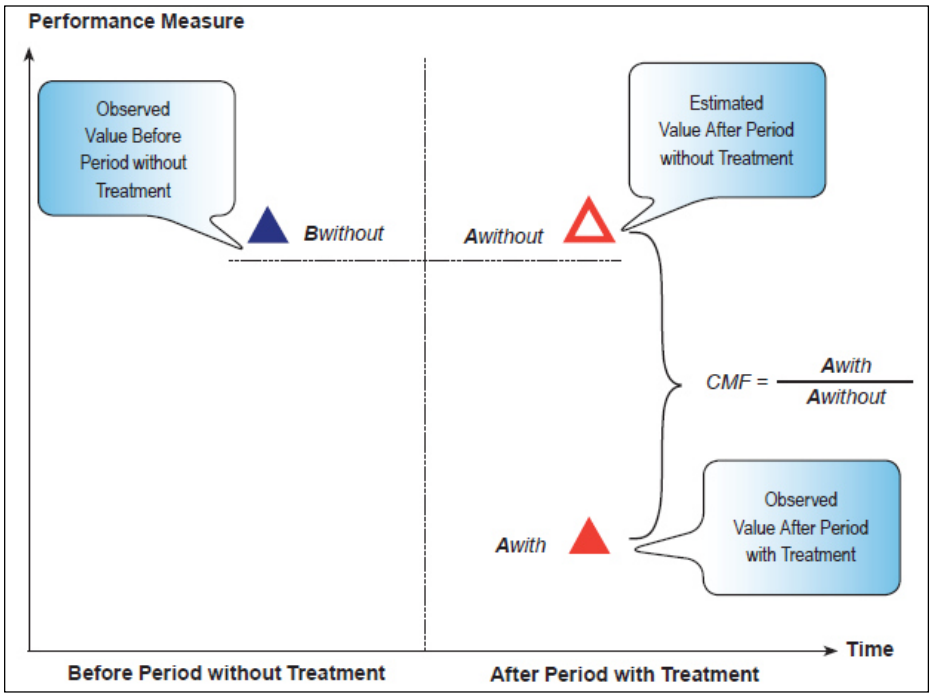

Figure 1.5 Schematic illustration of CMF significance within the framework of the EB Observational Before-After studies. Source: **(FHWA, 2012)**
:

Recommended values of CMF are provided by the FHWA Clearinghouse for different treatments and site attributes (FWHA, 2012; FWHA, 2014). The values are continually updated as more recent empirical information becomes available and is introduced into the Clearinghouse database.

Equation 1.24 shows also the calibration coefficient, which is intended to account for differences in crash patterns in different geographical areas that are not directly assessed by the SPFs. These differences involve multifarious factors widely variable between different places, such as, for instance, drivers' behaviour, vehicle fleet characteristics, crash reporting practices, road design standards (Hauer, 1997). Territorial jurisdiction may calibrate SPFs using local data in order to reflect local crash experience, but this would represent a major undertaking. Instead, calibration coefficients allow exploiting existing SPFs originally conceived for a certain geographical area by simply applying a multiplicative factor to the initial prediction. Basically, HSM proposes to calculate a calibration factor for each year by dividing the sum of observed crashes for all sites of a specific subtype to the sum of the predicted crashes for the same sites using SPFs (AASHTO, 2010).

1.5.1 Disadvantages affecting Empirical Bayes method observational before-after evaluation studies

The main drawback affecting the Bayesian approach and observational crash-based studies in general regards the unfeasibility to take into account complex causal relationships at the base of crashes occurred at a given site. The assessed safety effects of a certain treatment, expressed in terms of CMF, cannot unveil at what degree drivers' behaviour and operational performances of the road entity will change. However, these two aspects, too, contribute to the overall safety of a certain entity and should not be neglected for preventing the risk of accomplishing blind safety assessments where artificial and intangible result are obtained. This is evident by considering that, in EB approach, traffic volumes are expressed in terms of Annual Average Daily Traffic (AADT), i.e. the average number of vehicles that pass by a road section during a 24-hour period in a certain year. In this way, however, relevant changes that traffic operational condition may experience during the day cannot be considered. Starting from off-peak periods, vehicle flows can reach their daily pinnacles even in restricted time intervals. These sharp variations deeply influence drivers' behaviour with consequent safety repercussions (NCHRP, 2010). Annual means of traffic flows cannot take into account this variety of real conditions, which is profoundly correlated to crash patterns of a given road site (Svensson, 1992)

More explicitly, EB approach tends to lead to artificial outcomes not completely connected to the characteristics and peculiarities of the investigated site, acting like a sort of black box. This is more evident when safety assessments involve a plurality of treatments. In this case, it is difficult for the EB approach to distinguish the effect of one treatment from that of another. For instance, when estimating the effect on crashes of a permissive-protected left turn signal at a given intersection, a reliable estimate cannot be obtained if introduced at the same time with changes in signal phase (Shahdah, et al., 2014)

1.5.2 Empirical Bayes method observational before-after studies applied to roundabouts

Safety Performance Functions devoted to roundabouts can be sourced by numerous studies affecting the topic of Road Safety.

In the 1980's, the Transport and Road Research Laboratory conducted a study of accidents at four-arm roundabouts (Maycock & Hall, 1984). A sample of 84 four-arm roundabouts with approximately circular central island and no unconventional geometric features was selected. At each site, traffic and pedestrian flow counts were obtained and detailed geometric measurements were made. Fatal and injury crashes occurred over a six-year period were also obtained. Each crash was associated to a particular arm of the roundabout and classified by type, including those which involved pedestrian casualties. The generalized linear

models were used to investigate the relationships between the crash frequency and the traffic and pedestrian flows and geometry at the roundabout sites. The analyses were undertaken in two main stages. In the first part, roundabouts were considered as a whole. In the second one, investigations were focused on the single arms, which became the unit of the analyses. By considering the roundabouts as a whole, it stood out that injury crashes are expected to be higher at small roundabouts than normal roundabouts, presumably due to their wider flared entries, and that higher speeds are generally associated with higher crash frequencies. In the second part, where the single arms embodied the basic unit of the analysis, crash prediction models were specifically developed for single crash typologies. The major factors that were found to be statistically significant are entry width, circulatory width, entry path radius, approach curvature and angle between entries.

An Australian study (Arndt & Troutbeck, 1995) conceived crash prediction models for different crash typologies using both linear and non-linear Poisson-based regression models with independent variables related to driver behaviour and geometric design. These include flow, 85th percentile speed, changes in 85th percentile speed as the vehicle advances through the roundabout, vehicle path radius on each geometric element and the length of the driver path on this element. Construction of the vehicle paths allows the distance travelled and the estimated 85th percentile speed on each geometric element to be determined.

A French model for predicting the total number of fatal and injury crashes at a roundabouts does not contain any geometric variables and applies to roundabouts where the total incoming traffic ranges between 3,200 and 40,000 vehicles per day.

A study in Sweden surveyed roughly 650 roundabouts classifying them according to geometric design, speed level and other variables. A huge database was created collecting crash records and vehicle, bicycle and pedestrian volumes. The research unveiled a remarked influence of vehicle speeds, which could be safely lowered by providing central islands with radii between 10 and 20 m and by developing the approaches to be as perpendicular as possible at the roundabout entry. As for crashes involving cyclists and pedestrians, single lane roundabouts proved to be much safer for cyclists than multilane roundabouts. For pedestrians, roundabouts are no less safe than conventional intersections and single lane roundabouts are safer than multi-lane roundabouts (NCHRP, 2007).

Before-after studies exploiting the Bayes methodology in order to control the regression-to-the-mean bias have been mainly conducted in the United States (Persaud, et al., 2001). However, up to this time, such an approach has experienced a limited use in analysing the conversion from a traditional at-grade intersection into a roundabout. The AASHTO Highway Safety Manual does not currently include a full developed crash prediction method for roundabouts. The Manual only provides CMF achievable by converting traditional at-grade intersections, such as, for example, stop-controlled or signalised intersections into roundabouts. There is not the possibility of quantitatively assessing the crash reduction benefits of providing a roundabout at a specific intersection or to investigate the safety effects of complex design decisions at single-lane and

multilane roundabouts. Even the influence exerted by single geometric parameters cannot be clearly ascertained. As a reaction for this current gap, a NCHRP project (NCHRP 17-70) has been started with the aim to understand the influence of geometric and operational features on crash frequencies at roundabouts. This would allow designers to select the geometric layout able to guarantee the best safety performances for a given traffic demand.

This current lack of knowledge affecting roundabouts is a result of the difficulty of analysing in detail the articulated geometric framework characterising this intersection typology, where numerous geometric parameters may affect crash frequencies. This reflects the aforementioned disadvantage affecting EB approaches in ascertaining and capturing features and peculiarities of the analysed road entities (Davis, 2004; Hauer, 2010). After all, EB approach applied to before-after studies research for statistical regressions between values of different parameters; there is no consideration for crash patterns and dynamics which preceded them. As a result, there is not the possibility of unveiling the causes originating crashes, but only the consequences of criticalities which cannot be realised by the solely application of EB methods. There is also the concern of extending SPFs from the original site to other locations: no quantifiable variations of phenomena such as, for example, users' behaviour, traffic conditions and different attitudes between States about how a roundabout should work lead to such a dispersion of data to compromise the reliability of the results obtained by statistical approximations (Kennedy & Taylor, 2005).

1.6 Traffic Conflict Technique

An alternative metric to conventional crash-based analyses is focused on the so-called traffic conflicts, i.e. observable situations where two or more road users approach each other in space and time to such an extent that there is a risk of collision if their movements remain unchanged. In other words, traffic conflicts represent all the events where drivers must take evasive manoeuvres, such as breaking or swerving, for avoiding collisions (Guttinger, 1984). The gist of these branch of studies is that each crash is preceded by a dangerous situation; some turn into crashes and the rest into near-misses. Dangerous situations, in turn, follow incipient dangers within a continuum of events pictured by Figure 1.6 (Hauer, 1997).

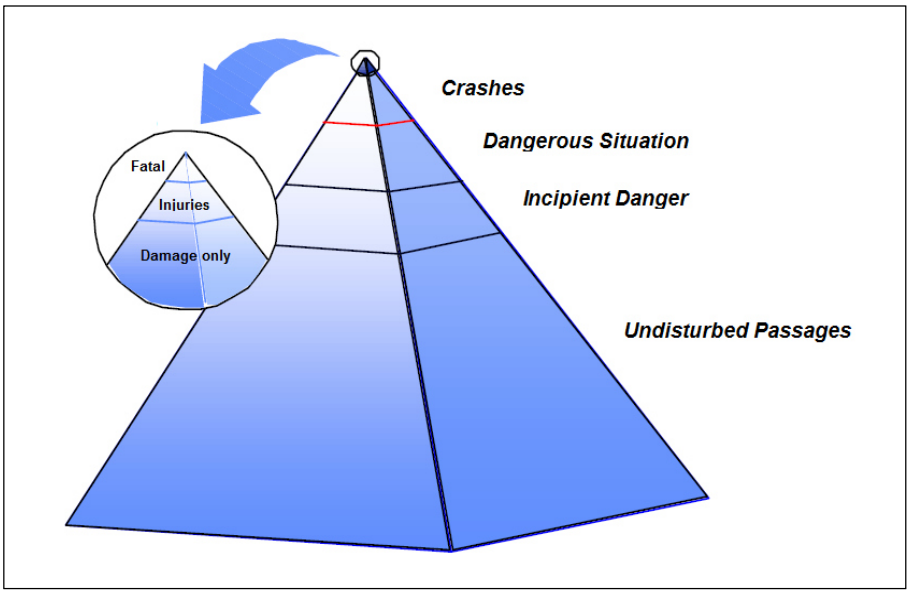

Figure 1.6 Heinrich's Triangle.
Source: **(Archer, 2005)**

The characteristic pyramid (Figure 1.6), also referred as the Heinrich's Triangle, is based on the hypothesis that events can be ranked in order of increasing severity but decreasing frequency (Hyden, 1987). The height of a section from the pyramid's base represents the severity of the corresponding class of events, while the volume of the section denotes the relative frequency for that class. It can be noted that crashes are actually rare events, while there are more dangerous situations per unit of time. Fatal crashes are the least frequent, so they occupy the tip of the pyramid. Below fatal accidents might be injury crashes and then non-injury crashes (i.e. proper damage only, PDO crashes), near misses crashes, and so forth. The underlying idea of traffic conflict studies is to assume that the frequency with which dangerous situation occur can provide an insight into crash frequency and safety performances of road entities (NHTSA, 2010). The reference measure for safety performances of road entities is now the frequency of dangerous situations, given that they are more frequent and easier to measure than real crashes. After a location is identified as hazardous, a study of conflict pattern can be used to gather a more accurate understanding of safety drawbacks and crash causation (Archer, 2005).

Raw counts of traffic conflicts have been made since traffic engineers first began making field observation for pursuing determination of appropriate safety improvements. Perkins and Harris of General Motors developed the first formalised procedure for identifying and recording traffic conflicts at intersections (1967). The technique, successively defined as traffic conflict technique (TCT), was applied at urban intersections with a view to ascertaining whether General Motors cars

performed more safely than those of other manufacturers. Conflicts were defined as those events involving swerving, braking or traffic violations; they were directly identified and recorded in normal operation and in real time by trained observers.

Originally, there was no scaling of conflicts by severity, but subsequent studies started to classify acquired traffic conflicts according to severity by means of specific factors, such as, for example, time to collision, complexity of evasive action and proximity of conflicting vehicles.

TCT moved then to acquisition of surrogate safety measures by field observers' crews specifically trained to collect the data and determine the potential number of conflicts along with their severities (FWHA, 2003; Saunier & Sayed, 2008; Highways Research Group, 2007). In the further research developments, two measures of movement in space and time emerged as the most notable surrogate measures of the severity of a conflict:

- Post Encroachment Time (PET): time between the first road user exiting from the conflicting space and the second road user arriving in that space;
- Time to Collision (TTC): time that will elapse before the two road users collide unless one of them takes an avoiding action (e.g. by braking or swerving).

However, TTC proved to be better suited for determining indices of severity and was then preferred to PET calculation.

Coherently to the Swedish TCT procedure, one of the most internationally accepted one, the TTC is calculated by conflict observers at the instant that one of the vehicles involved in the potential collision begin performing evasive manoeuvres. TTC value can be quantified based on two observers' estimates (Highways Research Group, 2007).

The first one is the distance between the relevant road user to the potential point of collision at the instant in which the evasive manoeuvre is performed. The second estimate is the speed of the only relevant user itself at the moment when evasive manoeuvre is taken. The TTC value together with the conflicting speed is used to determine whether or not a conflict is serious, as shown by the diagram reported in Figure 1.7, where the boundary between slight and serious conflicts was determined as a function of deceleration capabilities of vehicles involved in the potential collision.

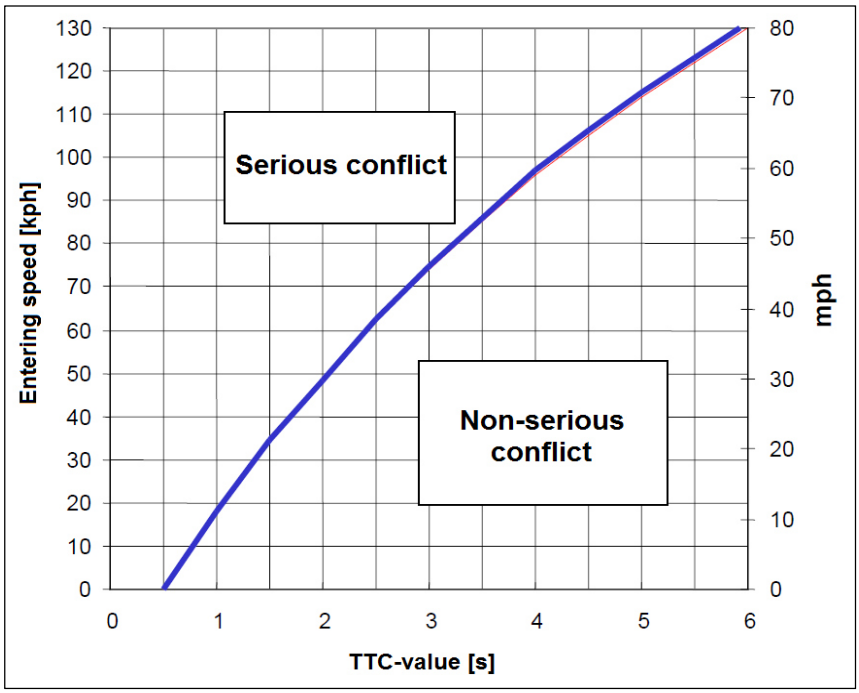

Figure 1.7 Graphical representation of the regression-to-the mean phenomenon
Source: **(Highways Research Group, 2007)**

The Swedish TCT technique has been applied for research, but it has also been used by highway authorities as a diagnostic and evaluation tool grounded in the ability to register the occurrence of near crashes directly in real-time traffic.

TCTs appear to have the potential to overcome shortcomings affecting EB method (Hauer & Hakkert, 1989; Davis, 2004; Saunier & Sayed, 2008; Shahdah, et al., 2014). First of all, as already specified, traffic conflicts are more numerous and frequent than real crashes. Therefore, there is no the necessity of waiting for prolonged times before having acquired an adequate amount of data. Second, output of EB method and observational road safety studies in general is highly influenced by crash records, which usually underreport less severe crashes, and ignore near-miss ones, which instead may be informative about lack of safety affecting the analysed site. Third, observers, during their conflict counts, have a direct vision of the investigated site, with the possibility of really understanding how the road entity works in terms of safety. In fact, they can appreciate actual driver' behaviour, how they interact each other and whether crashes or traffic conflicts can be explained by particular drivers' attitude, as well as the presence of possible punctual deficiencies affecting the investigate site, such as, for instance, obstacles impending mutual visibility. In other words, the dynamics leading to a crash can be investigated from a broader and more casual perspective than is possible from

observational crash data alone. Eventually, TCTs enable safety assessments taking into account the traffic flow changes influencing the operational performances of the road entities. Traffic conflict patterns recorded for a given road entity can be referred to precise time intervals, where it is possible to assume that traffic operations are constant and homogeneous. This is a key aspect for safety evaluations. Starting from off-peak periods, vehicle flows can reach their daily pinnacles even in restricted time intervals. These sharp variations deeply influence drivers' behaviour with consequent safety repercussions. As already explained, SPFs and Empirical Bayesian methods are not able to distinguish between these circumstances, given the fact that the traffic flow intensity figures in the covariates of the crash prediction model as an average value referred to an extended time period (Shahdah, et al., 2014).

1.6.1 Microscopic Traffic Simulations in synergy with Traffic Conflict Techniques

Recently, researchers have used microscopic traffic simulation to obtain high-risk vehicle interactions and collect surrogate measures of safety for intersections (FWHA, 2003; NHTSA, 2010; Shahdah, et al., 2014; Highways Research Group, 2007). This represents a sort of conjunction between software aimed to assess operational performances and road safety techniques. The main feature of microscopic software is the capability of modelling the analysed traffic systems by simulating and continuously updating position, speed, acceleration, lane position and other state variables of multiple vehicles advancing through the traffic network. These models were originally developed for planning purposes and operational analyses of multi-modal traffic network. The idea is to acquire surrogate measures of safety and crash severity directly from the traffic flow simulation offered by the software. In this regard, Federal Highway Administration has conceived a sort of post processor, called as Surrogate Safety Assessment Model (SSAM), able to analyse vehicle-to-vehicle interactions to identify conflict events and catalogues all of them. For each such event, SSAM also calculates numerous surrogate safety measures, such as the TTC, PET and others. The advantages ensured by this "modus operandi" based on microscopic models are obvious: there is no need for time-consuming field observation of traffic conflict; TCT can now be used also for not already existing road entities or for safety evaluation of possible treatments to be applied to the investigated sites; traffic evolution on time can be taken into account in safety assessments.

The main limit affecting this particular TCT procedure is that a single trajectory can be imposed to all of the simulated vehicles. This means that dispersion of trajectories is completely neglected. The researchers have to impose a unique path valid for the entire population of drivers, which is not consistent with actual drivers' behaviours. If this approximation can be accepted for signalised intersections, this is not the case for other road entities, such as roundabouts,

where trajectory followed by a driver can profoundly influence its speed with evident safety consequences.

The use of simulation continues to raise concerns about the credibility of modelled conflicts in real-world traffic applications, particularly as it is affected by different safety treatments. Establishing a link between simulated conflicts and observed crashes is of fundamental importance for identifying potential safety problems and suggesting the most effective ways to resolve them. Research is ongoing in this area, and as simulation models and video technology improve, this technique is expected to grow in use.

1.6.2 Validity and reliability of Traffic Conflict Techniques

Serious concerns have been raised for decades about validity and reliability of TCTs, given the fact that safety evaluations are built on indirect safety indicators. Reliability involve the operators' ability to distinguish serious conflicts from other events and correctly assessing their severity. No matter how the operators can be trained, a certain amount of subjectivity and variability in their evaluations will persist. In addition, the multifaceted interaction between cofounding variables involving human behaviour, vehicle and environmental factors could mislead the ascertainment of a potential critical situation (NHTSA, 2010). For example, a breaking action performed by an observed driver for causes not related to the need for prevent near-crashes could be erroneously interpreted as an evasive manoeuvre.

Video-recordings is an alternative tool to collect required data and ensures numerous advantages as compared to manual observation. In fact, it increases the possibility to accomplish long-period observations and to look through look the relevant situations over again. That is a crucial point because reliability of the conflict measurement is mostly connected with differences caused by subjective evaluation of traffic conflicts by individual observers. In this perspective, methods using video-recordings can ensure a more objective data acquisition due to the possibility of repeated assessments. However, it was pointed out that observers on site can benefit from a direct vision of all the events preceding a potential collision, which is preferable to a limited two-dimensional sequential analysis of video-recordings. The operators directly observing the site can be aware of safety problems affecting the investigated site. For example, there could be red-light violations, high flow rates, excessive vehicle speeds, large numbers of turning movements and other situations that influence road-user behaviour and interaction negatively.

In addition, even if with video-recordings the task of the observer is moved from being an outdoor to an indoor activity, the disadvantage of using a human operator as a detection unit still remain. A possible solution may be the automated video-recording analysis able to record and observe more than one road users at the same time. This may leads to shortening of the processing time and to significant increase of the measurement reliability. In fact, specific algorithms could

be developed in order that the system only acquire the situations that objectively matching the criteria at the base of a traffic conflicts. In other words, data collection could be based on objective measures of behaviours. However, a standard accepted methodology is still far from being assessed, so human observers continue to play a fundamental role. It must be highlighted that subjective element of outdoor or indoor observations implies the application and acquisition of safety knowledge and experience by the operators: they must be properly trained in order to reduce to the greatest extent possible the variations of judgements among them.

Validity of TCTs refers to two issues. The first is about to what extent the conflicts techniques are able to provide well-founded estimates of real crash frequencies with a satisfying variance. The second states the existence of a logical continuation between real crashes and traffic conflicts, that is whether patterns and dynamic of evasive manoeuvres allow predicting crashes by typology and severity, with particular attention to reliability of severity indicators.

Although various studies have found good correlations between conflicts and real crashes, it is known that number of crashes occurred during a certain year are not a good indicator of the real safety performances of a road entity. Therefore, rather than focusing on searching for these kinds of direct correlations, it was noted that if traffic conflicts are treated as crash opportunities, expected crash frequencies may be obtained via Equation 1.25

$$\begin{aligned} Expected\ crash\ frequencies & \\ = (Traffic\ conflicts\ frequencies) & \\ * (crash - to - conflcit\ ratio) & \end{aligned} \tag{1.25}$$

The number of traffic conflicts occurred in a given time provide the number of crash opportunities, while the crash-to-conflict ratio reflects the probability that a certain traffic conflict may result in a real crash. Equation 1.24 can be used as predictive method on the condition that crash-to-conflict ratios are estimated with acceptable precision and do not excessively vary across different entities of the same type. If conflicts of different degrees of severity have different probabilities of being followed by a real crash, then a study that mixes together conflicts of varying severity may find it difficult to identify a stable crash-to-conflict ratio. In this regard, various studies have shown that traffic conflicts seem to accord better with sever crashes than with all other crashes. However, issues of TCTs validity are still on debate, with particular mention for identification of groups of conflicts having stable crash-to-conflict-ratios and how combining them in a unique and coherent framework. Further validity problems can also derive from inaccurate and insufficiently processed crash data. It must be considered that another (Highways Research Group, 2007).

In addition to all of the aforementioned issues, TCTs show other two inadequacies of primary importance. By definition, traffic conflicts involve more than one vehicle, and for this reason, single-vehicle crashes are not considered. Furthermore, there is the impossibility of relating traffic conflicts to variables used in design and operational models. In this regard, even the traffic flow intensity cannot be directly implemented in analytical determinations. Although TCTs allow

the operators to appreciate possible influences of traffic flow daily changes on distribution for typology and severity of traffic conflicts, there is not a standard reference, and analyses about these aspects strictly depend on the personal sensibility and discernment of the operators.

1.6.3 Traffic Conflict Techniques Applied to Roundabouts

TCTs have been used to investigate roundabout safety issues (Guido, et al., 2011) and evaluate proposed changes to roundabout layouts (Al-Ghandour, et al., 2011). The proactive approach enabled by TCTs is of primary importance for roundabouts because injury and fatal crashes usually tend to occur at lower frequencies as compared to other kind of at-grade intersections. This means that numerous years would be required for collecting an adequate crash database for obtaining related SPF. Conversely, TCTs allow determining safety issues of analysed sites in a short time period.

Common surrogate safety measures have been successfully applied for roundabouts too, such as the deceleration rate, proportion of sight distance, and time to collision. The same measures have been widely exploited in microscopic traffic flow simulations with the aim of estimating traffic conflict frequencies for new designed roundabouts or for predicting possible safety concerns provoked by increases in traffic flows passing through already existing roundabouts.

Vehicle trajectories produced during the microscopic traffic simulation, as well as vehicle's position, speed and acceleration profiles, are automatically processed by specific suites, such as, for example, SSAM model developed by FHWA, in order to collect traffic conflicts and categorise them by typology and severity. This approach has all the generic advantages of simulation but there also various weakness. Firstly, microscopic traffic simulation software cannot take into account dispersion of trajectories, which is an essential factor for safety analyses of roundabouts: drivers who attempt to exploit shortest trajectories are likely to perform high speed value. Secondly, in these computer programs, vehicles are designed in order to maintain each other a safety to stop distance, in accordance to the car following model, a behavioural hypothesis which is not always complied with. As yet, the practical experience is rather limited and the results are not consensual. In front of promising outcomes, other studies have found that simulated conflicts are not good indicators for traffic conflicts generated by unexpected driving manoeuvres, such as illegal lane-changes. Specific procedures to calibrate simulation models for safety assessments have been proposed too (Cunto & Saccomanno, 2007) but this is still an ongoing research field.

Another approach for applying TCTs to roundabouts lies in intending traffic conflicts as violations of traffic rules, such as, for example, failures to yield to vehicles circulating in the ring.

This is accepted because roundabouts strictly rely on a complex mutual interaction between multiple vehicular flows approaching to the ring simultaneously; every time a traffic rule is not complied with, a crash may be arise.

However, by adopting this method, the problem arises of discerning whether the failure to observe the traffic rule is to be ascribed to driver's irresponsibility or to infrastructural weakness. For this particular application, video-apparatus is absolutely essential for the possibility to stop, slow down or replay the part of the video record in order to evaluate the monitored conflict exactly and objectively.

Whatever is the pursued approach, TCTs cannot be used for developing analytical models able to embody design and operational variables, and this gap is particularly relevant for roundabout intersections, whose geometric layout is quite complex and articulated. At most, sensitive analyses can be performed where applying TCTs to roundabouts with different geometric features in order to capture possible relationships between design aspects and safety performances. However, TCTs may provide appreciated results when analysing specific sites, but their adoption for unveiling general knowledge going beyond the investigated situations is still questionable.

1.7 Conflict Opportunities

The adoption of conflict opportunities (COs) in road safety assessments takes a common heritage from TCT techniques (Kaub & Kaub, 2005; Kennedy & Taylor, 2005; NCHRP, 2008). In fact, the same designation of conflict opportunity, which refers to any event where the vehicles involved will collide if the drivers do not make any evasive manoeuvres, resemble the already introduced definition of traffic conflict. The difference is that frequency of conflict opportunities, that is potentially dangerous situations, is no longer established by direct observation on the field or analyses of video-recordings but via probabilistic models where geometric and functional parameters can be directly implemented. The aim pursued by this alternative approach in assessing road safety is to hold advantages offered by TCT, in particular searching for the origins of crashes from a broader and more casual perspective as compared to a focus restricted to only crash counts, and, at the same time, to overcome the main TCTs limitations. In fact, estimation of COs does not require time and cost-expensive, as well as subjective, screening of crash surrogate event and enable considering the design and functional parameters.

However, this third approach is still uncommon and rarely exploited in safety analyses, and there is not a comprehensive definition of CO widely accepted by academic dimension. Practical applications of these analyses are quite limited too, and a consistent, standardised framework by means of which estimating real crashes from COs quantification is still absent.

The essence of conflict opportunities is sourced from traffic conflicts, but instead of considering the situations directly recorded on the field where drivers have already initiated a chain of events having the potential of resulting in a crash,

now the emphasis is placed on the exposition to possible collisions with other vehicles. There is a shift of perspective from situations already dangerous which may provoke crashes to the preceding traffic interactions not yet configured as traffic conflicts and with the potential for originating dangerous situations. By referring to Heinrich's triangle (Figure 1.6), it is as if consideration is given to the events categorised in a step below the traffic conflicts. Traffic conflicts precede possible crashes and are headed by conflict opportunities, which in turn occur every time certain prerequisites are met by traffic interactions. These prerequisites, without which the opportunity and therefore the likelihood of a given type of traffic conflict, and then a crash, does not exist, pertain to dynamic and spatial characteristics of vehicles, as well as features of the investigated infrastructure. COs can be directly recorded by traffic surveys conducted on the field, but they are susceptible to be analytically derived by statistical formulations suitable for modelling traffic flows. Surrogate measure of traffic conflicts rely on precise dynamic measures which describe the mutual interaction among vehicles and must be punctually evaluated. COs' prerequisites were conceived for taking into account more frequent situations where, in certain cases, there is only the need for the simultaneous presence of vehicles following conflicting trajectories.

For example, at a unsignalised intersection (Figure 1.8), a CO associated with left-turn crash will occur every time that there will be a vehicle turning to left and another one approaching along a conflicting path in a well-defined lag (i.e. the time interval that elapses from the passage of the nearest vehicle coming from the conflicting flow). The user' wrong evaluation of the time interval available between vehicles of the conflicting flow approaching to the intersection is the cause of this crash type (Kaub & Kaub, 2005; Ming, 2008). Extended lags do not constitute a threat and neither do the small ones since they would certainly be rejected. Instead, a CO occurs every time the lag assume intermediate values because he is susceptible to erroneously hazard to turn left even if safety conditions are not guaranteed. To sum up, the conflict opportunity is realized when a second user arrives in a conflicting manner, during the time of exposition to the risk.

Statistical representation of conflicting traffic flows, i.e. Poissonian distribution of the arriving vehicles, allows calculating the expected number of vehicles with at least a chance to collide for each vehicle intended to turn left. It is simply necessary calculating the expected number of conflicting vehicles arriving in the band of dangerous leg values. By multiplying this value for the total amount of vehicles turning to left, number of COs is then determined.

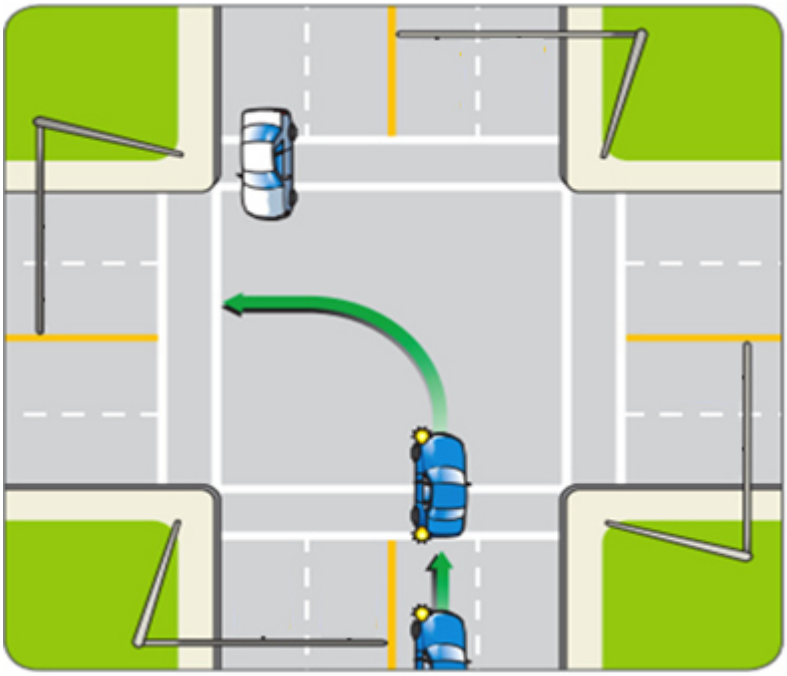

Figure 1.8 Graphical representation of the regression-to-the mean phenomenon
Source: http://www.drivesmartbc.ca/

An analytical representation could be (Equation 1.26):

$$CO_{ij,kl,P} = EN_{Rij} * Pr\left[A_{Ckl,ij}\right] * T_p \tag{1.26}$$

where:

- EN_{Rij} : expected number of risk manoeuvres on lane *j* of flow *i* per unit time in the period (i.e. movement opportunities exposed to opposition trajectories), usually estimating the number of risky manoeuvres as expressed by Equation 1.27;

$$EN_{Rij} = p_{Rij} * q_{ij} \tag{1.27}$$

  - p_{Rij} : probability of a risky manoeuvre;
  - q_{ij} : corresponding flow per unit of time;

- $\Pr[A_{Ckl,ij}]$: is the probability of a conflicting arrival to the risk manoeuvre from lane *l* of flow *k* evaluated as indicated by Equation 1.28;

$$Pr\left[A_{Ckl,ij}\right] = Pr\left[A_C / q_{Ckl,ij}, t_{Cij}\right] \quad (1.28)$$

- $q_{Ckl,ij}$: conflicting flow;
- t_{Cij} : time of exposition of the risky manoeuvre to the conflicting flow, given as (Equation 1.29):

$$t_{Cij} = L_{Cij}/V_{ij} + d_{ij} \quad (1.29)$$

- L_{Cij} : length of the conflicting area for the risky maneuver of flow *i* on lane *j*;
- V_{ij} : clearing speed of flow *i* on lane *j*;
- d_{ij} : the standing time on the conflicting area for vehicles of flow *i* on lane *j* (or delay);

- T_p : duration of time period characterised by homogeneous traffic operations.

The probability of a risky manoeuvre p_{Rij} can be 1 if mandatory or smaller if the manoeuvre is optional (e.g. as in lane changes for passing or overtaking). The probability of conflicting arrivals can be modelled via statistical distributions, such as Poisson or Erlang's one (Mauro, 2015).

Each type of CO event has its own operational concept and models. For the angle-crash at an unsignalised intersection, if the arrivals on the main flow are described by a simple Poisson model, $Pr\left[A_C / q_{Ckl,ij}, t_{Cij}\right]$ can be then expressed as (Equation 1.30):

$$Pr\left[A_{Ckl,ij}\right] = \left(e^{-q_{Ckl,ij} * t_{lower,Cij}} - e^{-q_{Ckl,ij} * t_{upper,Cij}}\right) \approx\approx q_{Ckl,ij} * \left(t_{upper,Cij} - t_{lower,Cij}\right) \quad (1.30)$$

The second term of Equation 1.30 represents the probability of arrivals on the main flow in a restricted time interval coinciding with the dangerous band of lag times where the driver being about to turn left may hazard dangerous manoeuvres. The two extremes of this time interval were assumed to be equal to +/- 2 seconds the crossing time. The geometrical parameters of the intersection appear in the calculation of the trajectory length performed by the vehicles, which is propaedeutic for the determination of the time required to cross.

The method for the estimation of Conflict Opportunities is directly affected by traffic volumes changes over time. EB methods adopted traffic flow volumes averaged on wide time intervals (e.g. AADT); TCT analyses can be related to specific temporal intervals where operational conditions may be considered homogeneous but there is not a procedure for analytically taking into account these

phenomena. Conversely, COs can be calculated for different time intervals, with the possibility of obtaining subsequent crash estimates really influenced by the actual way the vehicles interact each other. For example, free traffic flows conditions are completely different from situations where both manoeuvring and conflicting vehicle volumes are high. In the latter case, rear end collision and angle-crashes would be more likely to occur as compared to time periods characterised by low traffic flows, where, instead, single vehicle run off crash rates are expected to show an increase.

Another advantage offered by COs is the possibility of considering single-crashes involving a single vehicle, while TCTs can be used only for events with more than one vehicle (Kennedy & Taylor, 2005).

After acquisition of COs for a certain typology of possible collisions (e.g. rear-end, crossing, head-on, etc.) in relation to a specified position in the site and at a given time interval, crash expectations can be than obtained by exploiting the same hypothesis at the base of TCTs, that is a proportional relationships between incipient dangers and real crashes (Equation 1.31):

$$Expected\ crashes = (Conflict\ Opportunities) * (crash - to - conflict\ ratio) \quad (1.31)$$

By recalling Equation 1.26, the number of crashes expected to occur in a certain time period is then proportional to the number of time the analysed risky manoeuvre is performed.

Each type of CO events should have its own analytical formulation with specific variables to take into account. For example, a rear-end conflict should be based on different operational concepts and models as compared to an angle crash, because the dynamic leading to real crashes completely changes, as well as the variables to be taken into account (Mauro & Cattani, 2004; Mauro & Cattani, 2005; Kaub & Kaub, 2005; Kennedy & Taylor, 2005; Mauro & Cattani, 2010).

The ratio between crash and CO frequencies needs to be calibrated for obtaining an analytical expression whereby crash rates can be forecast (Equation 1.31). In previous researches, these coefficients, which reflect the probability that a given crash opportunity may result in a crash, were calculated by simply dividing the total amount of crashes by COs recorded in a certain time interval. Another possibility consists in searching for hypothetical correlations between the same coefficients and other factors supposed to be decisive for road safety, but not involved in CO calculations. The latter approach could be particularly useful when the conceptual model by which calculating the COs for a certain collision type cannot take into account aspects instead believed to exert influence on the crash patterns. For example, it could be problematic conceiving a CO model similar to Equation 1.30 involving the sight distance as an explicit variable. Therefore, its influence could be indirectly considered by inspecting possible correlations between this parameter and crash-to-conflict ratio. This modus operandi can also be intended as an investigation tool for uncovering possible significant influences on crash frequencies by unexpected parameters. The same concept is applied by

a software specifically conceived for estimating crash frequencies and based on COs technique. In fact, Traffic Safety prediction Computer Program (TRAF-SAFE) exploits regression relationships for obtaining crash-to-conflict ratios from the value of other significant variables not included in CO conceptual model but proved to be significantly correlated with crash frequencies. In particular, approach speed and density population were given a remarkably importance even if they were not embraced in CO calculation formulae. However, limited information and details were provided about acquisition of these regression relationships.

The ability of implementing design parameters in crash frequency expectations is fundamental in optimisation of geometrical and operational framework of road entities.

For traditional at-grade intersections where turning manoeuvres can be approximated as circle movements, the geometrical parameters appear in the calculation of the trajectory length performed by the vehicles, which is propaedeutic for the determination of the time required to cross.

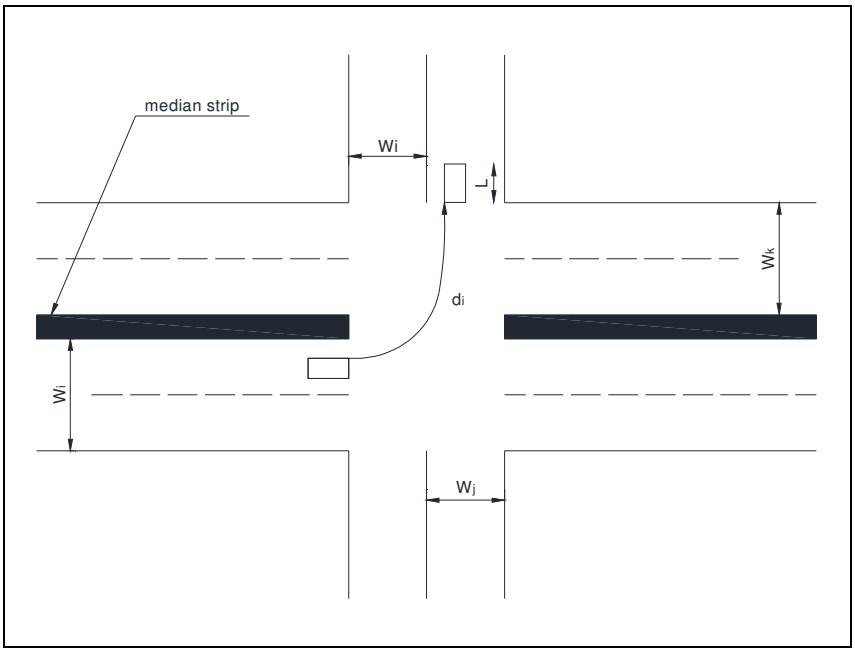

Figure 1.9 Geometric parameters which can be implemented in CO calculation for a traditional at-grade intersection. Source **(Ming, 2008)**

With reference to Figure 1.9, with the hypothesis of circular trajectory describing a right angle, crossing time included in Equation 1.31 can be calculated as:

$$t_i = \sqrt{\frac{2(d_i + L)}{a}} \tag{1.32}$$

$$d_i = \frac{\pi}{2}\left(W_k + W_{mi} + \frac{W_i}{2N_i}\right) \tag{1.33}$$

where:

- t_i: crossing time, that is the time where the turning vehicle is exposed to a conflict [s];
- d_i: distance to cross [m]
- a: acceleration value [m/s^2];
- N_i: number of lanes of the i-th approach leg;
- W_{mi}: width of median strip [m];
- W_k: width of the leg of provenience of the opposing flow [m];
- W_i: width of the approach leg [m].

However, certain road entities imposes quite complex trajectories to vehicles, and the possibility of implementing geometrical features is not always feasible. For example, vehicle‘s paths at roundabouts is particularly intricate. Adopting the aforementioned approach for implementing geometric features would be impracticable because trajectories are more dispersed than at traditional right-angled intersection. In addition, design of roundabouts is the result of numerous parameters which would deserve specific evaluations; a single analytical expression such as Equations 1.30, 1.31 cannot be developed for roundabouts. As yet, studies on COs technique are quite limited in number and do not implement geometrical features (Lakkundi, 2008; Rencelj, 2009). Among them are models limited to analyse safety performances of already existing roundabout and other ones where crash-to-conflict ratio can effectively derived from the vehicles' approach speed.

The only feasible approach for implementing geometric features in potential crash models based on COs consist in searching for possible statistical correlation between crash-to-conflict ratio and the single design factors. In other words, crash-to-conflict ratio should be calibrated via the values assumed by the geometrical features of roundabouts (Pecchini, et al., 2014). In this way, it should be possible to estimate crash frequencies for both already existing roundabouts and only designed ones.

References

AASHTO, 2010. *Highway Safety Manual.* Washington, DC, USA.

Al-Ghandour, Schroeder, B. J., Williams, B. M. & Rasdorf, W. J., 2011. Conflict models for single-lane roundabout slip lanes from microsimulation: development and validation. *Transportation Research Record: Journal of the Transportation Research Board No. 2236,* pp. 92-101.

Archer, J., 2005. *Indicators for traffic safety assessment and prediction and their application in micro-simulation modelling: A study of urban and suburban intersections. Doctoral Dissertation,* Stockholm, Sweden: Royal Institute of Technology.

Arndt, O. & Troutbeck, R., 1995. *Relationship between roundabout geometry and accident rates.* Boston, MA, Transportation Research Board of National Academies.

Arnold, L. S. et al., 2010. *Identifying Factors that Determine Bicyclist and Pedestrian-Involved Collision Rates and Bicyclist and Pedestrian Demand at Multi-Lane Roundabouts,* Sacramento, CA, USA: California Department of Transportation.

AUSTROADS, 1993. *Roundabouts. Guide to Traffic Engineering Practice, Part 6,* Sydney, Australia: Association of Australian State Road and Transport Authorities.

Bauer, K. M. & Harwood, D. W., 2014. *Safety Effects of Horizontal Curve and Grade Combinations on Rural Two-Lane Highways, FHWA-HRT-13-078,* Washington, DC, USA: Federal Highway Administration (FWHA).

Brilon, W., Wu, N. & Bondzio, L., 1997. *Unsignalized Intersections in Germany - A State of the Art.* Portland, OR, USA.

Cafiso, S. & D'Agostino, C., 2012. *Safety Performance Function for motorways using Generalized Estimation Equations.* Rome, Italy.

Cafiso, S., D'Agostino, C. & Persaud, B., 2013. *Investigating the influence of segmentation in estimating safety performance functions for roadway sections.* Washington, DC, USA.

Cunto, F. & Saccomanno, F., 2007. *Microlevel traffic simulation method for assessing crash potential at intersections.* s.l., Washington, DC, USA.

Daniels, S., Brijs, T., Nuyts, E. & Wets, G., 2010. Explaining Variable in Safety Performance of Roundabouts. *Accident Analysis and Prevention ,* 42(2), pp. 393-402.

Davis, G. A., 2004. Possible aggregation biases in road safety research and a mechanism approach to crash modelin. *Accident Analysis and Prevention,* 36(6), pp. 1119-1127.

De Brabander, B. & Vereeck, L., 2006. Safety effects of roundabouts in Flanders: Signal type, speed limits and vulnerable road users. *Accident Analysis and Prevention,* 39(3), pp. 591-9.

Department of Transport and Main Roads, 2014. *Road Planning and design manual - 2nd edition,* s.l.: Quuensalnd Government.

Elvik, R., 2003. *Effects on Road Safety ofconverting intersections to roundabouts: A review ofevidence from non-US studies.* Washington DC, USA, Transportation Research Board (TRB) of National Academies.

Elvik, R., Hoye, A., Vaa, T. & Sorensen, M., 2009. *The Handbook of Road Safety Measures - 2nd Edition.* Bingley, United Kingdom: Emerald Group Publishing Ltd.

FHWA, 2012. *Federal Highway Administration.* [Online] Available at: http://safety.fhwa.dot.gov/local_rural/training/fhwasa1108/ch3.cfm [Accessed 14 September 2004].

FWHA, 2003. *Surrogate Safety Measures From Traffic Simulation Models, Final Report,* McLean, VA, USA: Federal Highway Administration (FWHA).

FWHA, 2012. *A Guide to Developing Quality Crash Modification Factors,* Washington, DC, USA: Federal Highway Administration (FHWA).

FWHA, 2013. *Safety Performance Function Development Guide: Developing Jurisdiction-Specific SPFs,* Washington, DC, USA: Federal Highway Administration (FWHA) Office of Safety.

FWHA, 2014. *CMF - Crash Modification Factors Clearinghouse.* [Online] Available at: http://www.cmfclearinghouse.org/

Giaver, T., 1992. *Application, Design, and Safety of Roundabouts in Norway.* Nantes, France.

Guichet, B., 1993. *Typologie des accidents dans les giratoires urbains.* Bagneux, France, Service d'Etudes Techniques des Routes et Autorutes (SETRA), Centre d'Etudes des Transport Urbains, pp. 145-151.

Guichet, B., 1997. *Roundabouts In France: Development, Safety, Design, and Capacity.* Portland, OR, USA.

Guido, G. P. et al., 2011. Comparing safety performance measures obtained from video capture data. *Journal of Tranpsirtation Engineering,* 137(7), pp. 48-491.

Guttinger, V., 1984. *Conflict Observation in Theory and Practice.* Berlin, Germany: E. Asmussen.

Hauer, E., 1997. *Observational Before-After Studies in Road Safety - 1st Edition.* Bingley, United Kingdom: Emerald Group Pubblishing, Ltd.

Hauer, E., 2004. Statistical methods and safety data analysis and evaluation. *Transportation Research Record 1897,* pp. 81-87.

Hauer, E., 2010. Cause, effect and regression in road safety: A case study. *Accident Analysis and Prevention,* 42(4), pp. 1128-1135.

Hauer, E. & Bamfo, J., 1997. *Two Tools for Finding What Function Links the Dependent Variable to the Explanatory Variables.* Lund, Sweden.

Hauer, E. & Hakkert, S., 1989. The extent and some implications of incomplete crash reporting. *Transportation Research Record, No. 1185,* pp. 1-10.

Hels, T. & Orozova- Bekkevold, I., 2006. The effect of roundabout design features on cyclist accident rate. *Accident Analysis and Prevention,* 39(2), pp. 300-7.

Highway Agency, 2007. *Geometric Design of Roundabouts. Design Manual of Roads and Bridges - TD 16/07,* London, United Kingdom.

Highways Research Group, 2007. *Deliverable No. 2: Review of Literature and Experience on the,* Lund, Sweden: Lund University.

Hyden, C., 1987. *The Development of a Method for Traffic Safety Evaluation: The Swedish Traffic Conflicts Technqiue. Bulletin 70,* Lund, Sweden: Dept. of Traffic Planning and Engineering, Lund University.

Isebrands, H., 2011. *Quantifying safety and speed data for rural roundabouts with high-speed approaches.* s.l.:Iowa State University.

Isebrands, H., Hallmark, S., Fitzsimmons, E. & Stroda, J., 2008. *Toolbox to evaluate the Impacts of Roundabouts on a Corridor or Roadway Network,* St. Paul, MA, USA: Minnesota Department of Transportation Research Service Section.

ISTAT, 2014. *I.Stat, Fatalities and Injuries in road crashes.* [Online] Available at: http://dati.istat.it/Index.aspx?DataSetCode=DCIS_MORTIFERITISTR1 [Consulted on 30 September 2014].

ITE, 1999. *Traffic Safety Toolbox: A Primer on Traffic Safety,* Washington, DC, USA: Institute of Transportation Engineers (ITE).

Kaub, A. R. & Kaub, J. A., 2005. Predicting Annual Intersections Accident with Conflict Opportunities. *TRB Circular E109: Urban Street Symphosium Transportation Research Board .*

Kennedy, D. R. & Taylor, K. M., 2005. *Estimating Roundabout Performance using Delay and Conflict Opportunity Crash Prediction.* Vail, CO, USA, Transportation Research Board (TRB) of National Academies.

Kennedy, J., 2007. *International Comparison of Roundabout Design Guidelines - Report PPR206,* Workingham, United Kingdom: Transport Research Laboratory.

Kennedy, J. V., 2005. *Review of accident research at roundabouts.* Washington, D.C., USA, Transportation Reserach Board (TRB) of National Academies.

LAGS, 2010. *Le Intersezioni a Rotatoria. Tecniche, Costi, Efficacia - Online Textbook.* ww.lags.corep.it: Laboratorio per il Governo della Sicurezza Stradale (LAGS).

Lakkundi, V. R., 2008. *Development of left-turn guidelines for signalised andunsignalised intersections. Report No. FHWA NJ 2008 011,* Washington, DC, USA: Federal Highway Administration.

Liang, K. Y. & Zeger, S. L., 1986. Longitudinal data analysis using generalized linear models. *Biometrika,* Volume 73, pp. 13-22.

Lord, D. & Persaud, B., 2000. Accident prediction models with and without trend: application of the generalized estimating procedure. *Transportation Research Record: Journal of the Transportation Research Board,* 1717(1), pp. 102-108.

Mauro, R., 2015. *Traffic and Random Processes. An Introduction.* Berlin, Germany: Springer International Publishing.

Mauro, R. & Cattani, M., 2004. Model to evaluate potential accident rate at roundabouts. *ASCE Journal of Tranportation Engineering,* 130(5), pp. 602-609.

Mauro, R. & Cattani, M., 2005. *A model to evaluate the potential accident rate at single-lane roundabouts and double-lane roundabouts.* Linkoping, Sweden, Swedish National Road and Transport Research Institute (VIT).

Mauro, R. & Cattani, M., 2010. *Potential Accident Rate of Turbo-roundabouts.* Washington, DC, USA, Transportation Research Board (TRB) of National Academies.

Maycock, G. & Hall, R. D., 1984. *Accident at Four Arm Roundabouts,* Workingham, United Kingdom: Tranport and Road Research Laboratory.

McCullagh, P. & Nelder, J., 1989. *Generalized Linear Models - 2nd Edition.* London, United Kingdom: Chapman and Hall/CRC.

Ming, S. H., 2008. *Oportunitades de conflito de trafego:modelos de previsao.* Graduate Dissertation, Universidade de Sao Paulo.

Ministero delle Infrastrutture e dei Trasporti, 2006. *Geometrical and functional standards for road design. Official Italian Enhancement Act D.M. 19/04/2006.* Rome, Italy: s.n.

Montella, A., 2011. Identifying crash contributory factors at urban roundabouts and using association rules to explore their relationships to different crash types. *Accident Analysis and Prevention,* 43(4), pp. 1451-63.

Montella, A., Turner, S., Chiaradonna, S. & Aldridge, D., 2012. Proposals for Improvement of the Italian Roundabout Geometric Design Standard. *Procedia - Social and Behavioral Sciences,* Volume 53, pp. 189-202.

NCHRP, 1998. *Modern Roundabout Practice in the United States, NCHRP Synthesis 264,* Washington, DC, USA: Transportation Research Board (TRB) of National Academies.

NCHRP, 2003. *Review of Truck Characteristics as Factors in Roadway Design,* Washington, DC, USA: Transportation Research Board (TRB) of National Academies.

NCHRP, 2007. *Report 572: Roundabouts in the United States,* Washnigton D.C.: National Cooperative Highway Research Program (NCHRP), Transportation Research Board (TRB) of National Academies.

NCHRP, 2008. *Multimodal level of service analysis for urban streets,* Washington, DC, USA: Transportation Research Board (TRB) of National Academies.

NCHRP, 2010. *Roundabouts: An Informational Guide - Second Edition,* Washington D.C.: s.n.

NHTSA, 2010. *Task 3-Evaluating the Relationship Between Near-Crashes and Crashes: Can Near-,* Blacksburg, VA, USA: National Highway Traffic Safety Administration (NHTSA).

Ourston, L., 1996. *Comparative Safety of Modern Roundabouts and Signalized Cross Intersections.* [Online] Available at: http://www.roundabouts.com [Accessed 13 January 2014].

Pecchini, D., Mauro, R. & Giuliani, F., 2014. Model of Potential Crash Rates of Rural Roundabouts with Geometrical Features. *ASCE Journal of Tranposrtation Engineering,* 140(11), p. 04014055.

Perkins, S. R. & Harris, J. I., 1967. Traffic conflict characteristics: Accident potential at intersections. *Highway Research Record,* Volume 225, pp. 45-143.

Persaud, B. N., Retting, R. A., Garder, E. & Lord, D., 2001. Observational Before-After Study of the Safety Effect of U.S. Roundabout Conversions Using the Empirical Bayes Method. *Transportation Research Record, No. 1751.*

Persaud, B. N., Retting, R. A., Garder, P. E. & Lord, D., 2001. *Observational before–after study of the safety effect of U.S. roundabout conversions using the empirical Bayes method.* Washington, DC, USA.

Rencelj, M., 2009. *The methodology for predicting the expected level of traffic safety in the different types of level intersections. Doctoral Dissertation,* Trieste, Italy: Università degli Studi di Trieste.

Sacchi, E., Bassani, M. & Persaud, B., 2011. Comparison of safety performance models for urban roundabouts in Italy and other countries. *Transportation Research Record: Journal of the Transportation Research Board,* 2265(1), pp. 253-259.

Saunier, N. & Sayed, T., 2008. A Probabilistic Framework for the Automated Analysis of the Exposure to Road Collision. *Transportation Research Record, No. 2019,* pp. 96-104.

Saunier, N., Sayed, T. & Ismail, K., 2010. Large scale automated analysis of vehicle interactions and collisions. *Transportation Research Record: Journal of the Transportation Research Board,* Volume 2147, pp. 45-50.

Schoon, C. & Van Minnen, J., 1994. The safety of roundabouts in the Netherlands. *Traffic Engineering Control,* Volume 35, pp. 142-148.

Shahdah, U. E., Saccomanno, F. & Persaud, B., 2014. Developing a Crash-Conflict Model for Safety Performance Analysis and Estimation of Crash Modification Factors for Urban Signalized Intersections. *Transportation Research Board Annual Meeting 2014. Paper No. 14-4289.*

Shahdah, U. E., Saccomanno, F. & Persaud, B., 2014. Integrated traffic conflict model for estimating crash modification factors. *Accideny Analysis and Prevention,* 71(10), pp. 228-235.

Sheskin, D. J., 2003. *Handbook of Parametric and Nonparametric Statistical Procedures - 3rd Edition.* London, United Kingdom: Chapman & Hall/CRC.

Spacek, P., 2004. Basis of the Swiss Design Standard for Roundabout. *Transportation Research Record,* Volume 1881, pp. 27-35.

Svensson, A., 1992. *Further Development and Vlaidation of the Swedish Traffic Conflicts Techniques,* Lund, Sweden: Department of Traffic Planning and Engineering, Lund University.

Technical Committee 13 Road Safety, 2004. *Road Safety Manual.* Paris, France: PIARC - World Road Association.

Walden, T. D., 2008. *Analysison the Effectiveness of Photographic Traffic Signal Enforcement System in Texas,* Austin, TX, USA: Traffic Operations Division, Texas Department of Transportation.

Chapter 2

Problem statement and data collection

2.1 Problem statement

The aim of this study is to investigate the feasibility of developing crash rate models based on the calculation of Conflict Opportunities (COs) and expressly devoted to roundabouts and sensible to geometric features.

Investigating the feasibility of developing a model based on the calculation of Conflict Opportunities (COs) in order to estimate crash frequencies of rural roundabouts is the primary aim of this study. In particular, a model sensitive to geometric features of roundabouts is pursued, a goal which offers the opportunity of exploring to what an extent geometric layout influences safety performances.

The conceptual framework of conflict opportunities (COs) is sourced from the definition of traffic conflicts, but instead of recording on the field all of the events where drivers have already initiated a chain of events having the potential of resulting in a crash, now the attention is addressed toward the exposure to hypothetical dangerous situations.

For example, every time a vehicle stops at the entry of a roundabout before entering the ring, the presence of another vehicle coming from behind originates a CO, independently from its approach speed, driver's behaviour and other related factors. There is a probability, no matter how small, that a crash arises; in other words, the two vehicles are exposed to a collision event. There is no regard to the fact that drivers have or not subsequently adopted sudden corrective manoeuvres for avoiding the collision.

A traffic conflict can be recognised on the condition that certain parameters reach a predefined threshold, while a CO is mainly determined by the manifestation of certain traffic interactions. The latter can be reliably estimated by recurring to statistical models suitable for describing evolution of traffic flows. That is the point. While traffic conflict must be identified by means of observations on the field or analyses of video-recordings, CO can be analytically estimated via formulae which can embody design and operational parameters. The analytical framework for correlating real crashes to COs is simply based on the assumption that conflict opportunities represent the layer below the traffic conflicts in the Heinrich's Triangle (Hyden, 1987). Consequently, a linear relationship between the CO frequencies and crash frequencies can be established (Equation 2.1):

$$Expected\ crash\ frequencies = (Conflict\ Opportunities\ frequencies) * (crash - to - conflict\ ratio) \quad (2.1)$$

Conflict Opportunities can be estimated through methodological models differentiated for road entity and crash typology. For instance, analytical formulae for calculating exposure to rear-end collisions at signalised intersections are different from those suitable for roundabouts.

However, these analytical formulations strictly depend on traffic flows, and a direct implementation of geometric factors influencing crash frequencies is not feasible (Lakkundi, 2008; Rencelj, 2009). A possibility lies in including geometric variables within the determination process of crash-to-conflict ratios (Pecchini, et al., 2014).

These coefficients are the ratio between real crashes and COs occurred or estimated in a certain time period. Once the number of CO for each kind of manoeuvre is evaluated, crash rates can be derived by multiplying each value by its relative crash-to-conflict ratio, and then by adding up all the products.

Possible correlations of these coefficients with certain geometric variables could be investigated. If well-defined relations were effectively detected, crash-to-conflict ratios could be determined by simply knowing the values of geometric factors presumed to be significant for crash frequencies,

This path was followed in pursuing the development of a potential crash rate model based on calculation of COs and sensitive to geometrical features of roundabouts. The problem is that design layout for this kind of intersection is quite complex, and numerous are the parameters which potentially influence their safety performances.

The question arises of realising what are the factors actually conditioning crash occurrences with outcomes possibly disaggregated for crash typology. By considering a sample of roundabouts and collecting their geometric features and crash data, a complex arrangement of data may be obtained. Descriptive statistic techniques should be exploited in order to synthesis gathered information before trying to perform inferential analyses.

Crash frequency estimates should be disaggregated by crash types. In fact, they significantly differ from each other in terms of dynamics and related causes; considering them as a whole would not allow properly understanding influences of geometrical features on the various manifestation of safety concerns. As an example, origins of rear-end crashes are completely different from crashes due to failure to yield when entering the ring. Mixing up these two situations would compromise detection of influential design aspects. Therefore, for each crash typology, specific calibration functions associating crash-to-conflict ratios to geometric parameters should be obtained.

Additional peculiarity and advantage ensured by adoption of COs is the possibility of obtaining estimates of crash frequency related to actual traffic conditions at roundabouts. In fact, during the day, traffic flows passing through a given roundabout may experience marked variations with pinnacles reached in

restricted time intervals. These sharp fluctuations have obvious consequences on safety issues (NCHRP, 2010). For example, at roundabouts, free traffic flows conditions are completely different from situations where both entering and conflicting vehicle volumes are high. In the latter case, rear-end collision and failure to yield crashes would be more likely to occur as compared to time periods characterised by low traffic flows, where, instead, single vehicle run off crash rates are expected to show an increase. Annual means of traffic flows cannot take into account this variety of real conditions, which is profoundly correlated to crash patterns of a given road site (Svensson, 1992). As a result, for an investigated roundabout, vehicular traffic flows should be recorded for each hour during the day. In addition, analytical models by means of which calculating COs require to gather the travel demand between the origin and destination legs of analysed roundabouts. That is, for each leg, entering, exiting and circulating flows should be recorded for each hour of the day in order to properly calculate the total amount of COs associated to each crash typology.

Rural roundabouts out of Non-Motorised Users (NMUs) itineraries were considered for essentially two reasons.

Firstly, in urban contexts, road geometry is less important than road environment in influencing drivers' behaviour. In fact, they have to simultaneously perform a great number of tasks when driving in urban streets, and increased rates of workload induce drivers to decrease their speed (Desmond & Hancock, 2001; Desmond & Hancock, 2001). Therefore, dealing with urban setting could produce crash rates more difficult to interpret in terms of geometrical parameters.

Secondly, allowing for urban roundabouts and road vulnerable users, such as pedestrian, bicyclists and motorcyclists, would have implied to examine quite intricate crash patterns affected by numerous variables. Discerning the single effect of them would have been quite arduous. Definitely, dealing with urban setting could produce crash rates more difficult to interpret in terms of geometrical parameters.

After all, this study aims to verify the feasibility of applying a novel method. Before treating complex situations, preliminary results must be obtained for straightforward situations in order to understand whether the taken path is promising or not. Particular attention has been placed on trying to capture influence of geometric design of roundabouts on their safety performances.

In order to obtain the most possible detailed vision on geometric layout of roundabouts and its influences on their safety performances, the statistical unit considered in this study is not the roundabout as a whole but the single leg. Overall, 22 geometric factors were recorded for 151 legs of 43 sample roundabouts.

The problem arises of managing all of this information before making inferences from data and trying to develop analytical models. As the next chapter will show, exploratory data analyses have been exploited in order to identify the factors most likely to influence safety performance of roundabouts for each crash typology. These techniques allow maximizing the insight into a data set and uncovering underlying structures otherwise difficult to capture. They have proved to be very proficient in identifying significant factors from a multitude of data and suggesting what hypotheses should be tested for subsequent inferential analyses.

Preliminary treatments of collected data are not envisaged by current methodologies devoted to road safety. Even the most diffused ones, the empirical Bayes before-after studies, do not perform preliminary analyses on collected data, and stepwise approaches are directly adopted on them. This involves starting with a model deprived of any variable before gradually adding them one at a time, and the model is then selected which best performed in comparison criteria, such as, for instance, the Akaike's information criterion (AIC) and the Bayesian Information Criterion (BIC). However, this approach may lead to misplace the essence of investigated phenomenon by leading to select explanatory variables correlated with other factors excluded from the model (i.e. omitted variables bias). By supposing that the intent is to estimate the safety effects of chevrons on horizontal curves, a stepwise approach could omit the influence of roadside conditions. Consequently, the prediction model may incorrectly conclude that chevrons are associated with an increase in crashes while the main cause for collected crashes could be associated with the poor conditions of roadsides. There are additional reasons explaining why stepwise analysis results may not be reliable: the predictors selected at each step are conditioned on the previously selected covariates; stepwise analysis results are dependent on the sampling error present in any given sample (Hubert, 1989; Thompson, 1995).

All of these considerations enlighten how could be delicate the variable selection phase and explain the importance of adopting proficient exploratory analyses.

Awareness of these concerns lead to adopt other techniques in association with the regression stepwise approach in order to better discriminate real significant predictors and thus simplify subsequent inferential analyses. This will be explained in the following chapters, after the description of data collected here provided.

2.2 Data collected

As a first step, a database was collected of fatal and injury crashes occurred at rural roundabouts sited in the Province of Mantua, Lombardia Region, North Italy. For each counted crash, these data were recorded:

- date and time;
- area of the intersection where they occurred;
- description of the event;
- types of vehicles involved;
- number of injuries and casualties.

The information spans from 2005 to 2010. Police crash reports were used for reconstructing investigated vehicular collisions. Each of them was then assigned to a specific crash typology. In particular, the five most frequent ones were considered (Figure 2.1):

- Collision due to failure to yield starting from a stopped position (1);
- Collision due to a failure to yield without stopping (1);
- Single vehicle run off at the entry, the circulatory roadway, the exit (2, 3, 4);
- Rear end collision at the entry (5);
- Circulating exiting collision; only possible at multilane roadway circulatory roundabouts (6).

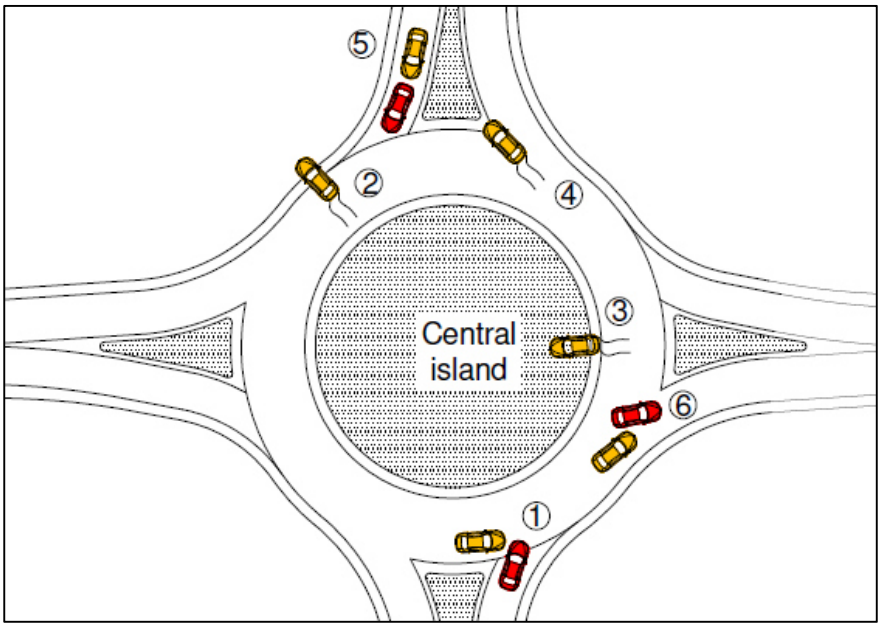

Figure 2.1 Graphical representation of the entry angle as indicated by Swiss norms.

These crash types cover by themselves nearly 80% of the entire number of crashes accordingly to numerous international inquiries (Guichet, 1993; Mauro & Cattani, 2004; NCHRP, 2010). In addition, each crash was conventionally assigned to the leg the involved vehicles or the driver who provoked the crash came from. Circulating exiting crashes were instead related to the leg through which one of the involved vehicles was about to exit the roundabout.

2.2.1 An overview of sampled roundabouts

The acquired sample consists of 43 rural roundabouts. Connected rural roads belong to the primary distribution network. Their section, according to C2 class proposed by Italian road standards (Ministero delle Infrastrutture dei Trasporti,

2001) presents a single carriageway with one traffic lane for each direction; the width of lanes and shoulders is 3.50 and 1.25 m respectively, and the design speed varies between 60 and 100 km/h.

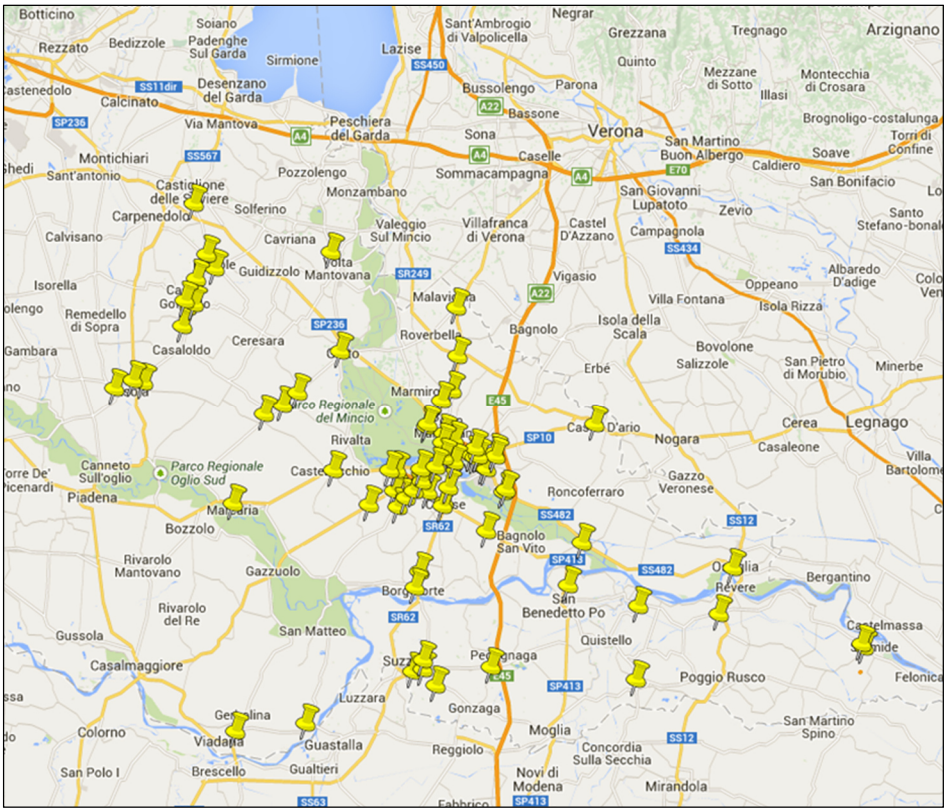

Figure 2.2 Localisation of sampled roundabouts.

The Province of Mantua is an entirely flat territory devoid of mountain or hilly regions; cross slope of roundabout plateaus is everywhere quite restricted, and converging roads have slight longitudinal slopes with no steep gradients. As a result, all of the sample roundabouts present usual vertical profiles for the central island and circulatory roadway with constant cross slope values of around 2%. It is worth noting that that all of the roundabouts built in the Province of Mantua have an inward cross slope, although the Regional guidelines suggest to adopt this configuration only for roundabout with inscribed circle diameters (ICD) greater than 50 metres. Given that all of the analysed roundabouts are characterised by quite similar cross slopes, this geometric aspect could not have been considered in the

subsequent analyses of the relationships between design of roundabouts and their safety issues.

A certain amount of entries have two lane for accommodating approaching traffic flows. In fact, two-lane roundabout at the junction of roads with one lane per direction is a typical Italian geometric configuration for these kinds of intersections: near the roundabout, legs are gradually enlarged for displacing two lanes available for entry vehicles. Homogeneous roundabouts located in the same area were selected for limiting inevitable dispersions caused by phenomena arduous to quantify such as, for example, discrepancy in drivers' behaviour or different environmental and traffic conditions. Roundabouts with unconventional geometry have not been considered.

Here is a list of main geometric features of investigated roundabouts

24 roundabouts with four legs;
18 roundabouts with three legs;
1 roundabouts with five legs;

7 roundabouts with only one circulatory lane;
37 roundabouts with two circulatory lanes;

2 roundabouts with ICD = 35 ÷ 40 m;
3 roundabouts with ICD = 40 ÷ 50 m;
14 roundabouts with ICD = 50 ÷ 60 m;
10 roundabouts with ICD = 60 ÷ 70 m;
5 roundabouts with ICD = 70 ÷ 80 m;
5 roundabouts with ICD = 80 ÷ 85 m;
4 roundabouts with ICD > 100 m.

Table 2.1 Mean and deviation standards for geometric parameters recorded for the 151 sampled roundabout legs.

	Mean	**Deviation Standard**	**N**
Internal Circle Diameter [m]	51.12	22.87	151
Inscribed Circle Diameter ICD [m]	68.03	22.91	151
Entry Kerb Radius [m]	77.76	117.54	151
Exit Kerb Radius [m]	123.31	274.79	151
R0 [m]	67.60	67.6	151
R1 [m]	95.27	77.74	151

R2 [m]	44.32	43.61	151
R3 [m]	92.46	97.49	151
R4 [m]	26.44	13.33	151
R5 [m]	69.19	66.02	151
R1sx [m]	95.81	86.32	151
R2sx [m]	46.92	51.31	151
Deviation Angle [°]	54.89	29.09	151
Entry angle [°]	49.93	12.29	151
Visibility Angle [°]	68.24	20.97	151
Distance entry preceding exit [m]	36.30	19.40	151
Distance entry consecutive exit [m]	37.91	21.50	151

Even from this essential report, inconsistencies between Italian requirements and building practice are evident, given that ICD higher than 50 meters are not allowed (Ministero delle Infrastrutture e dei Trasporti, 2006).

Roundabouts of greater dimensions must be designed by implementing weaving sections designed in order to guarantee adequate level of service (LOS) for the traffic demand. However, sampled roundabouts do not comply with this prescription.

After all, Italian and Regional official design standards for this type of intersections were developed in 2006, and numerous roundabouts had been already built. There is also to consider that Italian legislation proved to be affected by numerous inconsistencies and shortcomings to such an extent that significant improvements and enhancements are strongly encouraged by both academic and professional sphere (Montella, et al., 2012). Italian requirements only prescribe a minimal deviation for vehicles' trajectory, compliance with visibility requirements and widths of circulating, entry and exit lanes. However, International standards and guidelines, as well as scientific researches, offer abundant references about geometric configuration of roundabouts and factors which should be carefully pondered when designing these intersections. From these sources, parameters supposed to be decisive or significant, at least, were selected and measured for each leg. Overall, 22 geometric factors were recorded for 151 legs of 43 sample roundabouts. In the followings, these geometrical aspects are described, with particular mention to their influence on safety performances.

2.2.2 Geometrical parameters

2.2.2.1 Inscribed Circle Diameter

The inscribed circle diameter is the basic parameter used to define the size of a roundabout. It is measured between the outer edges of the circulatory roadway and is equal to the sum of the central island diameter and twice the circulatory roadway width. It represents the overall size of a roundabout and should be the outcome of various design choices, including accommodation of the design vehicle (i.e. the vehicle with the most obtrusive swept path), speed control and compliance with visibility requirements. However, the number of lanes that a roundabout needs to serve has the largest influence on the ICD (NCHRP, 2010). Two-lane roundabouts generally have larger ICDs than single-lane roundabouts to accommodate a greater number of lanes. There is also to consider that roundabouts with more than four legs are typically larger than roundabouts with four legs, given the same number of lanes. This is necessary to facilitate turning movements between consecutive legs.

ICD is also related to the alignment of individual approaches, that is the angles between consecutive approaches. Angles less than 90 degrees usually require a larger ICD to facilitate turning movements between those legs.

From these considerations, it is clear that an iterative process is strictly required to determine the optimal ICD size.

In fact, increasing ICD enable better geometry to be designed, such as a greater separation between adjacent entries and exit lanes, with evident safety benefits, and the provision of better approach geometry, which leads to a reduction in vehicle approach speeds, a decisive aspect when roundabout connects roads characterised by high desired speeds.

However, excessive ICD should be avoided because usually associated with high circulating speeds (Kennedy, 2007). Their beneficial reduction could be compromised, and safety concerns would be consequential. This is confirmed by numerous International inquiries where crash frequencies were observed to increase with the inscribed circle diameter, so much so that National standards usually dictate maximum acceptable values for ICD. In this regard, it is worth noting that even certain crash prediction models clearly identify ICD as a covariate whose increases are associated with higher crash frequencies, in particular for circulating entry collisions and exiting-circulating ones at multilane roundabouts.

2.2.2.2 Measurements of deviation imposed to vehicle trajectories

Adequate deviation of vehicle trajectories avoids dangerous driver' behaviours because it forces them to reduce their speed. In case that entering vehicles are not deviated sufficiently from the straight direction of travel by the central island, this will lead to failures to give way, increased pass through speeds and underestimations of these speeds by conflicting parties. Indeed, experimental studies showed a clear correlation between smaller deviation angles and higher crash rates.

Traditionally, the deviation is defined as the radius of the circle that goes to 1.50 m from the edge of the central island and 2 m from the entering and exiting

border lanes (NCHRP, 2010; SETRA, 1998; Highway Agency, 2007). The radius should be less than 100 m, with optimum values around 30 m. The circular arc of interest is those described by the so-called fastest path, that is the smoothest, flattest path possible for a single vehicle, in the absence of other traffic and ignoring all lane markings. Generally, the fastest path is the trajectory traced by two opposing arms; in particular circumstances, the fastest path is the right turn manoeuvre.

An alternative measure of the deviation imposed by the layout of roundabouts to vehicle trajectories is the so-called deviation angle (VSS-Norm, 2000; Ministero delle Infrastrutture e dei Trasporti, 2006).

It can be obtained by a graph construction. For drawing the tangent of the central island corresponding to a deflection angle equal to β, entry radius has to be increased by 3.5 m. The graph procedure, shown in Figure 2.3, is the same for single-lane roundabout and multilane roundabouts.

Deviation angle was firstly introduced by Swiss norms and subsequently selected by Italian standards as the prominent geometric factor to which all of the other measures are subordinated. It is, in fact, strictly required a deviation angle greater than 45 degrees for all the legs of roundabouts, no matter the values reached by other geometric variables, with the solely exception for entry, circulating carriageway and exit widths, which are fixed.

Swiss standards are more detailed, and angles of deviation greater than 40° (i.e. 45^{cc}) are imposed only for roundabouts with ICD greater than 32 m, unlike the Italian rules, which dictates great deviation angles for mini-roundabouts too, where this condition is practically unattainable. Sampled roundabouts are at least conventional ones with minimum ICD equal to 35 m, so respecting the aforementioned condition was potentially feasible at the design phase. However, a relevant part of them was built before the current Italian standards and do not have adequate deviation angle.

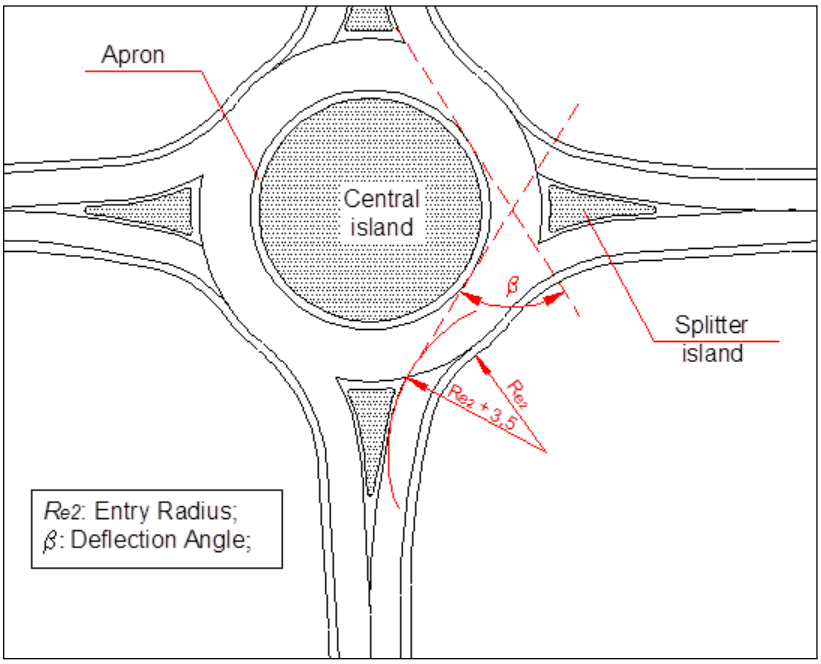

Figure 2.3 Graphical representation of the deviation angle as indicated by Swiss norms.

2.2.2.3 Critical path radii

Australian standards and American guidelines extend a perspective mainly focused on the deviation imposed by central island for capturing a complete framework of the speeds attained by drivers when manoeuvring through the roundabout (NCHRP, 2010; Austroads, 2011; Department of Transport and Main Roads, 2014). The underlying concept is that roundabouts operate safely and effectively when their geometry forces traffic to enter, circulate, and exit at slow speeds. Therefore, the emphasis is now placed on the aim of maintaining low and consistent speeds through the entire intersection. For achieving this aim, American guidelines propose a graphical and analytical procedure for identifying the manoeuvres where the highest vehicular speed could be attained, that is the so-called fastest paths. They are the smoothest, flattest paths possible for a single vehicle traversing through the entry, around the central island, and out the exit, in the absence of other traffic and without consideration for lane markings. The fastest paths must be drawn for each approach and possible manoeuvre, including left-turn movement and right-turn one. By following a graphical procedure explained in the guidelines, the vehicle centreline is depicted in its path through the roundabout by assuming a vehicle 2 m wide, which manoeuvres through the

roundabout maintaining 1.5 m from a concrete curb, 1.5 m from a roadway centreline, and 1.0 m from a painted edge line.

After identification of the fastest paths, the minimum radii can be measured. According to the US guidelines, there five critical path radii to be determined (Figure 2.4):

- R1: the entry path radius, is the minimum radius on the fastest through path prior to the entrance line;
- R2: the circulating path radius, is the minimum radius on the fastest through path around the central island;
- R3: the exit path radius, is the minimum radius on the fastest through path into the exit;
- R4: the left-turn path radius, is the minimum radius on the path of the conflicting left-turn movement;
- R5: the right-turn path radius, is the minimum radius on the fastest path of a right-turning vehicle.

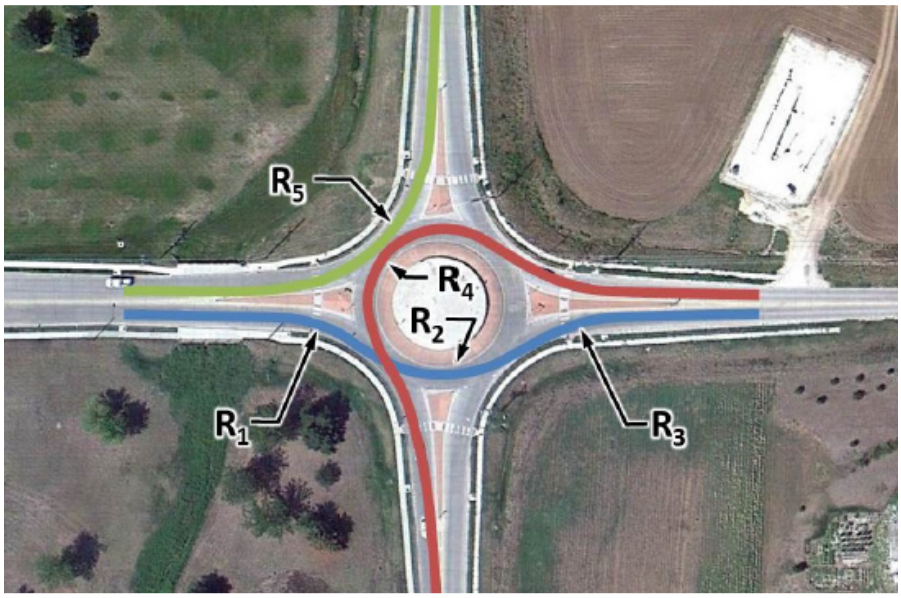

Figure 2.4 Graphical representation of fastest path radii. Source: (Kittelson & Associates, Inc., 2014)

From these radii, critical design speeds may be obtained via Equation 2.2, which represents the equilibrium of transversal forces acting on a vehicle moving along a superelevated curve, at the threshold of lateral slip:

$$\frac{V^2}{R} = 127(f_t + q) \qquad (2.2)$$

where:

- V = equilibrium speed [km/h];
- R = radius of curve [m];
- q = superelevation cross slope [m/m];
- f_t: coefficient of friction developed between the vehicle tyres and the road.

The coefficient of friction in turn is dependent on speed, so Equation 2.2 must be iteratively solved. Coefficients of friction proposed for various speeds by Italian technical norms were applied for eventually determining the design speeds associated with the five critical radii. A super elevation cross slope was fixed at 2%.

It must be enlightened that the fastest path methodology does not represent expected vehicle speeds, but rather theoretical attainable speeds for design purposes. As a matter of fact, actual speeds can vary substantially based on vehicles suspension, individual driving abilities, and tolerance for gravitational forces. In addition, R1 and R5 must not be confused with entry and exit kerb radius.

Figure 2.5 shows an application of the fastest method in acquiring the profile of design speed reached by vehicles for each step of their manoeuvres.

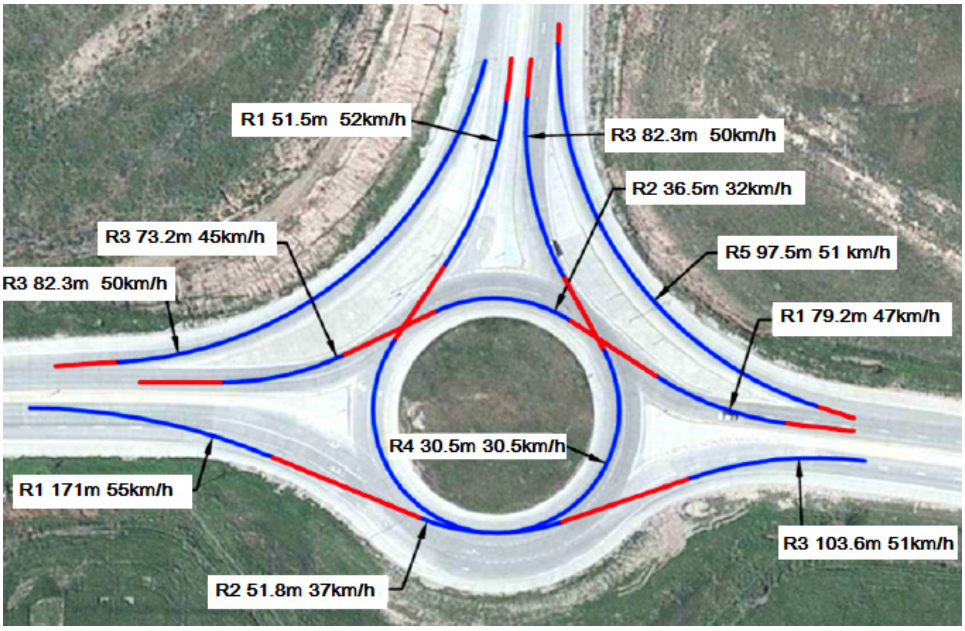

Figure 2.5 Fastest path example and identification of the five critical turning radii from which obtaining the design speed profile for the various manoeuvres

This method implies the control of the entire trajectory of each movements in order to detect possible critical locations with excessive theoretical speeds. Consistency between the speeds of various movements within the intersection can be checked, as well as the relative speeds between conflicting traffic streams. Both of them should be minimised such that the maximum speed differential between movements should be no more than approximately 15 to 25 km/h.

2.2.2.4 Entry path radius

Particular attention is devoted to the entry path radius R1, effectively recognised as a decisive factor for crashes by numerous scientific inquiries (Montella, et al., 2012) and norms of different Countries (Highway Agency, 2007; NCHRP, 2010; Austroads, 2011). The entry path radius is a measure of the deflection imposed on vehicles entering a roundabout; it can encourage drivers to slow down before entering the roundabout. Indeed, high entry radius may originate angle and rear-end crashes at the entry, and particular consideration should be given to the entry radius of the left approach, which is identified as the responsible for the arise of angle crash frequencies. Therefore, a maximum value of 100 m is provided by requirements of different States. However, at the same time, overly low values are not recommended because of the increased risk of single vehicle crashes. At multilane roundabouts, there could be additional concerns related to the path overlap when the geometry leads a vehicle in the left approach lane to naturally sweep across the right approach lane just before the approach line to avoid the central island.

The construction of the fastest path should begin at least 50 m prior to the entrance line using the appropriate offsets already introduced: 1.5 m from a concrete curb, 1.5 m from a roadway centreline, and 1.0 m from a painted edge line. The R1 radius should be measured as the smallest best-fit circular curve over a distance of at least 20 to 25 m near the yield line. Subsequently, Equation 2.2 can be used for calculating the associated design speed.

The radii of exit curves are commonly larger than those used at the entry. Large exit curve radii improve vehicle path alignment, avoid sideswipe collisions and increase exit capacity of roundabouts with drivers facilitated when exiting the roundabout. Loss of control crashes would be also prevented.

Therefore, R3 should not be less than R1 or R2.

The radius of the conflicting left-turn movement, R4, must be evaluated in order to ensure that the maximum speed differential between entering and circulating traffic is not excessive, given that the left-turn movement has the lowest circulating speed. Large differentials between entry and circulating speeds may result in an increase in single vehicle crashes due to loss of control and in failure to give the right of way to circulating traffic.

2.2.2.5 Entry kerb radius

The entry curb radius is defined as the minimum radius of curvature of the nearside kerb line in the region of the entry. It affects both capacity and safety of roundabouts (Kennedy, 2007). Excessively large entry curb radii have a higher potential to produce faster entry speeds than desired, but too sharped entry curb radii should be avoided since these may lead to single vehicle crashes, as well as provoke path overlap between traffic streams at multi-lane entries. Accommodation issues of heavy vehicles should be always carefully addressed. Various European countries require small entry radii of 10-15 m whereas UK and USA are more flexible and give chance of greater radii. Italian standard does not give any advice (Montella, et al., 2012).

2.2.2.6 Exit kerb radius

The exit kerb radius must be determined where the perpendicular from the corner of the deflection island intersect the kerb itself.

In general, standards and guidelines require using relatively large radius for making it quicker exit from the ring and improving capacity performances of roundabouts (Kennedy, 2007; NCHRP, 2010). The rationale is that a vehicle moving along the ring and being about to exit the intersection has already been slowed down by entry and circulating deviation, so that there is no reason for additional geometry aimed to reduce speed. In addition, large exit kerb radii are also typically used to promote good vehicle path alignment preventing possible sideswipe collisions when exit manoeuvres are performed.

Adequately large exit kerb radii represent a positive design practice for rural environments, while in urban areas tighter kerb radii are necessary for the safety of pedestrians using the nearby street-crossings; exiting vehicles must be forced to reduce their speeds for the presence of vulnerable road users.

Various European standards and guidelines recommend exit radii ranging from 15 to 20m for urban roundabouts and values spanning from 15 to 30m for rural areas, with the preference of higher values for larger roundabouts.

2.2.2.7 Angle of visibility

This parameter is proposed by American guidelines and refers to the angle between a vehicle's alignment at the entrance line and the sight line required according to intersection sight-distance standards (NCHRP, 2010). It can be basically intended as the supplementary angle of the angle drivers have to cover with their eyes by turning their heads in order to perceive oncoming traffic from the immediate upstream entry (Figure 2.6). Angle of visibility is a function of intersection sight distance (ISD), that is the distance required for a driver without

the right-of-way to perceive and react to the presence of conflicting vehicles, and achieved via the establishment of sight triangles. In this study, ISD was calculated in accordance to the same American guidelines in order to achieve coherent measures not subjected to biases due to adoption of different methodologies for calculating parameters mutually influencing each other. Equation 2.2 defines ISD value (NCHRP, 2010).

$$ISD = (0.2780) * (V_{entering})(t_c) \quad (2.2)$$

where:

- *ISD*: intersection sight distance, that is the length of entering leg of sight triangle [m];
- $V_{entering}$: design speed of conflicting movement approximated by taking the average of theoretical entering speed (entry path radius R_1) and the circulating (circulating path radius R_2) speed [km/h];
- t_c: critical headway for entering the major road, equal to 5.0s.

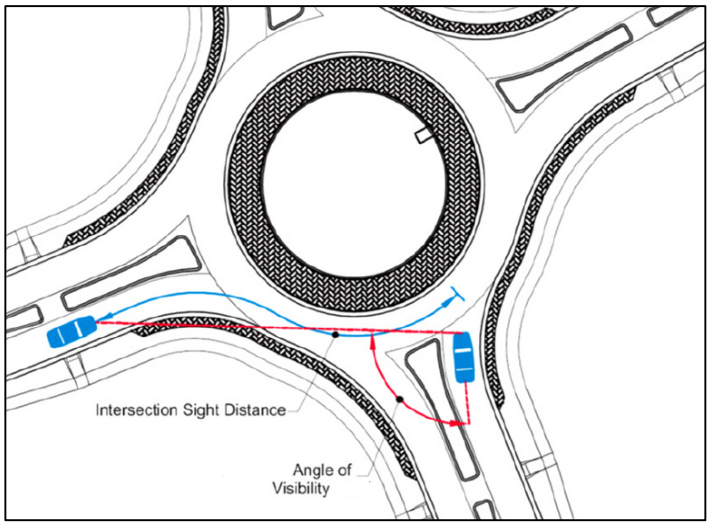

Figure 2.6 Example Design with severe angle of visibility to Left and possible solution with entry realignment. Source: (Kittelson & Associates, Inc., 2014)

Angle of visibility should not be excessively acute in order to allow drivers to comfortably turn their heads to the left, with particular mention for old motorists. A minimum value of 75° is then suggested. Too acute entry angles may be corrected by realigning the entries, but this may arise other challenges, such as the closer proximity of the entry with the successive one encountered along the clockwise

direction. As for other situations, a balance between contrasting requirements must be reached.

2.2.2.8 Approach curvature

It is the horizontal curvature preceding the entry of the roundabout (Figure 2.7). The higher the design speed before the entry, the higher the risk drivers pass the yield line at an excessive speed causing a potential threat for his safety and the other ones. This concern is particularly relevant for rural high speed environments, where long straight roads converge directly to the roundabouts without any horizontal element which can induce drivers to start to moderate their speed given the proximity of the intersection. In this regard, Australian scientific studies and guidelines strongly recommend adequate approach geometry with successive reverse curves to limit the decrease in speed between successive horizontal elements.

After all, preparing drivers to reduce their speed before reaching the entry is a necessary condition for achieving appropriate vehicular speeds for entering and traveling through the roundabout. Speed management is one of the most critical design objectives as it has profound impacts on safety of all users. The importance of approaching speed is also confirmed by its strong correlation with stopping sight distance, that is the distance travelled by a driver for decelerating and safely stopping the vehicle after having perceived the presence of an unexpected obstacle on the roadway ahead.

A driver who is approaching to the roundabout should have a clear line of sight to the nose of splitter island and entry yield line, and in this perspective.

The distance is dependent on the considered design speeds and assumptions for driver reaction time, as well as the braking ability of most vehicles under wet pavement conditions and the friction provided by most pavement surfaces (Montella, et al., 2012).

American guidelines recommend this formula (Equation 2.3) for calculating stopping sight distance (NCHRP, 2010).

$$d = (0.2780) * (V_{initial})(t_c) + 0.039 \frac{V_{initial}^2}{a} \quad (2.3)$$

where:

- d: stopping sight distance [m];
- t: perception-brake reaction time, assumed to be 2.5s;
- V: design speed at the approach phase [km/h];
- a: driver acceleration, assumed to be 3.41 m/s^2.

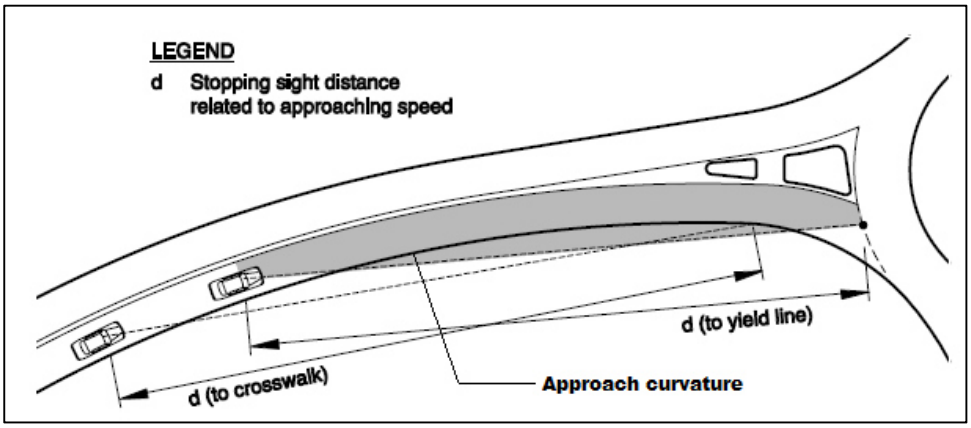

Figure 2.7 Graphical representation of the approach curvature for roundabouts and stooping sight distance on the approach itself. Source: (NCHRP, 2010)

The influence of speed in Equation 2.3 is clear, and higher approaching speeds imply longer driver reactions and greater physical stopping distances. In addition, excessive sight distance can lead to higher vehicle speeds, which creates safety and operational concerns.

In light of its influences on vehicle speed through the roundabout and safety aspect pertaining to stopping sight distance, approaching speed was selected as a candidate variable of potential crash rate model developed in this study.

2.2.2.9 Entry angle

The entry angle is the conflict angle between the entering and the circulating traffic (Figure 2.8). Low entry angles are generally associated with low angles of visibility, a situation where drivers have to uncomfortably strain to look over their shoulders for perceiving oncoming traffic flows. In addition to making the visibility to the left particularly troublesome, low entry angles may encourage merging behaviour with possible sideswipe collision between entering and circulating traffic streams.

Meanwhile, too high entry angles may produce excessive entry deflection, which may weaken traffic flow through the entry and overall operation performances of the roundabout, as well as lead to sharp braking at entries accompanied by rear-end crashes. However, there is not a general agreement about optimal values for this angle: Swiss standard requires entry angles between 70 and 90 degrees, thus producing perpendicular entries, whilst the UK standard requires angles between 20 and 60 degrees. Even the geometric definition of this angle proposed by the two national directives is slightly different. In this study the Swiss way of determining entry angle was adopted. Recommendation for entry angles great enough conditions the design of splitter island, which should be funnel

shaped for achieving flat enough entry angles or angles. Otherwise, drivers would have limited visual guidance and would be led to entering with inappropriate entry speeds. Possible consequence would be the failure to give way, head-on collisions or single-vehicle crashes.

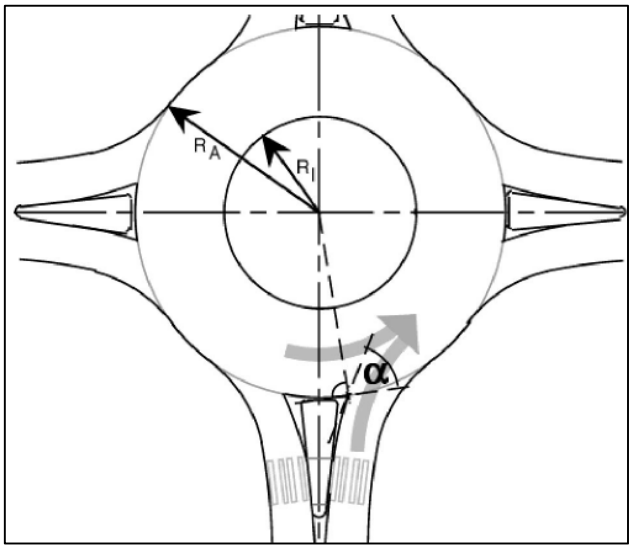

Figure 2.8 Graphical representation of the entry angle as indicated by Swiss norms. Source: (Spacek, 2004)

2.2.2.10 Angle between approach legs

Approaches should intersect at perpendicular angles. Higher values may provoke excessive speed for right-turn movements, while adoption of sharp angles could hamper manoeuvres performed by heavy vehicles. A possible solution for the latter concern could be the provision of a large corner radius in order to accommodate heavy vehicles, but there could be an unsafe rise in speed attained by other vehicles being about to enter the ring. Designing the approaches at perpendicular or near-perpendicular angles generally results in relatively slow and consistent speeds for all movements (Figure 2.9). In addition, an orthogonal configuration decreases driving workload by simplifying the task of selecting the correct lane for manoeuvring through the intersection, with particular regard for entries with multi-lane entry roundabouts.

However, acceptable designs can be achieved even with skewed angles between approaches with corresponding adjustments applied to other design components. Increasing the ICD may mitigate these criticalities, but this would mean greater costs and spatial requirements.

Alternative solutions could be the reduction of entry width and entry radii, as well as offsetting the approach centreline to the left of the centre of the roundabout For roundabouts in low-speed urban environments, the alignment of the approaches may be less critical (NCHRP, 2010; Department of Transport and Main Roads, 2014).

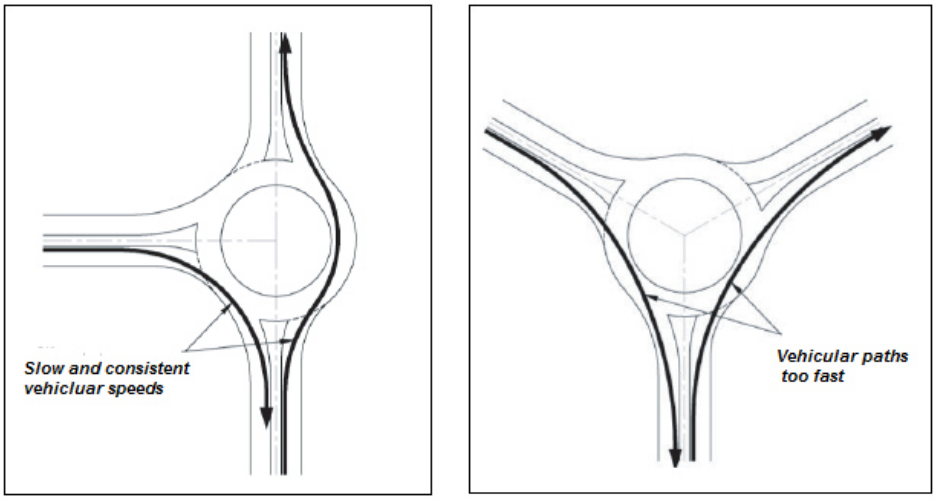

Figure 2.9 Perpendicular approach angles will generally provide slow and consistent speeds, while skewed angles may induce higher vehicle speeds. Source (NCHRP, 2010)

2.2.2.11 Spacing of entries and exits of consecutive legs

The spacing of entries and exits is particularly important at roundabouts with more than four legs, roundabouts with skewed legs, and multilane roundabouts. Excessive separation between the entry and exit of adjacent legs increase the probability of merging conflicts involving the entry and circulating vehicular paths, as well as the exit ones. An example of this collision pattern is provided by Figure 2.2, where an entering vehicle in the outside lane may be tempted to enter next to a circulating vehicle in the inside lane with the risk of commencing a circulating-exiting conflict.

A solution option would be realigning the approaches in order to reduce the separation between legs. By referring to Figure 2.10, realigning the eastbound approach by creating a more perpendicular intersection angle results in entry circulating paths that cross, rather than merge.

However, entries and exits should not be overly closely spaced. In fact, a similar geometric layout would require corner kerb radii smaller than the approach and departure curves, as well as higher angles between the entering and circulating vehicle paths. A consequence would be the increase in relative speeds of entering and circulating vehicles.

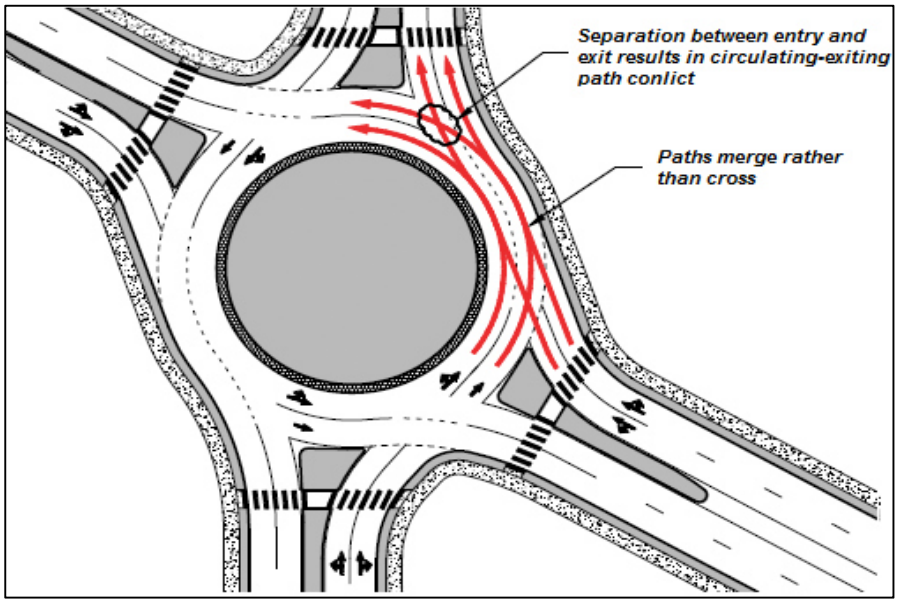

Figure 2.10 Graphical representation of safety concerns originated by excessively distanced entries and exits of consecutive approaches. The separation between legs causes the entry and circulatory paths to merge, creating conflicts at the downstream exit. Source: (NCHRP, 2010)

2.2.2.12 Circulating roadway

The required width of the circulatory roadway is fundamentally determined from the number of entering lanes and the radius of swept path described by the design vehicle when performing turn manoeuvres. However, at the same time, circulatory roadway of single lane roundabouts should not be too wide because drivers may suppose that two vehicles are allowed to circulate side-by-side. In addition, wider lanes and larger radii for lorries results in faster speeds for other vehicles. Truck aprons elevated above the surface of the circulatory roadway may be a solution because they are unattractive for light vehicles, while providing a mountable surface for articulated lorries to traverse. However, this arrangement is

not consistent with current Italian standards which limit the use of truck apron only for mini-roundabouts with 18 < ICD < 25 m.

At multi-lane roundabouts, there is the possibility of designing the width of circulatory roadway on the basis of the number of lanes and the design vehicle turning requirements of each approach, so that circulatory roadway does not have to be constant. Nevertheless, this solution is rarely exploited in Italy, and the sampled roundabouts of this study are basically characterised by a circular and regular shape, with constant widths for circulatory roadways and lanes. In this regard, it is worth recalling that Italian requirements for roundabouts strictly impose a single circulatory lane. However, intersections built before the enactment of National standards are not consistent with them, and the majority of samples roundabouts present two circulating lanes.

There is a debate about the safety appropriateness of providing more than one circulatory lane at the ring. This solution responds to the need of increasing capacity of roundabouts, but serious safety concerns arise.

Traffic streams must be properly channelized through pavement markings, splitter islands and the central island in order not to encourage drifts into adjacent lanes, in particular when exiting the ring starting from the inner lane.

Light vehicles and lorries advancing side-by-side along the ring is a critical situation too, where heavy vehicle drivers could not detect the presence of cars moving alongside them.

In addition, from an operational perspective, all of these situations confuse drivers, who could react by slowing down with deterioration of capacity performances. More research is then needed for addressing safety criticalities posed by circulatory roadway with more than one lanes, but it is clear that they have worse safety outcomes, and this is the reason why they are explicitly forbidden or strongly discouraged by numerous National guidelines. However, it can be stated that the number of circulating lanes should be limited to the minimum number that achieve desired capacity and operational requirements for projected future traffic volumes. This consideration should be extended to entry and exit lanes too.

2.2.2.13 Entry and exit widths

Entry and exit widths condition vehicle swept paths through the roundabouts and their speed profiles (Kennedy, 2007; NCHRP, 2010). In fact, small widths are usually associated to restricted curvature radii with consequent low speeds, and this may be beneficial from safety point of view, but criticalities could arise for turning requirements imposed by heavy vehicles.

As far as entry width is concerned, it is well recognised that wide entries must be avoided in order not to compromise the vehicle speed reduction through the roundabout. For single-lane entrances, typical entry widths range from 4.0 to 5.5 m (Ministero delle Infrastrutture e dei Trasporti, 2006). Italian standards require entry widths smaller than the lane width of rural collectors, which have one lane

per direction. A lane narrowing in the entry from 3.75 to 3.5 m is then necessary, with capacity reductions and safety concerns, but this is not a frequent situation for the analysed sample of roundabouts. Here, in fact, a recurrent approach configuration consists in gradually enlarging the entry lane of legs (i.e. flared approaches); in this way, two lanes are provided for accommodation of traffic flows being about to entry the roundabout. In addition, as already said, a substantial amount of sampled intersections was already built before the enactment of Italian standards pertaining roundabouts. For these two reasons, the lane narrowing imposed by norms is absent from the sample of this study.

Conventional wisdom in roundabout design is that wider entries increase capacity while they have detrimental effects on safety performances. Entry width was found to have direct relationship with frequencies of certain types of crashes (NCHRP, 2007).

However, deeper analyses unveiled that the simple distance measured along the entrance line from the left edge of travelled way to its right edge has not a significant correlation with crash frequencies. Conversely, entry width in the aggregate sense, that is the number of entry lanes, was recognised to be a decisive factor (NCHRP, 2010).

On the exit side, width values should be similar to, or slightly less than, entry widths. In this regard, American guidelines and British standards state the principle of easy exits, i.e. the need to provide a clear exit route with sufficient width to increase capacity and ease the flow of traffic departing from the circulatory roadway. Accordingly to this design philosophy, vehicles will not be able to accelerate significantly on easy exits if entry and circulatory speeds are sufficiently low, thus not compromising safety issues and improving operational performances.

Entry and exit widths shares various design principles (Kennedy, 2007). Exits must be checked for swept paths described by heavy vehicles to ensure they can be properly accommodated. In addition, from a safety perspective, the key factor is the number of lanes, not the bare measure of width. Indeed, multiple traffic streams entering, circulating and exiting the roundabout side-by-side may pose dangerous situations with drivers competing for the same space and natural path overlaps of different traffic flows. These concerns are even more relevant for exits because of the presence of circulating flows, which increases the number of conflict points and the likelihood of actual collisions: due to interactions of circulating flows with fast vehicles leaving the circle from the inner lane, two-lane exits often provoke serious crashes. This is the reason why exits arranged with multiple lanes are banned or not recommended, at least, in various Countries, such as Germany, Netherland, Italy and France for urban roundabouts. However, Italian standards allow two-lane entries with no suggestions of respecting the principle of lane continuity, and numerous recent roundabouts can be found affected by this inconsistency, which can confuse drivers expecting two circulatory and exit lanes (Alsop, 1998). Analysis of traffic conditions at congested roundabouts. In: Mathematics in Transport Planning and control. The potential crash rate model here proposed is consistent with all of these considerations about the critical aspects posed by lane arrangement of entries and exits, so much so that their

number of lanes is the only geometric aspect directly implemented in COs calculation. In fact, as the next chapters will show, two different analytical procedures are adopted depending on the presence of entries and exits arranged with one or multiple lanes.

Exit and entry widths, as well as the length of flared approaches, were not considered as possible candidate variables of the model, given that various researches have questioned about their real influence on safety performances of roundabouts.

To sum up, for each leg, the following 22 geometric aspect were recorded:

- Inscribed circle diameter of the roundabout to which the analysed leg belongs [m];
- Number of legs of the roundabout to which the analysed leg belongs;
- Number of lanes for the entry and the exit of the analysed leg;
- Number of circulating lanes of the roundabout to which the analysed leg belongs;
- Approach radius R_0 [m];
- Entry path radius R_1 [m]; circulating path radius R_2 [m]; exit path radius R_3 [m]; left-turn path radius R_4 [m]; right-turn path radius R_5 [m];
- Entry path radius $R1_{sx}$ [m]; circulating path radius $R2_{sx}$ of the left approach [m];
- Entry angle α [°];
- Deviation angle β [°];
- Angle between consecutive legs θ [°];
- Distance between entry of the analysed leg and the exit of the consecutive leg on the right [m]; distance between the entry of the analysed leg and the entry of the preceding leg on the left [m];
- Entry and exit width [m];
- Width of the circulating roadway [m];
- Entry and exit kerb radii [m];

As will be shown in the next chapters, exploratory analyses have been applied in order to seek for the most influencing parameters as regards frequencies of different typologies of vehicular crash.

However, this modus operandi should not convey the message that the successful design of roundabouts can be achieved by simply assembling the listed geometric components configured in such a way to comply with dimensions and values indicated by standards and guidelines (Kennedy, 2007). As a matter of fact, roundabout design is performance-based; that is, success is measured from its outputs, such as, for example, operational and safety performance and accommodation of heavy vehicles, rather than the individual design dimensions (Montella, et al., 2012). In addition, the fitting of the intersection with the

surrounding transportation system is another fundamental aspect to consider for achieving a successful design.

Therefore, possible identification of parameters which mostly influence safety performances of roundabouts may be only a preliminary step for improving the knowledge about the influence of geometric layout on the dynamic of crashes.

From the standpoint of the crash prediction model developed in this study, even if exploratory analyses clearly identified a set of influential geometric variables usable as input parameters, this would not guarantee the successful of the model in providing reliable estimates of crash frequencies. There are numerous other factors which can influence crash safety outcomes and their relation with geometry, including aspects difficult to embody in analytical formulation such as drivers' behaviour and their changes in conjunction with variation of traffic flows passing through the roundabout.

However, these kind of analyses could provide a guide for detecting the direction towards concentrating additional analyses, as well as getting an insight about major concerns which should be addressed for improving safety. For example, if approach radius R_0 was found to be significantly correlated with frequency of rear-end crashes, speeds attained before the entry could be presumed to be a factor deserving particular attention. Obviously, there could be other numerous concurrent causes, and R_0 could not explain on its own the entire occurrence of this kind of crash. Anyway, analysts may realise where focusing additional examinations for preventing rear-end crashes.

References

Alsop, R. E., 1998. *Analysis of traffic conditions at congested roundabouts.* Cardiff, United Kingdom, Oxford Pergamon.

Austroads, 2011. *Guide to Road Design, Part 4B Roundabouts. Report AGRD08/11,* Sydney, NSW, Australia-

Department of Transport and Main Roads, 2014. *Road Planning and design manual - 2nd edition,* s.l.: Quuensalnd Government.

Desmond, P. A. & Hancock, P. A., 2001. *Active and passive fatigue states..* Mahwah, NJ, USA, Lawrence Erlbaum Associates, Inc., pp. 455-465.

Guichet, B., 1993. *Typologie des accidents dans les giratoires urbains.* Bagneux, France, Service d'Etudes Techniques des Routes et Autorutes (SETRA), Centre d'Etudes des Transport Urbains, pp. 145-151.

Highway Agency, 2007. *Geometric Design of Roundabouts. Design Manual of Roads and Bridges - TD 16/07,* London, United Kingdom.

Hubert, C. J., 1989. Problems with stepwise methods: Better alternatives. *Advances in social science methodology,* Volume 1, pp. 43-70.

Hyden, C., 1987. *The Development of a Method for Traffic Safety Evaluation: The Swedish Traffic Conflicts Technqiue. Bulletin 70,* Lund, Sweden: Dept. of Traffic Planning and Engineering, Lund University.

Kennedy, J., 2007. *International Comparison of Roundabout Design Guidelines - Report PPR206,* Workingham, United Kingdom: Transport Research Laboratory.

Kittelson & Associates, Inc., 2014. *Kansas Roundabout Guide - 2nd Edition,* Topeka, KS, USA: Kansas Department of Tranpsortation .

Lakkundi, V. R., 2008. *Development of left-turn guidelines for signalised andunsignalised intersections. Report No. FHWA NJ 2008 011,* Washington, DC, USA: Federal Highway Administration.

Mauro, R. & Cattani, M., 2004. Model to evaluate potential accident rate at roundabouts. *ASCE Journal of Tranportation Engineering,* 130(5), pp. 602-609.

Ministero delle Infrastrutture dei Trasporti, 2001. *Geometrical and functional standards for the design of road intersections,* Rome, Italy.

Ministero delle Infrastrutture e dei Trasporti, 2006. *Geometrical and functional standards for road design. Official Italian Enhancement Act D.M. 19/04/2006.* Rome, Italy.

Montella, A., Turner, S., Chiaradonna, S. & Aldridge, D., 2012. Proposals for Improvement of the Italian Roundabout Geometric Design Standard. *Procedia - Social and Behavioral Sciences,* Volume 53, pp. 189-202.

NCHRP, 2007. *Report 572: Roundabouts in the United States,* Washnigton D.C.: National Cooperative Highway Research Program (NCHRP), Transportation Research Board (TRB) of National Academies.

NCHRP, 2010. *Roundabouts: An Informational Guide - Second Edition,* Washington D.C.

Pecchini, D., Mauro, R. & Giuliani, F., 2014. Model of Potential Crash Rates of Rural Roundabouts with Geometrical Features. *ASCE Journal of Tranposrtation Engineering,* 140(11), p. 04014055.

Rencelj, M., 2009. *The methodology for predicting the expected level of traffic safety in the different types of level intersections. Doctoral Dissertation,* Trieste, Italy: Università degli Studi di Trieste.

SETRA, 1998. *Aménagement des carrefours interurbains sur les routes principales. Carrefours plans - Guide technique,* Paris, France.

Spacek, P., 2004. Basis of the Swiss Design Standard for Roundabout. *Transportation Research Record,* Volume 1881, pp. 27-35.

Svensson, A., 1992. *Further Development and Vlaidation of the Swedish Traffic Conflicts Techniques,* Lund, Sweden: Department of Traffic Planning and Engineering, Lund University.

Thompson, B., 1995. Stepwise regression and stepwise discriminant analysis need not apply here: A guidelines editorial. *Educational and Psychological Measurement,* 55(4), pp. 525-534.

VSS-Norm, 2000. *Knoten, Knoten mit Kreisverkehr. SN 640 263,* Zurich, Switzerland: Swiss Association of Road and Transportation Experts (VSS-Norm).

Chapter 3

Calculation of Conflict Opportunities

3.1 Preliminary concepts

The crash rate code calculation based on the CO concepts denotes a common structure: for each crash typology, crash rates are estimated by multiplying the associated CO number for specific coefficients. Main assumption of Conflict Opportunities techniques is that (Ha & Berg, 1995):

$$Expected\ crash\ rates = (Number\ of\ Conflicts\ Opportunities) \times (crash\ to\ conflict\ ratio)$$

Once the number of COs for each kind of manoeuvre is evaluated, crash rates can be derived by multiplying each value by its relative coefficient ci, and then by adding up all the products. These coefficients are the ratio between crashes and CO number occurred or estimated in a certain time period. There are two options available for ci calibrations.

They can be calculated for all the manoeuvres recognised as potentially dangerous by simply dividing the total amount of crashes by CO number (Mauro & Cattani, 2004; Ming, 2008; Mauro & Cattani, 2010; Pecchini, et al., 2014). All the other factors involved in collision events would be implicitly considered in the determination of model coefficients. This is the case of CO application to signalised intersection. However, operating in this way for roundabouts too, would lead to potential crash prediction models not sensitive to geometric parameters. They could be used for ascertaining safety on existing roundabouts only. Another option consists in searching for hypothetical correlations between the same coefficients and other factors supposed to be decisive for road safety, but not involved in CO calculations (Kaub & Kaub, 2005; Kennedy & Taylor, 2005). In this way, crash to conflict ratios would be determined by geometric parameters, which, in turn, would belong to input data of the potential crash model.

3.1.1 Modelling traffic flow distribution

COs calculation is based on certain assumptions about traffic flow distribution. In particular, gap distribution, that is the interval time elapsing from the passage of consecutive vehicles, must be modelled.

For this purpose, the Erlang's distribution was adopted, with integer values of the parameter K related to the traffic volume (Mauro & Cattani, 2004; Mauro, 2015). Its probability density function is provided by Equation 3.1:

$$f(\tau) = \frac{KQ_e^{-KQ_\tau}(KQ_\tau)^{K-1}}{(K-1)} \tag{3.1}$$

To evaluate the probability that a vehicular gap is greater than or equal to a fixed time interval t, or included between two edge values t_{inf} and t_{sup}, the cumulative distribution function Fτ(t) must be used.

$$F(t) = P(\tau \geq t) = \int_0^t f(\tau)d\tau = 1 - e^{-KQ_t}\sum_{n=0}^{k-1}\frac{(KQ_t)^n}{n!}$$

$$P(\tau \geq t) = 1 - F(t)$$

$$P\left(t_{inf} < \tau < t_{sup}\right) = F(t_{inf}) - F(t_{sup})$$

With traffic flows lower than or equal to 400 passenger-car-unit/h/lane, gap distribution is supposed to follow a Poisson distribution, that is K=1. This assumption is justified by the consideration that in these operational condition the vehicle arrivals can be considered independent. Therefore, if Q_c < 400 (Equation 3.2, 3.3):

$$P\left(t_{inf} < t < t_{sup}\right) = e^{-Q_c t_{inf}} - e^{-Q_c t_{sup}} \tag{3.2}$$

$$P(t \geq t_c) = e^{-Q_c t} \tag{3.3}$$

If the volumes are higher, the gap distribution is not longer exponential, since the vehicles in the stream are often conditioned by the forward traveling vehicle. By following the indications provided by Scientific Literature, K was assumed equal to 2 for traffic flows ranging from 400 to 1000 pcu/h/lanes. Therefore, if 400 ≤ Q_c < 1000 (Equation 3.4, 3.5):

$$P(t_{inf} < t < t_{sup}) = e^{-2Q_C * t_{inf}}(1 + 2Q_c * t_{inf}) - e^{-2Q_C * t_{sup}}(1 + 2Q_c * t_{sup}) \quad (3.4)$$

$$P(t \geq t_c) = e^{-2Q_C t}(1 + 2Q_c t_c) \quad (3.5)$$

For greater traffic flows, K was fixed at 3.Therefore, if $Q_c \geq$ 1000 pcu/h (Equation 3.6, 3.7):

$$P(t_{inf} < t < t_{sup}) = e^{-3Q_C t_{inf}} * \left(1 + 3Q * t + \frac{9}{2}Q_C^2 * t_{inf}^2\right) - e^{-3Q_C t_{inf}} * (1 + 3Q * t + \frac{9}{2}Q_C^2 * t_{inf}^2) \quad (3.6)$$

$$P(t \geq t_c) = e^{-3Q_c t_c}(1 + 3Q_c t_c \frac{9}{2}Q_c^2 t_c^2) \quad (3.7)$$

3.1.2 Estimating Origin Destination matrix

In order to calculate the CO number it is necessary to know the Origin-Destination matrices. This means that traffic flows of all turning movements which can be performed at the roundabout must be collected.

On the other hand, the advantage to provide crash rates estimates related to temporal evolution of actual traffic condition offered by CO models require a complete daily acquisition of traffic flows.

Traffic flows were measured in passenger car units (pcu) with: 1 lorry = 1.5 pcu; 1 articulated lorry = 2 pcu and 1 motor bike = 1 pcu. The equivalences adopted by German Official Standards were used for being consistent with the adopted capacity calculation method (Brilon, et al., 1997; FGSV, 2006).

OD matrices were manually recorded by different operators and via the analysis of video records for night time flows. The flows are expressed in terms of equivalent vehicles.

The rural road network of the Mantua province and the neighbouring ones are characterized by traffic flows whose trend is constant during the week, with no substantial variations except for two peaks at 7:00 a.m. and 6:00 p.m.; there are very modest values during the night.

They revealed a good adaptation to the traffic counters set up by the Province for rural roads intersecting the analysed roundabouts. In detail, vehicle flows of

these roads manifest limited oscillation with pronounced values during the highest concentration of home to work travels (Provincia di Mantova, 2013)

It is not practical to number all the lane changes performed by the vehicles, given the evident difficulty of this survey, but this information is necessary to calculate the CO. Therefore, the distribution on the left and right lane for each turn, and consequently the drivers' behaviour, was hypothesized by using square matrices; they contain the percentages of vehicles circulating on the right or outer lane at the entry and at the roadway circle. Considering as improbable strongly unbalanced flows, matrices with less difference in vehicle flows between the major and minor road were chosen (Mauro & Cattani, 2005). Table 3.1 and 3.2 provide an example of these matrices for four-lagged roundabouts.

O / D	A	B	C	D
A	-	0,8	0,6	0,5
B	0,6	-	1	0,8
C	0,5	0	-	1
D	1	0,8	0,5	-

Table 3.1 Matrix of vehicle distributions at the entry lanes of a four legs roundabout. Each letter corresponds to a certain leg of the roundabout. Source: (Mauro & Cattani, 2005)

O / D	A	B	C	D
A	-	1	0,6	0,3
B	0,3	-	1	0,6
C	0,6	0,3	-	1
D	1	0,6	0,3	-

Table 3.2 Matrix of vehicle distributions at the ring lanes of a four legs roundabout. Each letter corresponds to a certain leg of the roundabout. Source: (Mauro & Cattani, 2005)

3.1.3 Capacity calculation

As will be shown in the following, capacity for each roundabout entries must be known for COs calculation. Capacity C of an entry is defined as the smallest

value of the leg flow that causes the permanent presence of vehicles queuing up to enter. To calculate C, the roundabout is considered as a series, along the development of the junction, of T intersections, with yielding to the circulating flows with only one interaction i.e., the mutual contribution to the formation of circulating flows that affect each entry as conflicting flows (Mauro, 2010).

Traffic data and Origin Destination matrix have been recorded on hourly basis during the data collection procedure. Operation conditions of roundabouts have been supposed to hold constant from one hour to the next.

The Capacity of a roundabout entry was calculated by the Brilon-Wu formula (Equation 3.8):

$$C = 3600 * \left(1 - \frac{t_m * Q_c}{n_c}\right)^{n_c} * \frac{n_E}{t_f} * e^{\left[-\frac{Q_c}{3600}(t_c - \frac{t_f}{2} - t_m)\right]} \quad (3.8)$$

Where:

- Q_c = circulating flow in front of the entry [pcu/h];
- n_E = entry lane number;
- n_c = circle lane number;
- t_c = critical gap, assumed to be equal to 4,12 s;
- t_f = follow up time, assumed to be equal to 2,88 s;
- t_m = minimum headway between the vehicles circulating in the ring assumed to be equal to 2,10 s.

Psycho Technical estimated times are derived from experimental data obtained by Brilon.

Traffic flows are measured in passenger car units (pcu) with: 1 lorry = 1.5 pcu; 1 articulated lorry = 2 pcu, 1 motor bike = 1 pcu, and 1 bicycle (on the roadway) = 0.5 pcu.

This formula should be only used for roundabouts with a single lane circle and single lane entries. In case of roundabouts with two circulatory lanes, Equation 3.9 can be used in order to calculate Capacity of entries.

$$C = 3600 * \frac{n_E}{t_f} * e^{\left[-\frac{Q_c}{3600}(t_c - \frac{t_f}{2})\right]} \quad (3.9)$$

where:

- n_E: parameter connected to the number of entry lanes; equal to 1 for single lane entries and 1.4 for double-lane entries;
- T_c = critical gap = 4.3 s;
- T_f = follow-up time = 2.5 s.

Other analytical formulation were tried, but it was noted that the use of different procedures for calculating capacity appeared to affect the final result very little.

3.2 Description of the analytical procedures for calculating COs for each crash typology

3.2.1 Collision due to failure to yield starting from a stopped position

The users' wrong evaluation of the time interval available between vehicles circulating in the ring is the cause of this crash type. The vehicle which is about to enter the ring is assumed to be stopped at the yield line. Situations where the *lag* (i.e. the time interval that elapses from the passage of the nearest vehicle circulating in the ring) is close to the critical value is considered as potentially susceptible to a collision. Extended *lags* do not constitute a threat and neither do the small ones since they would certainly be rejected. Instead, a CO occurs every time there are intervals between 3,5 and 5,5 s; these extremes were chosen considering critical time range, which varies from 4,11 to 5,19 s according to HCM 2010 estimations for single and multilane roundabouts.

For the *Headways* of the vehicles advancing along the ring a Poisson distribution for volumes up to 400 pcu/h and an Erlang one for major flows were assumed. The analytical details are shown in Equation 3.10.

$$N_{Ia} = Q_e * \big(1 - P(0)\big) * P(t_{inf} < t < t_{sup}) \quad (3.10)$$

where:

- *1-P(0)* = probability of having at least one vehicle waiting at the yield line;
- Q_e = Entering volume [pcu/h];
- $P(t_{inf} < t < t_{sup})$ = Probability of having vehicular "Headways" belonging to the dangerous interval (paragraph 3.1);

If there is a single waiting line service, from the queuing theory it is known that $1 - P(0) = \rho = \frac{Q_e}{C}$ .At double lane entries, the calculation of *P(0)* must be

performed independently for each lane by knowing the percentage of the vehicle dispositions. This implies using Table 1 in the way illustrated in Figure 3.1.

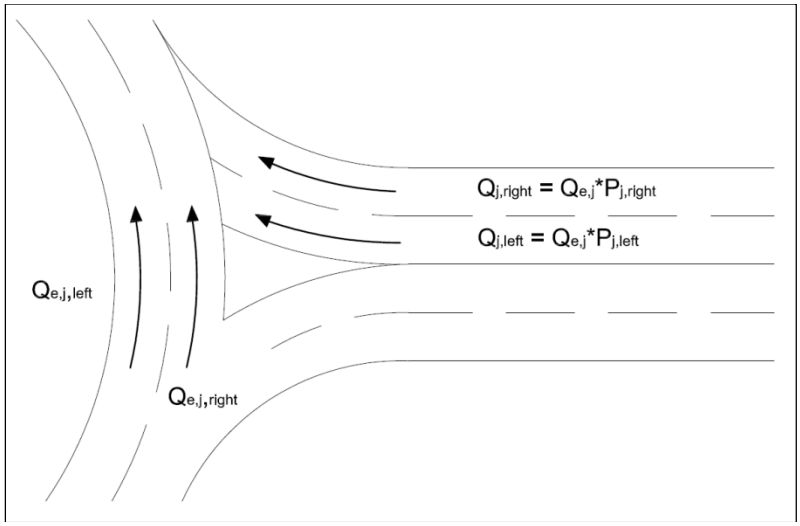

Figure 3.3 Entering and circulating flow distribution in the two lanes.

Where there is one lane only in the ring, the circulating flow Qc is to be considered entirely for both entry lanes. When two-lane ring roundabouts are considered, for the right entry lane, the part of disturbance flow advancing in the inner lane of the ring must be excluded.

3.2.2 Collision due to a failure to yield without stopping

Unlike the previous case, there is no vehicle waiting at the entry: the driver suddenly enters the ring without assessing safety issues. Blind entries performed by drivers pose dangerous situations. Non-perception of roundabout is the main cause for this type of crash, independently of events such as, for example, inattention, excessive speed, poor visibility that could lead drivers to act without appropriate risk consciousness (Guichet, 1993; SETRA, 1998; Mauro & Cattani, 2004)).

Whenever a vehicle which has not stopped tries to enter the roadway circle exploiting a "lag" smaller than 2s, a CO is originated. This time value, indicated as t_{coll}, is derived from dynamic evaluations in which the average approach speed is 25 km/h and the standard vehicle is 5m long and 2m wide (Mauro & Cattani, 2004). The number of vehicles entering the roundabout without coming across a waiting

line is equal to $Q_e * (1-\rho)$. The probability that one of these cars incurs the type of collision analysed here corresponds to the probability that the "lag" is less than t_{coll}, equal to $(1-e^{-Qc*tcoll}) \approx -Q_c * t_{coll}$. A Poisson distribution of the "headways" was assumed. Under this hypothesis, Equation 3.11 provides the number of CO per time unit for this kind of crash.

$$N_{1b} = Q_e * P(0) * t_{coll} * Q_c = Q_e * (1-\rho) * P(t < t_{coll}) \quad (3.11)$$

A Poisson distribution for volumes up to 400 equivalent-vehicles/h and an Erlang one for major flows were assumed as per Equations 3.2, 3.4, 3.6. There are no differences here between single lane and double lane roundabouts in terms of oncoming flow: a vehicle entering the roundabout without checking safety conditions affects all the ring lanes.

3.2.3 Single vehicle run off at the entry, the circulatory roadway, the exit

Apart from the location, overspeeding is the necessary condition for the loss of the road surface adherence and thus vehicle control. This situation may occur only if there are no waiting lines for approaching vehicles; another condition is that the first available "leg" is bigger than the critical one. Equation 3.12 gives the CO rates.

$$N_2 = Q_e * P(0) * P(t \geq t_c) \quad (3.12)$$

where:

- $P(t \geq t_c)$= probability that the first "*lag*" is superior than t_c critical time;

$P(t \geq t_c)$ was calculated by assuming a Poisson distribution for volumes up to 400 vehicles/h and an Erlang one for major flows, as previously shown in Equation 3.3, 3.5, 3.6.

Critical time was set equal to 4.65 s, the mean value of the range reported by HCM 2010.

Separate calculations must be performed in the presence of multiple entry lanes, each of which have its own $P(0)$.

3.2.4 Rear end collision at the entry

Whenever there is at least a waiting vehicle stopped at the yield line, there is the possibility of having a collision caused by a car coming from the rear. The crash rates for a given leg charged by entrance Q_e is provided by Equation 3.13.

$$N_3 = Q_e * (1 - P(0)) \quad (3.13)$$

3.2.5 Circulating exiting collision

This crash could occur every time the trajectory of a driver who is going to exit the roundabout by leaving the inner lane of the ring interferes with vehicles travelling on the outer lane towards the next exit.

For this situation too, a time of collision t_{coll} equal to 2s has been assumed; the difference is that in this case it is not necessary to consider the presence or absence of queues. Therefore, the CO frequencies for a leg subjected to an exiting traffic flow Q_{out}, was calculated as shown in Equation 3.14.

$$N_4 = Q_{out,int} * P(t < t_{coll}) \quad (3.14)$$

$P(t \geq t_{coll})$ should be ideally quantified by adopting a Poisson distribution or an Erlang one. However, analysed traffic flows are nearly always fewer than 400 pcu/h and in any case not greater than 500 pcu/h. It was decided to use a Poisson distribution to avoid analytical complications.

Successive Tables and Figures schematically depict a step by step procedure for calculating COs for each leg of the roundabout.

Figure 3.4 Roundabout S-420.

Table 3.5 Main features of Roundabout S-420-1. For each leg, all of the 22 geometric parameters of interest have been calculated. Here is reported only the deviation angle

Location

Municipality of Montanara (Mantua Province)

Main Geometric features

D ext	*D int*	*Number of legs*	*Number of inner lanes*
60 m	43 m	4	2

Legs features

	Entries	*Number of lanes*	*Angle of deflection β*
A	SS 420 twds Parma	1	63°
B	Morante Street	1	63°
C	SS 420 twds Mantua	1	58°
D	Santa Chiara Street	1	60°

Table 3.6 Preliminary calculations for estimating daily COs for the leg A

LEG A	Qe	Qc	Qc, ext	Qout	C	ρ	P(o)	P(tinf<t<tsup)	P (t>tsup)
6:00-7:00 a.m.	141	22	8	77	1230	0,11	0,89	0,0119	0,9699
7:00-8:00 p.m.	254	38	14	137	1215	0,21	0,79	0,0202	0,9486
8:00-9:00 p.m.	261	39	20	141	1214	0,21	0,79	0,0207	0,9473
9:00-9:00 a.m.	217	31	11,4	118	1221	0,18	0,82	0,0166	0,9579
10:00-9:00 a.m.	206	30	11,1	112	1222	0,17	0,83	0,0161	0,9592
11:00-9:00 a.m.	212	31	11	114	1221	0,17	0,83	0,0166	0,9579
12:00 a.m.-1:00 p.m.	219	34	13	119	1219	0,18	0,82	0,0182	0,9539
1:00-2:00 p.m.	177	26	10	96	1226	0,14	0,86	0,0140	0,9645
2:00-3:00 p.m.	175	26	10	94	1226	0,14	0,86	0,0140	0,9645
3:00-4:00 p.m.	256	35	15,3	118	1218	0,21	0,79	0,0187	0,9526
4:00-5:00 p.m.	227	34	13	123	1219	0,19	0,81	0,0182	0,9539
5:00-6:00 p.m.	275	40	15	148	1213	0,23	0,77	0,0213	0,9460
6:00-7:00 p.m.	316	48	18	171	1206	0,26	0,74	0,0253	0,9355
7:00-8:00 p.m.	206	30	11,1	112	1222	0,17	0,83	0,0161	0,9592
8:00-9:00 p.m.	157	23	8,4	85	1229	0,13	0,87	0,0125	0,9686
9:00-10:00 p.m.	102	16	6	55	1235	0,08	0,92	0,0087	0,9780
10:00-11:00 p.m.	61	14	6	53	1237	0,05	0,95	0,0077	0,9807
11:00 p.m. -6:00 a.m.	36	8	4	37	1242	0,03	0,97	0,0045	0,9886

Table 3.7 Estimation of COs for the leg A over hourly basis

LEG A	*Failure to yield starting from a stopped position*	*Failure to yield without stopping*	*Single vehicle run off*	*Rear end collision at the entry*	*Circulating exiting collision*
6:00-7:00 a.m.	0	2	121	16	0
7:00-8:00 p.m.	1	4	191	53	1
8:00-9:00 p.m.	1	4	194	56	2
9:00-9:00 a.m.	1	3	171	39	1
10:00-9:00 a.m.	1	3	164	35	1
11:00-9:00 a.m.	1	3	168	37	1
12:00 a.m.-1:00 p.m.	1	3	171	39	1
1:00-2:00 p.m.	0	2	146	26	1
2:00-3:00 p.m.	0	2	145	25	1
3:00-4:00 p.m.	1	4	193	54	1
4:00-5:00 p.m.	1	3	176	42	1
5:00-6:00 p.m.	1	5	201	62	1
6:00-7:00 p.m.	2	6	218	83	2
7:00-8:00 p.m.	1	3	164	35	1
8:00-9:00 p.m.	0	2	133	20	0
9:00-10:00 p.m.	0	1	92	8	0
10:00-11:00 p.m.	0	0	57	3	0
11:00 p.m. -6:00 a.m.	0	0	34	1	0

Table 3.8 Estimation of daily COs for each leg of the roundabout

Legs	*Failure to yield starting from a stopped position*	*Failure to yield without stopping*	*Single vehicle run off*	*Rear end collision at the entry*	*Circulating exiting collision*
Leg A	12	52	2945	640	14
Leg B	2	62	469	19	14
Leg C	26	84	3751	1094	11
Leg D	3	100	492	26	23

Table 3.9 A framework of COs calculation for each sampled leg

		Daily Conflict Opportunities					
I.D. Roundabout	*Daily Flows at legs [eq. Veh/day]*	*Failure to yield starting from a stopped position*	*Failure to yeld without stopping*	*Single vehicle run off*	*Rear End Collision at the entry*	*Circulating exiting collision*	*Total Daily Amount*
S236-1	15183	388	1431	8224	4804	336	15183
	13796	535	1590	6276	5155	240	13796
	8600	867	939	2283	4122	389	8600
S236-2	43423	6844	119	1510	34074	876	43423
	12928	2269	576	1189	8142	752	12928
	25883	4252	240	1563	19213	615	25883
	8382	1252	704	658	5042	726	8382
S236b-1	11260	1184	646	2507	6923	*	11260
	12620	1591	574	2246	8209		12620
	2908	278	829	775	1025		2908
	7082	471	654	2473	3484		7082
S236b-2	8673	340	404	4016	3798	115	8673
	10797	80	664	8177	1819	57	10797
	3014	26	779	1797	315	97	3014
S482-1	15331	1163	327	3009	10627	205	15331
	12742	1171	483	2582	8348	159	12742
	10992	1179	645	2500	6396	272	10992
S482-2	8610	828	706	2140	4785	151	8610
	3227	277	900	830	1022	198	3227
	7930	561	667	2368	3958	375	7930
	8106	565	634	2430	4217	260	8106
S62-1	3868	50	209	2779	794	35	3868
	2377	40	285	1628	375	49	2377
	3936	65	265	2692	856	58	3936
	3138	56	299	2129	586	68	3138
S62-2	4259	29	107	3229	871	23	4259
	4916	20	137	3664	1066	29	4916
	1300	14	144	1008	122	12	1300
S62-3	19748	656	85	3165	15762	80	19748
	12009	1025	512	2880	7544	48	12009
	4715	335	811	1718	1528	323	4715
S62-4	11518	470	1770	5617	3170	491	11518
	11420	266	1922	4714	3896	622	11420
	15248	2493	446	1505	10408	396	15248
	41036	8116	174	1227	30552	966	41036
S62-5	8759	52	84	5450	3154	20	8759
	1481	42	385	832	202	21	1481
	7320	132	228	4334	2571	55	7320
	798	6	156	511	35	90	798

* Rounadbout S236b-1 has only one circulatory lane

References

Brilon, W., Wu, N. & Bondzio, L., 1997. *Unsignalized Intersections in Germany– A State of the Art1997.* Portland, OR, USA.

FGSV, 2006. *Merkblatt für die Anlage von Kreisverkehren.* Köln, Germany: FGSV Verlag GmbH.

Guichet, B., 1993. *Typologie des accidents dans les giratoires urbains.* Bagneux, France, Service d'Etudes Techniques des Routes et Autorutes (SETRA), Centre d'Etudes des Transport Urbains, pp. 145-151.

Ha, T. J. & Berg, W. D., 1995. Development of safety-based level-of*service crietria for isolated signalised intersections. *Transportation Research Record 1484,* pp. 98-104.

Kaub, A. R. & Kaub, J. A., 2005. Predicting Annual Intersections Accident with Conflict Opportunities. *TRB Circular E109: Urban Street Symphosium Transportation Research Board .*

Kennedy, D. R. & Taylor, K. M., 2005. *Estimating Roundabout Performance using Delay and Conflict Opportunity Crash Prediction.* Vail, CO, USA, Transportation Research Board (TRB) of National Academies.

Mauro, R., 2010. *Calculation of Roundabouts. Capacity, Waiting Phenomena and Reliability - 1st Edition.* Berlin, Germany: Springer.

Mauro, R., 2015. *Traffic and Random Processes. An Introduction.* Berlin, Germany: Springer International Publishing.

Mauro, R. & Cattani, M., 2004. Model to evaluate potential accident rate at roundabouts. *ASCE Journal of Tranportation Engineering,* 130(5), pp. 602-609.

Mauro, R. & Cattani, M., 2005. *A model to evaluate the potential accident rate at single-lane roundabouts and double-lane roundabouts.* Linkoping, Sweden, Swedish National Road and Transport Research Institute (VIT).

Mauro, R. & Cattani, M., 2010. *Potential Accident Rate of Turbo-roundabouts.* Washington, DC, USA, Transportation Research Board (TRB) of National Academies.

Ming, S. H., 2008. *Oportunitades de conflito de trafego:modelos de previsao.* Dissertation Master Thesis, Universidade de Sao Paulo.

Pecchini, D., Mauro, R. & Giuliani, F., 2014. Model of Potential Crash Rates of Rural Roundabouts with Geometrical Features. *ASCE Journal of Tranposrtation Engineering,* 140(11), p. 04014055.

Provincia di Mantova, 2013. *Sicurezza stradale e mobilità sostenibile.* [Online] Available at:
http://www2.provincia.mantova.it/sicurezzastradale/
[Accessed 13 September 2013].

SETRA, 1998. *Aménagement des carrefours interurbains sur les routes principales. Carrefours plans - Guide technique,* Paris, France: s.n.

Capitolo 4

Statistical approach

4.1 Problem statement and introduction to exploratory data analyses

An attempt was made to implement geometric design of roundabout for the crash prediction model developed in this study by searching for possible significant correlation between crash-to-conflict ratios and geometric variables recorded for the sampled intersections.

For each of them, crash-to-conflict ratios were then calculated. The aim was to associate these coefficients to a limited set of geometric factors that actually proved to have a correlation with them.

Overall, data collected amount to 22 covariates for 151 legs of 43 different roundabouts. Attention was then focused on legs with one injury or fatal crash at least, so the sample reduced to 74 legs.

However, it still constitutes a wide ensemble of data that can be arduous to manage in order to find possible underlying information about investigated relationships.

The data from the surveys can be disposed into a rectangular array with one row for each experimental subject (i.e. the single leg of a roundabout) and one column for each original covariate. For this study, a 74 x 22 matrix should be discerned in order to capture useful details. The analyst could be overwhelmed by such an apparently chaotic assortment of variables and values.

Exploratory data analysis (EDA) techniques have been devised as an aid in this situation, an approach for summarising the main characteristics of collected data. Most of EDA techniques work in part by hiding certain aspects of the data while making other aspects more clear. They essentially have the potential of: maximising insight into a data set; uncovering underlying structure; extracting important variables; detecting outliers and anomalies; testing underlying assumptions; determining relationships among the explanatory variables;

developing parsimonious models; helping understand phenomena; suggesting hypotheses to test in confirmatory studies (Seltman, 2004).

For their properties, EDA are particularly recommended as a preliminary investigation of complex data, given the possibility of identifying significant variables where concentrating subsequent inferential analyses.

Thus, in classical analysis, the data collection is followed by the imposition of a model and the following analysis, estimation, and testing are focused on the parameters of that model. In EDA, the data collection does not precede a model imposition, but rather an analysis aimed to realise which variables should be considered, and what model may be appropriate for describing the examined phenomenon and fitting to the data (NIST, 2012). In a synthetic way:

- for classical analysis. the sequence is
  Problem => Data => Model => Analysis => Conclusions;

- For EDA. the sequence is Problem => Data => Analysis => Model => Conclusions.

EDA provides a variety of tools for summarising and gaining insight about a set of data. Factor analyses. Discriminant analyses and multiple regression with different hypotheses about statistical distribution of the residuals have been applied in this study in order to identify geometric variables having a significant correlation with crash-to-conflict ratios. A positive outcome would allow developing a sort of calibration curves by means of which determining the coefficients of the crash prediction model by simply knowing the values of certain geometric variables. Roundabout design would be then effectively implemented within the conversion from Conflict Opportunity frequency to estimation of crash frequencies.

However, as a first step for analysing collected data. a correlation matrix was obtained in order to quickly detect possibly highly correlated variables and eliminating redundant information.

4.2 Correlation matrix

It is the starting point for the study of principal components analysis and factor analysis. The Pearson correlation coefficient is a single number that describes the strength of a linear relationship between two variables on a scale which ranges from +1 to -1 (Kremelberg, 2011). A Pearson correlation coefficient equal to zero implies that no linear relationship can be observed for the two variables, but this does not mean that they are completely independent from each other (one of the variables may be a nonlinear function of the other). If the correlation is negative, there is a linear relationship with a negative slope; otherwise, a positive relationship can be established between them. When more than two random variables are involved, it is useful to draw up the correlations between each pair of

values into a matrix. The element of the matrix located at the *i-th* row and *j-th* column represents the correlation coefficient between *i-th* and *j-th* variables.

Conventionally, the correlation of a variable with itself is 1, so this matrix has elements equal to 1 on the main diagonal. as well as being symmetric.

Correlation coefficient between variables *X* and *Y* can be obtained from their covariance value by normalising their dispersion. In this way, the only degree of the linear relationship between *X* and *Y* is taken into account. Let *X* and *Y* random variables ϵ R^{1*n}. Formally, the correlation coefficient is defined as (Equation 4.1):

$$\rho_{XY} = \frac{Cov(X.Y)}{\sigma_X \sigma_Y} = \frac{E\left[(X - \mu_X)(Y - \mu_Y)\right]}{\sigma_X \sigma_Y} \tag{4.1}$$

where:

- $Cov(X.Y)$: covariance between r.v. X and Y;
- μ_X: population mean of r.v. X;
- μ_X: population mean of r.v. Y.
- σ_X: population standard deviation of r.v. X;
- σ_Y: population standard deviation of r.v. Y.

Starting from experimental data, unbiased estimate of ρ_{XY} is provided by Equation 4.2:

$$\widehat{\rho_{XY}} = \frac{\widehat{Cov(X.Y)}}{s_X s_Y}$$

$$\widehat{\rho_{XY}} = \frac{\sum_{i=1}^{n}(x_i - \bar{x})\,(y_i - \bar{y})}{\sqrt{\sum_{i=1}^{n}(x_i - \bar{x})^2 \sum_{i=1}^{n}(y_i - \bar{y})^2}} = \frac{\sum_{i=1}^{n}(x_i y_i - \bar{x}\bar{y})}{\sqrt{\sum_{i=1}^{n}(x_i - \bar{x})^2 \sum_{i=1}^{n}(y_i - \bar{y})^2}} \tag{4.2}$$

where:

- μ_X: unbiased sample mean of r.v. X;
- μ_X: unbiased sample mean of r.v. Y.
- s_X: unbiased sample standard deviation of r.v. X;
- s_Y: unbiased sample standard deviation of r.v. Y;

Table 4.1 represents the correlation coefficients for each pairs of variables considered in the study, excluded the number of entry and circulating lanes which are the only geometric features directly implemented in the COs calculations. Only the correlation values higher then 0.8 have been highlighted. It points out that R4 and Inscribed circle diameter are highly correlated, as well as entry kerb radii and R2. R1 and R0 seem to have a perfect linear relationship. In this way, redundancy of information provided by the single parameter is unveiled and can be properly taken into account in subsequent analyses. For instance, given that R4 and ICD manifest a great correlation coefficient, one of the two features can be excluded from the successive tests in order to avoid adding useless information with

unnecessarily more complicated analyses. These outcomes appear to be rational. R4, for its graphical definition, is effectively similar to the half of the ICD when the roundabouts is arranged with a circular shape, which is the case for the major part of the sampled intersections. The strong positive linear relationship between R0 and R1 confirms the absence of successions of reverse curves before the entries of roundabout (in this case. R0 and R1 would have opposite sign) and denotes a linear increase in transversal acceleration with the reduction of curvature radii when approaching the entries. It is interesting to note that R2 is strongly influenced by the entry kerb radius, while correlation between R2 and entry path radius is substantially lower. This suggests that circulating path radius is deeply influenced by the shape of the kerb at the entry, which therefore appear to be particular relevant for the entire deviation imposed by the roundabout to vehicle's trajectory.

Correlation matrix allow realising what pieces of information can be neglected, with a simplified pattern to deal with. However, once the correlation coefficients have been computed, a significance test should be conducted in order to verify whether the observed correlation is real or has occurred by chance. This implies testing the mutually exclusive hypotheses:

- Null hypothesis: $\widehat{\rho_{XY}} = 0$;
- Alternative hypothesis: $\widehat{\rho_{XY}} \neq 0$.

If the true Pearson correlation coefficient between X and Y within the general population is $\widehat{\rho_{XY}}$=0, and if the *n* sample size is equal to or greater than 6, then the quantity:

$$t = \frac{\widehat{\rho_{XY}}}{\sqrt{1 - \widehat{\rho_{XY}}^{2}}}\sqrt{n-2}$$

follows a t-Student random variable with N - 2 degrees of freedom (Howell, 2011). Application of this formula to any particular observed sample value of $\widehat{\rho_{XY}}$enable testing the null hypothesis that the observed value comes from a population in which there is actually no correlation between X and Y. By adopting a specific level of significance *α*, i.e. the probability of rejecting the null hypothesis given that it is true, correlation coefficient can be tested.

If $|t| > t_{\alpha/2}$, the null hypothesis must be rejected. and it can be stated that $\widehat{\rho_{XY}}$is significantly different from zero. Otherwise, the null hypothesis cannot be abandoned and no definitive conclusion can be drawn. Test results are shown in Table 4.2, where the only correlations found to be statistically different from zero have been highlighted. All of the three high correlation coefficients previously identified resulted to be statistically significant. In light of these outcomes, it may be stated that R4 could be neglected given its correlation with ICD. At the same time. R0 seems not to be relevant for subsequent analyses, given its redundancy

with the entry path radius R1. Eventually, also the possibility of abandoning entry kerb radius in favour of circulating radius R2 as a significant variable should be carefully evaluated. A part from these situations, there seems not to be an overall pronounced correlation among the considered geometric variables, which may give reasons for the path followed in this study, that is investigations focused on the single geometric features. In fact, if a general high correlation would have been found, this had implied a strictly reciprocal dependence among them, and different procedures taking into account the entire geometric layout of roundabouts should have been adopted.

Eventually, it is worth pointing out that the outcomes obtained from the correlation matrix cannot have a general validity because they are related to the sample of local roundabouts considered in this study. Other geographical areas where diverse design is adopted would have allegedly led to other results. Therefore, it cannot be stated, for example, that R0 is always entirely determined by the choice of entry path radius R1. For instance. Countries where successive reverse curves are implemented at the approaches of roundabout entries could not have shown this positive almost perfect correlation, given that, in this case, approach curvature would have had an opposite sign to the entry one.

	ICD	Carriageway width	R0	R1	R2	R3	R4	R5	R1 sx	R2 sx	Entry Angle	Deviation Angle	Angle consecutive legs	Angle of visibility	Distance entry-consec. exit	Distance entry-prev. exit	Entry kerb radii	Exit kerb radii
ICD	1	0.09	-0.22	-0.22	0.17	-0.2	0.9	0.12	-0.23	0.11	-0.55	0.35	0	-0.54	0.54	0.47	-0.01	0.06
Carriageway width	0.09	1	0.02	0.02	-0.15	-0.18	0	0.02	0	-0.07	-0.12	0.1	-0.1	-0.02	0	0.02	-0.08	-0.08
R0	-0.22	0.02	1	1	0.45	0.49	-0.24	-0.2	0.12	-0.09	0.28	-0.43	0.19	0.06	-0.17	-0.21	0.62	0.09
R1	-0.22	0.02	1	1	0.45	0.49	-0.23	-0.2	0.12	-0.09	0.28	-0.43	0.19	0.05	-0.17	-0.22	0.62	0.09
R2	0.17	-0.15	0.45	0.45	1	0.33	0.17	-0.01	-0.11	-0.02	-0.18	-0.27	0.13	-0.24	-0.01	0.07	0.81	0.04
R3	-0.2	-0.18	0.49	0.49	0.33	1	-0.18	-0.1	0.22	-0.03	0.35	-0.36	-0.02	0.11	-0.21	-0.12	0.35	0.22
R4	0.9	0	-0.24	-0.23	0.17	-0.18	1	0.19	-0.14	0.17	-0.47	0.33	-0.02	-0.43	0.47	0.5	-0.01	0.09
R5	0.12	0.02	-0.2	-0.2	-0.01	-0.1	0.19	1	0.18	0.38	-0.12	-0.02	-0.17	0.25	-0.02	0.37	-0.13	0
R1 sx	-0.23	0	0.12	0.12	-0.11	0.22	-0.14	0.18	1	0.52	0.42	-0.19	-0.09	0.57	-0.16	-0.17	-0.1	0.16
R2 sx	0.11	-0.07	-0.09	-0.09	-0.02	-0.03	0.17	0.38	0.52	1	0.19	0.06	-0.07	0.28	0.07	-0.04	-0.1	0.19
Entry Angle	-0.55	-0.12	0.28	0.28	-0.18	0.35	-0.47	-0.12	0.42	0.19	1	-0.19	-0.29	0.54	-0.43	-0.3	-0.15	0.13
Deviation Angle	0.35	0.1	-0.43	-0.43	-0.27	-0.36	0.33	-0.02	-0.19	0.06	-0.19	1	0.01	-0.26	0.31	0.22	-0.34	-0.15
Angle between consecutive legs	0	-0.1	0.19	0.19	0.13	-0.02	-0.02	-0.17	-0.09	-0.07	-0.29	0.01	1	-0.31	0.67	-0.24	0.26	-0.11
Angle of visibility	-0.54	-0.02	0.06	0.05	-0.24	0.11	-0.43	0.25	0.57	0.28	0.54	-0.26	-0.31	1	-0.48	-0.05	-0.2	0.16
Distance entry-consec exit	0.54	0	-0.17	-0.17	-0.01	-0.21	0.47	-0.02	-0.16	0.07	-0.43	0.31	0.67	-0.48	1	0	-0.02	-0.08
Distance entry-prev. exit	0.47	0.02	-0.21	-0.22	0.07	-0.12	0.5	0.37	-0.17	-0.04	-0.3	0.22	-0.24	-0.05	0	1	0.03	-0.12
Entry kerb radii	-0.01	-0.08	0.62	0.62	0.81	0.35	-0.01	-0.13	-0.1	-0.1	-0.15	-0.34	0.26	-0.2	-0.02	0.03	1	0.02
Exit kerb radii	0.06	-0.08	0.09	0.09	0.04	0.22	0.09	0	0.16	0.19	0.13	-0.15	-0.11	0.16	-0.08	-0.12	0.02	1

Table 4.1 Matrix correlation of various geometric aspects

	ICD	Carriageway width	R0	R1	R2	R3	R4	R5	R1 sx	R2 sx	Entry Angle	Deviation Angle	Angle consecutive legs	Angle of visibility	Distance entry-consec. exit	Distance entry-prev. exit	Entry kerb radii	Exit kerb radii
ICD		0.21	0.02	0.02	0.06	0.03	0	0.13	0.02	0.15	0	0	0.5	0	0	0	0.45	0.3
Carriageway width	0.21		0.43	0.44	0.08	0.04	0.49	0.42	0.48	0.25	0.14	0.17	0.17	0.43	0.48	0.44	0.22	0.24
R0	0.02	0.43		0	0	0	0.01	0.03	0.14	0.2	0	0	0.04	0.3	0.06	0.02	0	0.21
R1	0.02	0.44	0		0	0	0.01	0.03	0.13	0.2	0	0	0.04	0.31	0.06	0.02	0	0.21
R2	0.06	0.08	0	0		0	0.06	0.45	0.15	0.41	0.04	0.01	0.12	0.01	0.46	0.27	0	0.34
R3	0.03	0.04	0	0	0		0.05	0.17	0.02	0.41	0	0	0.43	0.15	0.03	0.14	0	0.02
R4	0	0.49	0.01	0.01	0.06	0.05		0.04	0.09	0.05	0	0	0.44	0	0	0	0.46	0.2
R5	0.13	0.42	0.03	0.03	0.45	0.17	0.04		0.05	0	0.13	0.41	0.06	0.01	0.44	0	0.12	0.49
R1 sx	0.02	0.48	0.14	0.13	0.15	0.02	0.09	0.05		0	0	0.04	0.2	0	0.06	0.05	0.19	0.06
R2 sx	0.15	0.25	0.2	0.2	0.41	0.41	0.05	0	0		0.04	0.3	0.27	0	0.25	0.37	0.18	0.04
Entry Angle	0	0.14	0	0	0.04	0	0	0.13	0	0.04		0.04	0	0	0	0	0.09	0.11
Deviation Angle	0	0.17	0	0	0.01	0	0	0.41	0.04	0.3	0.04		0.47	0.01	0	0.02	0	0.09
Angle between consecutive legs	0.5	0.17	0.04	0.04	0.12	0.43	0.44	0.06	0.2	0.27	0	0.47		0	0	0.01	0.01	0.15
Angle of visibility	0	0.43	0.3	0.31	0.01	0.15	0	0.01	0	0	0	0.01	0		0	0.31	0.03	0.07
Distance entry-consec exit	0	0.48	0.06	0.06	0.46	0.03	0	0.44	0.06	0.25	0	0	0	0		0.5	0.43	0.23
Distance entry-prev. exit	0	0.44	0.02	0.02	0.27	0.14	0	0	0.05	0.37	0	0.02	0.01	0.31	0.5		0.39	0.13
Entry kerb radii	0.45	0.22	0	0	0	0	0.46	0.12	0.19	0.18	0.09	0	0.01	0.03	0.43	0.39		0.44
Exit kerb radii	0.3	0.24	0.21	0.21	0.34	0.02	0.2	0.49	0.06	0.04	0.11	0.09	0.15	0.07	0.23	0.13	0.44	

Table 4.2 t-test of Matrix correlation

4.3 Factor analysis

Even if the analysis of the correlation matrix enables simplifying the aspects to take into account, remaining variables are still numerous; finding useful information lying in numerous collected data may be unfeasible. Factor analysis has the potential of reducing the set of variables to take into account by seeking underlying and unobservable variables (i.e. latent variables or factors) that are reflected in the observed and original variables (i.e. manifest variables).

The ultimate goal consist in reducing the original data set to a more manageable size while retaining as much of the original information as possible (Field, 2009).

An illustrative application of factor analysis is shown in **Figure 4.1**, where multiple psychological stress, that is the original manifest variables, have been grouped to a common and unobservable factor, the emotional instability.

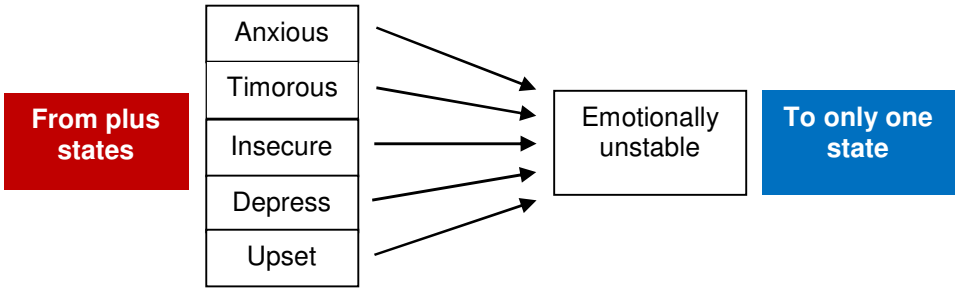

Figure 4.1 Illustrative depiction of the outcome of a successful factor analysis.

By referring to Figure 4.1, emotional instability is the latent variable of the example. It cannot be measured directly but only thought multiple manifest variables. Another possible example could be the inference of people's intelligence via observable and measurable tests such as, for example, short term memory. verbal, writing, reading, motor and comprehension skills.

In both the examples, a multitude of measurements have been summarised in a small number of factors without losing decisive information. At the same time. in addition to the economy of description factor analysis enable the analyst to quantify variables otherwise difficult to analytically define. Eventually. it is worth noting that no a priori assumptions about relationships among variables are required for the application of the method.

4.3.1 The Factor Analysis Model

Factor analysis attempts to represent a set of the manifest original variables by means of latent common factors plus a feature that is unique to each manifest variable. In details, factor analysis try to explain as much as possible of the total

variance of observed variables with as few latent common factors as possible, in order to obtain a more interpretable outcome.

All of the manifest variables are assumed to be dependent on a linear combination of the latent, common factors and to differ from each other by uncorrelated unique components.

With reference to *i-th* subject, if the observed variables are $X_1, X_2 \ldots X_n$, the common factors are $F_1, F_2, \ldots F_m$ and the unique factors are $U_1, U_2 \ldots U_n$, the observed variables may be expressed as linear functions of the common factors in accordance to Equation 4.3.

$$\begin{cases} X_{1i} = a_{11}F_{1i} + a_{12}F_{2i} + a_{13}F_{3i} + \cdots + a_{1m}F_{mi} + U_{1i} \\ X_{2i} = a_{21}F_{1i} + a_{22}F_{2i} + a_{23}F_{3i} + \cdots + a_{1m}F_{mi} + U_{2i} \\ \qquad\qquad\qquad\qquad \ldots \\ X_{ni} = a_{n1}F_{1i} + a_{n2}F_{2i} + a_{n3}F_{3i} + \cdots + a_{nm}F_{mi} + U_{ni} \end{cases} \tag{4.3}$$

These are regressive equations. Factor analysis seeks the coefficients a_{11}, a_{12}., a_{nm} which best reproduce the observed variables from the factors, that is the coefficients by means of which the fewest possible number of latent factors are able to explain the greatest amount of common variance related to the observed variables. In other terms, unique factors must be minimised (Taylor, 2004) (Field, 2009).

It is worth noting that factor analysis try to explain only the common variance shared by variables, that is the variance of the investigate phenomenon that can be related to the common factors.

Uniqueness for each observed variable is the portion of variance related to the manifest variable that cannot be predicted by the latent factors. Unique variance includes individual differences between subjects and the error variance inevitably affecting each survey response, which cannot be deterministically defined by the underlying factor structure. Unique factors are uncorrelated with the common ones. The latter, in turn, have been assumed to be uncorrelated with each other in this study.

The regression coefficients a_{11}. $a_{12} \ldots$. a_{nm} are the so-called *loadings*; so. a_{11} is the loading for variable X_1 on F_1. a_{23} is the loading for variable X_2 on F_3 and so on. Another property of loadings is that they are identical for each subject. Conversely, latent factors assume specific values for each subject. These values are indicated as *scores*; F_{2i} represents subject *i-th*'s score on F_2 factor. Loadings show the correlation between observed variables and the corresponding factor if the factors are uncorrelated with each other. Therefore, with this assumption, the sum of the squares of the loadings for variable X_1, namely ${a_{11}}^2 + {a_{12}}^2 + \cdots {a_{1m}}^2$. shows the proportion of variance of variable X_1 accounted for by the common factors. This is the so-called *communality* for variable X_1. Communality ranges from zero to 1; the latter extreme indicates an ideal situation where the manifest variable can be fully defined by the factors. In the analogy between factor analysis and multidimensional linear regression, communality can be intended as a sort of coefficient of determination R^2 because it practically explains the percentage of total variability explained by the model.

Variable uniqueness is instead equal to (*1- communality*) and is a measure of the proportion of variance associated to the analysed manifest variable not explained by the common factors.

Similarly, the sum of squares of the coefficient for a factor shows the proportion of the variance of all the variables explained by the factor itself. For example. ${a_{11}}^2 + {a_{21}}^2 + \cdots {a_{n1}}^2$. is the proportion of the variance of all the manifested variables explained by that factor. This quantity is defined as *eigenvalue*.

Given the system of equations 4.3 showing the variables $X_1 \ldots X_n$ in terms of the factors $F_1 \ldots F_m$. it should be possible to solve the equations for the factor scores, so as to obtain a score on each factor for each subject. In other words. equations of the following form (Equation 4.4) should be available.

$$\begin{cases} F_{1i} = b_{11}X_{1i} + b_{12}X_{2i} + b_{13}X_{3i} + \cdots + b_{1n}X_{ni} \\ F_{2i} = b_{21}X_{1i} + b_{22}X_{2i} + b_{23}X_{3i} + \cdots + b_{2n}X_{ni} \\ \ldots \\ F_{mi} = b_{m1}X_{1i} + b_{m2}X_{2i} + b_{m3}X_{3i} + \cdots + b_{mn}X_{ni} \end{cases} \quad (4.4)$$

However, exact solution for the factors is unfeasible for the presence of unique factors U_i (Equation 4.3). Various approximations are available and implemented by statistical package software. Among them is a procedure by means of which loadings are calculated in order that resulted factor scores have a mean of zero and a standard deviation of one if observed variables are expressed in the standardised form (Grice, 2001).

4.3.2 Outcomes of Factor analysis

Factor analysis pursues the best possible explanation of variance related to all of the observed variables with a restricted set of factors. As it will explained in the following, this implies to achieve an estimate of the observed correlation matrix as similar as possible to the actual one. The higher the discrepancy between these two matrices, the less successful the factor solution. In fact, when the factors are uncorrelated with each other, the correlation between variables X1 and X2 can be estimated by summing the products of the coefficients for the two variables across all common factors. A solution offered by factor analysis in estimating loadings is depicted in **Table 4.3**.

Table 4.3 An example of the solution achieved via a factor analysis

Variable	Loadings / Correlations		Communality
	Factor 1	*Factor 2*	
X_1	0.7	0.2	0.53
X_2	0.8	0.3	0.73
X_3	0.9	0.4	0.97
X_4	0.2	0.6	0.40
X_5	0.3	0.7	0.58
	$\sum x^2$ 2.07	$\sum x^2$ 1.14	

According to **Table 4.3**, the five variables can be expressed as a function of the two latent common factors F1. F2 in this way:

$$X_1 = 0.7F_1 + 0.2F_2$$
$$X_2 = 0.8F_1 + 0.3F_2$$
$$\ldots$$
$$X_5 = 0.3F_1 + 0.7F_2$$

The correlation between X_1 and F_1 is 0.7, that between X_1 and F_2 is 0.20, and so on. The sum of loading squares for each factor reported below the columns of Table 4.3 is the total variance of the observed variables explained by the single factor itself. For Factor F_1, the quantity $0.7^2 + 0.8^2 + 0.9^2 + 0.2^2 + 0.3^2 = 2.07$. Given that original variables are standardised, they have unitary standard deviation, so the total variance is equal to the number of observed variables. As a result. F_1 accounts for (2.07 / 5)*100 = 41.4% of the variance.

The quantities in the communality column show the proportion of the variance of each variable accounted for by the common factors. For X_1 this quantity is $0.7^2 + 0.2^2 = 0.53$, for X_2 it is $0.8^2 + 0.3^2 = 0.73$ and so on.

Eventually, the correlation matrix can be approximated by summing the products of the coefficients for the two variables across all common factors. By referring to Table 4.3, the correlation between variables X_1 and X_2 derived from the factor solution is equal to (0.7*0.8)+(0.2*0.3) = 0.62, while the correlation between variables X_3 and X_5 is equal to (0.9*0.3)+(0.4*0.7=0.55). This is why the quality of the outcome provided by factor analyses can be ascertained by comparing the actual correlation matrix of the observed variables with that estimated via factor solution. In particular, a reproduced correlation matrix quite similar to the original one is an denotes that the extracted factors accounted for a significant amount of the variance related to the original variables.

4.3.3 How Factor analysis works

The parameters and variables of factor analysis can be given a geometrical interpretation. The data, the factors and the unique factors can be viewed as vectors in multi-dimensional Euclidean spaces. Observational data are initially represented in an m-dimensional Euclidean space, where m is the number of the original, manifest and standardised variables, which are unit vectors defining the direction of the axes related to this space. Factor analysis try to identify a new Euclidean space with fewer variables, that is fewer dimensions; these new variables are the factors themselves. The aim is simplify the representation of the original data by perseverating as much as possible of the initial information by limiting the losses due to inevitable approximations. As already mentioned, factors are obtained from a linear combination of the original variables. In a geometrical perspective, this means that factors are attained via a rotation of the original reference system. Practically, a rotation to a simple structure is the effect performed by factor analysis on a complex layout of data arranged on numerous variables. It is worth noting that by assuming uncorrelated factors, axes of the new reference system are orthogonal to each other. This implies that only orthogonal rotations are performed. Propaedeutic for the factor analysis is the identification of directions where the projected data have the highest variances; these directions are obtained by orthogonal rotation of axes associated to the original reference system. This is the so-called Principal Component Analysis (PCA), which allows unveiling the most representative directions, that is the variables able to explain to the greatest extent the variance of the original data (Field, 2009). In details, PCA uses an orthogonal transformation to convert a set of observations of possibly correlated variables into a set of values of linearly uncorrelated variables called principal components (**Figure 4.2**).

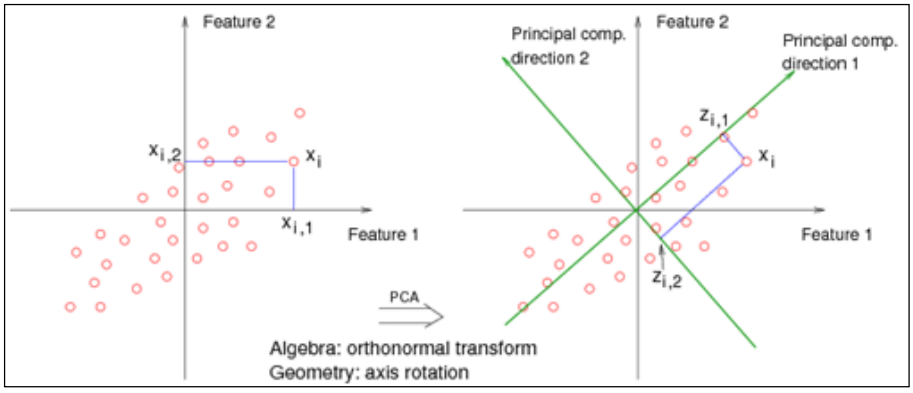

Figure 4.2 Illustrative depiction of a Principal Component Analysis; the original reference system is rotated in order to identify the directions where the variance of projected data is maximum.
Source: https://onlinecourses.science.psu.edu

This transformation is arranged in such a way that the first principal component has the largest possible variance, and each succeeding component in turn has the highest variance possible under the constraint that it is orthogonal to the preceding components. These new variables are the same in number as the old ones, and given that all of them are standardised, total variability does not change after the orthogonal rotation. Indeed, in PCA, all sources of variability (i.e. unique, shared and error variability) are analysed for each observed variable; therefore, no information vanishes, but it is simply expressed by means of a rotated reference system.

As a result, differently from factors, principal components do not present error terms taking into account uncertainties derived by approximations of the original information (Johnson & Wichern, 2007; Field, 2009). It is then possible to express PCA components as a function of the original variables without recurring to simplifications (Equation 4.5). Conversely, when using factors, such an exact solution is unattainable for the presence of uniqueness, and various approximation have to be used (Widaman, 1993).

$$PC_1 = b_{11}x_1 + b_{12}x_2 + b_{13}x_3 + \cdots b_{1n}x_n \tag{4.5}$$

The standardised original variables are practically versors in the original reference system. In the new one, they can be represented as vectors whose projections on the new axes define the analytical bound existing between the PCA components and these original variables. In fact, geometric interpretation confirms the mathematical solution of PCA techniques, according to which PCA components are a linear combination of manifest variables and vice-versa (Johnson & Wichern, 2007).

The mathematical base of PCA lies in the fact that the dispersion of sample point projections on the direction of a random unitary vector is equal to the scalar product between Γv vector, where Γ is the sample correlation matrix, and vector v itself. Mathematically speaking (Equation 4.6):

$$\sigma(v^2) = \langle \Gamma v, v \rangle \tag{4.6}$$

where:

- $\sigma(v^2)$: dispersion of sample point projection on the direction of unitary vector v;
- Γ: sample correlation matrix.

As already said, the principal component is the unitary vector whose direction is associated with the maximum variance of the projected sample points. In accordance to Equation 4.5, the problem of finding the principal component is reduced to defining the unitary vector such that $\langle \Gamma v, v \rangle$ is maximised. By exploiting Equation 4.5, it can be demonstrated that dispersion of sample points projected on the direction of a random unitary vector v_i is equal to the corresponding eigenvalue λ_i of the sample correlation matrix (Equation 4.7, 4.8):

$$\Gamma v = \lambda v \tag{4.7}$$

$$\sigma(v^2{}_i) = \langle \Gamma v_i, v_i \rangle = \langle \lambda_i v_i, v_i \rangle = \lambda_i \langle v_i, v_i \rangle = \lambda_i |v_i|^2 = \lambda_i \tag{4.8}$$

Therefore, the principal components are the eigenvectors v_i of the sample correlation matrix, and the first component will be the eigenvector with the highest eigenvalue.

Given that Γ is a symmetric matrix, there are as many eigenvalues λ_i as manifest variables; in addition, the equal in number corresponding eigenvectors v_i can be chosen in such a way that they are of unitary length and orthogonal to each other.

Importance of PCA lies in the fact that factors must be extracted from PCA components; in other terms, a decision is to be made about what components should be retained and exploited in the following steps featuring the factor analysis. The most widely accepted criterion is the so-called Kaiser's rule, which states that only components whose eigenvalues are greater than one should be preserved. As already specified, eigenvalues represents the total amount of variance explained by the single components, where the overall variance corresponds to the number of variables, given that they are standardised, that is they have unitary variance. A second graphical method for determining the number of factors is the so-called *scree test* and involves the examination of a scree plot, which is a graph representing the magnitude of each eigenvalue plotted against their ordinal number. In a typical scree plot, the magnitude of the first eigenvalues is relatively high before dropping off dramatically. The resulting line shapes a sort of knee representative of the fact that additional eigenvalues provide limited information with negligible contributions in explaining the total variance of the phenomenon. Consequently, only the components in the sharp descent of the line before the knee should be retained in accordance to this criterion (Stevens, 2002).

A third possibility consists of keep as many components as will account for a certain amount of total variance, usually the seventy percent at least (Stevens, 2002; Costello & Osborne, 2005).

After extraction of the most informative factors, they must be properly interpreted. They are obtained as a linear combination of the original variables and may express latent new variables embodied to the structure of sampled data. However, their interpretation and comprehension may be difficult. A possible solution consists in analysing the values assumed by loadings.

By referring to the example of Figure 4.1, if a new factor presented high loadings for anxiety, shyness, depression, insecurity and upset, it could be interpreted as a manifestation of emotional instability.

However, realisation of the underlying aspects represented by extracted factors can be significantly facilitated by proper rotation of the new reference system described by the factors extracted from the PCA (Field, 2009). As already specified, manifest variables can be expressed as a linear combination of the common factors and appear as vectors of unitary length, whose projection on factors give the loadings of Equation 4.3. A proper rotation of the factors, that is the axes of this new reference system, can bring them closer to the vectors

representing the manifest variables, with a reduction of the angular distances between their direction. As can be appreciated by **Figure 4.3**, where the manifest variables are represented by numbered vectors, certain variable projections are close to zero. This implies that part of the new loadings assumed by the manifest variables in this rotated reference system can be neglected, with a possible greater ease of unveiling the true meaning brought by the factors (**Figure 4.3**). The solution offered by factor analysis could be simplified with no alteration to its mathematical properties (Seltman, 2004; Field, 2009).

Researcher may decide to exploit orthogonal or oblique rotation. In the former, rotated factors remain uncorrelated with each other, and the size of the obtained loadings embodies the extent of the relationship between each observed variable and each factor.

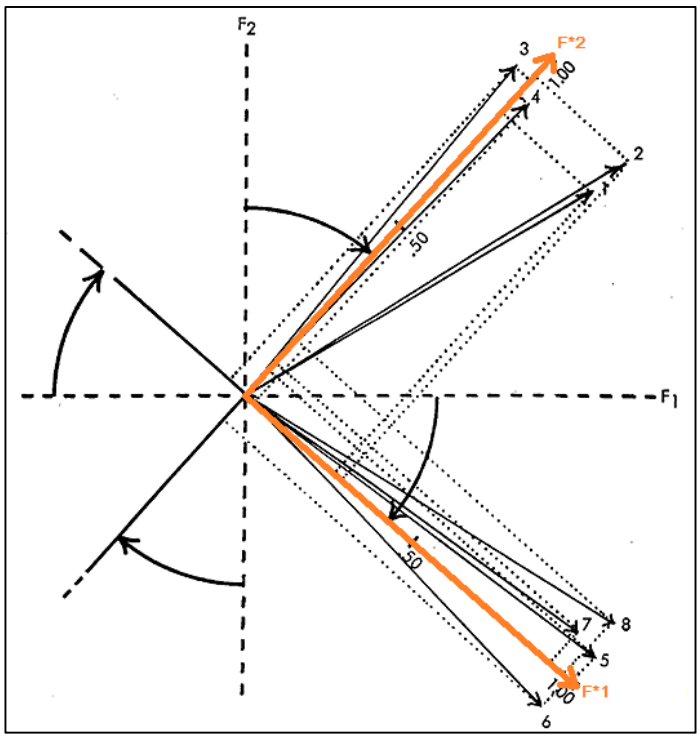

Figure 4.3 Orthogonal factor rotation. Vectors representing the manifest variables now correlate nearly perfectly with the two rotated factors.

The goal of factor analysis is to obtain underlying factors representing unique aspect of the underlying structure of the investigated phenomenon. Orthogonal rotation is then preferred to the oblique one, where factors are instead correlated with each other. Oblique rotation is usually adopted when the analyst has prior knowledge about the investigated phenomenon, with particular reference to the associations between the extracted factors themselves (Seltman, 2004). Such

deductive hypotheses were not available for this study; consequently, only orthogonal rotation has been adopted in this study. There are different types of orthogonal rotation procedure of which *Varimax* is the most commonly used.

For Varimax, a simple solution means that each factor has a small number of large loadings and a large number of zero, or small at least, loadings. This simplifies the interpretation because, after a Varimax rotation, each original variable tends to be associated with a small number of factors, and each factor represents only a small number of variables (Widaman, 1993; Stevens, 2002; Field, 2009)

Formally, Varimax searches for a rotation (i.e. a linear combination) of the original factors such that the variance of the loadings is maximized, which amounts to maximizing:

$$V = \sum \left(q_{j.l}^2 - \bar{q}_{j.l}^2\right)^2$$

where:

- $q_{j.l}^2$: square loading of the j-th variable on the l factor;
- $\bar{q}_{j.l}^2$: mean of the squared loadings.

This general brief description about the essence of factor analysis ends with emphasis placed on the fact that factor analysis consists in a sort of attempt to unveil concealed information about data collections apparently deprived of meanings and findings. The researcher cannot pretend to achieve a complete framework about the investigated phenomenon, and subsequent deepener analyses must be performed.

Particularly critical is the extraction of factors, a step that profoundly influences the resulting residuals between actual correlation matrix and that estimated by factor analysis. Even the addition of a single component in the group of extracted factors can bring remarkable different outputs.

As a result, despite there are various criteria for deciding which PCA components should be retained, plus iterations are required so as to find the best fitting solution with real data (Costello & Osborne, 2005).

4.3.4 Application of Factor analysis

In the followings, an exemplifying application of factor analysis is reported. Data collected refer to geometric features of legs from which vehicles involved in *single vehicle run-off crashes* entered the roundabout. In detail. 18 geometric aspects were recorded for 36 legs; therefore, a 36*18 sample matrix was obtained. The aim is to verify the existence of a well-defined geometric layout covered behind these 36 legs in order to possibly understand the design choices that increase the likelihood of run-off crashes.

The starting point for factor analysis technique is the correlation matrix. If unreliable correlations exist among variables, and those variables are involved into a factor analysis, the resultant factors could be affected by high uncertainties. The first step should be to verify that variables in the population correlation matrix are uncorrelated. If this hypothesis cannot be rejected, there is no reason to do a principal component analysis and consequently a factor one since the variables have nothing in common. The Bartlett's sphericity test specifically assesses the null hypothesis that the correlation matrix is an identity matrix whose all the diagonal elements are 1 and all off diagonal elements are 0 (Field, 2009). The direct implication of the null hypothesis is that covariates are reciprocally uncorrelated. Obviously, searching for factors able to share information provided by uncorrelated factors would be completely useless.

Subsequently to the Bartlett's sphericity test, the adequacy of the collected sample must be verified for realising whether factor analysis may provide proficient results or not. The measure of *Kaiser-Meyer-Olkin* (KMO) statistic predicts if collected data are likely to factor well, based on correlation and partial correlation.

There is a KMO statistic for each individual variable, and their sum is the KMO overall statistic. To compute KMO statistic, a fraction must be calculated. The numerator is the sum of squared correlations of all variables in the analysis, with the exception of the unitary self-correlations of variables with themselves. The denominator is equal to the same sum of the numerator plus the sum of squared partial correlations of each *i-th* variable with *j-th* each variable, where i ≠ j.

This ration is analytically expressed by Equation 4.4:

$$KMO = \frac{\sum_i \sum_{i \neq j} r_{ij}^2}{\sum_i \sum_{i \neq j} r_{ij}^2 + \sum_i \sum_{i \neq j} a_{ij}^2} \tag{4.4}$$

where:

- r_{ij}^2: squared correlation between *i-th* and *j-th* manifest variables;
- a_{ij}^2: squared partial correlation between *i-th* and *j-th* manifest variables.

Partial correlation represents the correlation between the two variables after common variance with other covariates has been removed from both of them. Consequently, it can be stated that partial correlation is a measure of the strength of linear dependence between a pair of variables with the exclusion of possible influences coming from other covariates.

Partial correlation can be intuitively understand in different ways.

The first one is based on a geometric perspective (Rummel, 1970). As an example, three normalised variables are represented as vectors belonging to a third dimensional Euclidean space (**Figure 4.4**). If variable X_3 was at right angle to the other two variables. X_1 and X_2 would be independent of it. Conversely, the X_1 and X_2 projections onto a plane orthogonal to X_3 would be uncorrelated with the third covariate. It can be analytically shown that the cosine of the angle between two random vectors is identical to their correlation coefficient. By considering the

angle described by the projections of X_1 and X_2 onto the aforementioned plane, its cosine can be intuitively interpreted as a measure of the partial correlation between the two variables. Possible influences of X_3 on the linear relationship between X_1 and X_2 are prevented by working on a plane at right angle to the third covariate.

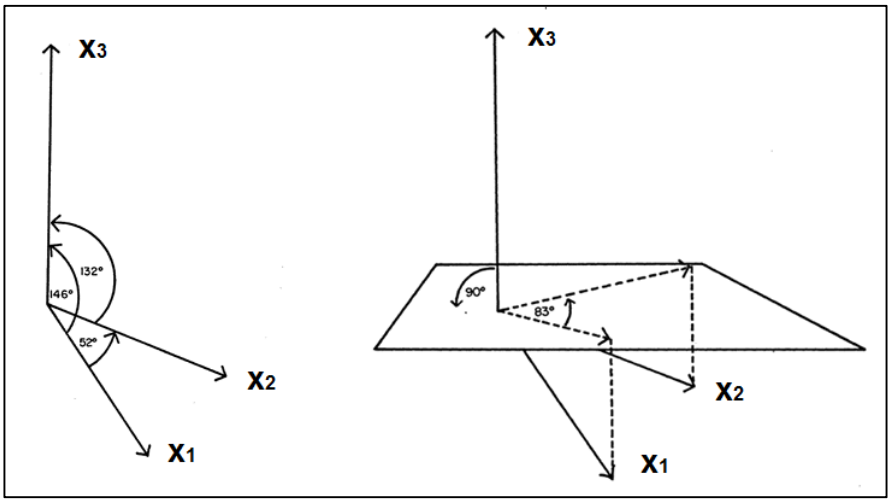

Figure 4.4 Graphical representation of partial correlation between two variables. The common variance with the other covariates is removed from the calculation. Practically, a correlation is calculated between the two variables derived of their variance shared with other covariates.

Image source: https://www.hawaii.edu/powerkills/UC.HTM

The second intuitive approach for understanding what partial correlation refers to lies in Venn's diagrams where the variances of variables are depicted as circles of unitary area (Cohen & Cohen, 2010). With reference to **Figure 4.5**:

- Total variance of X_2 = a+b+c+d;
- Correlation between X_1 and X_2 = a+c;
- Partial correlation between X_1 and X_2 = a/(a+d).

It appears clear that the partial correlation is the effectively the correlation between variables X_1 and X_2 with variable X_3 removed from both variables.

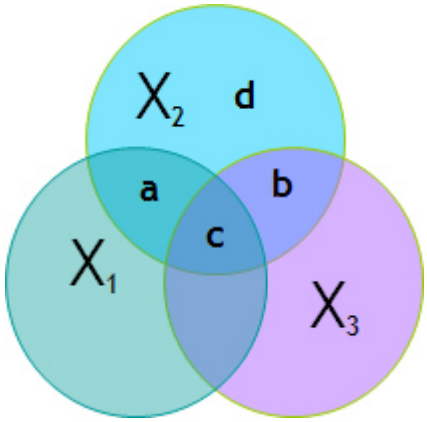

Figure 4.5 Graphical representation of partial correlation between two variables. The common variance with the other covariates is removed from the calculation. Practically, partial correlation is calculated between the two variables derived of their variance shared with other covariates.

Partial correlations should not be very large if distinct factors are expected to emerge from factor analysis. In fact, generally high partial correlations would implies that numerous sampled variables would be predominantly described by a single covariate; in such a circumstance, there could not be components or factors able to explain significant amounts of the whole variance of collected data. Factor analysis would be useless (**Table 4.4**).

As a result, KMO should be great enough in order to support the decision of proceeding with a factor analysis (Field, 2009). Given that KMO varies from 0 to 1, a threshold of 0.6 is conventionally assumed. If it is not, variables with the lowest individual KMO statistic values should be excluded until KMO overall rises above 0.6 (Seltman, 2004).

Taken together, Bartlett's test and KMO measure of sampling adequacy provide a minimum standard which should be passed before a factor analysis should be conducted. If both test are positive, PCA technique is then applied to the collected data in order to find the linear combinations of them that account for as much of the total variable as possible. Among them, the first principal component is the new unveiled variable that explain the maximum amount of the original variable. In this example, both tests are positive, so PCA was then applied (**Table 4.5**).

Table 4.4 Preliminary measures for testing the convenience of factor analysis for uncover concealed information from collected data

KMO Measure of sampling	0.677
Bartlett's test of sphericity (Sig.)	0.000

The analytic operations then proceed to uncover the second linear combination, uncorrelated with the first one, that accounts for the next largest amount of variance. The same criterion is applied for the other components, whose number will be the same of the original covariates. Components are arranged in the same way of Equation 4.3; after all, factors are extracted from them. Therefore. principal components have factor loadings and communality to be determined. As already said, factor loadings express the correlation between a specific observed variable and a certain component. Higher values mean a closer relationship and a better result. The communality is the proportion of each variable's variance that can be explained by the components; it is equal to the sum of squared factor loadings for the variables. Given that PCA analysis takes into account the entire, original variance and no information is lost, all of the communalities are unitary at this step.

The amount of variance accounted for by each component is shown by a quantity called the eigenvalue, which is equal to the sum of the squared loadings for a given component. The higher the eigenvalue, the higher the importance of this component and the probability it will be retained as a factor.

Table 4.5 reports the eigenvalues for all of the components defined by the PCA. They are arranged by decreasing order of magnitude, so that the first components are the most important ones. The total variance corresponds to the number of original variables used in the analysis because they were previously standardised. This can be confirmed by summing all the eigenvalues: the same result will be obtained. The proportion of variance explained by a single component can be determined by the ration between the corresponding eigenvalue and the overall variance. **Table 4.5** shows also the cumulative percentage of variance accounted for by the current and preceding factors.

Table 4.5 Eigenvalues of each component and their contribution in explaining the total variance

Component	Eigenvalues	% of variance	% cumulative
1	2.580	51.591	51.591
2	1.335	26.692	78.283
3	0.496	9.926	88.209
4	0.298	5.962	94.171
5	0.291	5.829	100.000

In accordance Kaiser's rule, only components whose eigenvalues are greater than one should be preserved. Another graphical method for determining the number of factors involves the examination of a scree plot, which graphs the magnitude of each eigenvalue plotted against their ordinal number. The resulting

line usually shapes a sort of knee representative of the fact that additional eigenvalues provide limited information with negligible contributions in explaining the total variance of the phenomenon. Consequently, in accordance to this criterion, only the components in the sharp descent of the line before the knee should be retained (**Figure 4.6**).

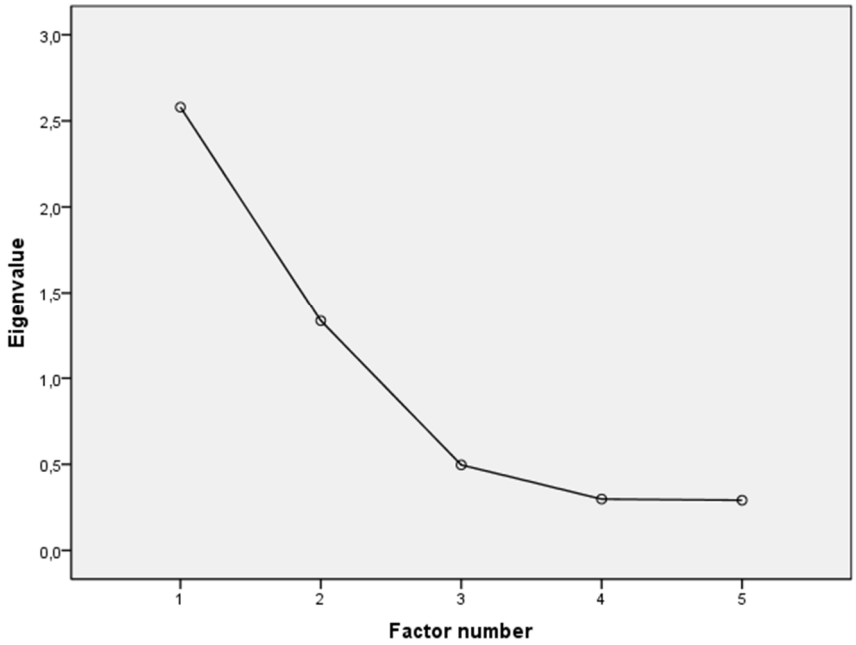

Figure 4.6 *Scatter plot graphing the eigenvalues related to each component*

In this example, the first two components were retained as factors. Both of them have eigenvalues greater than 1.0 and together explain more than 70 per cent of the entire variance. **Table 4.6**reports their loading factors for the manifest variables.

Table 4.6 Component matrix showing loadings of each variable

Manifest variables	*Extracted factors*	
	1	**2**
ICD	-0.849	0.206
R1	0.499	0.734
Angle of visibility	0.721	-0.557
R3	0.581	0.640
Entry angle	0.868	-0.186

Table 4.7 shows the communalities of each manifest variable for the two extracted factors, that is the proportion of each variables' variance explained by the retained factors.

Table 4.7 *Factor matrix showing loadings of each variable after Varimax rotation*

	Initial	*After extraction*
ICD	1.000	0.763
R1	1.000	0.787
R3	1.000	0.747
Angle of visibility	1.000	0.830
Entry angle	1.000	0.787

By analysing signs and values of factors (**Table 4.6**), their underlying and latent meaning may be realised.

The first factor seems to bring out entries with high design speeds. This geometrical arrangement could be consistent with pronounced entry and visibility angles; the negative correlation with inscribed circle diameter seems to confirm this interpretation. In fact, roundabouts require limited dimensions for inducing drivers to slow down thanks to the deviation imposed to their path when manoeuvring through the roundabout.

The second factor is even more difficult to interpret because the angle of visibility too now presents a negative correlation. An orthogonal rotation factor is then applied by following the Varimax criterion where the aim is to reduce for each factor the number of loadings significantly different from zero. This is obtained by rotating the new reference system in order to bring factors as near as possible to vectors representing the manifest variables.

The new factor loadings are listed in Table 4.8 and graphed in Figure 4.7.

Table 4.8 *Factor matrix showing loadings of each variable after Varimax rotation*

Manifest variables	*Extracted factors*	
	1	**2**
ICD	-0.836	-0.252
R1	0.059	0.885
Angle of visibility	0.904	-0.115
R3	0.177	0.846

Entry angle	0.842	0.279

Previous suppositions about the latent essence of the first factor have been confirmed by Varimax rotation. Now, the only geometric features with significant loading are ICD, Angle of visibility and the Entry angle. Therefore, the first factor is effectively focused on fast approaches. Particularly interesting is the correlation captured by factor analysis between entry angle and angle of visibility, which are design parameters identified by different National standards and not implemented by Italian requirements (Highway Agency, 2007; NCHRP, 2010). It is actually true that increasing the angle of visibility corresponds to a greater entry angle, as can be seen by **Figure 4.7**. Factor analysis proved to be able to identify the relationship despite an overly wide and diversified sample of roundabout legs built in a geographical context where roundabout design principles do not involve these two parameters. This is an evident demonstration of potentialities that factor analysis can guarantee when

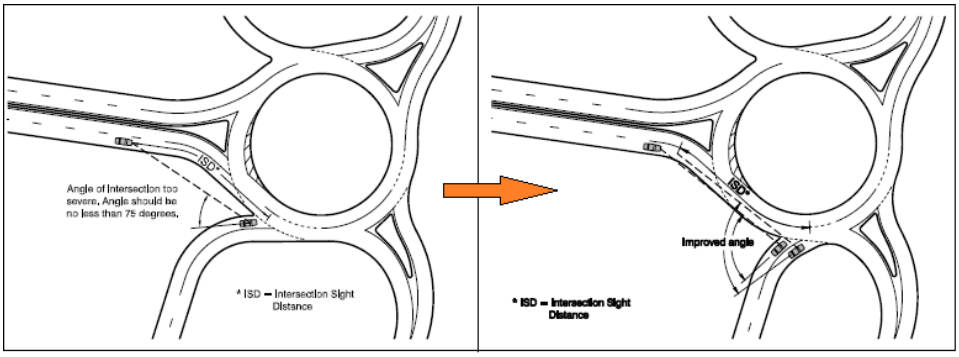

Figure 4.7 Improving the angle of visibility necessarily implies an increment of entry angle

Source: NCHRP Report No.672

Varimax has improved the interpretation of the second factor too. It is clear that it highlights roundabout legs with relevant entry and exit design speeds. Therefore, it can be stated that Varimax rotation has actually allowed better understanding the latent significances behind the factors. They both refer to entries characterised by high design speeds.

Figure 4.8 shows that the loadings of the manifest variables tend to be substantially concentrated on the two factors, which have simplified the interpretation of them.

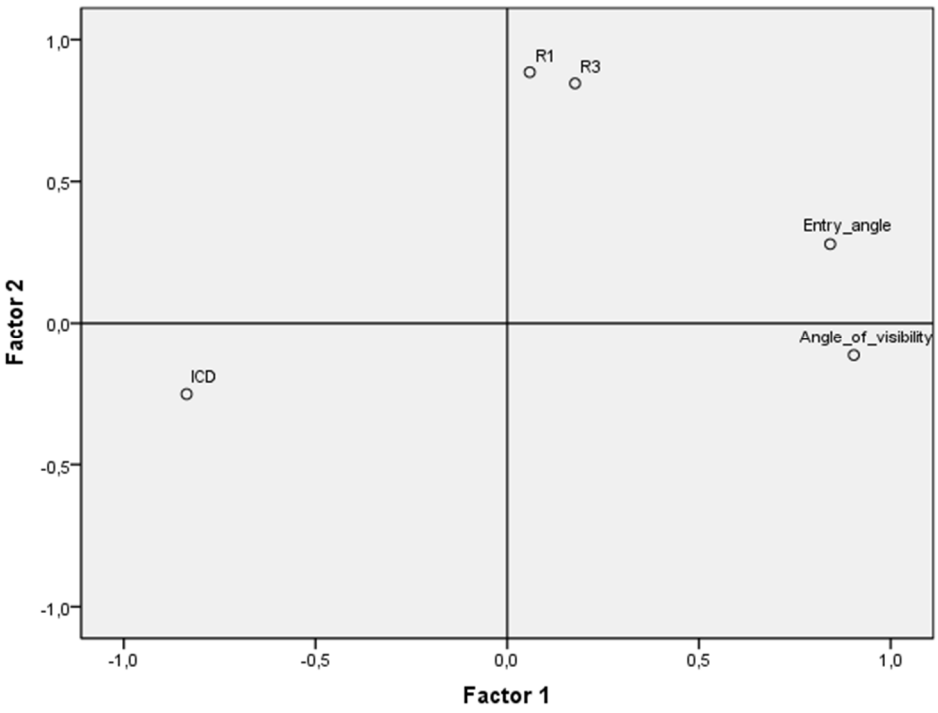

Figure 4.8 *Factor plot in rotated factor space.*

As already explained, the reproduced matrix correlation based on the extracted factors can be obtained from the matrix loadings (**Table 4.8**). It is desirable that corresponding values of the two variables are as close as possible, that is that residuals are close to zero. If the reproduced matrix was very similar to the original correlation matrix, this would prove the success of factor analysis, with extracted factors able to account for a great amount of the original variance. A threshold value of 0.05 is assumed for determining whether the obtained residual can be actually neglected. The limit condition is not respected by the fifty percent of the residuals. This implies that factor analysis, with its simplified perspective on the collected data, has not been able to perfectly reproduce the original framework of sampled information (**Table 4.9**). By visioning the magnitude of variable loadings, it stands out that fast entries with high entry path radius probably increase the likelihood of single vehicle run off crashes. However, given the significant discrepancies between estimated and sample correlation matrix, no definitive evidence has been found. Additional exploratory analyses are required.

Table 4.9 In the top part of the table there are the reproduced correlations, while the bottom part contains the residuals obtained by the difference with the sample correlation matrix.

		ICD	*R1*	*Visibility angle*	*R3*	*Entry angle*
Reproduced Correlation	*ICD*	0.763[a]	-0.273	-0.727	-0.361	-0.775
	V	-0.273	0.787[a]	-0.049	0.759	0.297
	Visibility angle	-0.727	-0.049	0.830[a]	0.062	0.729
	R3	-0.361	0.759	0.062	0.747[a]	0.385
	Entry angle	-0.775	0.297	0.729	0.385	0.787[a]
Residuals[b]	*ICD*		-0.034	0.102	0.084	0.111
	V	-0.034		0.039	-0.212	-0.047
	Visibility angle	0.102	0.039		0.043	-0.092
	R3	0.084	-0.212	0.043		-0.001
	Entry angle	0.111	-0.047	-0.092	-0.001	

Extraction method: principal component analysis.
a. Reproduced communalities.
b. Residuals are computed between observed and reproduced correlations. There are 5 (50.0%) non redundant residuals with absolute values greater than 0.05.

Differently from PCA components where no information vanishes, extracted factors inevitably simplify the original framework of collected data. As a result, each factor presents the already introduced uniqueness, which takes into account the portion of variance that cannot be explained by latent factors, such as, for example, differences between subjects and the error variance inevitably affecting each survey response.

The presence of uniqueness make it impossible to exactly express factors as functions of original variables because there would be more factors than variables. Approximation methods must be used. IBM® SPSS 21, the statistical package software adopted for performing part of the analyses performed in this study, uses as default method a least squares regression approach (IBM Support Portal, 2012). It is based on regression equations where factor scores are the dependent variables while the independent ones are represented by the standardised observed values assumed by the original variables for each different subject. The covariates are weighted by regression coefficients obtained by multiplying the inverse of the sample correlation matrix by the matrix of factor loadings. Under this process, the computed factor scores are standardised to a mean of zero with a unitary standard deviation.

Table 4.10 provides the Matrix Score for this example.

Table 4.10 Component matrix showing loadings of each variable

	ICD	*R1*	*Visibility angle*	*R3*	*Entry angle*
F1	-0.362	-0.112	0.452	-0.049	0.361
F2	-0.034	0.572	-0.218	0.527	0.050

As already specified, factor analysis should be applied for different sets of manifest variables until the best reproduction of sample correlation matrix is found (Costello & Osborne, 2005).

The corresponding manifest variables will receive additional attention in the subsequent more detailed exploratory analyses.

4.4 Discriminant Analysis

A conceptual evolution of factor analysis is the discriminant analysis (DA). In fact, DA also looks for linear combinations of variables which best explain the data. The difference is that sample survey have affected different groups of the same population, and the aim of the research is now focused in trying to model as well as possible the discrepancies existing between these groups (Burns & Burns, 2009; Agresti, 2010). From this standpoint, directions must be sought where projections of sampled data coming from separate categories can be differentiated to the greatest possible extent.

The concept of separation between population should be introduced before describing DA procedures.

Collected data are grouped in different classes on the base of values assumed by the variable of primary interest (i.e. *criterion variable*). Each of this group is a point cloud with a barycentre and an internal dispersion. The external dispersion refers to the point cloud whose barycentre is the one related to the entire sample and its other elements are the barycentre of each group.

It can be demonstrated that the distances between categories reach the greatest possible values when data points are projected on a direction such that internal dispersion is minimised and the external one is maximised. This direction is defined by the eigenvector corresponding to the lowest eigenvalue of the matrix obtained by the product between the inverse of correlation matrix and the within-groups correlation matrix (Baldi, 1999).

Figure 4.9 offers a pictorial explanation of DA. There are only two groups (withes and blacks) and two manifest variables. The new axis represents a new variable (i.e. discriminate function) which is a linear combination of the original variables. The two groups can be separated by these two variables, but there is a remarkable amount of overlap on each single axis. Conversely, dispersions of sampled point projected on the new directions do not intersect at all. For each

case, a D score is produced by means of the discriminate function, and a threshold value is defined so as to sampled points can be assigned to the correct group. If the discriminant score is less than or equal to the cut-off, the case is classed as a white member, otherwise as a black one.

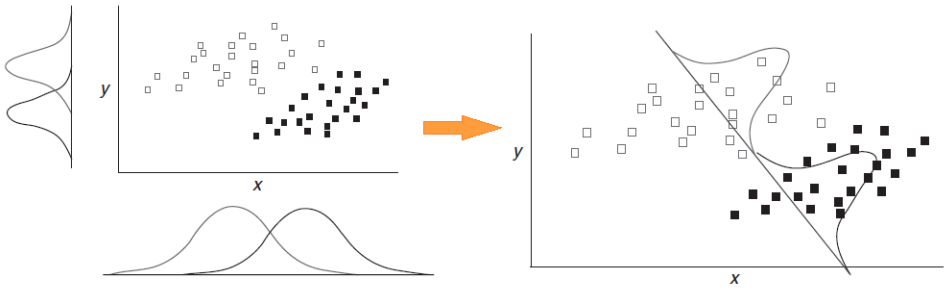

Figure 4.9 Pictorial explanation of discriminant analysis. Scatter plot with distribution of sample points along the axes. New axis has improved discrimination between the two groups.

Source:http://www.uk.sagepub.com/burns/website%20material/Chapter%2025%20-%20Discriminant%20Analysis.pdf

For this study, each roundabout leg has been associated with a categorical entity ranging from 1 to 3 after having evaluated its crash records. Discriminant analyses here conducted have the purpose of finding the linear combinations of manifest variables such that different safety performances of these groups are maximised. Therefore, the outcome is quite similar to a multiple linear regression, with the difference that dependent variable is not an estimated mean value pertaining to the analysed population but rather a global score allowing correct classification of elements (Equation 4.5).

$$D = v_1X_1 + v_2X_2 + v_3X_3 + \cdots v_iX_i + \cdots + v_nX_n + a \tag{4.5}$$

where:

- D: discriminate function;
- v_i: discriminant coefficient of the *i-th* variable;
- X_i: respondent's score for *i-th* variable;
- a: constant;
- n: number of predictor variables;

Each leg will take on as many D values as the number of the adopted discriminate functions. This will allow to assign legs to one of the three groups referencing to the different historic safety performances, from 1 (the category with the best results) to 3 (worst historic records).

DA allows reaching a more detailed view as compared to factor analysis because it clearly shows the contribute offered by geometric features in discriminating groups characterised by different safety performances. Good predictors tend to have large discriminant coefficients.

Factor analysis cannot take into account historic crash records. It simply attempts to simplify the whole amount of information in this case represented by the geometric parameters of legs involved in a fatal or death crash at least, with no additional specification for past crash events. Definitively, DA has the potential to provide a deep insights onto the relationship between geometric layout of roundabouts and their crash frequency.

4.4.1 Application of discriminant analysis

An application of discriminant analysis to the origin legs of vehicles having experienced fatal or injury single vehicle run-off crashes is here proposed. IBM® SPSS package software has been used for conducting discriminant analyses. The set of manifest variables which best reproduced the sample correlation matrix in factor analysis has been exploited in the discriminant analysis. Subsequently, stepwise procedures have been applied in order to refine the arrangement of parameters and individuate the most decisive ones. There are 5 initial geometric parameters and 36 legs which will be assigned to one of three groups defined on the base of their crash frequency magnitude. **Table 4.11** offers an overview about collected data.

Table 4.11 Group statistics

Class frequency		*Mean*	*Std. deviation*	*Valid cases*
1	ICD	69.3091	32.5477	22
	R1	45.5804	11.0688	22
	R3	96.2850	64.8785	22
	Entry angle	51.9545	12.1713	22
	Angle of visibility	75.3636	28.4396	22
2	ICD	78.1920	29.7393	10
	R1	48.0725	7.6565	10
	R3	69.1750	21.8970	10
	Entry angle	42.3000	10.3928	10
	Angle of visibility	67.7000	26.8991	10
3	ICD	53.3750	17.8109	4
	R1	72.1928	16.0827	4

	R3	337.2125	313.0506	4
	Entry angle	59.2500	29.2731	4
	Angle of visibility	66.2500	31.7949	4
Total	ICD	70.0061	30.6804	36
	R1	49.2296	13.4079	36
	R3	115.5242	132.3328	36
	Entry angle	50.0833	14.8061	36
	Angle of visibility	72.2222	27.8230	36

Within-groups correlation matrix is provided by **Table 4.12**.

Table 4.12 Within-groups correlation matrix. It corresponds to a correlation matrix of data points obtained by subtracting to them the barycentre of the group they belong to. Multicollinearity should not represent a possible concern for discriminant analysis given that no value is greater than 0.8.

	ICD	*R1*	*R3*	*Entry angle*	*Angle of visibility*
ICD	1.000	-0.260	-0.192	-0.645	-0.648
R1	-0.260	1.000	0.297	0.188	0.062
R3	-0.192	0.297	1.000	0.304	0.179
Entry angle	-0.645	0.188	0.304	1.000	0.671
Angle of visibility	-0.648	0.062	0.179	0.671	1.000

First of all, significant differences between groups on each of the independent variables are to be examined. If there were not significant differences between groups, it would not be meaningful proceeding any further with the analysis (Burns & Burns, 2009). From this standpoint, a summary vision of Group statistics represented in **Table 4.11** shows remarkable differences between the three sub-populations for entry and exit path radius

Table 4.12 shows two tests which can be used to evaluate the potential of the considered manifest variables in discriminating the three groups before the model is created. In particular, the significance of differences in group means for each variable is tested.

Wilks' Lambda is a direct measure of the proportion of variance in the combination of dependent variables that is unaccounted for by the independent variable. If a large proportion of the variance is accounted for by the independent variable then it suggests that there is an effect from the independent variable and that the groups have different mean values. In detail, the quantity (1 - Wilks' Lambda) is the proportion of variance in the dependent variable that can be explained by the considered predictor.

Therefore, a relatively small Wilks' Lambda value indicates that the analysed covariate has a potential in discriminating groups (Burns & Burns, 2009).

The other columns of Table 4.12 refers to an F-test performed in a one-way analysis of variance (ANOVA). The null hypothesis is that all population means are equal in regard to a particular variable; the alternative hypothesis is that at least one mean is different.

The F-test statistic is found by dividing the between group variance by the within group variance. The degrees of freedom for the numerator are the degrees of freedom for the between group (i.e. number of groups minus one) and the degrees of freedom for the denominator are the degrees of freedom for the within group. **Table 4.13** also reports the p-value related to the ANOVA test.

The p-value tests the null hypothesis that data from all groups are drawn from populations with identical means. Therefore, the p-value represents the chance that random sampling provides means with reciprocal distances at least greater than or equal to those observed in the survey.

If the null hypothesis is true, that is sub-populations really have the same means, F is expected to have a value close to 1.0; therefore, a large F implies that the variation among group cannot be entirely explained by chance. The threshold value of 0.05 is conventionally assumed in statistic studies. As a result, if p values are higher than 0.05, it can be stated that differences in group means related to the considered variable are effectively statistically significant.

The null hypothesis can be rejected. As can be seen by **Table 4.13**, both Wilk's lambda test and the ANOVA seem to suggest that only entry and exit path radius may discriminate the three sub-populations.

Table 4.13 Test of equality of group means table

	Wilks' Lambda	**F**	**df1**	**df2**	**p-value**
ICD	0.946	0.946	2	33	0.398
R1	0.616	10.282	2	33	0.000
R3	0.631	9.652	2	33	0.001
Entry angle	0.867	2.527	2	33	0.095
Angle of visibility	0.979	0.351	2	33	0.707

After this preliminary insight into potential of each manifest variable in separating sub-populations characterised by different crash frequency, discriminant functions can now be sought. The maximum number of discriminant functions produced is equal to the number of groups minus 1 (Burns & Burns, 2009). As a result, in this example, there are only two directions of interest; their eigenvalues and their contribution in explaining original variance are shown in **Table 4.14**. The canonical correlation is the multiple correlation between two sets of variables. The first is constituted by the manifest variables, while the second

refers to the dummy variables used for coding the three considered groups of different crash frequency. A high correlation indicates a function that discriminates well (Field, 2009).

Table 4.14 Eigenvalues table

Function	Eigenvalue	% of variance	% cumulative	Canonical correlation
1	0.981[a]	87.1	87.1	0.704
2	0.145[a]	12.9	100.0	0.355

The canonical correlation is then exploited in the statistical methods devoted to ascertain the significance of the acquired discriminant functions.

The focus is on the means of the independent variables. If they were equal for all of the three groups, these means would not be a useful basis for predicting the group to which a case belongs. As result, canonical correlation of discriminant functions would be equal to zero, with no relationship between the set of independent variables and the discriminant scores (i.e. the dependent variable). The discriminant functions would be worthless because the means of the discriminant scores would be the same in the considered groups (Burns & Burns, 2009).

This is exactly the null hypothesis of the Willk's lambda statistical test, by means of which it is possible to establish the significance of the discriminant functions. Wilks' lambda is the proportion of the total variance lying in the discriminant scores not explained by differences among the groups. It is calculated as the product of the values of *1-canonical correlation*^{2}. Therefore, smaller values of Wilks' lambda are desirable. In this example, canonical correlations are 0.704 and 0.355, so the Wilks' Lambda testing both canonical correlations is (1-0.704^2)*(1-0.355^2) = 0.441, and the Wilks' Lambda testing the second canonical correlation is (1-0.355^2) = 0.874.

The Chi-square statistic tests whether the canonical correlation of discriminant functions is equal to zero, which implies a unitary Wilk's lambda. This is exactly the null hypothesis, a situation characterised by a negligible contribution offered by discriminant functions in explaining the total variance of the independent variables.

Table 4.15 represents the output of Willk's lambda statistical test carried out on the two discriminant functions obtained for this example. The Chi-square statistic is compared to a Chi-square distribution with the degrees of freedom stated in the specific column of the table. It is also indicated the p-value associated with the Chi-square test. If this p-value is less than the significance level, usually established as 0.05, the null hypothesis is rejected. If not, the null hypothesis cannot be rejected, and no definitive conclusions can be drawn. The first test presented in this table tests both canonical correlations ("1 through 2") and the second test presented tests the second canonical correlation alone.

Table 4.15 Wilk's lambda table

Function	Wilks' Lambda	Chi-square	df	p-value
1 through 2	0.441	25.376	10	0.005
2	0.874	4.188	4	0.381

The first line of **Table 4.15** tests the null hypothesis that the mean discriminant scores for the two possible functions are equal in the subgroups of the dependent variable. Since the probability of the chi-square statistic for this test is less than 0.05, the null hypothesis can be rejected, and it can be stated that there is at least one statistically significant function. If the probability for this test had been larger than 0.05, the definitive conclusion would have been that concluded that there are no discriminant functions to separate the groups of the dependent variable.

Discriminant analysis would have been concluded here (Burns & Burns, 2009).

The second line of the Wilks' Lambda table tests the null hypothesis that the mean discriminant scores for the second possible discriminant function are equal in the subgroups of the dependent variable. Since the probability of the chi-square statistic for this test is greater than 0.05, the null hypothesis cannot be rejected. In conclusion, there is only one discriminant function to separate the groups of the dependent variable.

Table 4.16 provides the standardised coefficients for the two discriminant functions. Their interpretation enable unveiling the latent aspects they represent, in a similar way to the identification of the meaning embraced by factors adopted in factor analysis. The sign indicates the direction of the relationship, while the magnitudes define how strongly the discriminating variables effect the score (Field, 2009).

As for the first function, the only one that actually separates the three groups, Entry and Exit path radius have the preponderant coefficients. Entry angle and Angle of visibility score were less successful as predictors, while ICD score is insignificant.

Table 4.16 Standardised canonical discriminant function coefficients table

	Functions	
	1	2
ICD	-0.082	0.019
R1	0.583	-0.549
R3	0.597	0.152
Entry angle	0.156	1.164
Angle of visibility	-0.376	-0.434

The standardised coefficients of **Table 4.16** together with standardised independent variables can be used to calculate the standardised discriminant score for a given case. The distribution of the scores from each function will be then standardized to have a mean of zero and standard deviation of one. For discriminant function 1, score achieved by a new case will be equal to (Equation 4.5):

$$D_1^* = -0.082 * ICD^* + 0.583 * R1^* + 0.597 * R3^* + 0.156 * (Entry\ angle^*) - 0.376 * (Angle\ of visibility^*) \quad (4.5)$$

There is an alternative way of specifying the relative importance of the predictors. The structure matrix table (**Table 4.17**) provides the correlations of each independent variable with the discriminant functions (Burns & Burns, 2009; Field, 2009). These correlations serve as factor loading in factor analysis. By identifying the largest loadings, the researcher gains an insight into how to correctly interpret the discriminant function.

Table 4.17 Structure matrix table

	Functions	
	1	**2**
R1	0.788	-0,317
R3	0.766	0,261
Entry angle	0.247	0,803
ICD	-0.204	-0,336
Angle of visibility	-0.076	0,328

Pooled within-groups correlations between discriminating variables and standardised canonical discriminant functions. Variables ordered by absolute size of correlation within function.

Loadings of Entry and exit path radius stand out as predictor strongly influencing the allocation of legs to the three groups characterised by different frequency values for single run-off crashes. Structure matrix table confirms the vision obtained standardised canonical distribution function coefficients.

Discriminant functions are eventually created by unstandardized coefficients, which are reported in **Table 4.18**. Non standardised values of manifest variables will give the score for the discriminant functions. The greatest coefficients are referred to entry and exit path radius again.

Table 4.18 Canonical discriminant function coefficients table. Unstandardized coefficients

	Functions	
	1	**2**
ICD	-0.003	0.002
R1	0.053	-0.031
Angle of visibility	-0.013	0.003
R3	0.006	0.000
Entry angle	0.014	0.070
(Constant)	-2.813	-2.378

A further way of interpreting the DA results is insert the average discriminant score (non standardised) in the three groups (**Table 4.19**). In detail, the discriminant score for each group when the variable means (rather than individual values for each case) are entered into the discriminant equation. These group means are called centroids.

Table 4.19 Functions at group centroids table

	Functions	
Class frequency	**1**	**2**
1,00	-0.275	0.312
2,00	-0.437	-0.494
3,00	2.685	-0.081

Unstandardized canonical discriminant functions evaluated at group means

SPSS also provides a graphical representation of DA output. As can be seen from **Figure 4.10**, the contribution offered by the second discriminant function is effectively negligible.

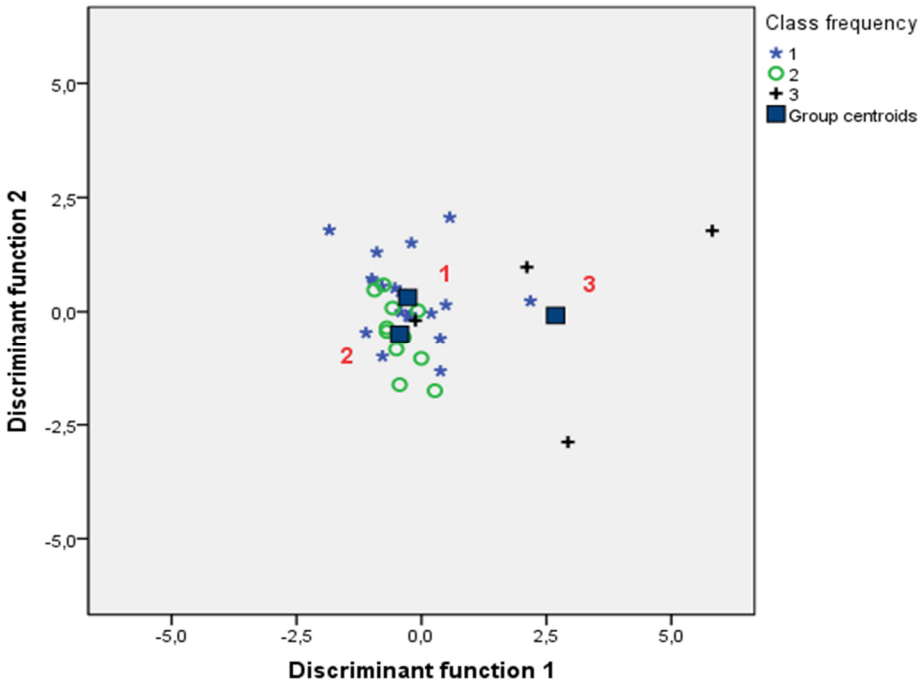

Figure 4.10 Graph of individuals on the discriminant dimensions.

The output of discriminant analysis is the classification table, whose rows are the observed categories of the dependent variable while the columns are the predicted categories. When prediction is perfect all cases lie on the diagonal. The percentage of cases on the diagonal is the percentage of correct classifications. The cross validated set of data is a more authentic representation of the outcome achieved by discriminant function. The cross validation is often termed a 'jack-knife' classification, given that successively classifies all cases but one to develop a discriminant function and then categorizes the case that was left out. This process is repeated with each case left out in turn. This cross validation produces a more reliable function. The ratio is that one should not use the case the researcher is trying to predict as part of the categorization process. The classification results for the crash type "Single vehicle run-off" (**Table 4.20**) reveal that 44.3% of legs were classified correctly into the three categories of crash frequency. The third group suffers from the least accuracy.

This overall predictive accuracy of the discriminant functions is called the 'hit ratio'. Via a random classification of the collected legs, there would be a 33.3% probability of correctly collocating the 36 subjects into the three categories (Burns & Burns, 2009).

Accordingly to a conventional approach, acceptable hit ratios must be greater than this probability increased by 25%, which gives a threshold value equal to 41.63%. The output of discriminant analysis seems to be up to standard.

Table 4.20 Classification results table.72,2% of original grouped cases correctly classified. 50,0% of cross validated grouped cases correctly classified.

			Predicted group membership			
		Class frequency	**1.00**	**2.00**	**3.00**	**Total**
Original	Count	1.00	15	4	1	20
		2.00	4	8	0	12
		3.00	0	1	3	4
	%	1.00	75.0	20.0	5.0	100.0
		2.00	33.3	66.7	.0	100.0
		3.00	.0	25.0	75.0	100.0
Cross-validated [a]	Count	1.00	10	9	1	20
		2.00	5	7	0	12
		3.00	1	2	1	4
	%	1.00	50.0	45.0	5.0	100.0
		2.00	41.7	58.3	.0	100.0
		3.00	25.0	50.0	25.0	100.0

a. Cross validation is done only for those cases in the analysis. In cross validation, each case is classified by the functions derived from all cases other than that case

A discriminant analysis was then conducted to predict the categorical variable *crash frequency* for analysed roundabout legs. Predictor variables were inscribed circle diameter, entry radius, radius of deflection, angle of visibility and entry angle. These are the same geometric features previously identified via the factorial analysis. Significant mean differences were observed for entry radius and radius of deflection. Only one of the two discriminate functions was found to be statistically significant, that is able to effectively separate legs of different crash frequency category. By analysing the standardised coefficients of the discriminant function and the pooled within-groups correlations of the structure table matrix, conclusion can be drawn that entry radius and radius of deflection are the only predictors which can explain safety performances of roundabout legs in regard to the crash type single vehicle run-off.

The cross validated classification showed that overall 44.3% of analysed legs were correctly classified. However, the most important finding is that the two radius appear to be the decisive factors for this crash typology. Starting from a list of 19 parameters, now the attention is focused on only two parameters. Further

exploratory analyses were then conducted with the purpose of validating these outcomes and reaching a better insight into the geometric features actually conditioning the dynamics which lead to single vehicle run-off.

4.5 Multiple linear models

In the discriminant analysis, crash frequency figures as a categorical dependent variable which can take on fixed values from a limited set of possibilities.

By interpreting coefficients of discriminate functions, it is possible to identify the geometrical features best discriminating legs with high or low crash frequencies. An improvement would be better understanding how geometric parameters influence likelihood of single vehicle run-off crashes.

In this sense, multiple regression models whit crash frequency as a continuous dependent variable may allow understanding the portion of variance affecting crash frequency explained by the single geometric parameter. Indeed, the core of multiple regression techniques is modelling the relationship between two or more explanatory variable and a response variable by searching for the analytical expression which best fits the observed data. Among these models, the Multiple Linear Regression is the simplest one and offers numerous analytical tools devoted to assess the predictor's contribution in explaining variance of the dependent variable.

All multiple linear regression models can be expressed in the following general form, where the observed value of the variable of interest equals the expected value provided by the linear combination of the covariates corrected by means of a random error (Chiorri, 2010; Weisberg, 2013).

$$Y_i = \beta_0 + \beta_1 x_{i1} + \beta_2 x_{i2} + \cdots + \beta_k x_{ik} + \varepsilon_i \tag{4.5}$$

where:

- Y_i: value assumed by the dependent variable for the *i-th* observation;
- x_{ki}: value assumed by the *k-th* explanatory variable for the *i-th* observation;
- β_k: coefficient of the *k-th* explanatory variable;
- ε_i: random error term related to the *i-th* observation.

The assumptions at the base of the multiple linear regression models refer to the generation process of the *n* collected observations, which can be intended as vectors of *k+1* components $(x_{11}, x_{12}, \ldots, x_{1k}, y_1)$, $(x_{21}, x_{22}, \ldots, x_{2k}, y_2)$,… $(x_{n1}, x_{n2}, \ldots, x_{nk}, y_n)$. The general hypotheses are the following (Chiorri, 2010; Dupont, 2010):

- $Y_i = \beta_0 + \beta_1 x_{i1} + \beta_2 x_{i2} + \cdots + \beta_k x_{ik} + \varepsilon_i$ for each observation i = 1, …, n;

- ε_i are independent random variables normally distributed with an expected value E (ε_i) = 0 and a constant variance V(ε_i) = σ^2.
  Analytically:

  $\varepsilon_i \sim N(0, \sigma^2)$ for i = 1,…, n.
  $V(\varepsilon_i) = \sigma^2$, ∀ i = 1,…, n.
  $Cov(\varepsilon_i, \varepsilon_i) = 0$, ∀ i = 1,…, n, with i≠j.

  The condition of constant variance for the error terms is known as the *homoscedasticity* hypothesis;

- There are no uncertainties affecting the values of explanatory variables;

- Y_i observations are realisations of normally distributed random variables with expected values equal to the linear combination of predictors and the same variance σ^2 of the error term.
  Analytically, $Y_i \sim N(\beta_0 + \beta_1 x_{i1} + \beta_2 x_{i2} + \cdots + \beta_k x_{ik}, \sigma^2)$ for i = 1,…, n.

The last assumption derives from the fact that dependent variable is expressed in the model as the linear combination of a deterministic component and a stochastic one. The error terms represent the discrepancies between the estimated Y_i resulted from the linear combination of predictors, that is the deterministic component, and the *i-th* observation for the variable of interest (Chiorri, 2010).

The first hypothesis may appear to be excessively restrictive, but it should be noted that only the linearity of parameters is imposed. This implies a certain amount of flexibility. Polynomial regression models contain squared and higher order terms of the predictor variables but they are still linear regression models. For example, the following model includes a squared term and even the product between two variables in order to allow for an possible interaction effect.

$$Y_i = \beta_0 + \beta_1 x_{i1} + \beta_2 x_{i2} + \beta_3 x_{i1}^2 + \beta_4 x_{i1} x_{i2} + \cdots + \beta_k x_{ik} + \varepsilon_i$$

This model can be still represented as a multiple linear regression one. In fact, by replacing x_{i3} with x_{i1}^2 and $x_{i1}x_{i2}$ with x_{i4}, it can be obtained the canonical analytical expression of linear regression models.

$$Y_i = \beta_0 + \beta_1 x_{i1} + \beta_2 x_{i2} + \beta_3 x_{i3} + \beta_4 x_{i4} + \cdots + \beta_k x_{ik} + \varepsilon_i$$

Even non-linear regression forms can be re-arranged to a linear model by means of an adequate transformation. For instance, $Y_i = \beta_0 x_{i1}^{\beta_1} \varepsilon_i$ can be rewritten as a linear combination of covariates. In fact, $\ln(Y_i) = \ln(\beta_0 x_{i1}^{\beta_1} \varepsilon_i) = ln\beta_0 + \beta_1 \ln(x_{i1}) + ln(\varepsilon_i)$ and by proper substitution, a linear model is obtained again.

The true regression model is usually never known, as well as the values of the random error terms corresponding to observed data points. However, the regression model can be estimated by calculating the regression coefficients of the model for the available set of observational data.

In a matrix form, Equation 4.6 can be rewritten in this way:

$$Y = X\beta + \varepsilon \tag{4.6}$$

where:

$$Y = \begin{bmatrix} y_1 \\ y_2 \\ \vdots \\ y_n \end{bmatrix} \quad \beta = \begin{bmatrix} \beta_1 \\ \beta_2 \\ \vdots \\ \beta_n \end{bmatrix} \quad \varepsilon = \begin{bmatrix} \varepsilon_1 \\ \varepsilon_2 \\ \vdots \\ \varepsilon_n \end{bmatrix} \quad X = \begin{bmatrix} 1 & x_{1i} & \dots & x_{1k} \\ 1 & x_{2i} & \dots & x_{2k} \\ \vdots & \vdots & \ddots & \vdots \\ 1 & x_{3i} & \dots & x_{nk} \end{bmatrix}$$

Equation 4.6 is then a system of n equation. The matrix X is referred as the design matrix. It contains information about the levels of the predictor variables at which the observations are obtained. The vector β contains all the regression coefficients and can be estimated by using the ordinary least square (OLS) method.

This technique estimates coefficients able to minimise the sum of the squared residuals between the actual value of the dependent variable and the value predicted by the model. The goal is then to find the coefficients of the model through which this function reaches its minimum value:

$$G(\beta) = \sum_{i=1}^{n} (y_i - \beta_0 + \beta_1 x_{i1} + \beta_2 x_{i2} + \cdots + \beta_k x_{ik} + \varepsilon_i)^2$$

It can be demonstrated that required coefficient vector is given by Equation 4.7:

$$\hat{\beta} = (X'X)^{-1}X'Y \tag{4.7}$$

where:

- $\hat{\beta}$: OLS estimate of coefficient vector;
- X': transpose of the design matrix.

The estimated regression model is also referred to as the *fitted model*. The observations Y_i, may be different from the fitted values $\hat{Y}_i$ obtained from this model. As already specified, the difference between these two values is the residual $\boldsymbol{\varepsilon_i}$. The vector of residuals $\boldsymbol{\varepsilon_i}$, is defined as (Equation 4.8):

$$\varepsilon = Y - \hat{Y} \tag{4.8}$$

In particular, ε is a vector of r.v. independently and identically distributed with an expected value equal to zero and a variance-covariance matrix V(εi) = Iσ².

The fitted model can also be written as follows by exploiting Equation 4.7 (Equation 4.9):

$$\hat{Y} = X\hat{\beta} = X(X'X)^{-1}X'Y = HY \tag{4.9}$$

where $H = X(X'X)^{-1}X'Y$ is referred to as the *hat matrix*, which transforms the vector of the observed response *Y* values to the vector of fitted values $\hat{Y}$.The OLS estimates $\hat{\beta}_0, \hat{\beta}_1, \dots, \hat{\beta}_k$ are unbiased estimators of $\beta_0, \beta_1, \dots, \beta_k$, provided that the random error terms are independently and normally distributed. The variance-covariance matrix of estimated regression coefficient is obtained as follows (Equation 4.10):

$$C = \sigma^2(X'X)^{-1} \tag{4.10}$$

C is a symmetric matrix whose diagonal elements C_{jj} represent the variance of the estimated *j-th* regression coefficient $\hat{\beta}_j$. The off-diagonal elements C_{ij} represent the covariance between the *i-th* and *j-th* estimated regression coefficients $\hat{\beta}_i$ and $\hat{\beta}_j$. σ^2 is the constant variance of the error terms.

To sum up, OLS estimations of regression coefficients are normally distributed with an expected value $E(\beta_i) = \beta_i$ and a variance-covariance matrix $V(\beta_i) = \sigma^2(X'X)^{-1}$.

Therefore, it can be stated that (Equation 4.11):

$$\frac{\beta_i - \hat{\beta}_i}{\sigma\sqrt{c_{ij}}} \sim N(0,1) \tag{4.11}$$

The problem is that σ^2 cannot be ascertained if the entire population is not known. An unbiased estimate of σ^2 can be obtained by the residuals ε_i in accordance to Equation 4.12:

$$s^2 = \frac{\sum_{i=1}^{n} \varepsilon_i^2}{n-k-1} \tag{4.12}$$

By replacing *s* with *σ*, Equation 4.11 is transformed into a t-student distribution with *n-k-1* degrees of freedom (Equation 4.13):

$$\frac{\beta_i - \hat{\beta}_i}{s\sqrt{c_{ij}}} \sim t_{n-k-1} \tag{4.13}$$

In addition, the *s* estimator allows estimating the standard errors for the estimated regression coefficients by exploiting Equation 4.10. Estimated standard

error of the *j-th* regression coefficient $se(\hat{\beta}_j)$ is given by the positive square root of diagonal elements of the variance-covariance matrix (Equation 4.14).

$$se(\hat{\beta}_j) = \sqrt{C_{jj}} \tag{4.14}$$

It is now possible to define the confidence intervals related to OLS estimations of regression coefficients. A confidence interval gives an estimated range of values which is likely to include an unknown population parameter, the estimated range being calculated from a given set of sample data. The confidence level α of a *I* confidence interval gives the probability that the interval produced by the method employed includes the true value of the parameter. For the selected confidence level α, a $100\ (1-\alpha)$ percent confidence interval on the regression coefficient is obtained as follows (Equation 4.15)

$$I = \hat{\beta}_j \pm t_{\alpha/2} se(\hat{\beta}_j) \tag{4.15}$$

The threshold $t_{\alpha/2}$ defines the value for which the probability that the t-Student distribution with n-k-1 degrees of freedom reaches or exceed $t_{\alpha/2}$ is equal to $\alpha/2$.

4.5.1 Testing statistical significance of regression coefficients

Regression analysis generates an equation by means of which describing the statistical relationship between one or more predictor variables and the response variable. $\hat{\beta}_j$ coefficients are supposed to represent the *Y* (i.e. the dependent variable) variation due to a unitary increase of the *j-th* explanatory variable when all of the other predictors are held constant. However, they may be simply the result of analytical calculations aimed to describe as well as possible the collected data (Kraha, et al., 2012). As a result, even high values of regression coefficients cannot demonstrate the relevance of related predictors in explaining the analysed phenomenon. The existence of significant relationships between predictors and the dependent variable must be proved.

For addressing these issues, the first step consists in testing whether explanatory variables collectively have an effect on the response variable. If this assumption is verified, the focus shifts to test statistical significance of single regression coefficients while controlling for the other variables in the model.

The starting point involves testing the null hypothesis that all of the predictors offer no contribution in explaining Y variance, that is $H_0: \beta_0 = \beta_1 = \cdots = \beta_k$. This implies that the selected regression model is not able to provide reliable estimates and should be abandoned in favour of other set of covariates. The F-test allows answering to these questions, but the so-called sum of squares must be explained before introducing it (Chiorri, 2010; Weisberg, 2013).

Sums of squares are actually sums of squared deviations about a mean. For the F-test, the interest is focused on the total sum of squares (SST), the regression sum of squares (SSR), and the error sum of squares (SSE) also known as the residual sum of squares (**Table 4.21**). Sum the squares of the explained deviations.

Table 4.21 Sums of squares with degree of freedom.

Source	Formula	degrees of freedom
SST	$\sum_{j=1}^{n}(Y_i - \bar{Y})^2 = SSR + SSE$	n-1
SSR	$\sum_{j=1}^{n}(\hat{Y}_i - \bar{Y})^2 = SST - SSE$	k
SSE	$\sum_{j=1}^{n}(Y_i - \hat{Y}_i)^2 = SST - SSR$	n-k-1

With reference to **Table 4.21**:

- Y_j: j-th observation for the variable of interest;
- $\bar{Y}$: mean value for the variable of interest;
- $\hat{Y}_i$: value provided by the model for the j-th subject;

SSR is the Y deviation explained by the model; SSE represents the Y deviation not explained by the model; SST quantifies the total amount of Y deviation (**Figure 4.11**).

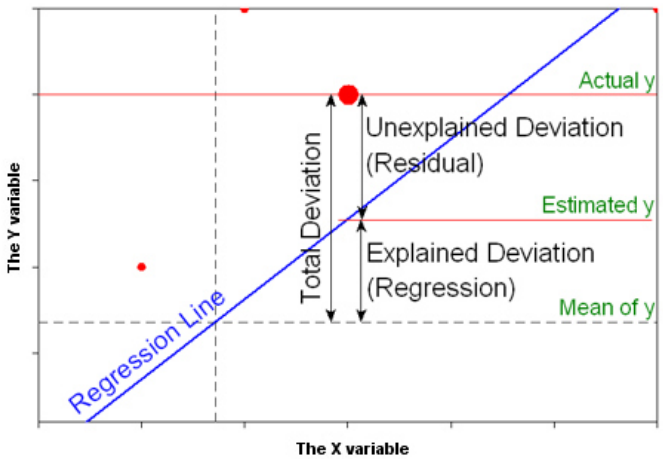

Figure 4.11 Graphical representation of various sums of squares.

Source: https://people.richland.edu/james/ictcm/2004/weight.html

Mean squares are then obtained by dividing the sum of squares by their degrees of freedom, but given that the sum of squares are deviations values, it follows that mean squares are practically variance values.

$$MSST = \frac{SST}{n-1} \qquad MSR = \frac{SSR}{k} \qquad MSE = \frac{SSE}{n-k-1}$$

Eventually, the F statistic can be calculated as the ratio between explained and unexplained variance (Equation 4.16):

$$F = \frac{MSR}{MSE} = \frac{expalined\ variance}{unexplained\ variance} \tag{4.16}$$

As already said, *F statistic* is used to test the hypothesis $all\ \beta_i = 0$ against the alternative $at\ least\ one\ \beta_i = 0$. Larger values of F indicate more evidence for the alternative. Under the null hypothesis, F-statistic is distributed as an F – Fisher random variable with k and $n-k-1$ degrees of freedom. After having selected a certain level of confidence α, the related interval of confidence $I = (1-\alpha)100$ expressed in percentage is then determined. The null hypothesis will be rejected if F does not belong to *I* confidence interval. Analytically, it means that (Equation 4.17):

$$F \geq f_{k,n-k-1} \rightarrow H_0\ rejected \tag{4.17}$$

where $f_{k,n-k-1}$ is a threshold for the acceptance of the null hypothesis; the probability that r.v. F-Fisher is greater than or equal to it exactly matches the level of confidence α. If F-Fisher is less than $f_{k,n-k-1}$, the null hypothesis cannot be rejected, and no definitive conclusions about the significance of the model as a whole can be drawn.

An equivalent way for testing the null hypothesis lies in calculating the p-value, which is the estimated probability of obtaining an effect at least as extreme as that observed from collected sample, with the assumption that the null hypothesis is true. P-value can be seen as the probability of obtaining actually observed data by chance alone. This probability tends to be lower when the predictor is significant.

If the p-value is equal or smaller than the significance level α, it suggests that the observed data are likely to be inconsistent with the assumption that the null hypothesis is true, and thus that hypothesis must be rejected.

F test can be alternatively used for comparing nested models (Chiorri, 2010; Weisberg, 2013). Two models are nested if both contain the same terms and one has at least one additional term. The latter will be the full model (k parameters), while the other one will be the reduced model ($h < k$ parameters). Parsimonious models are preferable to complex models as long as both have similar predictive power.

It is then desired to ascertain whether the full model contributes additional information about the association between *Y* and the predictors. In this case, the null hypothesis is that the additional covariates are not significant, and their related coefficients will be therefore equal to zero. If the difference between SSE for the reduced model (i.e. SSE_R) and the SSE for the complete model (i.e. SSE_C) reaches high values, the null hypothesis is likely to be rejected because this would mean that the additional $k - h$ parameters significantly improve the model's fit to the data. The full model should be preferred. For assessing the size of the difference, test statistic provided by Equation 4.18 is to be used.

$$F = \frac{(SSE_R - SSE_C)/(k-h)}{(SSE_C)/(n-k-1)} \tag{4.18}$$

After having selected a certain level of confidence α, the related interval of confidence $I = (1-\alpha)100$ expressed in percentage is then determined. The null hypothesis will be rejected if F does not belong to *I* confidence interval. Analytically, it means that (Equation 4.19):

$$F \geq f_{k-h,n-k-1} \rightarrow H_0\, rejected \tag{4.19}$$

where $f_{k-h,n-k-1}$ is a threshold for the acceptance of the null hypothesis; the probability that r.v. F-Fisher is greater than or equal to it exactly matches the level of confidence α. If F-Fisher is less than $f_{k-h,n-k-1}$, the null hypothesis cannot be rejected. There is no evidence supporting the predilection for the reduced model.

The p-value calculation can be used as an alternative to test the null hypothesis (Sellke, et al., 2001).

If the selected model provided with a specific set of covariates proves to be statistically significant, the OLS inferences on the single regression coefficient must be analysed. The aim is to test the statistical significance of single regression coefficients while controlling for the other variables in the model. For this purpose, statistical *one-sample t-test* are exploited. In particular, the *t-test* may be particularly useful in order to assess whether a new variable should be added or not in the model. A *one-sample t-test* compares the expected value of the population with a hypothetical specified value. The population of interest is here represented by the values that the regression coefficient can assume, while the hypothetical value to be tested is those proposed by the null hypothesis. Given that the significance of predictors is questioned, the null hypothesis forecasts that their coefficients are equal to zero, that is H_0: $\hat{\beta}_j = 0$. The null hypothesis practically states that the regression coefficient has no effect in the model and therefore should not be implemented. Under the H_0 hypothesis, the test statistic is expressed by Equation 4.20 and is supposed to have a t-Student distribution with n-k-1 degrees of freedom.

$$T_0 = \frac{\hat{\beta}_j}{se(\hat{\beta}_j)} \sim t_{n-k-1} \tag{4.20}$$

Given a certain confidence level α, the null hypothesis must be rejected if the test statistic lies in the acceptance region $|T_0| \geq t_{\alpha/2}$. The threshold $t_{\alpha/2}$ defines the value for which the probability that the t-Student distribution with n-k-1 degrees of freedom reaches or exceed $t_{\alpha/2}$ is equal to $\alpha/2$.

A p-value can also be calculated representing the probability of obtaining an outcome greater than or equal to the value taken on by the test statistic. The less the p-value is, the greater is the evidence against the null hypothesis. In particular, for p-values smaller than level of confidence α, the null hypothesis can be rejected, and it can be stated that the analysed variable is statistically significant and appears to offer a substantial contribution in explaining Y variance.

The problem with inferential test is that they strictly depend on the sample size. A certain predictor may result to be insignificant for restricted collected data, while for increased sample size the same predictor may reveal itself to be important for the analysed phenomenon. An inferential test may be statistically significant (i.e., unlikely to have occurred by chance), but this does not necessarily indicate how large the effect of the predictor is on the dependent variable. There may be non-significant, notable effects especially in low powered tests.

Therefore, there is the need for measures capable of measuring the actual importance of predictors. This is where measure of model adequacy and correlation coefficients come in.

4.5.2 Measures of model adequacy

There are various measures and techniques which can be used in order to check the appropriateness of the multiple linear regression model for describing collected data (Chiorri, 2010; Dupont, 2010; Weisberg, 2013).

The coefficient of determination R^2 is a measure of the amount of variability in the data accounted for by the regression model. It is practically a measure of how well the variable of interest Y can be predicted by using a linear function of a set of covariates.

As mentioned, previously, the total variability of data is quantified by the total sum of squares $SST = (Y_i - \bar{Y})^2$, while the amount of this variability explained by the regression model is the regression sum of squares $SSR = (\hat{Y}_i - \bar{Y})^2$. The coefficient of determination R^2 is the ratio of SSR to SST (Equation 4.23):

$$R^2 = \frac{SSR}{SST} = 1 - \frac{SSE}{SST} \tag{4.23}$$

R^2 can take on values between 0 and 1, with a value of one indicating that the predictions are exactly correct and a value of zero indicating that no linear combination of the independent variables is a better predictor than is the fixed mean of the dependent variable.

It may appear that larger values of R^2 indicate a better fitting regression model. However, the value of R^2 increases as more terms are added to the model, even if the new terms do not contribute significantly to the model. Therefore, an increase in the value of R^2 cannot allow assessing that the new model is to be preferred to the older one. A better statistic to use is the $adjusted\ R^2$ statistic defined as follows (Equation 4.24):

$$R^2 = 1 - \frac{SSE/(n-k-1)}{SST/(n-1)} \tag{4.24}$$

The $adjusted\ R^2$ only increases when significant terms are added to the model. Addition of unimportant terms may lead to a decrease in the value of $djusted\ R^2$.

Coefficients of determination only quantify the strength of relationship between the dependent variable and the entire set of covariates. Correlation coefficients may give an insight into the magnitude of the effect each predictor exerts on the dependent variable. However, this also requires the knowledge of the reciprocal influence among predictors.

4.5.3 Multicollinearity

Problems occur in regression analysis when a model is specified that has multiple independent variables that are highly correlated. The main effect would

be an increase in the variance of OLS estimates for the regression coefficients (Chiorri, 2010). As an example, a model is considered with only two standardised predictors (zero mean value and unitary variance). In this case, it can be demonstrated that (Equation 4.21):

$$(X'X)^{-1} = \frac{1}{1-\rho_{12}^2}\begin{bmatrix} 1 & \rho_{12} \\ \rho_{12} & 1 \end{bmatrix} \tag{4.21}$$

where ρ_{12} is the correlation coefficient between X_1 and X_2. Consequently, variance of estimated regression coefficients β_1 and β_2 is $V(\beta_1) = V(\beta_1) = \sigma^2 \frac{1}{1-\rho_{12}^2}$

High reciprocal correlations between predictors inflate the variance of their coefficients. The reliability of their OLS estimates would be compromised given that the t-statistic adopted for proving their statistical significance is the ratio of the estimated coefficient to the standard error (Equation 4.17). Consequently, high multicollinearity tends to result in insignificant outputs for the t-test, with the impossibility of rejecting the null hypothesis stating the predictors are negligible.

In such a model, an estimated regression coefficient may not be found to be significant even if a statistical relation is captured between the response variable and the set of the predictor variables via the F-test.

And beyond the statistical tests, the coefficient values themselves could not be trusted in case of high multicollinearity.

In the previous example, both of the highly-correlated predictors contribute to explain the variance of dependent variable. However, multiple regression model is likely to estimates a near-zero coefficient for one of the two predictors while assigning a substantial weight for the other one. As a result, there is a highly probability of estimating regression coefficients that are poor reflections of actual variable relationships, as well as being extremely sensitive to models changes. Adding or removing variables from the model may change the nature of the small differences existing between the two original predictors and drastically modify their estimates. It may even lead to change in the sign of the regression coefficient (Kraha, et al., 2012).

The variance inflation factor (VIF) quantifies the severity of multicollinearity in an OLS regression analysis (Field, 2009; Chiorri, 2010). It provides an index that measures how much the variance of an estimated regression coefficient is increased because of multicollinearity. The VIF factor for β_i coefficient related to the X_i predictor is given by the following formula (Equation 4.22):

$$VIF_i = \frac{1}{1-R_i^2} \tag{4.22}$$

where R_i^2 is the coefficient of determination for a multiple linear regression that has X_i as a function of all the other explanatory variables in the first equation.

If i = 1, for example, R_i^2 related to this multiple linear regression:

$$x_1 = \beta_0 + \beta_2 x_2 + \beta_3 x_3 + \beta_4 x_4 + \cdots + \beta_k x_{ik} + \varepsilon_i$$

A VIF factor must then be calculated for each predictor. The VIF minimum value of one implies X_i is uncorrelated to the other ones, while values greater than 2 are a sign of severe multicollinearity (Chiorri, 2010).

4.5.4 Correlation coefficients

After recognition of multicollinearity presence, strategies must be applied for capturing the actual amount of Y variance explained by the predictors and corrected for their reciprocal correlations. In particular, the main goal consists in determining the amount of association existing between each predictor and the dependent variable.

When independent variables are pairwise orthogonal, their importance in the regression can be expressed by the squared coefficient of correlation between each of the independent variable and the dependent variable. By summing them, coefficient of determination R^2 is obtained (Equation 4.22).

$$R^2 = {r_{Y-X1}}^2 + {r_{Y-X2}}^2 + \cdots + {r_{Y-Xk}}^2 \quad (4.22)$$

Equation 4.22 works only because the predictors explain different and unique portions of the dependent variable Y.

The problem is when the dependent variables are correlated. In this case, the aforementioned strategy would overestimate the contribution of each variable, as their variance is counted multiple times. The coefficient of determination would no longer be equal to the simple sum of the single squared coefficient of correlations (Kraha, et al., 2012).

One answer to the concern of covariates sharing the same variance of the dependent variable is the calculation of standardised regression coefficients $\hat{\beta}^*$.

They are the estimates resulting from a multiple linear regression analysis carried out on independent variables that have been standardised in order to have a unitary variance. Each variable can be standardized by subtracting its mean from each of its values and then dividing these new values by the standard deviation of the variable. Standardizing all variables in a multiple regression yields standardized regression coefficients that show the change in the dependent variable measured in standard deviations. In fact, $\hat{\beta}^*$ coefficient of a single predictor refers to changes in standard deviations that will affect the standardised dependent variable *Y* per unitary standard deviation increase in the standardised predictor, while all of the other predictors are held constant.

Therefore, it can be stated that $\hat{\beta}^*$ coefficients outline the importance that each predictor variable is receiving in the regression model for predicting Y. As evidence thereof, $\hat{\beta}^*$ can be used for calculating the coefficient of determination R^2 when predictors are not reciprocally orthogonal (Equation 4.23).

$$R^2 = \beta_1(r_{Y-X1}) + \beta_2(r_{Y-X2}) + \cdots + \beta_k(r_{Y-Xk}) \quad (4.23)$$

However, various concerns persist about the reliability of standardised regression coefficients as a measure of actual relationships between each predictor and the dependent variable. As a matter of fact, $\hat{\beta}^*$coefficients can dramatically change in numerical value, and even in sign, as new variables are introduced or as old variables are removed. They simply reflect the amount of credit given to the related predictors. It can be said that they are context-specific to a given model characterised by a specific set of covariates. The problem is that the true model is rarely, if ever, known.

In addition, $\hat{\beta}^*$ coefficients are still sensitive to multicollinearity, and their values may be affected by the amount of Y variance shared with the other predictors. As a result, it can happen that a predictor explaining a consistent part of Y variance may have a near-zero $\hat{\beta}^*$ because another predictor is receiving the credit for the explained variance (Kraha, et al., 2012).

Other techniques are then required for correctly evaluating the importance of single predictors in explaining the analysed phenomenon. There is the need for estimating the relationship between a predictor variable and the outcome variable after controlling for the effects of other predictors in the equation. This means that is required to determine the degree of association between the two variables that would exist if all influences exerted by other predictors could be removed. This process of exercising statistical control, also known as partialing or residualization, is the essential concept underlying the *partial and semipartial correlation coefficients*. As of now, the standard Pearson correlation coefficients are defined as *zero order correlation coefficients*.

Partial correlation represents the correlation between the dependent variable Y and a predictor after common variance with other predictors has been removed from both Y and the predictor of interest. The squared partial correlation denotes the explained by the predictor portion of Y variance not estimated by other predictors. That is, the *partial correlation* expresses the correlation between the residualized predictor and the residualized criterion. Partial correlation can be computed directly from the zero order correlation coefficients between each predictor and the dependent variable. Analytical formulations will be showed in the followings.

Semipartial correlation coefficient (also called part correlation) indicates the unique contribution of an independent variable. Specifically, it represents the correlation between the criterion and a predictor that has been residualized with respect to all other predictors in the equation. It may appear quite similar to the partial correlation, but the significant difference lies in the fact that dependent variable remains unaltered without removing part of variance explained by other predictors.

It is worth noting that the total variance of outcome variable Y is held constant, no matter which predictor is being examined. This means that the square of the semipartial can be interpreted as the proportion of the criterion variance associated uniquely with the predictor. The squared semipartial represents the unique variance of that predictor shared with the dependent variable. This means that the

squared semipartial correlation for a variable denotes the decrease in coefficient of determination R^2 if that variable is removed from the regression equation.

Semipartial correlation can be computed directly from the zero order correlation coefficients between each predictor and the dependent variable. Analytical formulations will be showed in the followings.

Eventually, there are the so-called structure coefficients. They are simply bivariate Pearson correlation coefficients, but they are not zero-order correlations between two observed variables. Indeed, they are related to the association existing between a single predictor and the predicted values for the dependent variable, often called $Yhat\ \hat{Y}\ scores$. These scores are just the values estimated by the model for the outcome variable. Their variance represents the portion of total variance that can be explained by the predictors (Field, 2009; Kraha, et al., 2012).

A squared structure coefficient denotes the amount of variance estimated by the model that the predictor is able to explain. This is equivalent to say that a squared structure coefficient denotes the amount of variance related to R^2 that the predictor is able to explain. Structure coefficients definitely clarify the contribution of each predictor in explaining the phenomenon described via a multiple linear regression, and they provide support in trying to identify multicollinearity effects. For example, predictors with high standardised regression coefficients and near to-zero structure coefficients are allegedly simple suppressor predictors. This means that their high coefficient values only respond to the need for OLS estimation to reduce residuals with observed values. In other words, for suppressor variables, high coefficient values do not correspond to a significant effect on the dependent variable.

Conversely, a small standardised coefficient but a high structure coefficient suggest the presence of shared variance between the analysed predictor and another one at least. $\hat{\beta}^*$ calculations have presumably assigned this shared variance to other independent variables. Structure coefficients have not the potential for identifying these other covariates, but an evidence is provided about the actual importance of the analysed predictor, which instead would have been considered as unessential and removed from the model.

A graphical representation supported by Venn diagrams can ease comprehension of introduced coefficients. By referring to **Figure 4.12**, a multiple linear regression model has been established. The outcome variable Y is explained by only two covariates, X_1 and X_2.

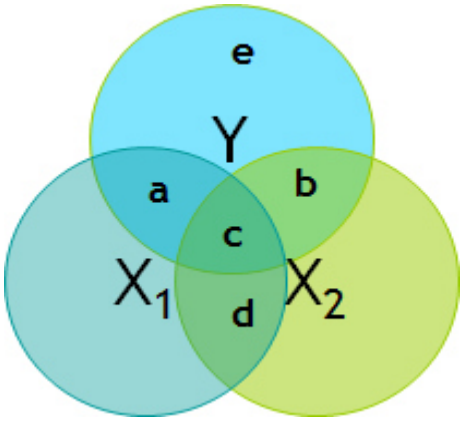

Figure 4.12 Graphical representation of correlation coefficients and measures of adequacy for multiple linear regressions. Areas of shared variance are labelled with lower case letters and these are then used to define coefficients.

In the following, analytical definitions of introduced measures and their correspondent graphical illustration are provided (Sheskin, 2003).

- $Total\ variance\ of\ Y\ =\ a + b + c + e;$
- $Variance\ of\ Y\ explained\ by\ the\ model\ =\ a + b + c;$
- $Variance\ of\ Y\ not\ explained\ by\ the\ model\ =\ e;$
- $R^2 = (a + b + c)/(a + b + c + e);$
- $Multicollinearity\ =\ c + d;$
- $Squared\ Zero\ order\ correlation\ coefficients$

  $r^2Y_1 = a\ +\ c;\ r^2Y_2 =\ b\ +\ c;$
- $Squared\ Semipartial\ correlation\ for\ X_1$

  $R^2\ - r^2Y_1 =\ a\ /\ (a\ +\ b\ +\ c\ +\ e);$
- $Squared\ Partial\ correlation\ for\ X_1$

  $(R^2\ -\ r^2Y_1\ )/(1\ -\ r^2Y_1\ )\ =\ a\ /\ (a\ +\ e);$
- $Structure\ coefficient\ of\ X_1\ =\ r^2Y_1\ /R^2\ \ =\ a\ /\ (a\ +\ b\ +\ c).$

Correlation coefficients and structure coefficients offer substantial guide in better understanding actual importance of single covariates. In addition, as already said, combining information provided by structure coefficients and standardised regression coefficients enable recognising the presence of suppressor independent variables and avoiding the removal of decisive variables with small regression coefficient because of multicollinearity effects (Kraha, et al., 2012). Eventually, after identification of substantial covariates for the prediction power of the model, partial and semipartial correlations may give an insight into the actual strength of the associations between predictors and the dependent variable.

4.5.5 Cohen's f^2 effect size

The magnitude of these relationships may be directly and synthetically measured by the so-called *Cohen's f^2 effect size*, which is focused on the strength of the association between the predictor of interest and the dependent variable (Cohen, 1988; Field, 2009).

Its outcome is a measure of practical significance in terms of the magnitude of the effect exerted by the single predictor. It is independent of the sample size and is appropriate for calculating the effect size within a multiple regression model in which the independent variable of interest and the dependent variable are both continuous.

Cohen's f^2 effect size for the predictor of interest can be assessed by comparing the proportion of variance explained by the full model with the proportion of variance explained by the same model deprived of the predictor whose effect is investigated (Equation 4.24)

$$f^2 = \frac{R^2_{full\ model} - R^2_{model\ without\ the\ predictor}}{1 - R^2_{full\ model}} \tag{4.24}$$

$R^2_{model\ without\ the\ predictor}$ can be easily calculated by exploiting Equation 4.23 without the predictor of interest.

Cohen's f^2 ranging from 0.15 to 0.35 should indicate a moderate effect size, while for values greater than or equal to 0.35 it could be stated that the predictor is quite significant (Cohen, 1988)).

4.5.6 Verifying the assumptions of multiple linear models

A multiple linear model is based on certain assumptions that must be verified in order to trust its outputs. As an introductory premise, the fact must be enlighten that regressions here proposed have an exploratory essence. They are not aimed

to propose exact prediction models, but rather they have been arranged in order to refine previous exploratory analyses. They are the last step of the path aiming to the disclosure the most prominent geometric factors related to crash frequency and deserve to be implemented in crash prediction model based on Conflict Opportunities. For these reasons, even if assumptions of multiple linear models were not fully satisfied, this would not aprioristically imply the abandon of model outputs. Certain assumptions, in particular normal distribution and homoscedasticity of residuals, must be complied if the aim is obtaining new data points, but that is not the case. In accordance to a famous quotation, "…the statistician knows…that in nature there never was a normal distribution, there never was a straight line, yet with normal and linear assumptions, known to be false, he can often derive results which match, to a useful approximation, those found in the real world." (Box, 1976). Correlation and structure coefficients may provide interesting information anyhow. For example, although general hypothesis would not fully respected, a relevant structure coefficient standing out from the other ones would remark the importance of the covariate, with even stringer reason in case the same covariate was identified by previous exploratory analyses.

4.5.6.1 Dependent variable follows a normal distribution

Multiple linear regression assumes that the dependent variable has a normal distribution. Descriptive statistics such as Skewness and Kurtosis may help easily and quickly understand if outcome variable can actually follow a normal distribution. Both of them are unitless.

Skewness is a measure of symmetry of the distribution, that is if it looks the same to the left and right of the centre point. More precisely, skewness denotes the lack of symmetry affecting the variable, which is said to be positively skewed if it has an asymmetrical distribution with a long tail to the right, negatively skewed otherwise. As a rule of thumb, skewness greater than 1.0 (or less than -1.0) is considered substantial and the distribution is far from symmetrical. Skewness can be calculated as the ratio of the third moment and the variance raised to the power of 3/2. The third moment about the mean is the sum of each value's deviation from the mean cubed.

Kurtosis coefficient quantifies whether the shape of the data distribution matches the Gaussian distribution: a Gaussian distribution has a kurtosis of 0; a flatter distribution has a negative kurtosis; a distribution more peaked than a Gaussian distribution has a positive kurtosis.

Kurtosis coefficient can be calculated as the ratio of the fourth moment and the variance (approximated by its unbiased estimator s^2) minus 3.0. The ratio is also known as the kurtosis index, which defines a distribution similar to the normal one for values near 3.0. As a rule of thumb, kurtosis coefficient should range between -1.0 and 1.0 for approximating variable distribution as a normal one (Chiorri, 2010).

The fourth moment is the sum of each value's deviation from the mean raised to the power of 4. The whole sum is then divided by the number of values.

Skewness and kurtosis are provided by statistical package IBM® SPSS 21.

However, violation of normal distribution of collected values of the dependent variable should not compromise the regression model at all (Box, 1976).
According to this perspective, numerous authors and statisticians question the utility of testing the hypothesis about normal distribution for Y data, where Y is the dependent variable. In fact, they note that this assumption is only a consequence of the analytical structure of the model: a linear combination of independent variables supposed to be perfectly known and residuals normally distributed. Even if collected data for Y did not follow a normal distribution, this does invalidate neither OLS estimation coefficients nor correlation coefficients. There is no reason for not exploiting outcomes coming from these analyses. There could be numerous causes behind the non-normal distribution of Y collected data, such as restricted sample or other factors not still identified and implemented in the regression equation, but if the current model proved to be the best possible, using its results for better understanding the analysed phenomenon would be correct.

From a more analytical point of view, **Figure 4.13** shows a regression models with only one covariate where Y is actually non-normally distributed. This would mean that individuated regression model could not be accepted, which is obviously unacceptable. In addition, in Figure 4.13, *Y* reveals itself to be conditional normally distributed as error term is from normal distribution (Xiang, et al., 2012). The very important aspect is that residuals are normally distributed, but again the researcher must use the results coming from the best possible model

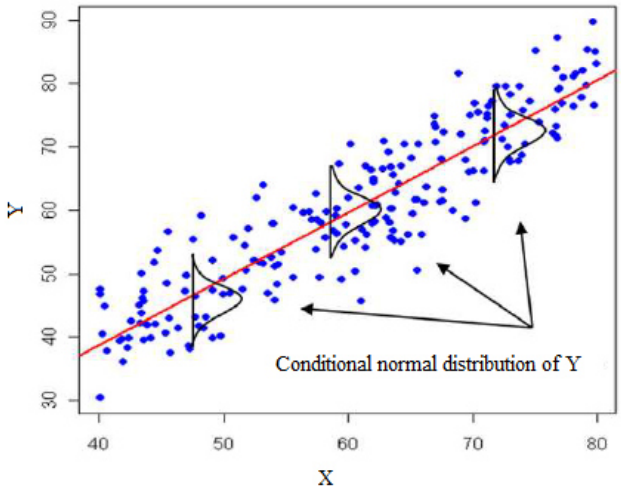

Figure 4.13 Testing homoscedasticity of residuals by plotting standardised residuals against standardised predicted values

Source: (Xiang, et al., 2012)

4.5.6.2 Dependent variable follows a normal distribution

Normality of residuals is strictly required for valid hypothesis testing, that is, the normality assumption assures that the p-values for the t-tests and F-test will be valid. Normality is not required in order to obtain unbiased OLS estimates of the regression coefficients. OLS regression merely requires that the residuals errors be identically and independently distributed. Also the correlation coefficients do not assume random variables are normally distributed, so possible negative results about testing normality of residuals would not prevent exploiting outcome of linear regression in case there were parameter strongly correlated with crash frequency (Chiorri, 2010).

The most intuitive way for testing normality of residuals consists in trying to graph a histogram by plotting obtained residuals and placing them in regularly spaced cells. The histogram should approximate a normal distribution of residuals. However, with small sample sizes, which is the case of various crash type here in this study, this is not be the best choice for judging the distribution of residuals (**Figure 4.14**).

A more sensitive graph is the $normal\ probability\ plot$ (also called P-P plot). It is obtained by sorting the standardised residuals into ascending order and then calculating the cumulative probability of each residual using the Equation 4.25:

$$P(i-th\ residual) = i/(N+1) \tag{4.25}$$

where P denotes the cumulative probability, *i* is the order of the value in the list and *N* is the number of residuals. Eventually, the so calculated P values are then plotted versus the normalised cumulative frequency distribution of residuals themselves, that is $(\varepsilon_i - \mu)/\sigma)$, where μ and α are approximated via the mean and standard deviation of residuals respectively. The normal probability plot should produce an approximately straight line if the points come from a normal distribution (**Figure 4.14**).

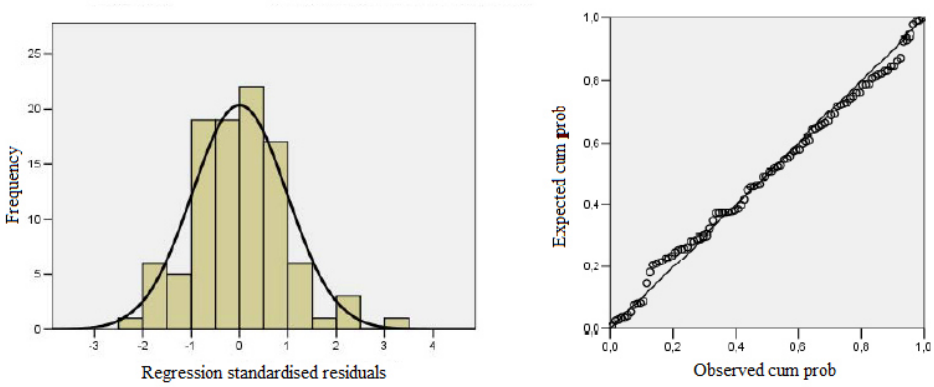

Figure 4.14 Testing normality distribution of residuals

Source: (Chiorri, 2010)

4.5.6.3 Homoscedasticity of residuals

Vector of residuals is supposed to be homoscedastic; this means that residuals should have a constant variance σ^2. The complementary notion is called heteroscedasticity. Homoscedastic assumption can be checked by visual examination of a plot of the standardized residuals (the errors) by the regression standardized predicted value. Ideally, residuals are randomly scattered around 0 (the horizontal line) providing a relatively even distribution. There is heteroscedasticity when the residuals are not evenly scattered around the line and a certain trend can be recognised (**Figure 4.15**).

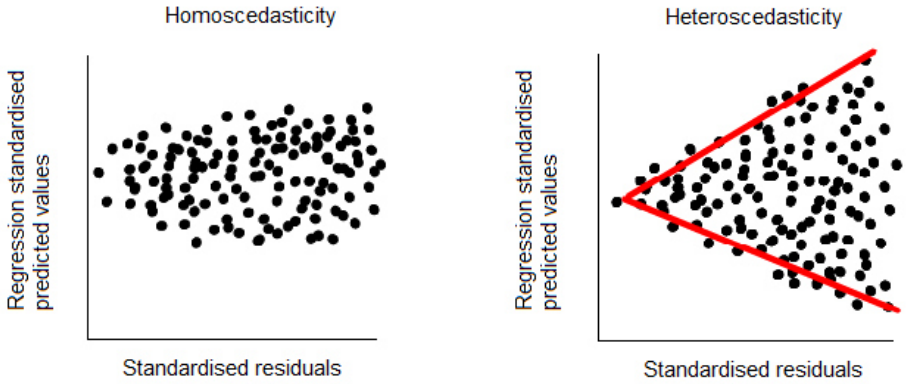

Figure 4.15 Testing homoscedasticity of residuals by plotting standardised residuals against standardised predicted values

Source: (Chiorri, 2010)

Independence of residuals can be taken for granted given that statistical units of this study are the roundabout legs, which are cross-sectional data (Wayne & Zappe, 2009). Certain analytical tools such as the Durbin-Watson test are useful for detecting autocorrelation of time-series data, but this is not the case.

4.5.7 Application of multiple linear regression model

An application of discriminant analysis to the legs from which vehicles involved in fatal or injury run-off crashes is here proposed. IBM® SPSS package software has been used for developing multiple linear models.

From FA and DA, a set of geometric features apparently related to crash frequency was found and then investigated in MLR models. Stepwise regression procedures were applied by exploiting the F-test in order to establish which of these five models should be preferred for analysing the investigated phenomenon.

- *Model 1.* Predictors: Constant, R1;
- *Model 2.* Predictors: Constant, R1, Visibility Angle;
- *Model 3.* Predictors: Constant, R1, R3, Visibility Angle;
- *Model 4* Predictors: Constant, R1, R3, Visibility Angle, ICD;
- *Model 5.* Predictors: Constant, Entry Angle, R1, R3, Visibility Angle, ICD;

It must be ascertained whether the full model contributes additional information about the association between Y and the predictors. The null hypothesis is that the additional covariates are not significant, and their related coefficients are therefore equal to zero. If the difference between error sum of squares for the reduced model (i.e. SSE_R) and the error sum of squares for the complete model (i.e. SSE_C) reaches high values, the null hypothesis is likely to be rejected because this would mean that the additional parameters significantly improve the model's fit to the data. Output of F-test for the five tested models are reported in Table 4.22, which shows that the independent variables statistically significantly predict the dependent variable for all of tested models.

Table 4.22 F-test for the five models.

Model		Sum of squares	df	Mean squares	F	Sig.
1	*Regression*	1.307E-06	5	2.614E-07	3.905	7.606E-03
	Residual	2.008E-06	30	6.693E-08		
	Total	3.315E-06	35			
2	*Regression*	1.307E-06	4	3.267E-07	5.044	3.004E-03
	Residual	2.008E-06	31	6.478E-08		
	Total	3.315E-06	35			
3	*Regression*	1.303E-06	3	4.343E-07	6.906	1.026E-03
	Residual	2.012E-06	32	6.288E-08		
	Total	3.315E-06	35			
4	*Regression*	1.297E-06	2	6.484E-07	10.601	2.780E-04
	Residual	2.018E-06	33	6.116E-08		
	Total	3.315E-06	35			
5	*Regression*	1.272E-06	1	1.272E-06	21.175	5.609E-05
	Residual	2.043E-06	34	6.008E-08		
	Total	3.315E-06	35			

Measures of model adequacy were calculated, with particular emphasis to adjusted R square, since it increases only when significant terms are added to the model (Table 4.23).

Table 4.23 Measures of adequacy for the five models

Model	R	R-square	Adjusted R square	Standard error of the estimate
1	0.619	0.384	0.366	2.45E-01
2	0.625	0.391	0.354	2.47E-01
3	0.627	0.393	0.336	2.51E-01
4	0.628	0.394	0.316	2.55E-01
5	0.628	0.394	0.293	2.59E-01

By analysing R-square coefficients, in particular adjusted R square, it appears that the simplest model having the entry path radius as the only covariate perform

better than the others do. This obviously represents a strong evidence about the prominence of R1 in relation to other parameters.

However, it was decided to investigate the full model in order to establish the degree of correlation with crash frequency for all of the covariates.

Unstandardized coefficients indicate the increase experienced by the dependent variable for a unitary increment of the independent variable when all other independent variables are held constant (Table 4.24).

The same table reports the outputs of tests pertaining to the statistical significance of each of the independent variables. The null hypothesis is that the related coefficient of the investigated predictor is equal to zero. If p-value < 0.05, the null hypothesis can be rejected, and it can be stated that coefficients are statistically significantly different to zero, which is the case for *entry path radius R.*

Table 4.24 Calculating regression coefficients and testing statistical significance of the independent variables.

Model		Unstandardized coefficients		Standardised Coefficients		
		β	*Std. Error*	$\hat{\beta}$	*t*	*Sig.*
1	*Constant*	3.975E-4	3.514E-4		1.131	0.267
	ICD	4.588E-7	2.129E-6	0.046	0.216	0.831
	R1	2.307E-6	7.449E-7	0.601	3.098	0.004
	Visibility Angle	-6.310E-7	2.321E-6	-0.057	-0.272	0.788
	R3	1.360E-7	4.414E-7	0.058	0.308	0.760
	Entry Angle	-2.129E-7	4.554E-6	-0.010	-0.047	0.963

The variance inflation factor (VIF) quantifies the severity of multicollinearity in MLS analyses. It provides an index that measures how much the variance of an estimated regression coefficient is increased because of multicollinearity.

Table 4.25 warns against possible critical multicollinearity spread along all of the covariates. There is a strong need for detecting the actual degree of correlation with crash frequency for each covariate, whose estimated coefficients may be affected by reciprocal correlation between each other.

As already noted, there are additional concerns pertaining reliability of standardised regression coefficients as a measure of actual relationships between each predictor and the dependent variable. As a matter of fact, $\hat{\beta}^*$coefficients can dramatically change in numerical value, and even in sign, as new variables are introduced or as old variables are removed. They simply reflect the amount of credit given to the related predictors. It can be said that they are context-specific to a given model characterised by a specific set of covariates. The problem is that the true model is rarely, if ever, known.

In addition, $\hat{\beta}^*$ coefficients are still sensitive to multicollinearity, and their values may be affected by the amount of Y variance shared with the other

predictors. As a result, it can happen that a predictor explaining a consistent part of Y variance may have a near-zero $\hat{\beta}^*$ because another predictor is receiving the credit for the explained variance.

Other techniques are then required for correctly evaluating the importance of single predictors in explaining the analysed phenomenon. There is the need for estimating the relationship between a predictor variable and the outcome variable after controlling for the effects of other predictors in the equation.

Partial correlation represents the correlation between the dependent variable Y and a predictor after common variance with other predictors has been removed from both Y and the predictor of interest.

The squared *semipartial correlations* represent the unique variance of that predictor shared with the dependent variable. This means that the squared semipartial correlation for a variable denotes the decrease in coefficient of determination R^2 if that variable is removed from the regression equation (Table 4.25). From correlation coefficients, R1 turns out to be the only covariate to offer a significant contribution in explaining crash frequency variance.

Table 4.25 Verifying the presence of severe multicollinearity and calculation of correlation coefficients

	Correlation coefficients			**Collinearity**	
	Zero-order	*Partial*	*Semipartial*	*Toll*	*VIF*
ICD	-0.121	0.039	0.031	0.448	2.231
R1	0.619	0.492	0.440	0.537	1.863
Visibility Angle	-0.085	-0.050	-0.039	0.459	2.181
R3	0.413	0.056	0.044	0.560	1.784
Entry Angle	0.128	-0.009	-0.007	0.421	2.377

A squared structure coefficient denotes the amount of variance estimated by the model that the predictor is able to explain. This is equivalent to say that a squared structure coefficient denotes the amount of variance related to R^2 that the predictor is able to explain.

Structure coefficients definitely clarify the contribution of each predictor in explaining the phenomenon described via a multiple linear regression, and they provide support in trying to identify multicollinearity effects. Structure coefficients confirm previous analyses of partial and semipartial correlations.

Structure coefficient confirms the preponderance of R1.

The magnitude of correlations may be directly and synthetically measured by the so-called *Cohen's f^2 effect size*, which is focused on the strength of the association between the predictor of interest and the dependent variable.

Its outcome is a measure of practical significance in terms of the magnitude of the effect exerted by the single predictor. It is independent of the sample size

and is appropriate for calculating the effect size within a multiple regression model in which the independent variable of interest and the dependent variable are both continuous. The effect size corroborates previous results: *entry path radius* appears to have a remarkable relationship with crash frequency as compared to other 21 investigated geometric factors (Table 4.26). This output is partially consistent with the findings of discriminant analysis, which identified the inscribed circle diameter too as a significant geometric factor for safety performance of roundabout as pertaining to rear-end crashes at entry. However, correlation coefficients and the effect size point out its restricted contribution in explaining crash frequency.

Eventually, exploratory analyses reach the conclusion that these aspects should deserve the maximum attention in order to design more safety roundabouts for collisions due to failure to yield starting from a stopped position.

Table 4.26 Calculation of structure coefficients and effect size f^2

	Structure coefficient	**Effect size f^2**
ICD	0.027	0.000
Deviation Angle	0.955	0.504
R1	0.018	0.008
Visibility Angle	0.416	0.079
Entry Angle	0.125	0.000

A multiple linear model is based on certain assumptions that must be verified in order to trust its outputs. However, the multiple linear models here proposed have only an exploratory essence: they are not aimed to propose exact analytical forecasts, but rather they were arranged in order to refine previous exploratory analyses. They are the last step of the path aimed to disclosure the most prominent geometric factors related to crash frequency and deserving to be implemented in crash prediction model based on CO technique.

For these reasons, even if assumptions of multiple linear models were not fully satisfied, this would not aprioristically imply the abandon of model outputs.

In this perspective, correlation and structure coefficients may provide interesting information anyhow. Even if general hypothesis would not fully respected, a relevant structure coefficient standing out from the other ones would remark the importance of the covariate, with even stringer reason in case the same covariate was identified by previous exploratory analyses. In the following, test are reported which should be performed in order to verify whether the assumptions at the base of the multiple linear model are satisfied or not.

The most intuitive way for testing normality of residuals consists in trying to graph a histogram by plotting obtained residuals and placing them in regularly spaced cells. The histogram should approximate a normal distribution of residuals.

However, with small sample sizes, which is the case of various crash type here in this study, this is not be the best choice for judging the distribution of residuals (Figure 4.16).

A more affordable way is proposed by the $normal\ probability\ plot$ (also called P-P plot). It is obtained by sorting the standardised residuals into ascending order and then calculating the cumulative probability of each residual.

Eventually, the so calculated P values are then plotted versus the normalised cumulative frequency distribution of residuals themselves, that is $(\varepsilon_i - \mu)/\sigma)$, where μ and α are approximated via the mean and standard deviation of residuals respectively. The normal probability plot seems to be able to produce an approximately straight line, which means that residuals may come from a normal distribution (Figure 4.17).

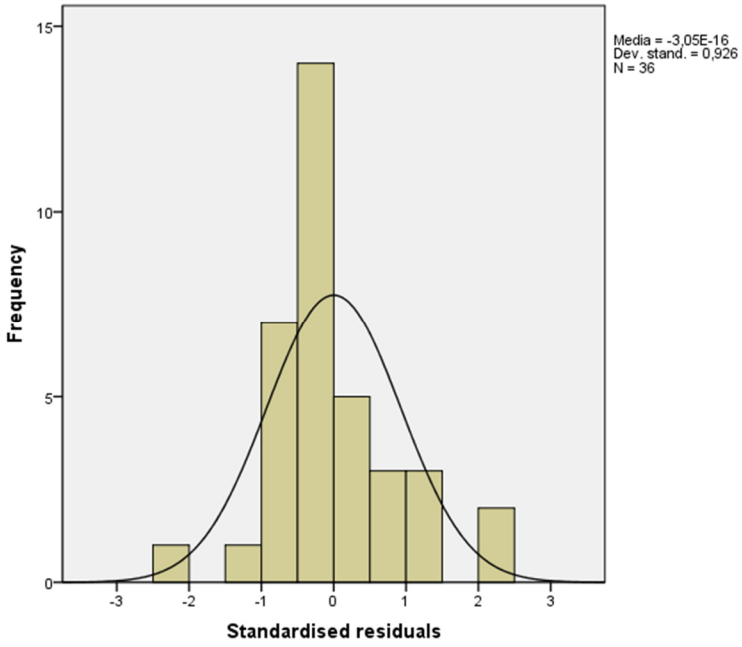

Figure 4.16 Testing normality distribution of residuals. Histogram

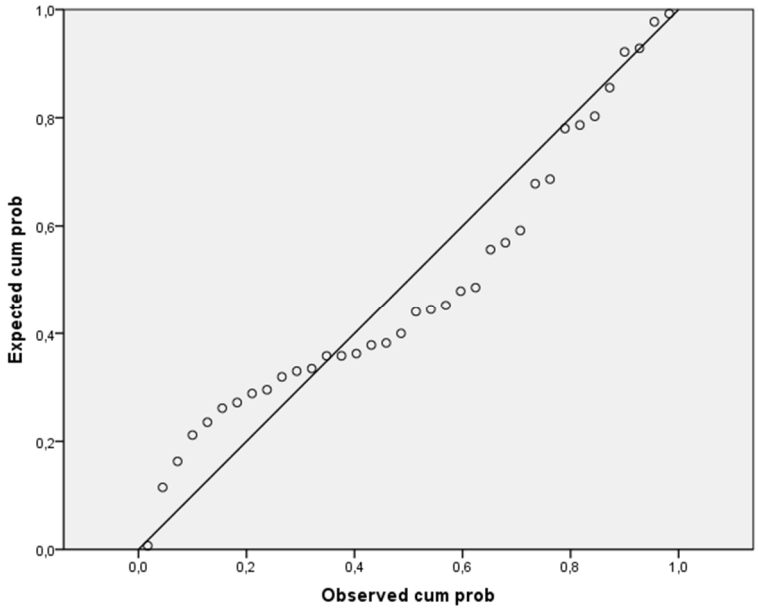

Figure 4.17 Testing normality distribution of residuals. Normal probability plot

There are instead serious concerns about the homoscedastic nature of residuals, which should have a constant variance σ^2. Homoscedastic assumption can be checked by visual examination of a plot of the standardized residuals (the errors) by the regression standardized predicted value. Residuals are not evenly scattered around the line and a certain trend can be recognised (Figure 4.18). This means that homoscedastic assumption is not verified. However, as already said, this cannot compromise results obtained with correlation coefficients and the effect size, which gave substantial results also consistent with previous exploratory analyses.

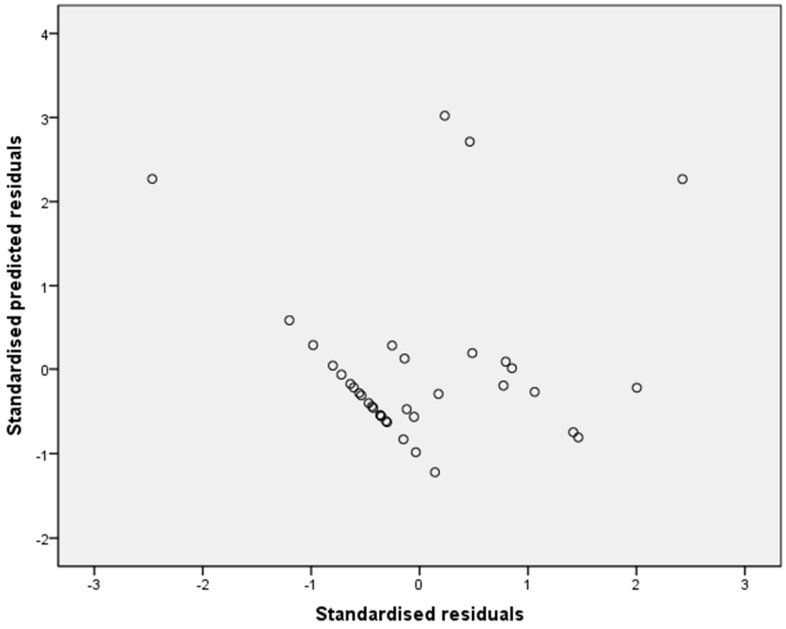

Figure 4.18 Classification results table.68.8% of original grouped cases correctly classified. 62.5% of cross validated grouped cases correctly classified.

Even if a certain degree of homoscedasticity was revealed affecting the residuals, correlation coefficients and the effect sizes cannot be neglected, given that they clearly identified deviation angle and R1 as predominant factors in explaining crash frequency as compared to the other geometric features.

4.6 Bootstrap regressions

Bootstrapping is a nonparametric approach to statistical inference that does not require distributional assumptions, such as, for example, normally distributed residuals. It has the potential for providing accurate inferences when the data are not well behaved or when the sample size is small, which is exactly the shortcoming for certain types of crash as will be shown in Chapter 5.

Bootstrapping uses the sample data to estimate relevant characteristics of the population in such a way that the sampling distribution of a statistic is constructed empirically by resampling from the collected sample itself. In other words, given a random sample of size *n*, each bootstrap sample selects n values with replacement from among the *n* values of the original sample.

The underlying concept of this statistical method is that each data set is not only a sample from a population but can also be considered to be the only and best available approximation to the population itself. Therefore, it is possible to compute numerically the variability of an estimate, not by repeatedly sampling from a theoretically well-defined population distribution, which is not available, but by resampling with replacement from the data (Davison & Hinkley, 1997).

In synthesis, the population is to the sample as the sample is to the bootstrap samples (**Figure 4.19**).

In accordance to this statement, *r* bootstrap samples are generated by sampling with replacement *n* times from the original data set. Therefore, certain observations are drawn only once, others multiple times and some never at all.

Typical values for *r*, the number of bootstrap samples, range from 50 to 500 depending on the pursued statistical inference.

For sufficiently large data sets, as those obtained through bootstrap procedure, the Central Limit Theorem can be applied. As a result, it can be hypothesised the bootstrap sample mean follows a normal distribution whit the same mean of the reference population and a standard deviation $\sigma_y = (\sigma / n)^{1/2}$, where σ is the unknown variance of the reference population and *n* the sample size.

The estimator $\hat{\theta}$ is a function of the observed sample. For instance, the sample mean is an unbiased estimator of the population mean. By calculating an estimate for each bootstrap sample, *r* bootstrap estimates $\hat{\theta}_b^*$ are then obtained and successively exploited in order to inference the statistical parameter of interest. The mean of *r* Bootstrap means matches the mean of the original sample, while the related bootstrap standard error $se^*(\hat{\theta})_B$ is provided by Equation 4.26:

$$se^*(\hat{\theta})_B = \sqrt{\frac{\sum_{b=1}^{r}(\hat{\theta}_b^* - \bar{\vartheta}^*)^2}{r-1}} \tag{4.26}$$

where:

- $\hat{\theta}_b^*$ = estimate of the investigated parameter obtained from the r-th bootstrap sample;
- $\bar{\vartheta}^* = \frac{\sum_{b=1}^{r}\hat{\theta}_b^*}{r}$

For sufficiently numerous bootstrap replication, central limit theorem can be applied, and it can be demonstrated that Equation 4.26 approaches asymptotically to $\sigma_y = (\sigma / n)^{1/2}$, while the bootstrap mean matches the mean of the reference population.

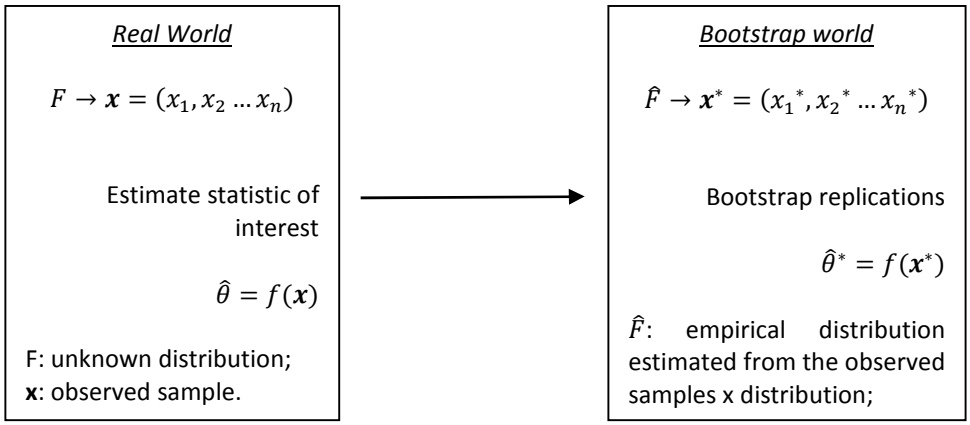

Figure 4.19 Schematic of the concepts underlying the Bootstrap procedure for statistical inferences

Typical application of Bootstrap procedures consists in assessing the accuracy of the estimated parameters without the need for hypotheses concerning the statistical distribution of the investigated population or properties of residuals. In detail, Bootstrap procedure was firstly developed to provide standard errors and confidence intervals for regression coefficients and predicted values in situations in which the standard assumptions are not valid. For example, if residuals were not normally distributed, analytical formulas previously introduced for calculating standard error of regression coefficients would not be valid. Bootstrap procedure allows overcoming these limits. However, regression analyses previously described were essentially aimed to understand the amount of crash frequency's variance explained by geometric features (Efron & Tibshirani, 1998). The attention was then focused on correlation coefficients rather than the predictor coefficients. Bootstrap procedure was instead adopted for validating trend of calibration curves conceived in Chapter 5. After having plotted crash-to-conflict ratios against geometric features most correlated to crash frequency, regression curves were successively obtained.

The problem arises of their reliability because of the restricted sample size. Beyond the analytical expression relating crash-to-conflict ratios with geometric parameters, the same regression trend could not be trusted, with the result that the feasibility of the crash prediction model proposed in this study would remain questionable at all. There is the need for assessing whether the model properly recognises the beneficial or negative effect related to geometric design choices.

There is no information concerning the nature or properties related to the reference population of this calibration curves, with the result that no consideration can be drawn from them. In this perspective, Bootstrap procedures proved to be

particularly useful in corroborating regression trend of the obtained calibration curves.

The main assumption underlying the Bootstrap method is that collected sample approximates the population fairly well. Because of this hypothesis, Bootstrapping does not work well for samples that are quite likely not to be representative of the population. This means that if bootstrap regression curves had trends and shape entirely different from the curve fitting obtained from the original data set, the model would completely mistake the repercussions of a geometric design choice on safety performances. Conversely, if the original curve maintained itself under bootstrap sampling, this would mean that original calibration curves are representative of their reference population despite of the restricted sample sizes. The final step will consist in comparing trend of model predictions concerning influence of geometric parameters on crash frequency with scientific knowledge and empirical evidence. This will definitively prove the ability of the model to give trustworthy results.

Given that no reliance can be placed on calibration curves, the so-called bootstrap by pairs was selected, since it does not require the knowledge of the analytical structure of the regression model. In fact, it does not come from a parametric model and simply consists in resampling the dependent variable and regressors together from the original data. It is a non-parametric statistical procedure for making inferences with only one assumption, that is the original pairs (y_i, x_i) are randomly sampled from a certain reference population. Therefore, the single observation is now the couple formed by the value of the outcome variable and the related value of the geometric covariate. Two hundred bootstrap replications were performed for each calibration curve, which means that each original pair had a probability equal to 1/200 of being selected at every extraction.

A polynomial curve was fitted to each bootstrap sample, and the mean value, as well as related standard error, was calculated along restricted intervals of the geometric covariate. **Figure 4.21** reports an example of Bootstrap procedure. In the upper part, there is the original regression curve, while below the bootstrap outcome is depicted. The crash type here analysed is the rear-end collision at the entry of a roundabout The geometric feature deserving of being analysed for its high correlation with crash frequency is the entry path radius.

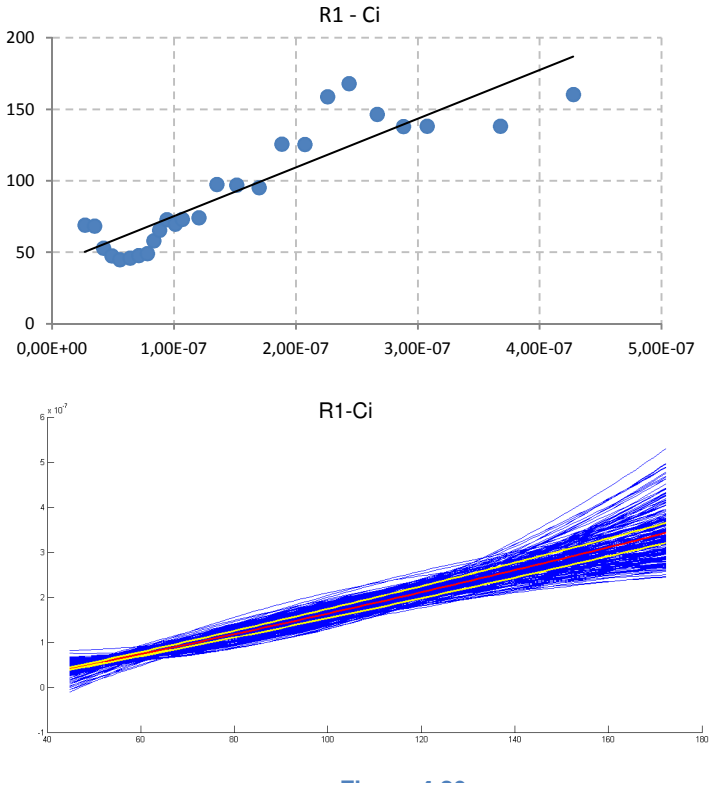

Figure 4.21 Schematic of the concepts underlying the Bootstrap procedure for statistical inferences

The central tendency of analysed data set provided by Bootstrap analyses seems to replicate well the original calibration curve. It can be stated that obtained regression model is quite likely to be able to represent the reference population. In other terms, reliance can be placed on the regression trend. The final stage will consist in verifying whether trend of calibration curve is realistic and consistent with scientific knowledge. Given that high crash-to-conflict ratios represent dangerous situations, as the entry path radius increases, the model indicates that the occurrence probability of a rear-end collision increases. This is consistent with Scientific Literature, and conclusions can be drawn that the crash prediction model based on CO technique proved to be able to provide a realistic pattern concerning the influence of geometric design on this kind of crash.

References

AASHTO, 2010. *Highway Safety Manual.* Washington, DC, USA: s.n.

Agresti, A., 2010. *Categorical Data Analysis - 2nd Edition.* New York, NY, USA: John Wiley & Sons Inc..

Baldi, P., 1999. *Appunti di Metodi Matematici e Statistici - 2nd Edition.* Bologna, Italy: CLUEB.

Box, G. E. P., 1976. Science and statistics. *Journal of the American Statistical Association,* 71(356), pp. 791-799.

Burns, R. P. & Burns, R., 2009. *Business Research Methods and Statistics Using SPSS.* Thousand Oaks, CA, USA: SAGE Publications Ltd .

Cafiso, S. & D'Agostino, C., 2012. *Safety Performance Function for motorways using Generalized Estimation Equations.* Rome, Italy, s.n.

Chiorri, C., 2010. *Fondamenti di psicometria.* Milano, Italy: McGraw-Hill Italia.

Cohen, J., 1988. *Statistical Power Analysis for the Behavioral Science - 2nd Edition.* Hilldale New Jersey: Lawrence Erlbaum Associates.

Cohen, J. & Cohen, P., 2010. *Applied Multiple Regression/correlation Analysis for the Behavioral Sciences.* New York, NY, USA: Taylor & Francis e-Library.

Costello, A. B. & Osborne, J. W., 2005. Best Practices in Exploratory Factor Analysis: Four Recommendations for Getting the Most From Your Analysis. *Practical Assessment, Research & Evaluation,* 10(7), pp. 1-9.

Davison, A. C. & Hinkley, D. V., 1997. *Bootstrap Method and their Application.* Cambridge, United Kingdom: Cambridge University Press.

De Brabander, B. & Vereeck, L., 2006. Safety effects of roundabouts in Flanders: Signal type, speed limits and vulnerable road users. *Accident Analysis and Prevention,* 39(3), pp. 591-9.

Department of Transport and Main Roads, 2014. *Road Planning and design manual - 2nd edition,* s.l.: Quuensalnd Government.

Desmond, P. A. & Hancock, P. A., 2001. *Active and passive fatigue states..* Mahwah, NJ, USA, Lawrence Erlbaum Associates, Inc., pp. 455-465.

Dupont, W. D., 2010. *Statistical modeling for biomedical researchers: a simple introduction to the analysis of complex data - 2nd Edition.* Cambridge, United Kingdom: Cambridge University Press.

Efron, B. & Tibshirani, R. J., 1998. *An Introduction to the Bootstrap - 2nd Edition.* New York, NY, USA: Chapman & Hall/CRC.

Field, A., 2009. *Discovering Statistic using SPSS.* London, United Kingdom: SAGE Pubblications Ltd.

Giaver, T., 1992. *Application, Design, and Safety of Roundabouts in Norway.* Nantes, France, s.n.

Grice, J. W., 2001. Computing and evaluating factor scores. *Psychological Methods,* 6(4), pp. 430-450.

Guichet, B., 1997. *Roundabouts In France: Development, Safety, Design, and Capacity.* Portland, OR, USA, s.n.

Highway Agency, 2007. *Geometric Design of Roundabouts. Design Manual of Roads and Bridges - TD 16/07,* London, United Kingdom: s.n.

Highways Research Group, 2007. *Deliverable No. 2: Review of Literature and Experience on the,* Lund, Sweden: Lund University.

Howell, D. C., 2011. *Statistical methods for psychology.* Boston, MA, United States: Wadsworth Cengage Learning.

Hubert, C. J., 1989. Problems with stepwise methods: Better alternatives. *Advances in social science methodology,* Volume 1, pp. 43-70.

IBM Support Portal, 2012. *IBM SPSS Statistics 21 Core System User's Guide.* [Online]
Available at: http://www-01.ibm.com/support/docview.wss?uid=swg27024972#it

Johnson, R. A. & Wichern, D. W., 2007. *Applied Multivariate Statistical Analysis - 6th Edition.* Upper Saddle River, NJ, USA: Prentice Hall Inc..

Kraha, A. et al., 2012. Tools to support interpreting multiple regression in the face of multicollinearity. *Frontiers in Psychology,* 3(44), pp. 1-16.

Kremelberg, D., 2011. *Practical Statistics: A Quick and Easy Guide to IBM®.* London, United Kingdom: SAGE Pubblications Ltd.

Ministero delle Infrastrutture dei Trasporti, 2001. *Geometrical and functional standards for the design of road intersections,* Rome, Italy: s.n.

Ministero delle Infrastrutture e dei Trasporti, 2006. *Geometrical and functional standards for road design. Official Italian Enhancement Act D.M. 19/04/2006.* Rome, Italy: s.n.

Montella, A., 2011. Identifying crash contributory factors at urban roundabouts and using association rules to explore their relationships to different crash types. *Accident Analysis and Prevention,* 43(4), pp. 1451-63.

Montella, A., Turner, S., Chiaradonna, S. & Aldridge, D., 2012. Proposals for Improvement of the Italian Roundabout Geometric Design Standard. *Procedia - Social and Behavioral Sciences,* Volume 53, pp. 189-202.

NCHRP, 1998. *Modern Roundabout Practice in the United States, NCHRP Synthesis 264,* Washington, DC, USA: Transportation Research Board (TRB) of National Academies.

NCHRP, 2010. *Roundabouts: An Informational Guide - Second Edition,* Washington D.C.: s.n.

NIST, 2012. *NIST/SEMATECH e-Handbook of Statistical Methods.* [Online] Available at: http://www.itl.nist.gov/div898/handbook/index.htm [Accessed 22 February 2014].

Pecchini, D., Mauro, R. & Giuliani, F., 2014. Model of Potential Crash Rates of Rural Roundabouts with Geometrical Features. *ASCE Journal of Tranposrtation Engineering,* 140(11), p. 04014055.

Rummel, R. J., 1970. *Applied factor analysis.* Northwestern University Press: Evanston, IL, USA.

Saunier, N. & Sayed, T., 2008. A Probabilistic Framework for the Automated Analysis of the Exposure to Road Collision. *Transportation Research Record, No. 2019,* pp. 96-104.

Seltman, H. J., 2004. *Experimental Design and Analysis.* s.l.:On-line textbook, Carnegie Mellon University, Department of Statistic.

Sheskin, D. J., 2003. *Handbook of Parametric and Nonparametric Statistical Procedures - 3rd Edition.* London, United Kingdom: Chapman & Hall/CRC.

Stevens, J. P., 2002. *Applied Multivariate Statistics for the Social Sciences - 4th Edition.* Mahwah, New Jersey, USA: Lawrence Erlbaum Associates Inc..

Taylor, A., 2004. *A Brief Introduction to Factor Analysis.* s.l.:Online Textbook, Macquarie University, Department of Psychology.

Technical Committee 13 Road Safety, 2004. *Road Safety Manual.* Paris, France: PIARC - World Road Association.

Thompson, B., 1995. Stepwise regression and stepwise discriminant analysis need not apply here: A guidelines editorial. *Educational and Psychological Measurement,* 55(4), pp. 525-534.

Wayne, S. A. & Zappe, V. C., 2009. *Data Analysis and Decision Making with Microsoft Excel - 2nd Edition.* Mason, OH, USA: South-Western Cengage Learning.

Weisberg, S., 2013. *Applied Linear Regression - 4th Edition.* New York, NY, USA: John Wiley & Sons Inc.

Widaman, K. F., 1993. Common factor analysis versus principal component analysis: Differential bias in representing model parameters?. *Multivariate Behavioral Research,* 28(3), pp. 263-311.

Xiang, L., Wang, L. W., Ecosse, L. L. & Tien, Y. W., 2012. Are linear regression techniques appropriate for analysis when the dependent (outcome) variable is not normally distributed? - Letter. *Invest Ophthalmol Vis Science,* 56(6), pp. 3082-3.

Capitolo 5

Implementation of geometric features in the model

In Chapter 4, exploratory analyses have been discussed and explained before being applied for each crash typology. The purpose of their applications is to unveil possible geometric features showing a certain degree of association with occurrence probability of crashes. In this chapter, outputs of exploratory analyses are exposed, and then calibration curves relating the coefficients (i.e. *crash-to-conflict ratios*) of the model to the most relevant geometric features are proposed and analogies and contradictions with Scientific Literature and empirical evidences are then provided.

Factorial analyses (FA) combined with principal component analyses (PCA) have allowed identifying the geometric features that best represent the sampled legs where crashes of a certain type have occurred. After recognition of these candidate variables for geometric aspects that could be correlated to crash-to - conflict ratios, Discriminant analyses (DA) and multiple linear regressions (MLR) have skimmed design aspects previously found by placing emphasis only on those actually correlated to crash frequency.

As for MLR, alternative models were tested, such as polynomial regression models containing squared original variables and log-normal models linearized via the logarithmic transformation $Y_i = \beta_0 x_{i1}^{\beta_1} \varepsilon_i \rightarrow \ln(Y_i) = \ln\left(\beta_0 x_{i1}^{\beta_1} \varepsilon_i\right) = ln\beta_0 + \beta_1 \ln(x_{i1}) + ln(\varepsilon_i)$. In particular, the latter model was tested because from theory it is widely recognised that historic crashes occurred at a given site tend to follow a Poisson distribution. Both the quadratic and the logarithmic transformation have worsened the original MLR model, where the dependent variable is a one-degree polynomial function of geometric covariates. However, given that the real distribution of historic crashes and conflict opportunities cannot be known, graphical analyses were then conducted in order to discover the actual association existing between the variable of interest and better understand information underlying calibration curves. Eventually, they were resampled via Bootstrap procedure for taking into account the shortage of the available sample size and verifying whether they can be trusted or not. In particular, it is worth pointing out

that the interest is not addressed toward the exact analytical expression of calibration curves. More data are needed for achieving this aim. The attention has been focused on trend of these curves, that is the ability of the proposed model to properly capture the effect of geometric features on safety performances. A positive output may encourage successive enhancements of the model, such as increasing the sample size.

5.1 Collision due to failure to yield starting from a stopped position

5.1.1 Factor analysis

Factor analysis attempts to represent a set of the manifest original variables by means of latent common factors plus a feature that is unique to each manifest variable. In details, factor analysis try to explain as much as possible of the total variance of observed variables with as few latent common factors as possible, in order to obtain a more interpretable outcome.

All of the manifest variables are assumed to be dependent on a linear combination of the latent, common factors and to differ from each other by uncorrelated unique components.

Various factors analyses have been performed for the 32 roundabout legs involved in crash type *Collision due to failure to yield starting from a stopped position* at least one time in their operational life. Various attempt were performed, and it was found that the following set of covariates allows reaching the best results.

- Deviation angle;
- Angle of visibility;
- Entry angle;
- R1sx;

There are two preliminary steps to be conducted in order to assess whether factor analysis may be actually useful for better understanding the collected sample. The first one consists in verifying that variables are uncorrelated. If this hypothesis cannot be rejected, there is no reason to do a principal component analysis and consequently a factor one since the variables have nothing in common. **Table 5.1** clearly shows that the null hypothesis can be rejected: there are certain degree of correlation between considered variables. The measure of *Kaiser-Meyer-Olkin* (KMO) statistic predicts if collected data are likely to factor well, based on correlation and partial correlation. KMO index is substantially higher than the conventional threshold value of 0.6. Therefore, even this step gave positive outcomes.

Table 5.1 Preliminary measures for testing the convenience of factor analysis for uncover concealed information from collected data

KMO Measure of sampling	0.712
Bartlett's test of sphericity (Sig.)	<0.001

Taken together, Bartlett's test and KMO measure of sampling adequacy provide a minimum standard which should be passed before a factor analysis should be conducted. Given that both test are positive, PCA technique is then applied to the collected data in order to find the linear combinations of them that account for as much of the total variable as possible.

PCA technique is then applied to the collected data in order to find the linear combinations of original variables that best explain the total variable. Among them, the first principal component is the new unveiled variable that explain the maximum amount of the original variables (**Table 5.2**).

The amount of variance accounted for by each component is shown by the eigenvalue, which is equal to the sum of the squared loadings for a given component. The higher the eigenvalue, the higher the importance of this component and the probability it will be retained as a factor. The proportion of variance explained by a single component can be determined by the ration between the corresponding eigenvalue and the overall variance. Table 5.2 also shows the cumulative percentage of variance accounted for by the current and preceding factors.

Table 5.2 Eigenvalues of each component and their contribution in explaining the total variance

Component	Eigenvalues	% of variance	% cumulative
1	2.199	54.984	55.0
2	0.925	23.132	78.1
3	0.482	12.060	90.2
4	0.393	9.827	100.0

For this crash type, the first two components were retained as factors, since together they explain more than 70 per cent of the entire variance and the knee of the scree plot graphing the magnitude of eigenvalues seems to occur nearby the second factor (**Figure 5.1**).

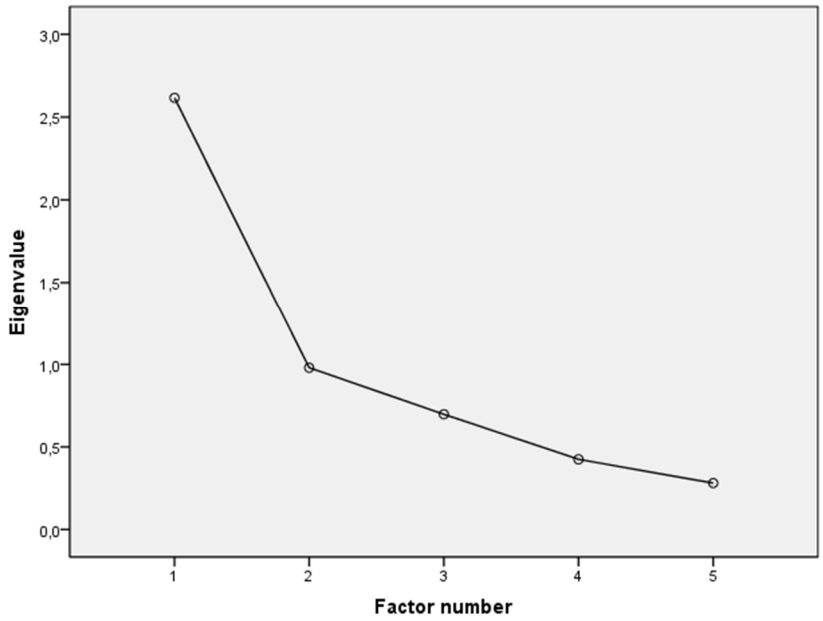

Figure 5.1 Scatter plot graphing the eigenvalues related to each component

Table 5.3 reports loadings of the two retained factors.

Table 5.3 Component matrix showing loadings of each variable

Manifest variables	*Extracted factors*	
	1	**2**
Deviation angle	-0.381	0.921
Angle of visibility	0.833	0.249
Entry angle	0.819	0.071
R1sx	0.830	0.102

Table 5.4 shows the communalities of each manifest variable for the two extracted factors, that is the proportion of each variables' variance explained by the retained factors.

Table 5.4 *Factor matrix showing loadings of each variable after Varimax rotation*

	Initial	*After extraction*
Deviation angle	1.000	0.993
Angle of visibility	1.000	0.756
Entry angle	1.000	0.676
R1sx	1.000	0.700

By analysing signs and values of factors (**Table 5.3**), their underlying and latent meaning may be realised.

The first factor seems to bring out entries with high design speeds with a fast circulating traffic. High angles of visibility are associated to high entry angles, as already specified in Chapter 4. This layout tends to increase vehicle speeds, as confirmed by the negative sign of deviation angle. The loading related to the entry radius of the left approach seems to be important too. As matter of fact, if vehicles coming from the left moves at higher speeds, the likelihood of *collision due to failure to yield starting from a stopped position* will inevitably increase.

The second factor appears to be prevalently focused on the legs with accentuated deviation of trajectories followed by vehicles.

For the sake of an easier interpretation of manifest meanings of the factors, an orthogonal rotation factor was then applied by following the Varimax criterion where the aim is to reduce for each factor the number of loadings significantly different from zero (**Table 5.5** and Figure 5.2).

Table 5.5 *Factor matrix showing loadings of each variable after Varimax rotation*

Manifest variables	*Extracted factors*	
	1	**2**
Deviation angle	-0.109	0.990
Angle of visibility	0.870	0.007
Entry angle	0.806	-0.161
R1 sx	0.826	-0.134

In this situation, Varimax rotation did not offer a significant additional perspectives about the essence of factors. Loadings are practically unaltered, and **Figure 5.2** clearly shows that interpretation of the factors is identical to the previous conceived one.

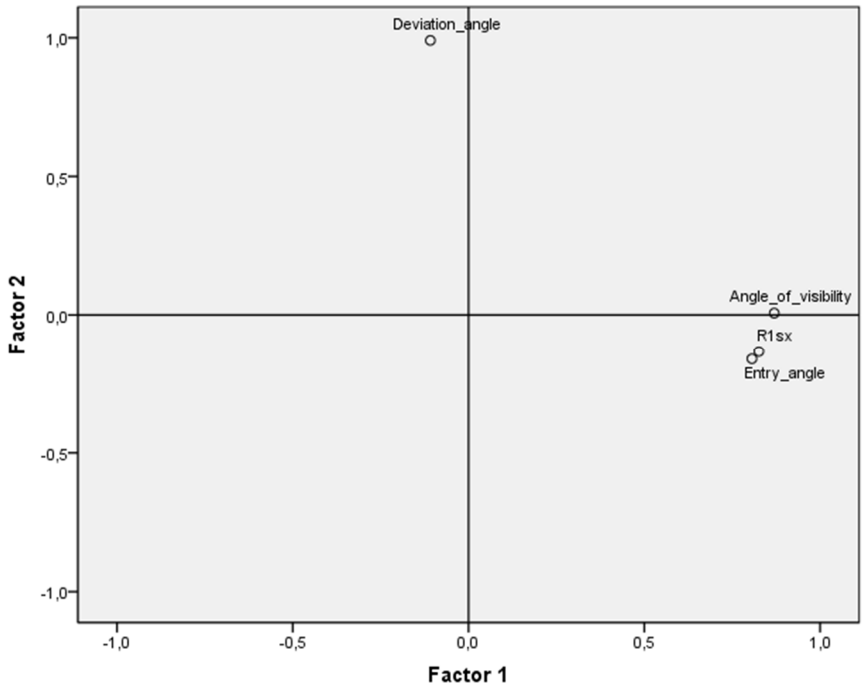

Figure 5.2 *Factor plot in rotated factor space.*

As already explained, the reproduced matrix correlation based on the extracted factors can be obtained from the matrix loadings (Table 5.6). It is desirable that corresponding values of the two variables are as close as possible, that is that residuals are close to zero. Correlation matrix estimated by Factor analysis proved to approximate well the original one, with only three residuals greater than the threshold value of 0.05.

Table 5.6 In the top part of the table there are the reproduced correlations, while below there are the residuals obtained by the difference with the sample correlation matrix.

		Deviation angle	*Visibility angle*	*Entry angle*	*R1sx*
Reproduced Correlation	*Deviation angle*	0.993[a]	-0.088	-0.247	-0.222
	Visibility angle	-0.088	0.756[a]	0.700	0.717
	Entry angle	-0.247	0.700	0.676[a]	0.687
	R1sx	-0.222	0.717	0.687	0.700[a]
Residuals[b]	*Deviation angle*		-0.041	0.031	0.014
	Visibility angle	-0.041		-0.138	-0.128
	Entry angle	0.031	-0.138		-0.168
	R1sx	0.014	-0.128	-0.168	

Extraction method: principal component analysis.
a. Reproduced communalities.
b. Residuals are computed between observed and reproduced correlations. There are 3 (50.0%) non redundant residuals with absolute values greater than 0.05.

Errore. L'origine riferimento non è stata trovata. provides the Matrix Score where factors are expressed as a function of original variables. However, this in an approximated solution, given that exact scores cannot be known for the presence of uniqueness factors (IBM® SPSS 21 uses the so-called coarse method).

Table 5.7 Component matrix showing loadings of each variable

	Deviation angle	*Visibility angle*	*Entry angle*	*R1sx*
F1	-0.112	-0.439	0.379	-0.393
F2	-1.004	0.153	-0.030	0.001

5.1.2 Discriminant analysis

Discriminant analysis, similarly to factor analysis, looks for linear combinations of variables which best explain the data. The difference from FA is that the items of the collected sample have been catalogued in different groups, and the aim of the research is now focused in trying to model as well as possible the discrepancies existing between these groups. Items are grouped in accordance to their dependent variable's values. This means that dependent variable is now introduced in the analysis and is implemented as a categorical variable. Outputs of DA will then provide basilar information about the correlation between dependent variable and the covariates of the model, and these evidences will be successively examined in depth via multiple linear regression models.

There are 4 initial geometric parameters identified by FA and 32 legs which has been assigned to one of three groups defined on the base of their crash frequency magnitude. Table 5.8 offers an overview about collected data.

Table 5.8 Group statistics

Class frequency		*Mean*	*Std. deviation*	*Valid cases*
1	Deviation angle	55.8667	27.29172	15
	Visibility angle	78.8000	16.89548	15
	Entry angle	52.5333	14.15156	15
	R1sx	109.4133	101.31787	15
2	Deviation angle	63.2727	38.01076	11
	Visibility angle	69.1818	22.58237	11
	Entry angle	53.5455	17.07257	11
	R1sx	149.3909	136.69385	11
3	Deviation angle	20.3333	18.43547	6
	Visibility angle	60.8333	25.26988	6
	Entry angle	54.3333	23.82156	6
	R1sx	110.6333	96.31008	6
Total	Deviation angle	51.7500	33.22067	32
	Visibility angle	72.1250	21.11222	32
	Entry angle	53.2188	16.62826	32
	R1sx	123.3844	111.91698	32

Table 5.9 shows the Within-groups correlation matrix. It corresponds to a correlation matrix of data points obtained by subtracting to them the barycentre of the group they belong to. Multicollinearity should not represent a possible concern for discriminant analysis given that no value is greater than 0.8.

Table 5.9 Within-groups correlation matrix.

	Deviation angle	*Visibility angle*	*Entry angle*	*R1 sx*
Deviation angle	1.000	-0.275	-0.231	-0.288
Visibility angle	-0.275	1.000	0.612	0.654
Entry angle	-0.231	0.612	1.000	0.525
R1sx	-0.288	0.654	0.525	1.000

First of all, significant differences between groups on each of the independent variables are to be examined. If there were not significant differences between groups, it would not be meaningful proceeding any further with the analysis. Table 5.10 shows two tests which can be used to evaluate the potential of the considered manifest variables in discriminating the three groups before the model is created. In particular, the significance of differences in group means for each variable is tested. The quantity *(1 - Wilks' Lambda)* is the proportion of variance in the dependent variable that can be explained by the considered predictor. Therefore, a relatively small Wilks' Lambda value indicates that the analysed covariate has a potential in discriminating groups. The other columns of Table 5.10 refers to an F-test performed in a one-way analysis of variance (ANOVA). The null hypothesis is that all population means are equal in regard to a particular variable; the alternative hypothesis is that at least one mean is different.

As can be seen by **Table 5.10**, the Wilk's lambda test presents similar results for the variables, while the ANOVA seem to suggest that only Deviation angle may discriminate the three sub-populations.

Table 5.10 Test of equality of group means table

	Wilks' Lambda	**F**	**df1**	**df2**	**p-value**
Deviation angle	0.777	4.167	2	29	0.026
Visibility angle	0.889	1.804	2	29	0.183
Entry angle	0.998	0.027	2	29	0.974
R1sx	0.971	0.436	2	29	0.651

After this preliminary insight into the potential of each manifest variable in separating sub-populations characterised by different crash frequency, discriminant functions can now be sought. The maximum number of discriminant functions produced is equal to the number of groups minus 1. As a result, in this example, there are only two directions of interest; their eigenvalues and their contribution in explaining original variance are shown in **Table 5.11**. The canonical correlation is the multiple correlation between two sets of variables. The first is

constituted by the manifest variables, while the second refers to the dummy variables used for coding the three considered groups of different crash frequency. A high canonical correlation indicates a function that discriminates well.

Table 5.11 Eigenvalues table

Function	Eigenvalue	% of variance	% cumulative	Canonical correlation
1	0.532[a]	70.7	70.7	0.589
2	0.220[a]	29.3	100.0	0.425

The canonical correlation is then exploited in the statistical methods devoted to ascertain the significance of the acquired discriminant functions.

If canonical correlation of discriminant functions were be equal to zero, no relationship between the set of independent variables and the discriminant scores (i.e. the dependent variable) would be found. The discriminant functions would be worthless because the means of the discriminant scores would be the same in the considered groups.

This is exactly the null hypothesis of the Willk's lambda statistical test, by means of which it is possible to establish the significance of the discriminant functions. Wilks' lambda is the proportion of the total variance lying in the discriminant scores not explained by differences among the groups. It is calculated as the product of the values of *1-canonical correlation*^{2}. Therefore, smaller values of Wilks' lambda are desirable. In this example, canonical correlations are 0.704 and 0.355, so the Wilks' Lambda testing both canonical correlations is $(1-0.589^2)*(1-0.425^2) = 0.5351$, and the Wilks' Lambda testing the second canonical correlation is $(1-0.425^2) = 0.819$.

The Chi-square statistic tests whether the canonical correlation of discriminant functions is equal to zero, which implies a unitary Wilk's lambda. This is exactly the null hypothesis, a situation characterised by a negligible contribution offered by discriminant functions in explaining the total variance of the independent variables.

Table 5.12 represents the output of Willk's lambda statistical test carried out on the two discriminant functions obtained for this example. The first test presented in this table tests both canonical correlations ("1 through 2") and the second test presented tests the second canonical correlation alone.

Table 5.12 Wilk's lambda table

Function	Wilks' Lambda	Chi-square	df	p-value
1 through 2	0.535	17.203	8	0.028
2	0.819	5.479	3	0.140

From **Table 5.12**, it can be stated that there is at least one statistically significant function. If the probability for this test had been larger than 0.05, the

definitive conclusion would have been that there are no discriminant functions able to separate the groups of the dependent variable.

Discriminant analysis would have been concluded here.

The second line of the Wilks' Lambda table tests the null hypothesis that the mean discriminant scores for the second possible discriminant function are equal in the subgroups of the dependent variable. Since the probability of the chi-square statistic for this test is greater than 0.05, the null hypothesis cannot be rejected. In conclusion, there is only one discriminant function to separate the groups of the dependent variable.

In **Table 5.13**, the standardised coefficients are provided for the two discriminant functions. Their interpretation enables unveiling the latent aspect they represent, similarly to the identification of the meaning embraced by factors adopted in factor analysis. The sign indicates the direction of the relationship, while the magnitudes define how strongly the discriminating variables effect the score.

As for the first function, the only one that actually separates the three groups, Entry and Exit path radius have the preponderant coefficients. Entry angle and Angle of visibility score were less successful as predictors, while ICD score is insignificant.

Table 5.13 Standardised canonical discriminant function coefficients table

	Functions	
	1	**2**
Deviation angle	-0.779	0.629
Visibility angle	1.068	-0.925
Entry angle	0.393	0.196
R1 sx	-0.254	-1.052

The standardised coefficients of **Table 5.13** together with standardised independent variables can be used to calculate the standardised discriminant score for a given case. The distribution of the scores from each function will be then standardized to have a mean of zero and standard deviation of one. For discriminant function 1, score achieved by a new case will be equal to (Equation 5.1):

$$D_1^* = -0.779 * Deviation\ angle^* + 1.068 * Visibility\ angle^* - 0.393 * Entry\ angle^* - 0.264 * (R1sx^*) \quad (5.1)$$

There is an alternative way of specifying the relative importance of the predictors. The structure matrix table (Table 5.14) provides the correlations of each independent variable with the discriminant functions. These correlations serve as factor loadings in factor analysis. By identifying the largest loadings, the researcher gains an insight into how correctly interpreting the discriminant function.

Table 5.14 Structure matrix table

	Functions	
	1	**2**
Deviation angle	0.649	0,536
Visibility angle	0.446	-0,289
Entry angle	-0.053	0,038
R1 sx	0.014	0,369

Pooled within-groups correlations between discriminating variables and standardised canonical discriminant functions. Variables ordered by absolute size of correlation within function.

Loadings of Deviation angle and angle of visibility stand out as predictors that strongly influence the allocation of legs to the three groups characterised by different crash frequencies. Structure matrix table confirms the vision obtained from standardised canonical distribution function coefficients.

Discriminant functions are eventually created by unstandardized coefficients, which are reported in **Errore. L'origine riferimento non è stata trovata.**. Non standardised values of manifest variables will give the score for the discriminant functions. The greatest coefficients are referred to entry and exit path radius again.

Table 5.15 Canonical discriminant function coefficients table. Unstandardized coefficients

	Functions	
	1	**2**
Deviation angle	0.026	0.021
Visibility angle	0.052	-0.045
Entry angle	-0.023	0.011
R1sx	-0.002	0.009
(Constant)	-3.580	0.417

A further way of interpreting the DA results consists in inserting the average discriminant score (unstandardized) in the three groups (**Errore. L'origine riferimento non è stata trovata.**). In detail, the discriminant score for each group is obtained when the variable means (rather than individual values for each case) are entered into the discriminant equation. These group means are called centroids.

Table 5.16 Functions at group centroids table

	Functions	
Class frequency	**1**	**2**
1,00	0.499	0.351
2,00	0.078	-0.616
3,00	-1.391	-0.251

Unstandardized canonical discriminant functions evaluated at group means

SPSS also provides a graphical representation of DA output. As can be seen by **Figure 5.3**, the contribution offered by the second discriminant function is effectively negligible.

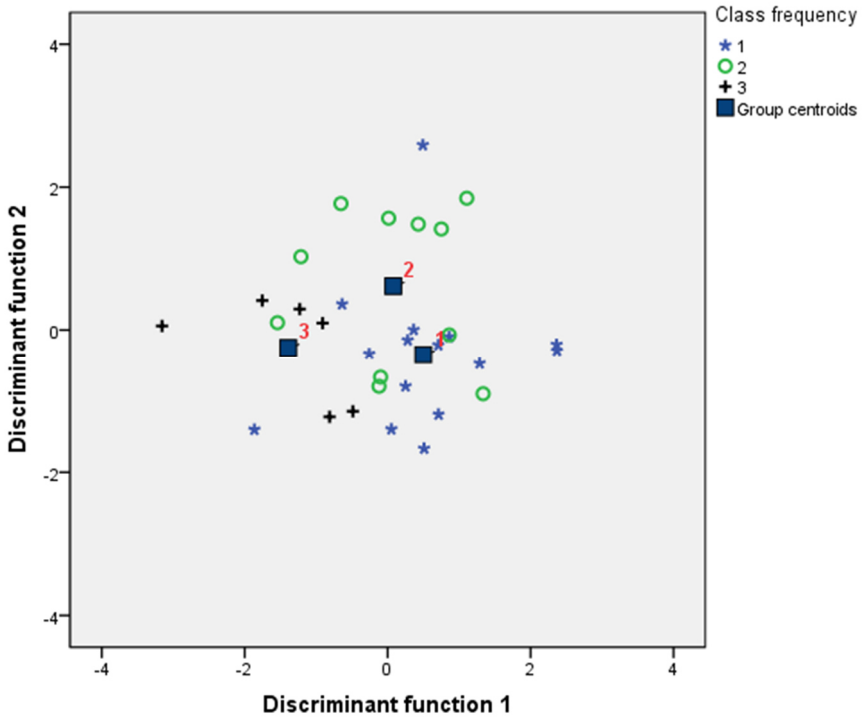

Figure 5.3 Graph of roundabout legs on the discriminant dimensions.

The output of discriminant analysis is the classification table, whose rows are the observed categories of the dependent variable while the columns are the predicted categories. When prediction is perfect, all cases lie on the diagonal (**Table 5.17**). The percentage of cases on the diagonal is the percentage of correct

classifications. The cross validated set of data is a more authentic representation of the outcome achieved by discriminant function. The cross validation is often termed a 'jack-knife' classification, given that successively classifies all cases but one to develop a discriminant function and then categorizes the case that was left out. This process is repeated with each case left out in turn. This cross validation produces a more reliable function. The ratio is that one should not use the case the researcher is trying to predict as part of the categorization process. The classification results for the crash type reveal that 62.5% of legs were classified correctly into the three categories of crash frequency. The third group suffers from the least accuracy.

This overall predictive accuracy of the discriminant functions is called the *hit ratio*. Via a random classification of the collected legs, there would be a 33.3% probability of correctly collocating the 32 subjects into the three categories. Accordingly to a conventional approach, acceptable hit ratios must be greater than this probability increased by 25%, which gives a threshold value equal to 41.63%. The output of discriminant analysis is substantially up to standard.

Table 5.17 Classification results table. 68.8% of original grouped cases correctly classified. 62.5% of cross-validated grouped cases correctly classified.

			Predicted group membership			
		Class frequency	**1.00**	**2.00**	**3.00**	**Total**
Original	Count	1.00	12	2	1	15
		2.00	4	5	2	11
		3.00	1	1	5	6
	%	1.00	80.0	13.3	6.7	100.0
		2.00	36.4	45.5	18.2	100.0
		3.00	.16.7	0	83.3	100.0
Cross-validated [a]	Count	1.00	11	3	1	15
		2.00	4	5	2	11
		3.00	2	0	4	6
	%	1.00	73.7	20.0	6.7	100.0
		2.00	36.4	45.5	.18.2	100.0
		3.00	33.3	0	66.7	100.0

a. Cross validation is done only for those cases in the analysis. In cross validation, each case is classified by the functions derived from all cases other than that case.

A discriminant analysis was then conducted to predict the categorical variable *crash frequency* for analysed roundabout legs. Predictor variables were *deviation angle, angle of visibility, entry angle* and *entry path radius of the left approach*.

These are the same geometric features previously identified via the factorial analysis. Significant mean differences were observed for the deviation angle. Only one of the two discriminate functions was found to be statistically significant, that is able to effectively separate legs of different crash frequency category.

By analysing the standardised coefficients of the discriminant function and the pooled within-groups correlations of the structure table matrix, conclusion can be drawn that $deviation\ angle$ and $angle\ of\ visibility$ are the only predictors which can explain safety performances of roundabout legs in regard to the crash type collision due to failure to yield starting from a stopped position.

5.1.3 Regression analyses

Multiple linear regression models whit crash frequency as a continuous dependent variable may allow understanding the portion of variance affecting crash frequency explained by the single geometric parameters. From FA and DA, a set of geometric features apparently related to crash frequency was found and then investigated in MLR models. Stepwise regression procedures were applied by exploiting the F-test in order to establish which of these four models should be preferred for analysing the investigated phenomenon.

- Model 1. Predictors: Constant, Deviation angle;
- Model 2. Predictors: Constant, Deviation angle, Angle of visibility;
- Model 3. Predictors: Constant, Deviation angle, Angle of visibility, R1sx;
- Model 4. Predictors: Constant, Deviation angle, Angle of visibility, R1sx; Entry angle.

It is then desired to ascertain whether the full model contributes additional information about the association between Y and the predictors. The null hypothesis is that the additional covariates are not significant, and their related coefficients are therefore equal to zero. If the difference between error sum of squares for the reduced model (i.e. SSE_R) and the error sum of squares for the complete model (i.e. SSE_C) reaches high values, the null hypothesis is likely to be rejected because this would mean that the additional $k - h$ parameters significantly improve the model's fit to the data. Output of F-test for the four tested models are reported in **Table 5.18**, which shows that the independent variables statistically significantly predict the dependent variable for all of tested models.

Table 5.18 F-test carried out for testing statistical significance of various models

Model		Sum of squares	df	Mean squares	F	Sig.
1	*Regression*	<0.001	1	<0.001	9.696	0.004
	Residual	<0.001	30	<0.001		
	Total	<0.001	31			
2	*Regression*	<0.001	2	<0.001	10.824	<0.001
	Residual	<0.001	29	<0.001		
	Total	<0.001	31			
3	*Regression*	<0.001	3	<0.001	9.450	<0.001
	Residual	<0.001	28	<0.001		
	Total	<0.001	31			
4	*Regression*	<0.001	4	<0.001	9.959	<0.001
	Residual	<0.001	27	<0.001		
	Total	<0.001	31			

In order to definitively decide on which model focusing the attention, measures of model adequacy were calculated, with particular emphasis to adjusted R square, since it increases only when significant terms are added to the model (**Table 5.19**). After analysis of Table 5.19, the full model was then selected.

Table 5.19 Measure of adequacy for the various MLR models.

Model	R	R-square	Adjusted R square	Standard error of the estimate
1	0.712	0.508	0.435	0.003
2	0.494	0.244	0.219	0.004
3	0.654	0.427	0.388	0.003
4	0.709	0.503	0.450	0.003

Unstandardized coefficients indicate the increase experienced by the dependent variable for a unitary increment of the independent variable when all other independent variables are held constant (**Table 5.20**).

The same table reports the outputs of tests pertaining to the statistical significance of each of the independent variables. The null hypothesis is that the related coefficient of the investigated predictor is equal to zero. If p-value < 0.05, the null hypothesis can be rejected, and it can be stated that coefficients are

statistically significantly different to zero. It appears that *Entry path radius of the left approach, deviation angle* and the *angle of visibility* are statistically significant.

Table 5.20 Calculating regression coefficients and testing statistical significance of the independent variables.

	Model	Unstandardized coefficients		Standardised Coefficients		
		β	*Std. Error*	$\hat{\beta}$	*t*	*Sig.*
1	*Constant*	1.79E-03	2.82E-04		6.34	0.000
	R1sx	1.27E-06	6.94E-07	0.322	1.84	0.077
	Deviation angle	-6.58E-06	1.86E-06	-0.494	-3.55	0.001
	Visibility angle	-1.39E-05	3.78E-06	-0.663	-3.68	0.001
	Entry angle	2.27E-06	4.57E-06	0.085	0.498	0.623

The variance inflation factor (VIF) quantifies the severity of multicollinearity for linear regressions with OLS estimates of the coefficients. It provides an index that measures how much the variance of an estimated regression coefficient is increased because of multicollinearity. Given that VIF factor is substantially lower than 2.0 for each predictor, there rea not severe reciprocal correlations between independent variables (**Table 5.21**).

Various concerns persist about the reliability of standardised regression coefficients as a measure of actual relationships between each predictor and the dependent variable. As a matter of fact, $\hat{\beta}^*$coefficients can dramatically change in numerical value, and even in sign, as new variables are introduced or as old variables are removed. They simply reflect the amount of credit given to the related predictors. It can be said that they are context-specific to a given model characterised by a specific set of covariates. The problem is that the true model is rarely, if ever, known.

In addition, $\hat{\beta}^*$ coefficients are still sensitive to multicollinearity, and their values may be affected by the amount of Y variance shared with the other predictors. As a result, it can happen that a predictor explaining a consistent part of Y variance may have a near-zero $\hat{\beta}^*$ because another predictor is receiving the credit for the explained variance.

Other techniques are then required for correctly evaluating the importance of single predictors in explaining the analysed phenomenon. There is the need for estimating the relationship between a predictor variable and the outcome variable after controlling for the effects of other predictors in the equation.

Partial correlation represent the correlation between the dependent variable Y and a predictor after common variance with other predictors has been removed from both Y and the predictor of interest.

The squared *semipartial correlations* is the unique variance of that predictor shared with the dependent variable. This means that the squared semipartial correlation for a variable denotes the decrease in coefficient of determination R^2 if that variable is removed from the regression equation.

Table 5.21 Verifying the presence of severe multicollinearity and calculation of correlation coefficients

	Correlation coefficients			**Collinearity**	
	Zero-order	*Partial*	*Semipartial*	*Toll*	*VIF*
R1sx	0.079	0.333	0.248	0.592	1.69
Deviation angle	-0.494	-0.564	-0.479	0.939	1.06
Visibility angle	-0.361	-0.578	-0.497	0.562	1.78
Entry angle	-0.013	0.095	0.067	0.618	1.62

A squared structure coefficient denotes the amount of variance estimated by the model that the predictor is able to explain. This is equivalent to say that a squared structure coefficient denotes the amount of variance related to R^2 that the predictor is able to explain.

Structure coefficients definitely clarify the contribution of each predictor in explaining the phenomenon described via a multiple linear regression, and they provide support in trying to identify multicollinearity effects. Structure coefficients confirm previous analyses of partial and semipartial correlations. Crash frequency variance seems to be basically explained by Deviation angle and angle o visibility.

The magnitude of these relationships may be directly and synthetically measured by the so-called *Cohen's f^2 effect size*, which is focused on the strength of the association between the predictor of interest and the dependent variable.

Its outcome is a measure of practical significance in terms of the magnitude of the effect exerted by the single predictor. It is independent of the sample size and is appropriate for calculating the effect size within a multiple regression model in which the independent variable of interest and the dependent variable are both continuous. The effect size corroborates previous results: *deviation angle and angle of visibility* appear to have a marked relationship with crash frequency as compared to other 23 investigated geometric factors (**Table 5.22**). It is worth noting that discriminatory analyses gave importance to *R1sx* too, while correlation coefficients and effect sizes proved its irrelevant association with crash frequency.

Eventually, exploratory analyses reach the conclusion that these aspects should deserve the maximum attention in order to design safer roundabouts from collisions due to failure to yield starting from a stopped position.

Table 5.22 Calculation of structure coefficients and effect size f^2

	Structure coefficient	**Effect size f^2**
R1sx	0.012	0.052
Deviation angle	0.481	0.496
Visibility angle	0.256	0.485
Entry angle	0.000	-0.002

A multiple linear model is based on certain assumptions that must be verified in order to trust its outputs. As an introductory premise, the fact must be enlighten that regressions here proposed have an exploratory essence. They are not aimed to propose exact prediction models, but rather they have been arranged in order to refine previous exploratory analyses. They are the last step of the path aimed to disclose the most prominent geometric factors related to crash frequency and deserve to be implemented in crash prediction model based on Conflict Opportunities. For these reasons, even if assumptions of multiple linear models were not fully satisfied, this would not aprioristically imply the abandon of model outputs. Certain assumptions, in particular normal distribution and homoscedasticity of residuals, must be complied if the aim is obtaining new data points, but that is not the case.

Correlation and structure coefficients may provide interesting information anyhow. For example, although general hypothesis would not fully respected, a relevant structure coefficient standing out from the other ones would remark the importance of the covariate, with even stringer reason in case the same covariate was identified by previous exploratory analyses.

The most intuitive way for testing normality of residuals consists in trying to graph a histogram by plotting obtained residuals and placing them in regularly spaced cells. The histogram should approximate a normal distribution of residuals. However, with small sample sizes, which is the case of various crash type here in this study, this is not be the best choice for judging the distribution of residuals (**Figure 5.4**).

A more affordable way is proposed by the $normal\ probability\ plot$ (also called P-P plot). It is obtained by sorting the standardised residuals into ascending order and then calculating the cumulative probability of each residual. Eventually, the so calculated P values are then plotted versus the normalised cumulative frequency distribution of residuals themselves, that is $(\varepsilon_i - \mu)/\sigma)$, where μ and α are approximated via the mean and standard deviation of residuals respectively. The normal probability plot seems to be able to produce an approximately straight line, which means that residuals may come from a normal distribution (**Figure 5.5**).

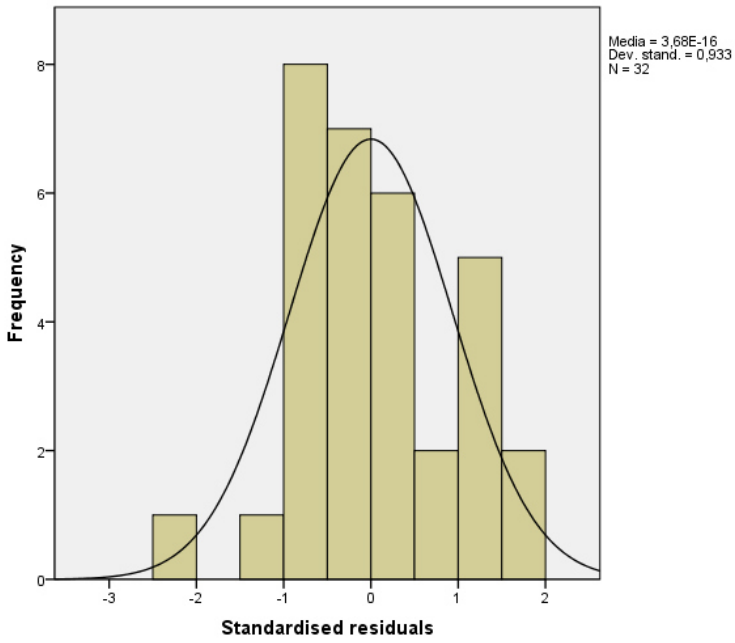

Figure 5.4 Testing normality distribution of residuals. Histogram

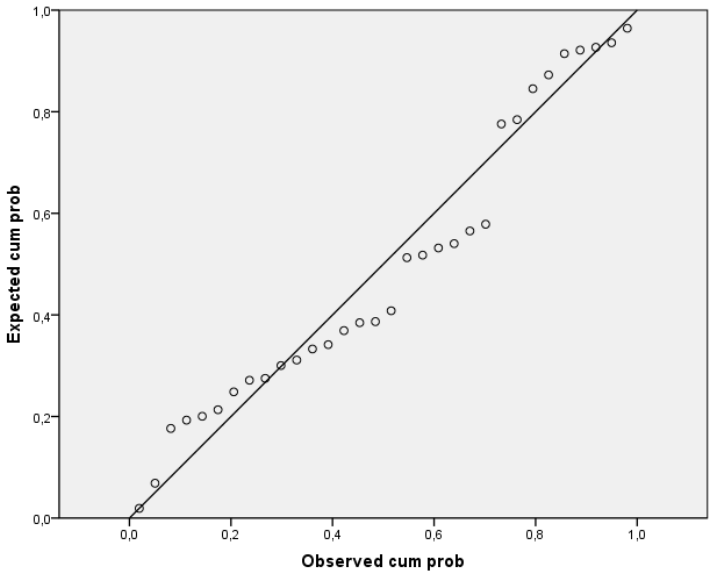

Figure 5.5 Testing normality distribution of residuals. Normal probability plot

There are instead serious concerns about the homoscedastic nature of residuals, which should have a constant variance σ^2. Homoscedastic assumption can be checked by visual examination of a plot of the standardized residuals by the regression standardized predicted value. Residuals are not evenly scattered around the line and a certain trend can be recognised (**Figure 5.6**). This means that homoscedastic assumption is not verified. However, as already said, this cannot compromise definitive results obtained with correlation coefficients and the effect size.

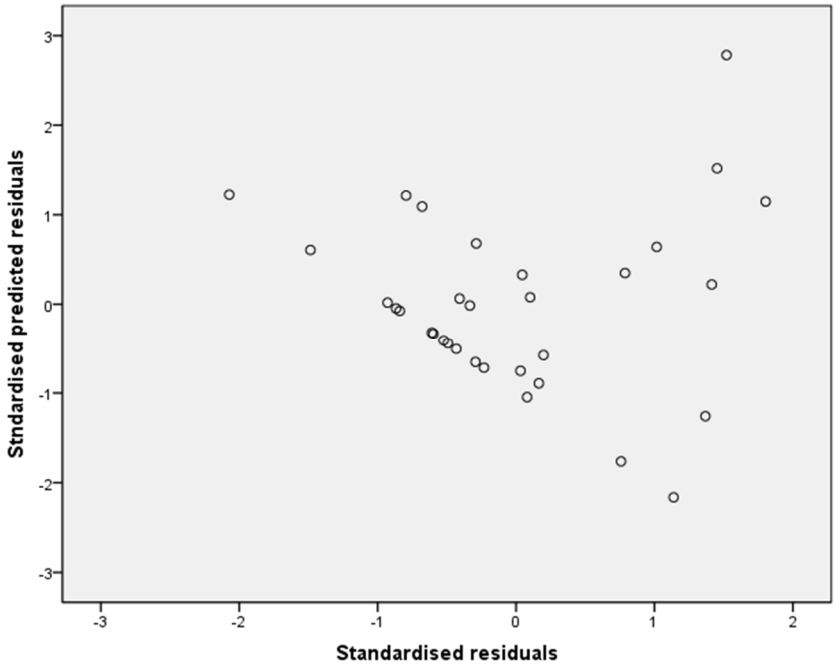

Figure 5.6 Scatter plot for detecting homoscedasticity of residuals

5.1.4 Estimating the calibration curves

The output of the crash prediction model based on COs techniques is practically the calibration curve relating geometric features to crash-to-conflict ratios. These coefficients allow converting calculated COs frequency in crash frequency. Exploratory analyses were performed in order to focus the attention only on geometric features with a significant association with crash frequency when trying to ascertain calibration curves.

Multiple linear models and their correlation coefficients, as well as the effect size, provides information about the strength of the association between two

variables. However, their range is limited to linear relationships only. As already said in Chapter 4, MLR are quite flexible and it is possible implementing polynomial and Poisson relationships.

However, in order to extend and verify the acquired knowledge of the correlation between geometric features and crash frequency, graphical analyses were carried out. They enabled assessing possible reciprocal relationships among geometric features, their links with traffic flows and their correlation with the number of COs and the crash frequency. For example, traffic flows proved to be statistically insignificant in MLS model for all the crash typologies, but graphical analyses unveiled a certain influence of these parameters on the calibration curves. The same MLS models did not find correlations between geometric features and COs frequency, while graphical analyses disclosed significant trends in certain situations. Simple moving average technique proved to be very useful in avoiding that erratic elements could conceal possible clear tendencies.

Exploratory analyses identified the *deviation angle* and the *angle of visibility* as the geometric features most correlated to frequency of crashes due to failure to yield when starting from a stopped position. Conversely, no geometric parameters were found to be correlated to the potential crash frequency.

$$N_{1a} = Q_E * \big(1 - P(0)\big) * P\big(t_{inf} < t < t_{sup}\big)$$

For this type of crash, COs related to the analysed leg and calculated for each hour of the day show a peculiar monotone increase, that is, COs increase as traffic flows increase (**Figure 5.7**). This trend also emerges when considering the average daily traffic flow entering a roundabout and passing through the analysed leg (**Figure 5.8**).

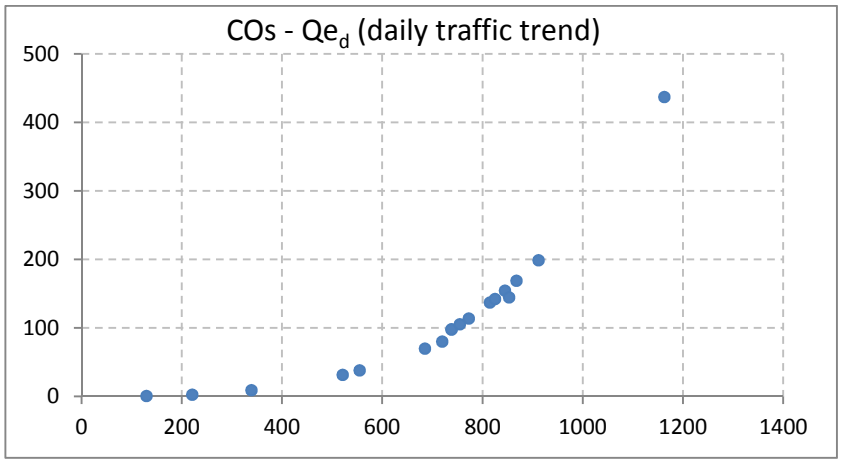

Figure 5.7 Daily evolution of Conflict Opportunities plotted against entering traffic flows measured on an hourly basis for a single roundabout leg

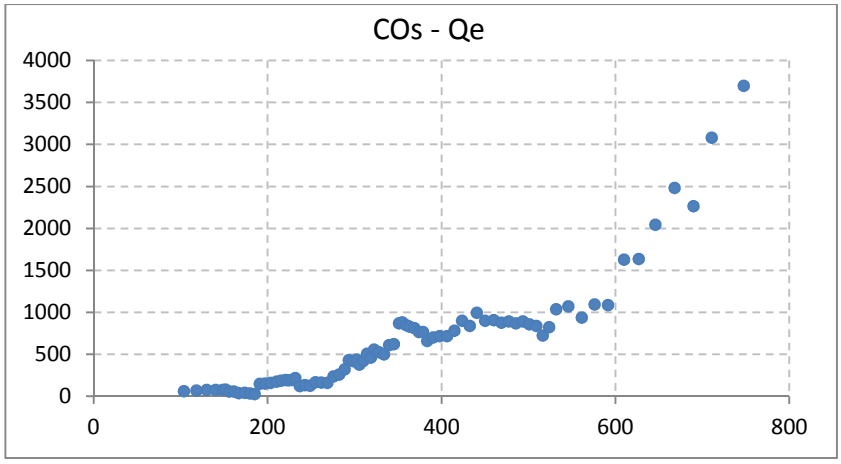

Figure 5.8 Conflict Opportunities plotted against average daily traffic flows entering roundabouts. Each point represent a different leg. All of the 87 legs analysed in this study were considered

5.1.4.1 Deviation angle β

By considering all of the sampled roundabouts, overall monotonic trend can be detected between inscribed circle diameters and entering traffic flows measured on an hourly basis (**Figure 5.9**). Greatest roundabouts are exposed to the most intense traffic flows.

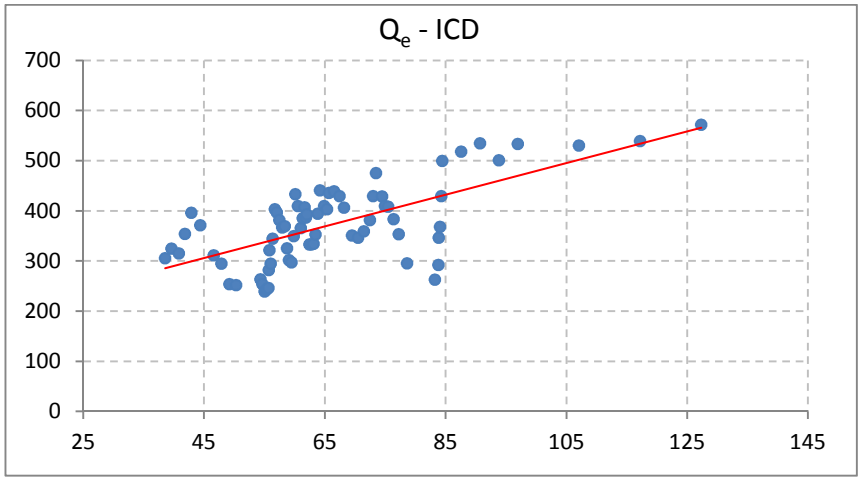

Figure 5.9 Average daily traffic flows plotted against inscribed circle diameter. All of the 87 sampled legs were considered. A Simple Moving Average was applied

From **Figure 5.10**, a certain dependency can be noticed between ICD and deviation angle: as the former increases, the latter reaches higher values too. In particular, by analysing in depth the same graph, a direct relationship stands out involving small ICD and deviation angles, that is between small traffic flows and deviation angles. Conversely, similar associations were not found for great roundabouts (**Figure 5.11**).

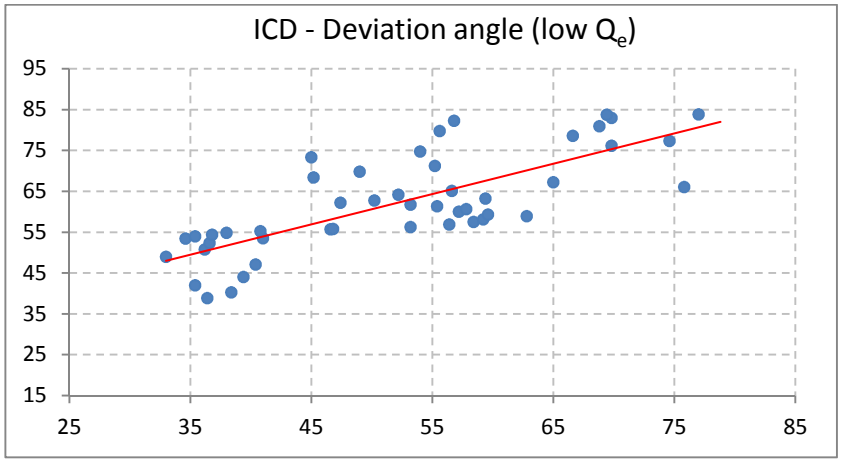

Figure 5.10 Inscribed circle diameters plotted against deviation angles for legs with low traffic flows.

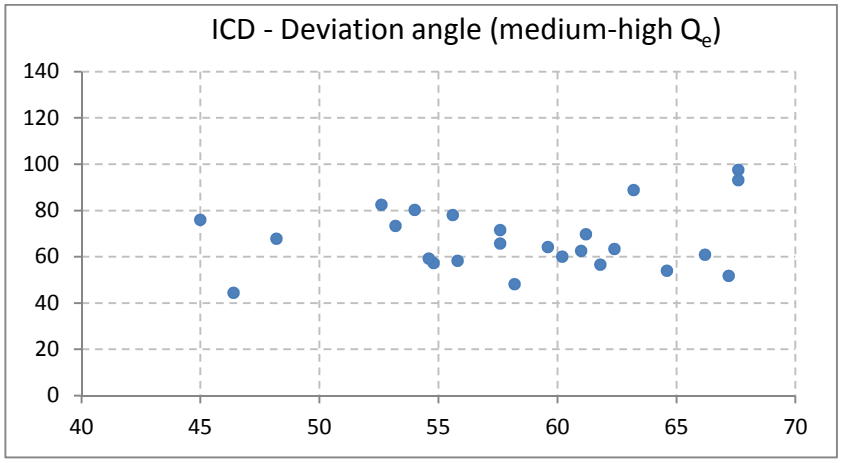

Figure 5.11 Inscribed circle diameters plotted against deviation angles for legs with high traffic flows

Overall, evolution of deviation angles along COs appears to provide no useful information. However, two significantly different trends can be obtained by differentiating legs affected by medium-high traffic flows (Qe > 400 passenger per car unit / hour) from legs experiencing low vehicular volumes (Qe < 400 pcu/h). If COs reduction associated with an increase in deviation angle is recorded for medium-high vehicular flows, the number of potentially dangerous situations arises as deviation angle increases.

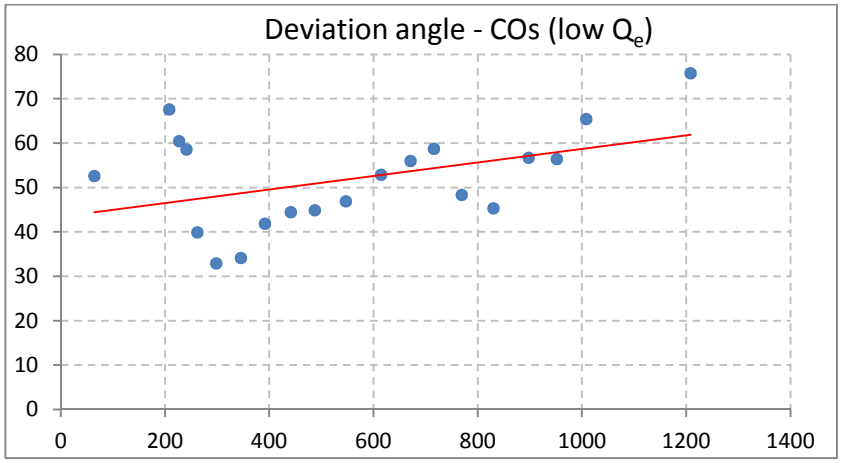

Figure 5.12 Deviation angle plotted against COs for legs experiencing low traffic flows (Qe < 400pcu/h). A simple moving average was applied

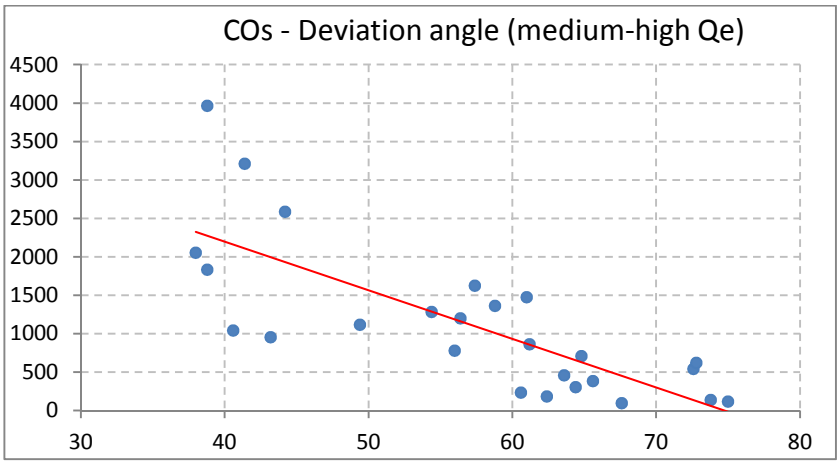

Figure 5.13 Deviation angle plotted against COs for legs experiencing medium-high traffic flows (Qe > 400 pcu/h). A simple moving average was applied

The apparently contradictory increase in COs as vehicle trajectories are more deviated, can be explained by taking into account relationships between Qe and ICD, β and ICD and eventually between COs and Qe.

Practically, β angles raise as traffic flows increase. However, higher traffic flows imply more numerous COs. This provokes peculiar monotonic function between COs and deviation angle itself for roundabout legs affected by low traffic flows. In a synthetic way, only for roundabout legs experiencing small vehicular volumes:

$$\begin{cases} \beta = \beta(De) \\ De = De(Q) \Rightarrow \beta = \beta(De) \Rightarrow \beta = \beta(Q) \Rightarrow \beta = \beta(CO) \\ CO = CO(Q) \end{cases}$$

For busy roundabout legs, no relation was found between ICD and deviation angle and consequently between the same angle and traffic flows. Therefore, the relationship between deviation angle and medium – high traffic flows is not influenced by other parameters.

Conversely, for leg subjected to low traffic flows Qe, correlations between COs and deviation angles proved not to be affordable. After all, the geometric layout may condition the occurrence probability of crashes due to failure to yield only if a persistent interaction between entering and circulating flows exists.

As for the crash frequency, it raises as deviation angle decreases, in accordance to theoretical and empirical expectations (**Figure 5.14**).

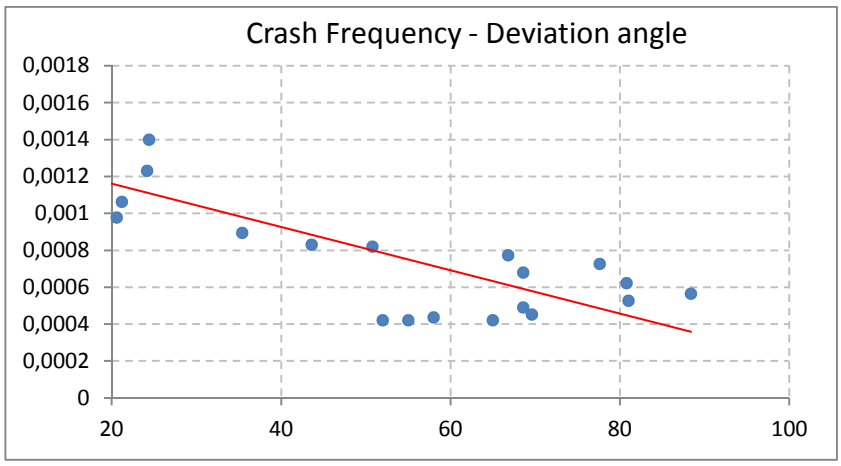

Figure 5.14 Crash frequency plotted against deviation angle. A simple moving average was applied

As for the interaction between deviation angle and ci coefficients, an overall safety increase can be noted for increasing deviation angles. This is corroborated by the fact that *ci* decreases when *deviation angle* reaches higher values. For low traffic flows, as *deviation angle* increases*, crash frequency* decreases, while *COs* raise. Therefore, coefficient *c*i quickly decreases.

For medium high traffic flows, both *COs* and *crash frequency* decrease with more pronounced vehicle trajectory deviations, and a decreasing trend is recorded.

Figure 5.15 suggests that reduction is faster for legs affected by low Qe.

As for legs affected by low Qe, even if relationships between COs and deviation angles have no meaning, the calibration curve is consistent with the ratio that diverging vehicles' trajectory enhance safety performance of roundabouts.

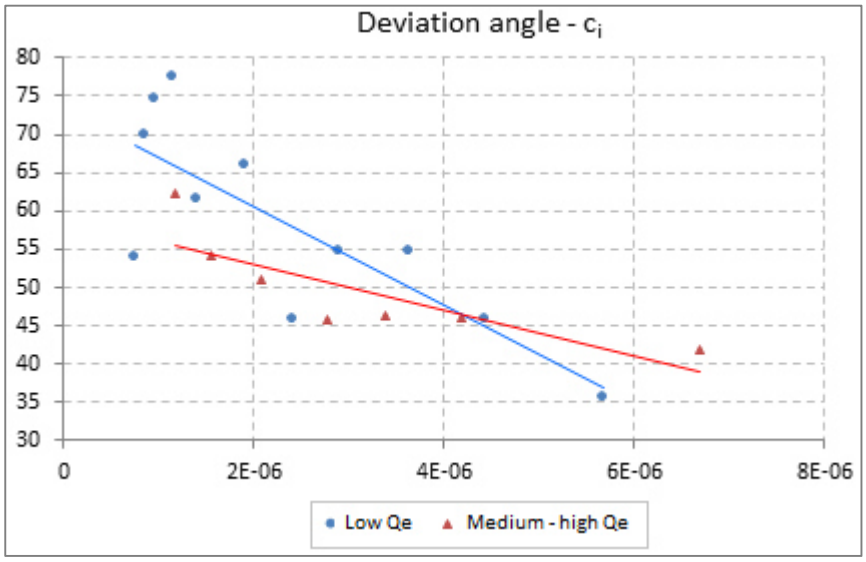

Figure 5.15 Calibration curve. Deviation angle plotted against crash to conflict ratio. Distinction between great and small roundabouts

Bootstrap procedure has been adopted for validating trend of calibration curves, whose reliability may be compromised by the restricted sample size.

If bootstrap regression curves had trends and shape entirely different from the curve fitting of the original data set, the trend of the calibration curve would not be robust. With a different sample, other trends would be gathered. Reliability of calibration curve would be questionable.

. Conversely, if the original curve maintained itself under bootstrap sampling, this would mean that original calibration curves are representative of their reference population despite of the restricted sample sizes.

Two hundred bootstrap data sets were generated by sampling with replacement the original pairs *(Deviation angle; ci)*$_i$ of **Figure 5.15**, and for each bootstrap sample, a polynomial regression was successively fitted. The mean value, as well as related standard error, was calculated along restricted intervals of the geometric covariate. The so obtained curve represents the Bootstrap estimate of the calibration functions. Decreasing trend is confirmed for both low and medium-high average daily traffic flows Qe. Bootstrap also corroborates the difference in slope between the two calibration functions (**Figure 5.16**, **Figure 5.17**).

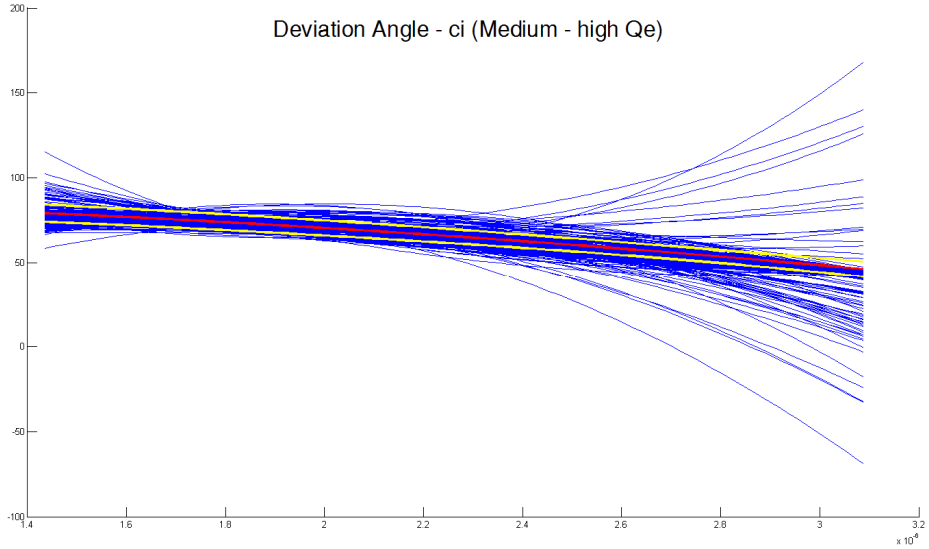

Figure 5.16 Calibration curve for roundabout legs affected by medium high average daily traffic flow. Bootstrap estimation

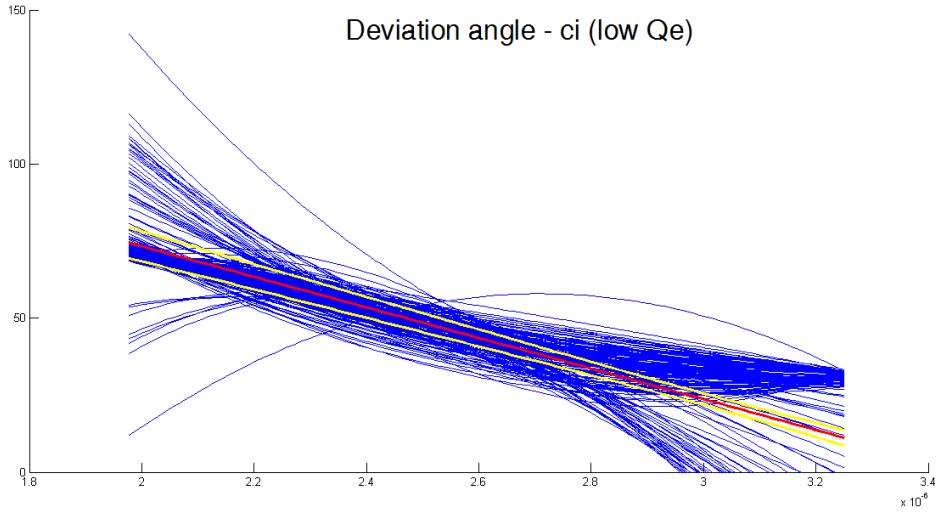

Figure 5.17 Calibration curve for roundabout legs affected by low average daily traffic flow. Bootstrap estimation

5.1.4.2 Angle of visibility

Figure 5.18 denotes a certain association existing between visibility angle and ICD and consequently with entering traffic flows (string relationship between Qe and ICD). Distinguishing between medium high and low traffic flows does not provide additional information.

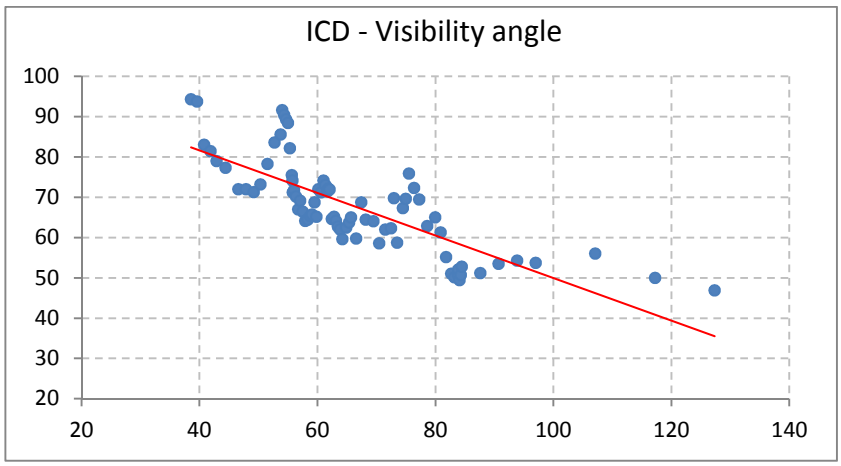

Figure 5.18 ICD plotted against angle of visibility

Possible interaction between visibility angle and COs was firstly analysed by considering all of the legs involved by the analysed crash type, and then by considering separately legs affected by high and low traffic flows. A general diminution of *visibility angle* can be noticed when *COs* increase until an asymptotically behaviour is reached for a visibility angle nearby 60° (**Figure 5.19**). Instead, for high traffic flows, when visibility angle decreases, CO increases (**Figure 5.20**).

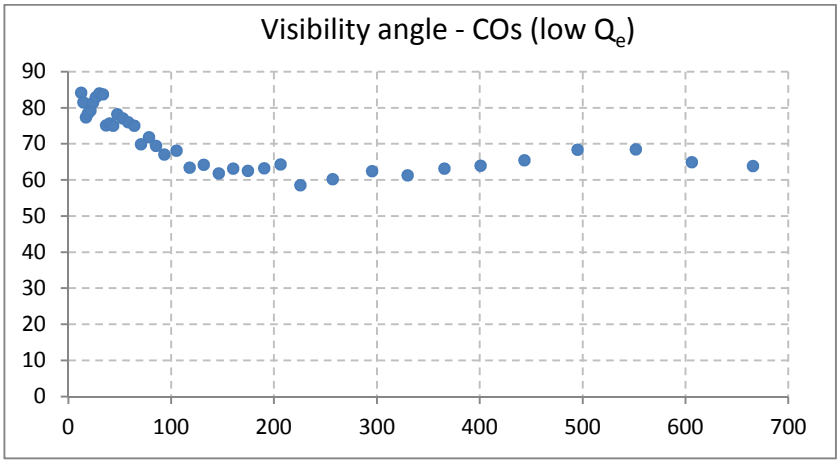

Figure 5.19 Angle of visibility plotted against COs for legs affected by low Qe. A simple moving average was applied

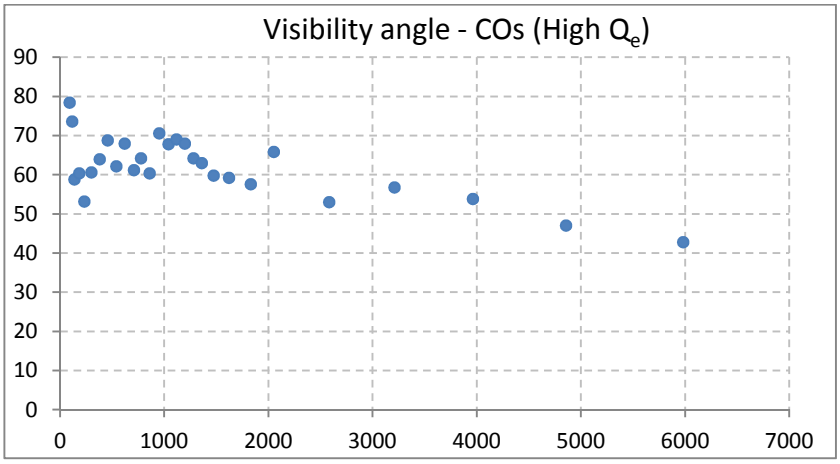

Figure 5.20 Angle of visibility plotted against COs affected by medium-high Qe. A simple moving average was applied

Crash frequency does not show any particular relationships with *visibility angle* for low traffic flows (**Figure 5.21**). On the contrary, by focusing on legs affected by medium-high traffic flows, a significant reduction of crash frequency can be appreciated when visibility angle increases (**Figure 5.22**).

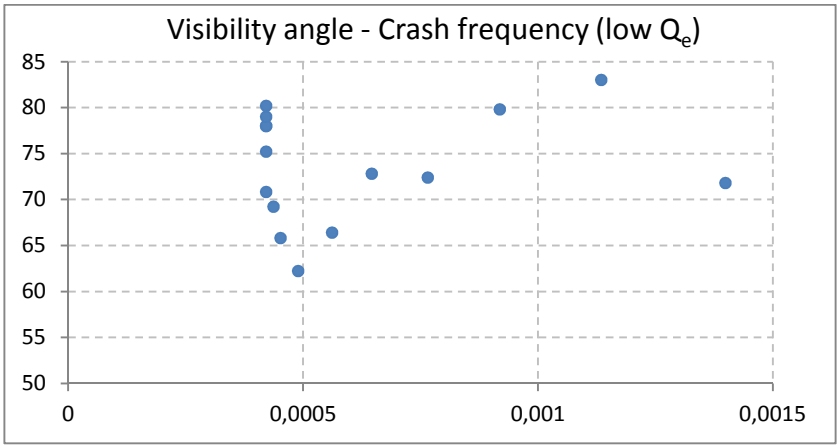

Figure 5.21 Angle of visibility vs COs (low Qe). A simple moving average was applied

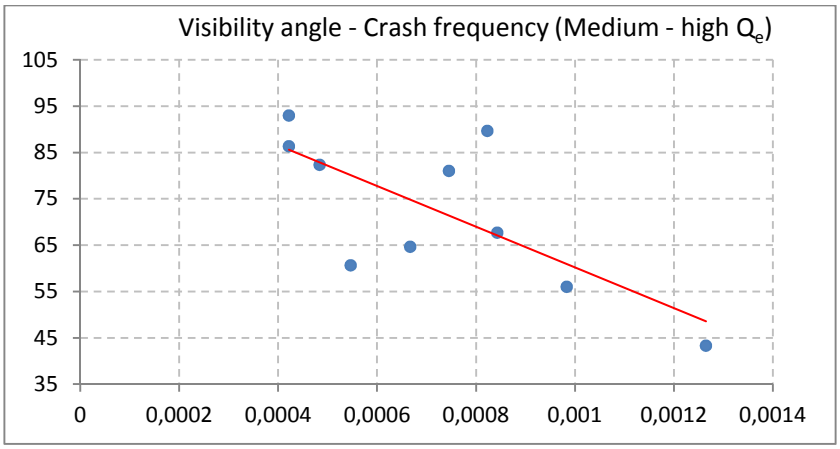

Figure 5.22 Angle of visibility vs COs (medium - high Qe). A simple moving average was applied

In accordance with previous considerations, *ci* coefficients have no relationships with *visibility angle* for low traffic flows (**Figure 5.23**), while a marked decrease can be noticed for medium-high traffic flows as *visibility angle* increases (**Figure 5.24**). It is worth noting that also for visibility angle, geometric layout of roundabouts does not seem to be able to explain crash frequency. Bootstrap estimations of the calibration curves were then carried out in order to verify whether their trends can be trusted.

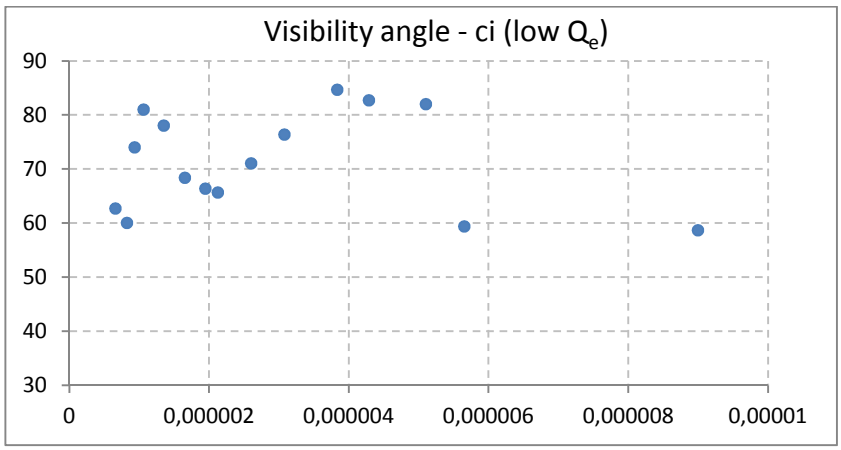

Figure 5.23 Angle of visibility plotted against ci (low Qe). A simple moving average was applied

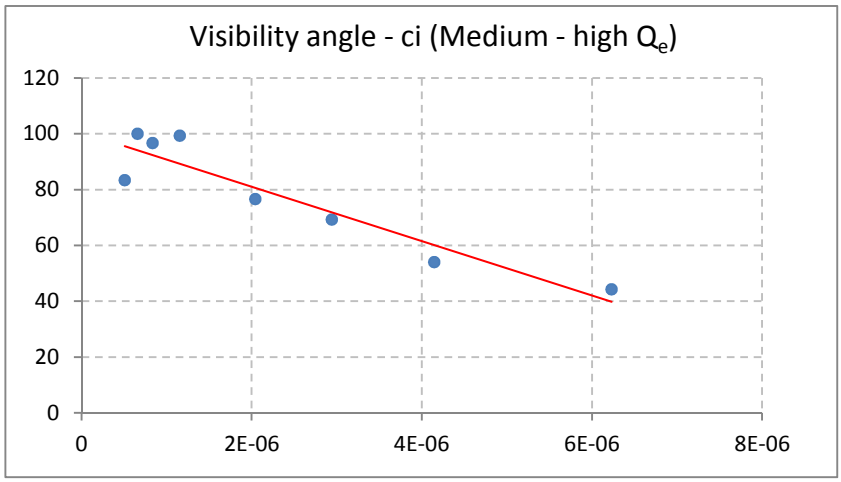

Figure 5.24 Angle of visibility plotted against crash frequency recorded for the same leg (medium-high Qe). A simple moving average was applied

Bootstrap estimates of the calibration curves is consistent with output provided by the original data. A negative slope was found for legs affected by medium – high Qe, while an almost horizontal line was obtained for low Qe. This confirms the supposition that for low entering flows, geometric configuration of

roundabout has no remarkable effect on safety performances (**Figure 5.25**, **Figure 5.26**).

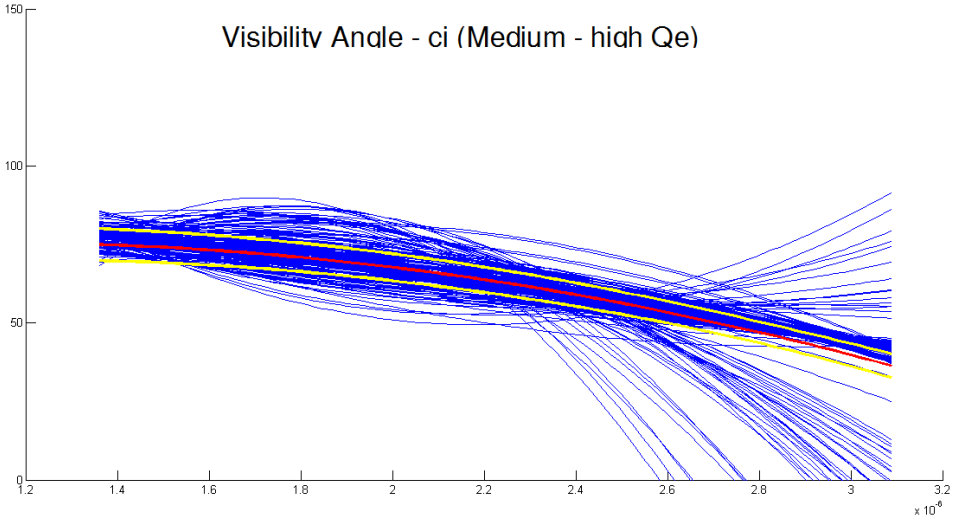

Figure 5.25 Calibration curve for roundabout legs affected by medium-high average daily traffic flow. Bootstrap estimation

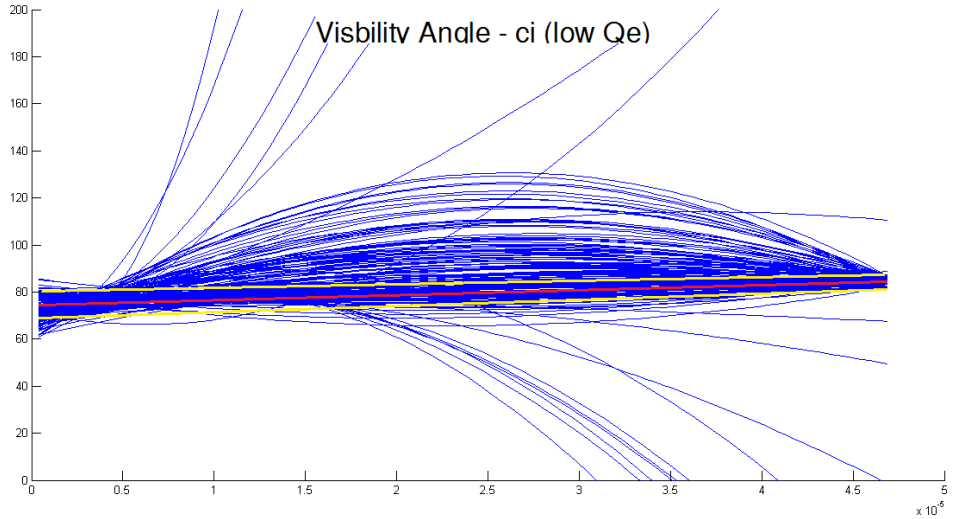

Figure 5.26 Calibration curve for roundabout legs affected by low average daily traffic flow. Bootstrap estimation

5.2 Collision due to a failure to yield without stopping

5.2.1 Factor analysis

Various factors analyses have been performed for the 24 roundabout legs involved in crash type *Collision due to failure to yield without stopping* at least one time in their operational life. Various attempt were performed, and it was found that the following set of covariates allows reaching the best results.

- R1 sx;
- Deviation angle;
- Visibility angle;
- Entry angle;
- Angle between consecutive legs;
- R1.

There are two preliminary steps to be conducted in order to assess whether factor analysis may be actually useful for better understanding the collected sample. The first one consists in verifying that variables are uncorrelated. If this hypothesis cannot be rejected, there is no reason to do a principal component analysis and consequently a factor one since the variables have nothing in common. **Table 5.23** clearly shows that the null hypothesis can be rejected: there are certain degrees of correlation between considered variables. The measure of *Kaiser-Meyer-Olkin* (KMO) statistic predicts whether collected data are likely to factor well, based on correlation and partial correlation. KMO index is substantially higher than the conventional threshold value of 0.6. Therefore, even this step gave positive outcomes.

Table 5.23 Preliminary measures for testing the convenience of factor analysis for uncover concealed information from collected data

KMO Measure of sampling	0.722
Bartlett's test of sphericity (Sig.)	<0.001

Taken together, Bartlett's test and KMO measure of sampling adequacy provide a minimum standard which should be passed before a factor analysis should be conducted. Given that both test are positive, PCA technique is then applied to the collected data in order to find the linear combinations of them that account for as much of the total variable as possible.

PCA technique is then applied to the collected data in order to find the linear combinations of them accounting for as much of the total variable as possible. Among them, the first principal component is the new unveiled variable that explain the maximum amount of the original variable. (**Table 5.24**).

The amount of variance accounted for by each component is shown by the eigenvalue, which is equal to the sum of the squared loadings for a given component. The higher the eigenvalue, the higher the importance of this component and the probability it will be retained as a factor. The proportion of variance explained by a single component can be determined by the ration between the corresponding eigenvalue and the overall variance. **Table 5.24** also shows the cumulative percentage of variance accounted for by the current and preceding factors.

Table 5.24 Eigenvalues of each component and their contribution in explaining the total variance

Component	Eigenvalues	% of variance	% cumulative
1	2.941	49.012	49.012
2	1.486	24.762	73.773
3	0.520	8.664	82.438
4	0.483	8.054	90.492
5	0.352	5.859	96.351
6	0.219	3.649	100.000

For this crash type, the first two components were retained as factors, since together they explain more than 70 per cent of the entire variance and the knee of the scree plot graphing the magnitude of eigenvalues seems to occur nearby the second factor (**Figure 5.27**).

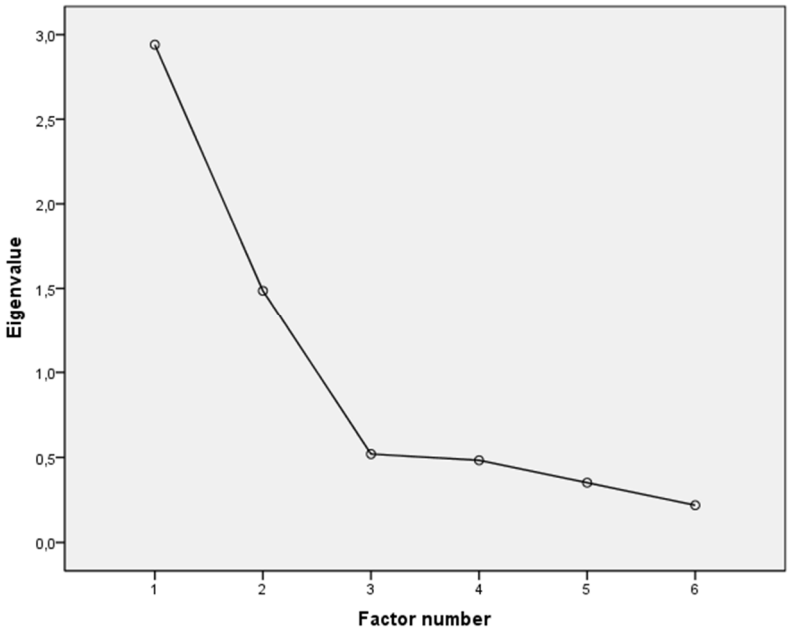

Figure 5.27 Scatter plot graphing the eigenvalues related to each component

Table 5.25 reports loadings of the two retained factors.

Table 5.25 Component matrix showing loadings of each variable

Manifest variables	*Extracted factors*	
	1	**2**
Deviation angle	-0.458	0.733
R1	0.303	-0.834
Visibility angle	0.862	0.294
R1sx	0.816	0.060
Entry angle	0.849	< 0.001
Angle between legs	-0.712	-0.403

Table 5.26 shows the communalities of each manifest variable for the two extracted factors, that is the proportion of each variables' variance explained by the retained factors.

Table 5.26 *Factor matrix showing loadings of each variable after Varimax rotation*

	Initial	*After extraction*
Deviation angle	1.000	0.747
R1	1.000	0.788
Visibility angle	1.000	0.830
R1sx	1.000	0.670
Entry angle	1.000	0.721
Angle between legs	1.000	0.670

By analysing signs and values of factors (**Table 5.25**), their underlying and latent meaning may be realised.

The first factor seems to bring out entries with high design speeds and affected by fast circulating traffic flows. High angles of visibility are associated to high entry angles, as already specified in Chapter 4, and pronounced angles between consecutive legs may provoke excessive speed too, in particular for right-turn movements. The negative sign of deviation angle confirms this idea. The loading related to the entry radius of the left approach seems to be important too. As matter of fact, if vehicles coming from the left proceed at higher speeds, the likelihood of *collision due to failure to yield without stopping* will inevitably increase.

The second factor appears to be focused on fast approaches too, with deviation angle and entry path radius having the highest scores and opposite sign.

For the sake of an easier interpretation of the factors, an orthogonal rotation factor was then applied by following the Varimax criterion where the aim is to reduce for each factor the number of loadings significantly different from zero (**Table 5.27** and **Figure 5.28**).

Table 5.27 *Factor matrix showing loadings of each variable after Varimax rotation*

Manifest variables	*Extracted factors*	
	1	**2**
Deviation angle	-0.174	-0.847
R1	0.006	0.888
Visibility angle	0.911	0.025
R1sx	0.786	0.228
Entry angle	0.796	0.298
Angle between legs	-0.808	0.129

In this situation, Varimax rotation did not offer significant additional perspectives about the essence of factors. Loadings are practically unaltered, and

Figure 5.28 clearly shows that interpretation of the factors is identical to the previous conceived one.

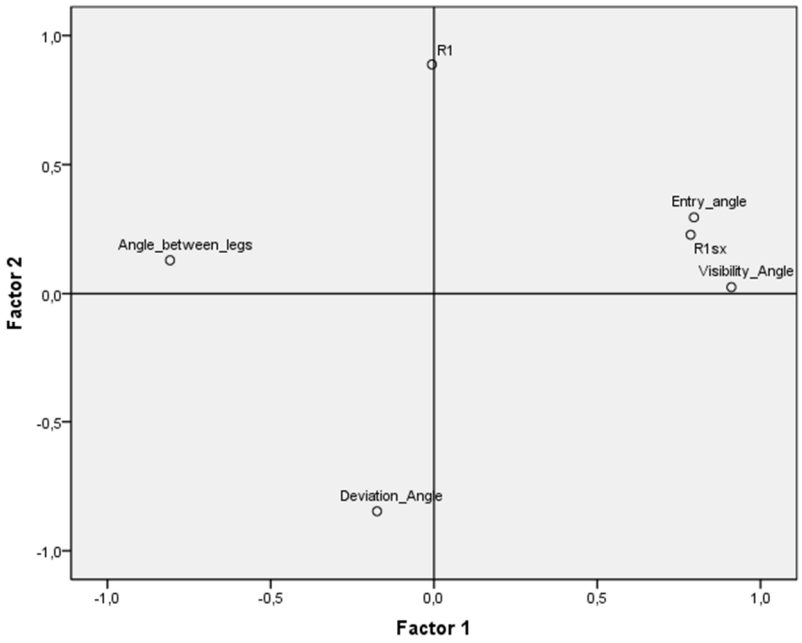

Figure 5.28 *Factor plot in rotated factor space.*

As already explained, the reproduced matrix correlation based on the extracted factors can be obtained from the matrix loadings (**Table 5.28**). It is desirable that corresponding values of the two variables are as close as possible, that is that residuals are close to zero. Correlation matrix estimated by Factor analysis proved to approximate well the original one, with only three residuals greater than the threshold value of 0.05.

Table 5.28 In the top part of the table, there are the reproduced correlations, while the bottom part contains the residuals obtained by the difference with the sample correlation matrix.

		R1	*Angle between legs*	*Entry angle*	*Visibility Angle*	*Deviation Angle*	*R1sx*
Reproduced correlation	*R1*	0.788	0.120	0.257	0.017	-0.751	0.198
	Angle between legs	0.120	0.670	-0.605	-0.733	0.031	-0.606
	Entry angle	0.257	-0.605	0.721	0.732	-0.389	0.693
	Visibility Angle	0.017	-0.733	0.732	0.830	-0.180	0.721

	Deviation Angle	-0.751	0.031	-0.389	-0.180	0.747	-0.330
	R1sx	0.198	-0.606	0.693	0.721	-0.330	0.670
Residuals	*R1*		-0.046	-0.008	0.055	0.198	-0.058
	Angle between legs	-0.046		0.121	0.084	0.085	0.138
	Entry angle	-0.008	0.121		-0.031	0.079	-0.105
	Visibility Angle	0.055	0.084	-0.031		0.046	-0.069
	Deviation Angle	0.198	0.085	0.079	0.046		0.011
	R1sx	-0.058	0.138	-0.105	-0.069	0.011	

Extraction method: principal component analysis.
Residuals are computed between observed and reproduced correlations. There are 10 (66.0%) non redundant residuals with absolute values greater than 0.05.

Table 5.29 provides the Matrix Score, that is the coefficient values related to the manifest variables linearly combined in order to obtain the factor score. However, the presence of uniqueness makes it unfeasible reaching an exact solutions, and approximation methods must be applied.

Table 5.29 Component matrix showing loadings of each variable

	Deviation angle	*Visibility angle*	*Entry angle*	*R1sx*
F1	-0.112	-0.439	0.379	-0.393
F2	-1.004	0.153	-0.030	0.001

5.2.2 Discriminant analysis

There are 4 initial geometric parameters identified by FA and 24 legs which have been assigned to one of three groups defined on the base of their crash frequency magnitude. Table 5.30 offers an overview about collected data.

Table 5.30 Group statistics

Class frequency		*Mean*	*Std. deviation*	*Valid cases*
1	*Deviation Angle*	50,4615	38,0342	13
	R1sx	82,1000	70,9331	13
	R1	54,3391	17,9662	13
	Angle between legs	119,0000	37,5921	13
	Visibility Angle	60,7692	16,3409	13
	Entry angle	49,4615	11,9416	13

2	*Deviation Angle*	58,8333	6,4936	6
	R1sx	52,4667	22,8287	6
	R1	48,2915	8,4110	6
	Angle between legs	106,8333	43,9610	6
	Visibility Angle	63,8333	23,9451	6
	Entry angle	48,0000	14,0855	6
	Deviation Angle	25,8000	28,0393	5
3	*Deviation Angle*	277,7200	149,1626	5
	R1sx	61,9269	17,3534	5
	R1	96,8000	52,6089	5
	Angle between legs	83,4000	38,4487	5
	Visibility Angle	61,8000	25,8496	5
	Entry angle	47,4167	32,2718	24
	Deviation Angle	115,4458	118,3032	24
Total	*Deviation Angle*	54,4080	16,0690	24
	R1sx	111,3333	41,5113	24
	R1	66,2500	24,5662	24
	Angle between legs	51,6667	16,1963	24
	Visibility Angle	50,4615	38,0342	13
	Entry angle	82,1000	70,9331	13
	Deviation Angle	54,3391	17,9662	13

Table 5.31 shows the Within-groups correlation matrix. It corresponds to a correlation matrix of data points obtained by subtracting to them the barycentre of the group they belong to. Multicollinearity should not represent a possible concern for discriminant analysis given that no value is greater than 0.8.

Table 5.31 Within-groups correlation matrix.

	Deviation Angle	*R1sx*	*R1*	*Angle between legs*	*Visibility Angle*	*Entry Angle*
Deviation Angle	1.000	-0.087	-0.505	0.072	-0.013	-0.218
R1sx	-0.087	1.000	-0.081	-0.520	0.618	0.538
R1	-0.505	-0.081	1.000	0.107	-0.011	0.181
Angle between legs	0.072	-0.520	0.107	1.000	-0.635	-0.465
Visibility Angle	-0.013	0.618	-0.011	-0.635	1.000	0.666
Entry angle	-0.218	0.538	0.181	-0.465	0.666	1.000

First of all, significant differences between groups on each of the independent variables are to be examined. If there were not significant differences between groups, it would not be meaningful proceeding any further with the analysis. **Table 5.32** shows two tests which can be used to evaluate the potential of the considered manifest variables in discriminating the three groups before the model is created. In particular, the significance of differences in group means for each variable is tested. The quantity *(1 - Wilks' Lambda)* is the proportion of variance in the dependent variable that can be explained by the considered predictor. Therefore, a relatively small Wilks' Lambda value indicates that the analysed covariate has a potential in discriminating groups. The other columns of **Table 5.32** refers to an F-test performed in a one-way analysis of variance (ANOVA). The null hypothesis is that all population means are equal in regard to a particular variable; the alternative hypothesis is that at least one mean is different.

As can be seen by **Table 5.32**, the Wilk's lambda test presents similar results for the variables, while the ANOVA seem to suggest that only *R1sx* may discriminate the three sub-populations.

Table 5.32 Test of equality of group means table

	Wilks' Lambda	F	df1	df2	p-value
Deviation Angle	0.865	1.642	2.000	21.000	0.218
R1sx	0.472	11.739	2.000	21.000	< 0.001
R1	0.915	0.980	2.000	21.000	0.392
Angle between legs	0.951	0.541	2.000	21.000	0.590
Visibility Angle	0.863	1.661	2.000	21.000	0.214
Entry angle	0.891	1.284	2.000	21.000	0.298

After this preliminary insight into potential of each manifest variable in separating sub-populations characterised by different crash frequency, discriminant functions can now be sought. The maximum number of discriminant functions produced is equal to the number of groups minus 1. As a result, in this example, there are only two directions of interest; their eigenvalues and their contribution in explaining original variance are shown in **Table 5.33**. The canonical correlation is the multiple correlation between two sets of variables. The first is constituted by the manifest variables, while the second refers to the dummy variables used for coding the three considered groups of different crash frequency. A high canonical correlation indicates a function that discriminates well.

Table 5.33 Eigenvalues table

Function	Eigenvalue	% of variance	% cumulative	Canonical correlation
1	1.541	97.29	97.29	0.779
2	0.043	2.71	100.00	0.203

The canonical correlation is then exploited in the statistical methods devoted to ascertain the significance of the acquired discriminant functions.

If canonical correlation of discriminant functions were be equal to zero, no relationship between the set of independent variables and the discriminant scores (i.e. the dependent variable) would be found. The discriminant functions would be worthless because the means of the discriminant scores would be the same in the considered groups.

This is exactly the null hypothesis of the Willk's lambda statistical test, by means of which it is possible to establish the significance of the discriminant functions. Wilks' lambda is the proportion of the total variance lying in the discriminant scores not explained by differences among the groups. It is calculated as the product of the values of *1-canonical correlation*^{2}. Therefore, smaller values of Wilks' lambda are desirable. In this example, canonical correlations are 0.779 and 0.203, so the Wilks' Lambda testing both canonical correlations is $(1-0.779^2)*(1-0.203^2) = 0.377$ and the Wilks' Lambda testing the second canonical correlation is $(1-0.203^2) = 0.959$.

The Chi-square statistic tests whether the canonical correlation of discriminant functions is equal to zero, which implies a unitary Wilk's lambda. This is exactly the null hypothesis, a situation characterised by a negligible contribution offered by discriminant functions in explaining the total variance of the independent variables.

Table 5.34 represents the output of Willk's lambda statistical test carried out on the two discriminant functions obtained for this example. The first test presented in this table tests both canonical correlations ("1 through 2") and the second test presented tests the second canonical correlation alone.

Table 5.34 Wilk's lambda table

Function	Wilks' Lambda	Chi-square	df	p-value
1 through 2	0.377	18.032	12.000	0.115
2	0.959	0.778	5.000	0.978

From **Table 5.34**, it can be stated that there is no statistically significant function. If the probability for this test had been larger than 0.05, the definitive conclusion would have been that concluded that there are no discriminant functions to separate the groups of the dependent variable.

Discriminant analysis may concluded here. However, it was decided to keep the analysis going in order to capture possible interesting information, even if their reliability would be seriously questioned.

Table 5.35 provides the standardised coefficients for the two discriminant functions. Their interpretation enables unveiling the latent aspect they represent, in a similar way to the identification of the meaning embraced by factors adopted in factor analysis. The sign indicates the direction of the relationship, while the magnitudes define how strongly the discriminating variables effect the score.

As for the first function, *R1sx* has the preponderant coefficient. *R1* and *Angle between consecutive legs* are less successful as predictors, while the scores of the other covariates are insignificant.

Table 5.35 Standardised canonical discriminant function coefficients table

	Functions	
	1	**2**
Deviation Angle	-0.162	0.128
R1sx	1.203	0.116
R1	0.256	0.432
Angle between legs	0.323	0.571
Visibility Angle	-0.074	-0.675
Entry Angle	-0.249	0.411

There is an alternative way of specifying the relative importance of the predictors. The structure matrix table (**Table 5.36**) provides the correlations of each independent variable with the discriminant functions. These correlations serve as factor loading in factor analyses. By identifying the largest loadings, the researcher gains an insight into how to correctly interpret the discriminant function. However, the pattern seems to be completely different from previous analyses, and the prominence of R1sx is not confirmed.

Table 5.36 Structure matrix table. Pooled within-groups correlations between discriminating variables and standardised canonical discriminant functions. Variables ordered by absolute size of correlation within function.

	Functions	
	1	**2**
Deviation Angle	0.849	-0.424
R1sx	-0.318	-0.140
R1	0.280	-0.191
Angle between legs	-0.124	0.803
Visibility Angle	0.298	-0.698
Entry Angle	0.232	0.500

Deviation angle stands out as the predictor most strongly influencing the allocation of legs to the three groups characterised by different frequency values for the analysed crash type.

Discriminant functions are eventually created by unstandardized coefficients, which are reported in **Table 5.37**. Non standardised values of manifest variables will give the score for the discriminant functions. The greatest coefficients are referred to *R1, R1sx* and the *Entry angle*.

Table 5.37 Canonical discriminant function coefficients table. Unstandardized coefficients

	Functions	
	1	**2**
Deviation Angle	-0.005	0.004
R1sx	0.014	0.001
R1	0.016	0.027
Angle between legs	0.008	0.014
Visibility Angle	-0.003	-0.028
Entry Angle	-0.016	0.026

A further way of interpreting the DA results consists in inserting the average discriminant score (unstandardized) in the three groups (**Table 5.38**). In detail, the discriminant score for each group when the variable means (rather than individual values for each case) are entered into the discriminant equation. These group means are called centroids.

Table 5.38 Functions at group centroids table. Unstandardized canonical discriminant functions evaluated at group means

	Functions	
Class frequency	**1**	**2**
1.00	-0.379	0.167
2.00	-1.017	-0.290
3.00	2.205	-0.086

SPSS also provides a graphical representation of DA output (**Figure 5.29**).

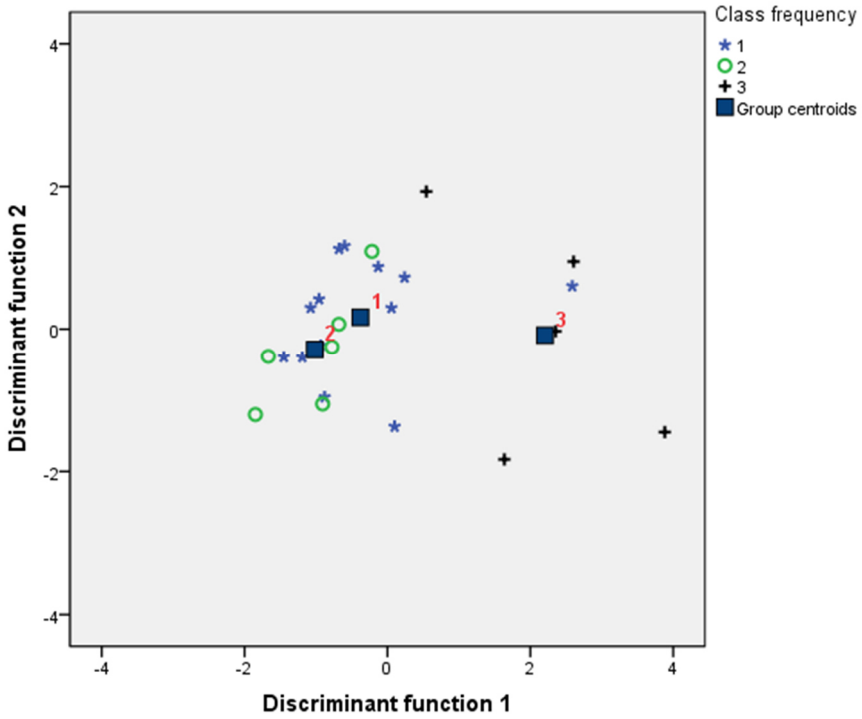

Figure 5.29 Graph of roundabout legs on the discriminant dimensions..

The first direction seems to perform better than the second one in discriminating the three groups.

The output of discriminant analysis is the classification table, whose rows are the observed categories of the dependent variable while the columns are the predicted categories (**Table 5.39**). When prediction is perfect all cases lie on the diagonal. The percentage of cases on the diagonal is the percentage of correct classifications. The cross-validated data set is a more authentic representation of the outcome achieved by discriminant function. The cross validation is often termed a *jack-knife* classification, given that successively classifies all cases but one to develop a discriminant function and then categorizes the case that was left out. This process is repeated with each case left out in turn. This cross validation produces a more reliable function. The ratio is that one should not use the case the researcher is trying to predict as part of the categorization process. The classification results for the crash type reveal that 41.7% of legs were classified correctly into the three categories of crash frequency. The third group suffers from the least accuracy.

This overall predictive accuracy of the discriminant functions is called the *hit ratio*. Via a random classification of the collected legs, there would be a 33.3% probability of correctly collocating the 24 subjects into the three categories.

Accordingly to a conventional approach, acceptable hit ratios must be greater than this probability increased by 25%, which gives a threshold value equal to 41.63%. The output of discriminant analysis is substantially up to standard.

Table 5.39 Classification results table. 58.3% of original grouped cases correctly classified. 41.7% of cross validated grouped cases correctly classified.

			Predicted group membership			
		Class frequency	**1.00**	**2.00**	**3.00**	**Total**
Original	Count	1.00	6	6	1	13
		2.00	2	4	0	6
		3.00	1	0	4	5
	%	1.00	46.15	46.15	7.69	100.00
		2.00	33.33	66.67	0.00	100.00
		3.00	20.00	0.00	80.00	100.00
Cross-validated [a]	Count	1.00	4	8	1	13
		2.00	3	3	0	6
		3.00	2	0	3	5
	%	1.00	30.76	61.53	7.69	100.00
		2.00	50.00	50	0.00	100.00
		3.00	40.00	0.00	60.00	100.00

a. Cross validation is done only for those cases in the analysis. In cross validation, each case is classified by the functions derived from all cases other than that case

A discriminant analysis was then conducted to predict the categorical variable *crash frequency* for analysed roundabout legs. Predictor variables were *Entry Angle, R1, Angle between legs, Deviation Angle, R1sx* and *Visibility Angle*. These are the same geometric features previously identified via the factor analysis. Significant mean differences were observed for the deviation angle.

None of the two discriminate functions were found to be statistically significant, that is able to effectively separate legs of different crash frequency category. A proper application of discriminate analysis should end here.

However, it was prosecuted in order to verify whether interesting results would have been emerged. Standardised coefficients of the discriminant functions and the pooled within-groups correlations of the structure table matrix offered contrasting outputs, and the same scatter plot does not seem to offer a coherent

perspective. Discriminate analysis ultimately failed in differentiating covariates on the basis of their influence on the likelihood of collisions due to failure to yield without stopping.

5.2.3 Regression analyses

Multiple linear regression models whit crash frequency as a continuous dependent variable may allow understanding the portion of variance affecting crash frequency explained by the single geometric parameters. From FA and DA, a set of geometric features apparently related to crash frequency was found and subsequently investigated in MLR models. Stepwise regression procedures were applied by exploiting the F-test in order to establish which of these five models should be preferred for analysing the investigated phenomenon.

- *Model 1.* Predictors: Constant, Entry Angle, R1, Angle between legs, Deviation Angle, R1sx, Visibility Angle;
- *Model 2.* Predictors: Constant, Entry Angle, R1, Deviation Angle, R1sx, Visibility Angle;
- *Model 3.* Predictors: Constant, Entry Angle, Deviation angle, R1sx, Visibility Angle;
- *Model 4.* Predictors: Constant, Deviation angle, Angle of visibility, R1sx; Entry angle;
- *Model 5.* Predictor: Constant, R1sx.

It is then desired to ascertain whether the full model contributes additional information about the association between Y and the predictors. The null hypothesis is that the additional covariates are not significant, and their related coefficients are therefore equal to zero. If the difference between error sum of squares for the reduced model (i.e. SSE_R) and the error sum of squares for the complete model (i.e. SSE_C) reaches high values, the null hypothesis is likely to be rejected because this would mean that the additional parameters significantly improve the model's fit to the data. Output of F-test for the four tested models are reported in **Table 5.40**, which shows that the independent variables statistically significantly predict the dependent variable for all of tested models.

Table 5.40 F-test carried out for testing statistical significance of various models

Model	Sum of squares	df	Mean squares	F	Sig.

1	*Regression*	0.028	6	0.005	2.911	0.039
	Residual	0.027	17	0.002		
	Total	0.055	23			
2	*Regression*	0.028	5	0.006	3.698	0.018
	Residual	0.027	18	0.002		
	Total	0.055	23			
3	*Regression*	0.028	4	0.007	4.878	0.007
	Residual	0.027	19	0.001		
	Total	0.055	23			
4	*Regression*	0.028	3	0.009	6.804	0.002
	Residual	0.027	20	0.001		
	Total	0.055	23			
5	*Regression*	0.028	2	0.014	10.588	<0.001
	Residual	0.027	21	0.001		
	Total	0.055	23			

The fifth model with R1sx as the only covariate shows the best fit to collected data, as confirmed by the adjusted R square values (**Table 5.41**). This is a perceivable evidence of the importance assumed by R1sx in conditioning likelihood of collisions due to failure to yield without stopping. However, it was finally decided to analyse the full model for the possibility of comparing the amount of crash frequency variance explained by the single predictors and discovering whether other geometric features can have certain effects.

Table 5.41 Measures of adequacy for the considered multiple linear models

Model	R	R-square	Adjusted R square	Standard error of the estimate
1	0.712	0.507	0.333	0.040
2	0.712	0.507	0.370	0.039
3	0.712	0.507	0.403	0.038
4	0.711	0.505	0.431	0.037
5	0.709	0.502	0.455	0.036

Unstandardized coefficients indicate the increase experienced by the dependent variable for a unitary increment of the independent variable when all other independent variables are held constant (**Table 5.42**).

The same table reports the outputs of tests pertaining to the statistical significance of each of the independent variables. The null hypothesis is that the related coefficient of the investigated predictor is equal to zero. If p-value < 0.05, the null hypothesis can be rejected, and it can be stated that coefficients are statistically significantly different to zero. After the conduction of significance tests, only *Entry path radius of the left approach* resulted to be statistically significant. This confirms even more the previous evidence of R1sx as the solely decisive geometric factor.

Table 5.42 Calculating regression coefficients and testing statistical significance of the independent variables.

	Model	Unstandardized coefficients		Standardised Coefficients		
		β	*Std. Error*	$\hat{\beta}$	*t*	*Sig.*
1	*Constant*	0.054	0.067	<0.001	0.805	0.432
	Deviation Angle	<0.001	<0.001	-0.041	-0.189	0.853
	R1sx	<0.001	<0.001	0.766	3.183	0.005
	R1	<0.001	0.001	0.011	0.053	0.958
	Angle between legs	<0.001	0.000	0.006	0.024	0.981
	Visibility Angle	<0.001	0.001	-0.171	-0.572	0.575
	Entry angle	<0.001	0.001	0.057	0.221	0.828

The variance inflation factor (VIF) quantifies the severity of multicollinearity in MLS models with ordinary-least-squares estimations of regression coefficients. It provides an index that measures how much the variance of an estimated regression coefficient is increased because of multicollinearity. **Table 5.43** denotes the presence of severe multicollinearity given the presence of VIF factors significantly higher than the aforementioned threshold. Therefore, it is strictly required understanding actual contributions offered by predictors in explaining Y variance. Estimates of standardised regression coefficients may be seriously misled by shared variance between predictors. As a result, it can happen that a predictor explaining a consistent part of Y variance may have a near-zero β^* because another predictor is receiving the credit for the explained variance.

In addition, $\hat{\beta}^*$coefficients can dramatically change in numerical value, and even in sign, as new variables are introduced or as old variables are removed. They simply reflect the amount of credit given to the related predictors. It can be said that they are context-specific to a given model characterised by a specific set of covariates. The problem is that the true model is rarely, if ever, known.

Other techniques are then required for correctly evaluating the importance of single predictors in explaining the analysed phenomenon. There is the need for

estimating the relationship between a predictor variable and the outcome variable after controlling for the effects of other predictors in the regression equation.

Partial correlation represents the correlation between the dependent variable Y and a predictor after common variance with other predictors has been removed from both Y and the predictor of interest.

The squared *semipartial correlations* represent the unique variance of that predictor shared with the dependent variable. This means that the squared semipartial correlation of a certain variable denotes the decrease in coefficient of determination R^2 if that variable is removed from the regression equation.

Table 5.43 Verifying the presence of severe multicollinearity and calculation of correlation coefficients

	Correlation coefficients			**Collinearity**	
	Zero-order	*Partial*	*Semipartial*	*Toll*	*VIF*
Constant	-0.286	-0.046	-0.032	0.607	1.647
Deviation Angle	0.700	0.611	0.542	0.501	1.994
R1sx	0.144	0.013	0.009	0.643	1.555
R1	-0.273	0.006	0.004	0.547	1.829
Angle between legs	0.371	-0.137	-0.097	0.323	3.096
Visibility Angle	0.400	0.053	0.038	0.435	2.297

A squared structure coefficient denotes the amount of variance estimated by the model that the predictor is able to explain. This is equivalent to say that a squared structure coefficient denotes the amount of variance related to R^2 that the predictor is able to explain. Partial and semipartial correlation coefficients clearly indicate that the only geometric feature capable of explaining a significant part of Y variance is the *Entry path radius of the left approach*.

The successive steps in this exploratory path consists in the determination of the structure coefficients, which can definitely clarify the contribution of each predictor in explaining the phenomenon described via a multiple linear regression, as well as providing additional support in trying to identify multicollinearity effects. Structure coefficients confirm previous analyses of partial and semipartial correlations. Crash frequency variance seems to be basically explained by *R1 sx* (**Table 5.44**).

The magnitude of these relationships between predictors and the dependent variable may be directly and synthetically measured by the so-called *Cohen's f^2 effect size*.

Its outcome is a measure of practical significance in terms of the magnitude of the effect exerted by the single predictor on Y variable. It is independent of the sample size and is appropriate for calculating the effect size within a multiple regression model in which the independent variable of interest and the dependent

variable are both continuous. The effect size corroborates previous results: only *R1sx* appears to have a marked relationship with crash frequency as compared to other 22 investigated geometric factors (**Table 5.44**).

Eventually, exploratory analyses reach the conclusion that R1sx design seems to have primary importance for achieving safer roundabouts which can prevent collisions due to failure to yield without stopping.

Table 5.44 Calculation of structure coefficients and effect size f^2

	Structure coefficient	**Effect size f^2**
Deviation angle	0.162	0.024
R1	0.041	0.003
Visibility angle	0.271	-0.129
R1sx	0.966	1.086
Angle between legs	0.316	0.046
Entry angle	0.147	-0.003

The most intuitive way for testing normality of residuals consists in trying to graph a histogram by plotting obtained residuals and placing them in regularly spaced cells. The histogram should approximate a normal distribution of residuals. However, with small sample sizes, which is the case of various crash type here in this study, this is not be the best choice for judging the distribution of residuals (**Figure 5.30**).

A more affordable way is the analysis of the $normal\ probability\ plot$ (also called P-P plot). It is obtained by sorting the standardised residuals into ascending order and then calculating the cumulative probability of each residual. Eventually, the so calculated P values are then plotted versus the normalised cumulative frequency distribution of residuals themselves, that is $(\varepsilon_i - \mu)/\sigma)$, where μ and α are approximated via the mean and standard deviation of residuals respectively. The normal probability plot seems to be able to produce an approximately straight line, which means that residuals may come from a normal distribution (**Figure 5.31**).

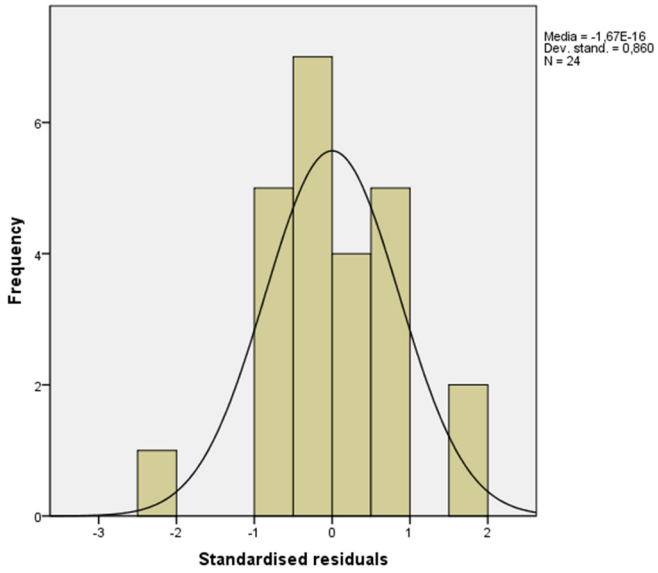

Figure 5.30 Testing normality distribution of residuals. Histogram

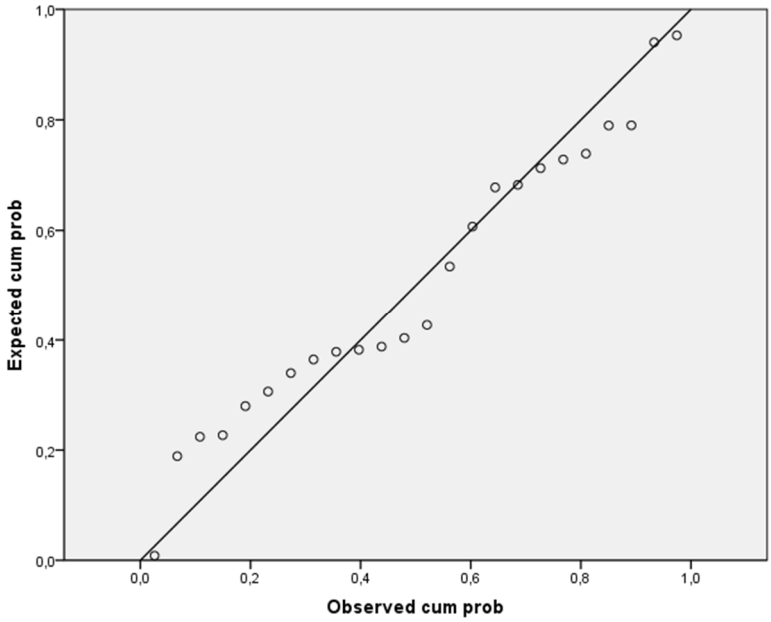

Figure 5.31 Testing normality distribution of residuals. Normal probability plot

There are instead serious concerns about the homoscedastic nature of residuals, which should have a constant variance σ^2. Homoscedastic assumption can be checked by visual examination of a plot of the standardized residuals (the errors) by the regression standardized predicted value. Residuals are not evenly scattered around the line and a certain trend can be recognised (**Figure 5.32**). This means that homoscedastic assumption is not verified. However, as already said, this cannot compromise results obtained with correlation coefficients and the effect size, which gave substantial results also consistent with previous exploratory analyses.

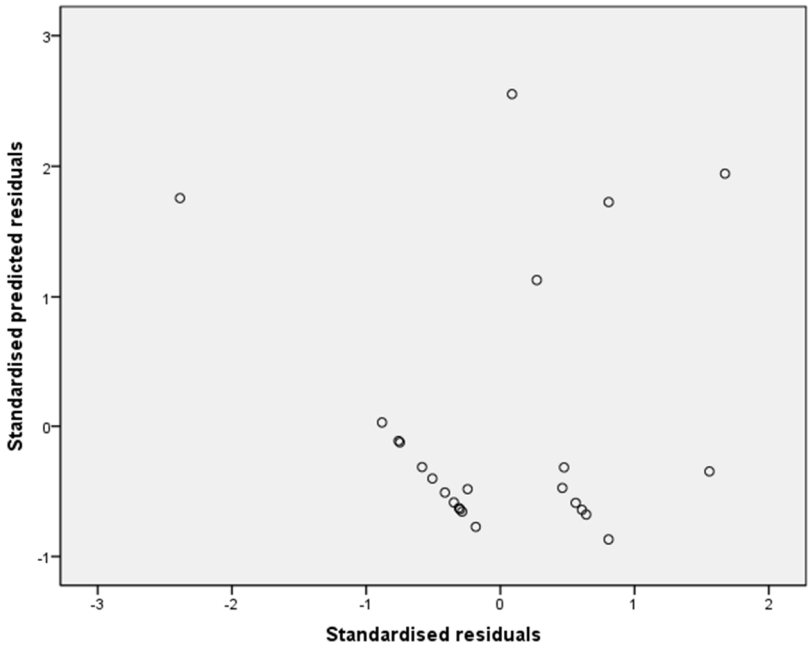

Figure 5.32 Scatter plot for detecting homoscedasticity of residuals

5.2.4 Estimating the calibration curves

Exploratory analyses R1sx as the geometric feature most correlated to frequency of crashes due to *failure to yield without stopping*. Conversely, no geometric parameters were found to be correlated to the potential crash frequency.

$$N_{1b} = Q_e * P(0) * t_{coll} * Q_c = Q_e * (1 - \rho) * P(t < t_{coll})$$

For this type of crash, theoretical trend of COs over hourly changes of traffic flows shows an initial increase followed by a pronounced decline after having reach a peak (**Figure 5.33**). It is quite similar to a parabolic curve. This trend also emerges by considering the average daily entering traffic flow related to the analysed single roundabout leg (**Figure 5.34**).

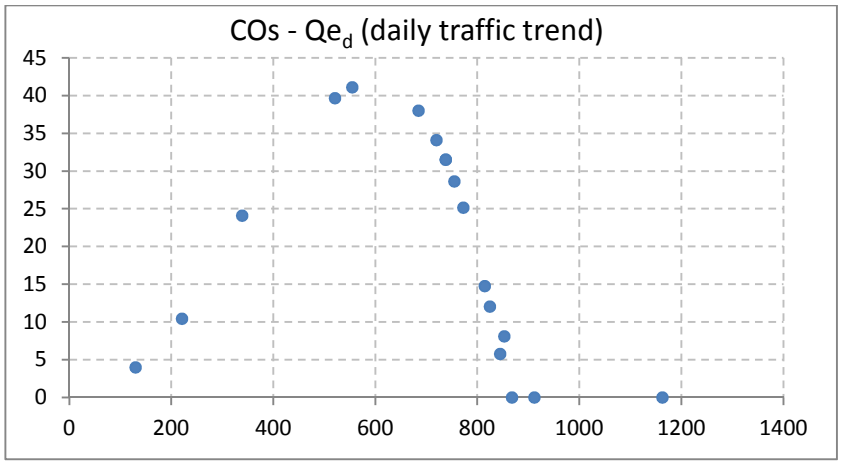

Figure 5.33 Daily evolution of Conflict Opportunities plotted against entering traffic flows measured on an hourly basis for a single roundabout leg

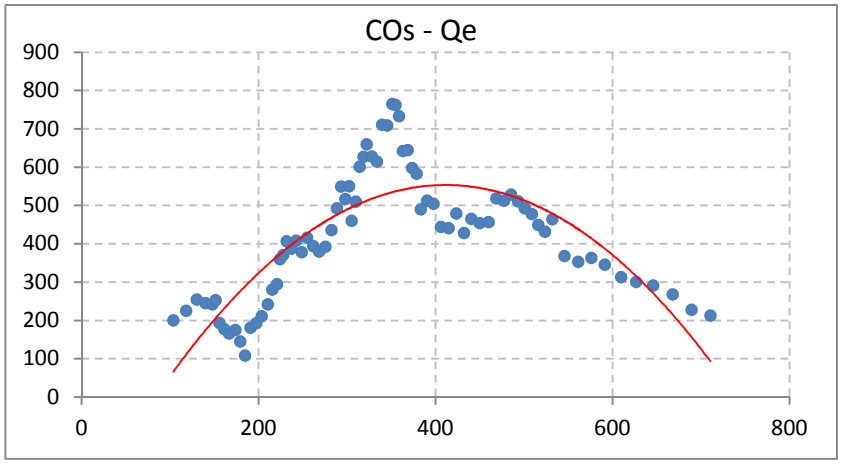

Figure 5.34 Conflict Opportunities plotted against average daily traffic flows Qe

There is no relation between ICD and R1sx for low average daily traffic flows entering the roundabout through the analysed leg (Qe < 400 pcu/h) (Figure 5.35), while a negative trend can be traced for medium-high traffic volumes (Figure 5.36), with a decline of ICD when R1sx rises.

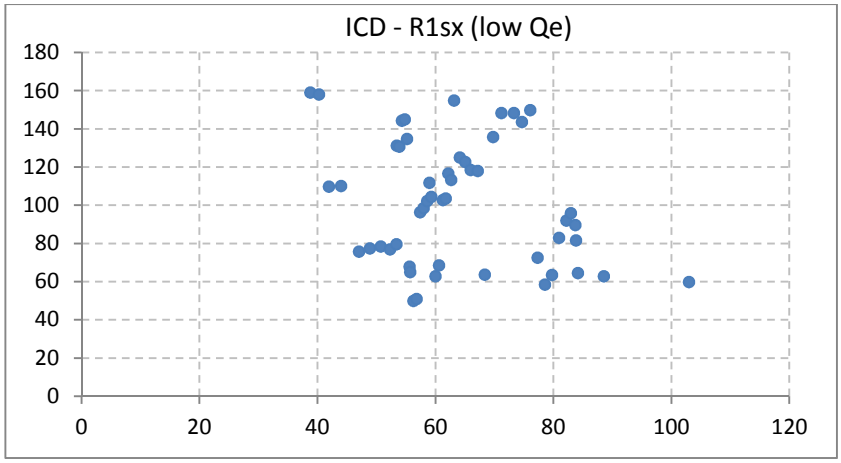

Figure 5.35 Conflict Opportunities plotted against average daily entering traffic flows

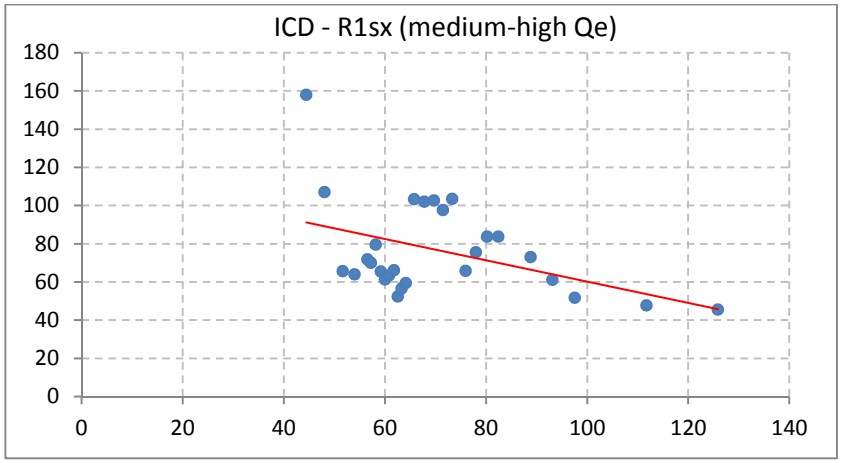

Figure 5.36 Conflict Opportunities plotted against average daily entering traffic flows

Possible connection between R1sx and daily average COs was then analysed by initially considering all of the legs involved in collisions due to failure to yield

without stopping and then by analysing separately legs affected by low and medium-high traffic flows. In all of these situations, COs arise as R1sx increases (**Errore. L'origine riferimento non è stata trovata.**).

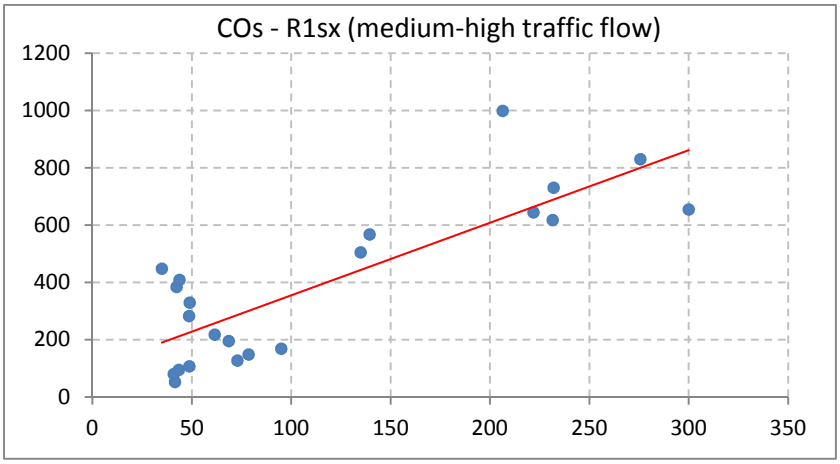

Figure 5.37 Conflict Opportunities plotted against entry path radius of legs affected by medium-high traffic flows

Crash frequency presents an expected and well defined growth for increased *R1sx* values (**Figure 5.38**), but this occurs only for medium high traffic flows (**Figure 5.40**), while for legs with low *Qe* no association can be detected (**Figure 5.39**).

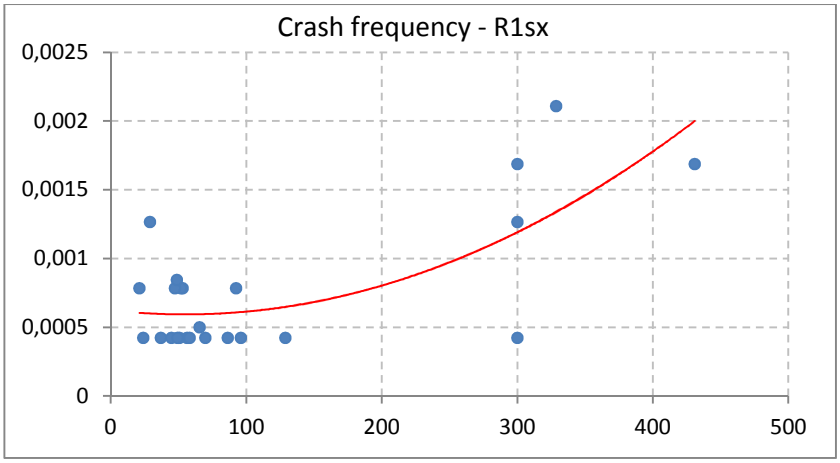

Figure 5.38 Crash frequency plotted against entry path radius of legs affected by medium-high traffic flows

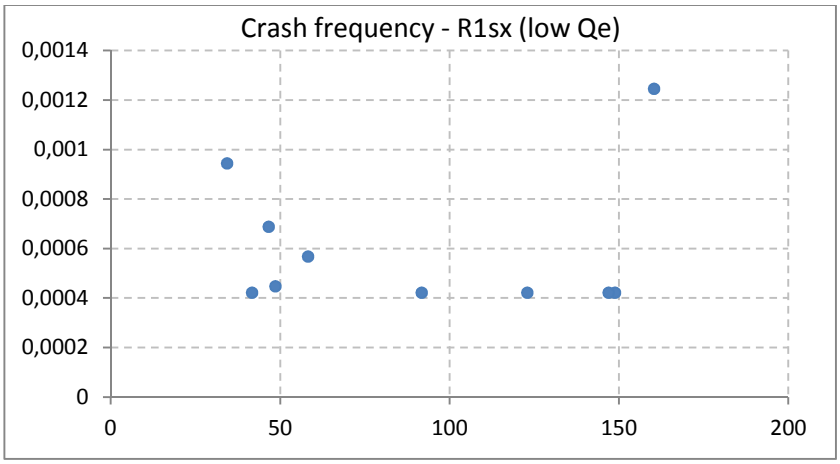

Figure 5.39 Crash frequency plotted against entry path radius of legs affected by medium-high traffic flows

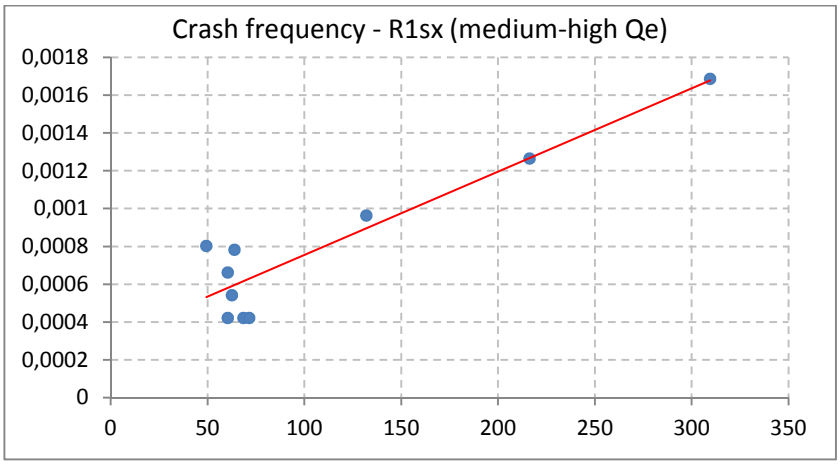

Figure 5.40 Crash frequency plotted against entry path radius of legs affected by medium-high traffic flows

Expressing *ci* coefficients as a function of *R1sx* gives a growing trend consistent with scientific knowledge and empirical evidence, in accordance to which great entry path radii induce drivers to enter the ring at high speeds, with consequent safety issues. Possible explanation for trend proposed by the model is to be ascribed to the greater increasing rate of crash frequency as compared to the increasing rate of COs (**Figure 5.43**).

However, this is true only for legs characterised by medium-high average daily entering traffic flows (**Figure 5.42**). No relationship was found for legs with low Qe (**Figure 5.41**), probably because of the absence of any degree of interconnection between their crash frequency and their R1sx (**Figure 5.39**).

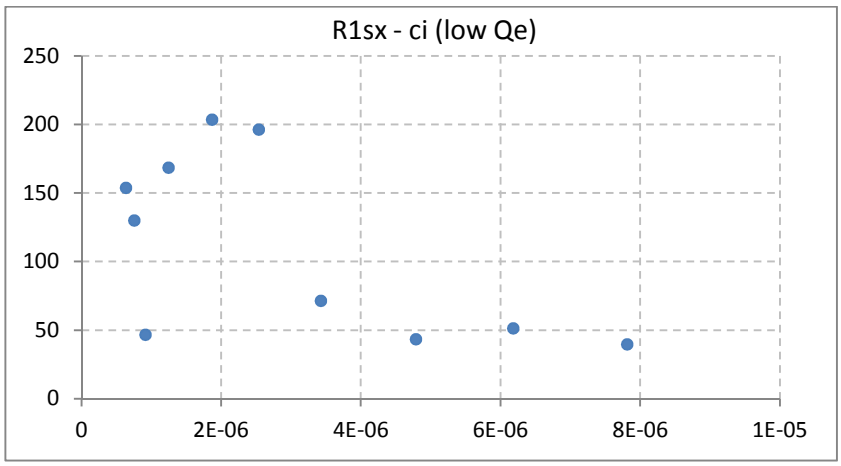

Figure 5.41 Entering traffic flows measured on an hourly basis plotted against inscribed circle diameter (Simple Moving Average)

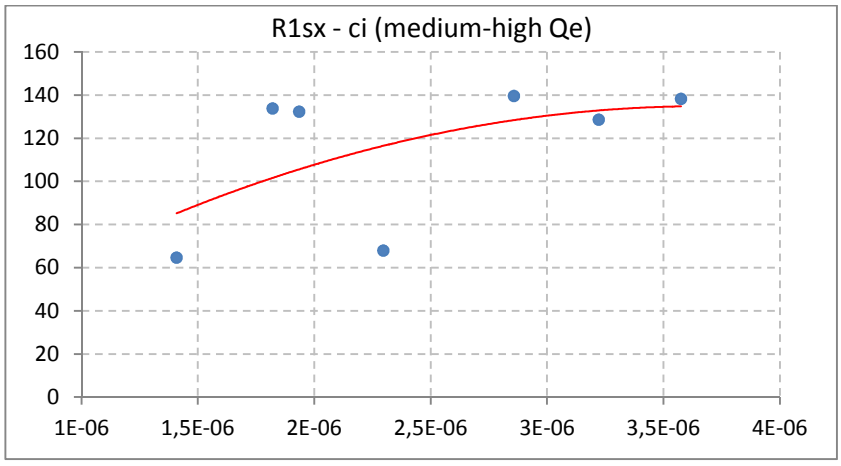

Figure 5.42 Entering traffic flows measured on an hourly basis plotted against inscribed circle diameter (Simple Moving Average)

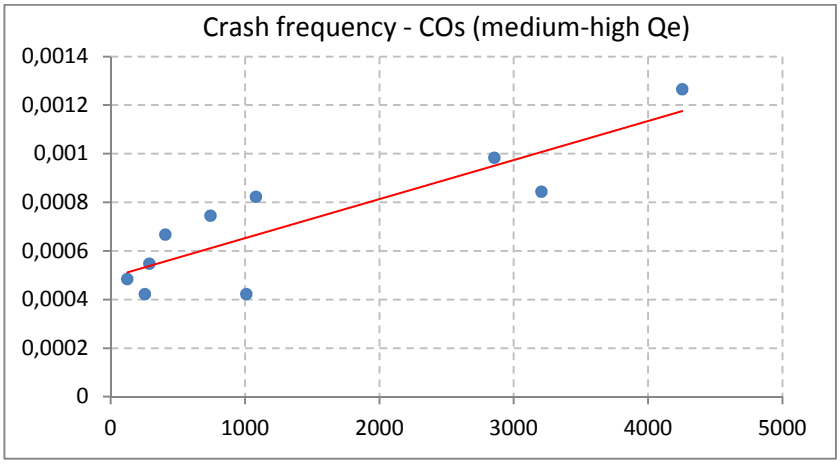

Figure 5.43 Crash frequency of legs subjected to medium-high average daily entering traffic flows plotted against estimation of their COs. The graph demonstrates that crash frequency increases at an higher rate as compared to COs. A simple moving average was applied

Only for legs subjected to medium-high entering traffic flows there seems to be the possibility of estimating a calibration curve able to predict the crash-to-conflict ratio by knowing the entry path radius of the analysed approach. The calibration curve limited to roundabout legs with high Qe appears to follow findings of Scientific Literature and empirical evidence, seems not to have been corroborate.

In summary, as for the *collisions due to failure to yield without stopping*, the crash prediction model based on CO technique proved to offer affordable estimates for only legs with high Qe. For small traffic flows, geometric layout of the roundabout seems to be completely ineffective. Bootstrap estimation confirms this last statement, given that the resulting line is quite flatten (**Figure 5.45**). However, the increasing trend of the relationship R1sx-ci is poorly pronounced in Bootstrap reproductions (**Figure 5.44**). TThis enlightens the needs for enhancing the sample size in order to obatine more reliable results.

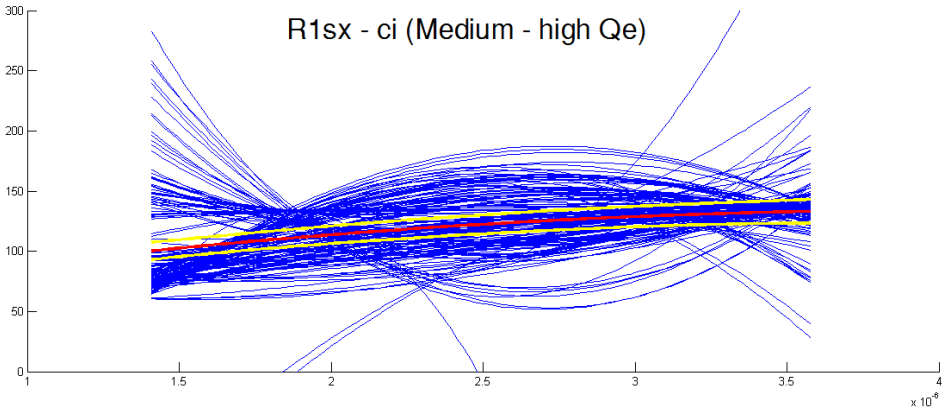

Figure 5.44 Calibration curve for roundabout legs affected by medium-high average daily traffic flow. Bootstrap estimation

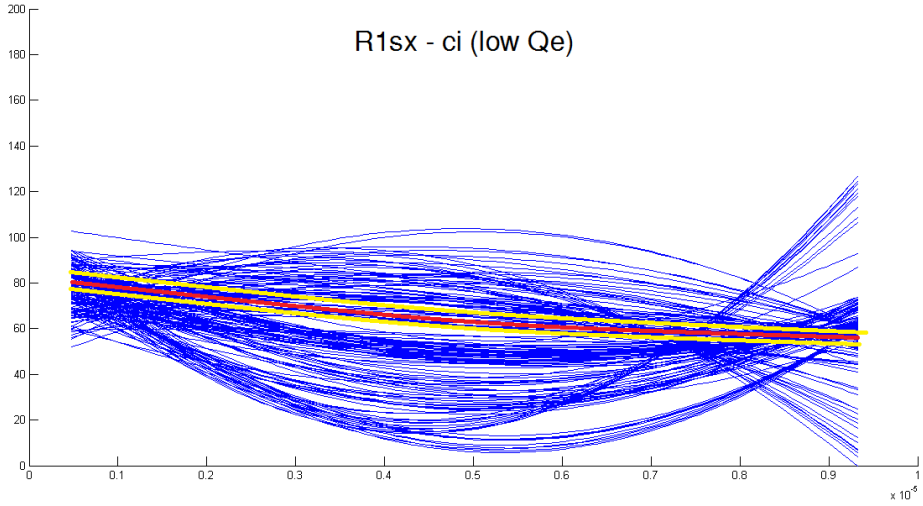

Figure 5.45 Calibration curve for roundabout legs affected by low average daily traffic flow. Bootstrap estimation

5.3 Single vehicle run-off

Exploratory analyses for this kind of crash were carried out in Chapter 4. It turned out that only entry path radius R1 offers a significant contribution in explaining variance of crash frequency.

5.3.1 Estimating the calibration curves

Exploratory analyses identified deviation angle and angle of visibility as the geometric features mot correlated to frequency of crashes due to failure to yield when starting from a stopped position. Conversely, no geometric parameters were found to be correlated to the potential crash frequency.

$$N_2 = Q_e * P(0) * P(t \geq t_c)$$

where

- $P(t \geq t_c)$= probability that the first "*lag*" is superior than t_c critical time

For this type of crash, COs related to the analysed leg and calculated for each hour of the day initially increase and then decline after having reached a peak for an entering traffic flow of about 400 pcu/h (**Figure 5.46**). This trend also emerges by considering the average daily traffic flow entering a roundabout and passing through the analysed leg (**Figure 5.47**).

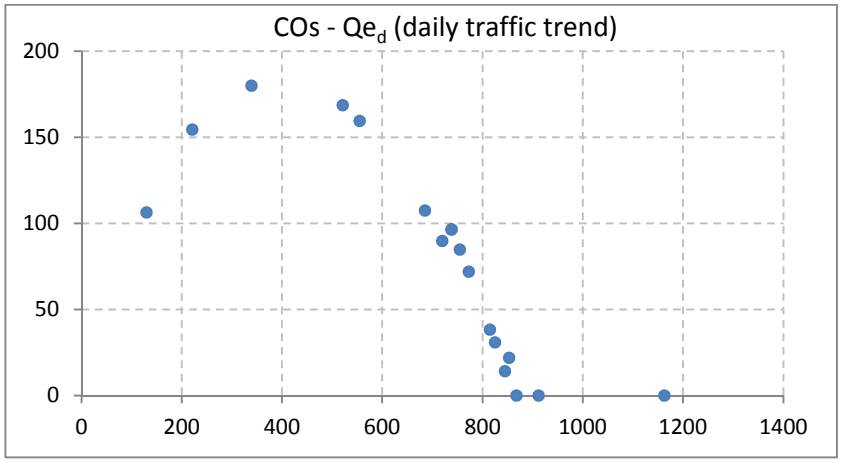

Figure 5.46 Daily evolution of Conflict Opportunities plotted against entering traffic flows measured on an hourly basis for a single roundabout leg

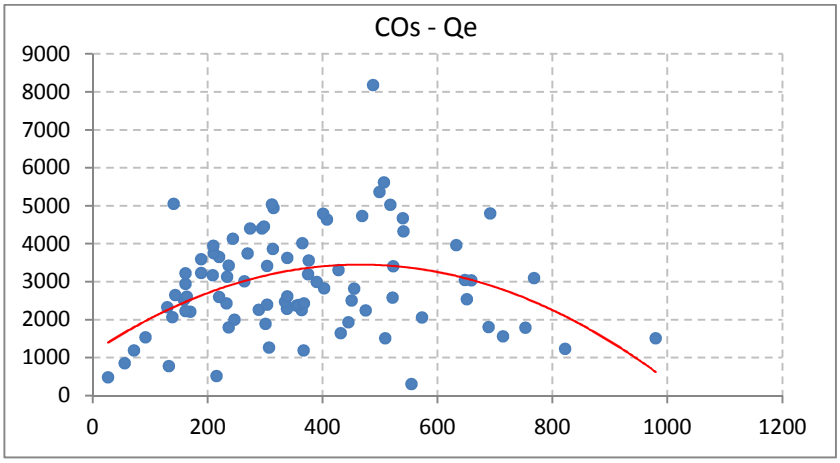

Figure 5.47 Conflict Opportunities plotted against average daily traffic flows entering roundabouts. Each point represent a different leg. All of the 87 legs analysed in this study were considered

By considering all of the sampled legs, Entry path radius R1 is substantially independent of inscribed circle diameter of the related roundabout and entering flows Qe averaged over the day (**Figure 5.48**, **Figure 5.49**). Distinguishing between low and medium-high Qe do not change this pattern.

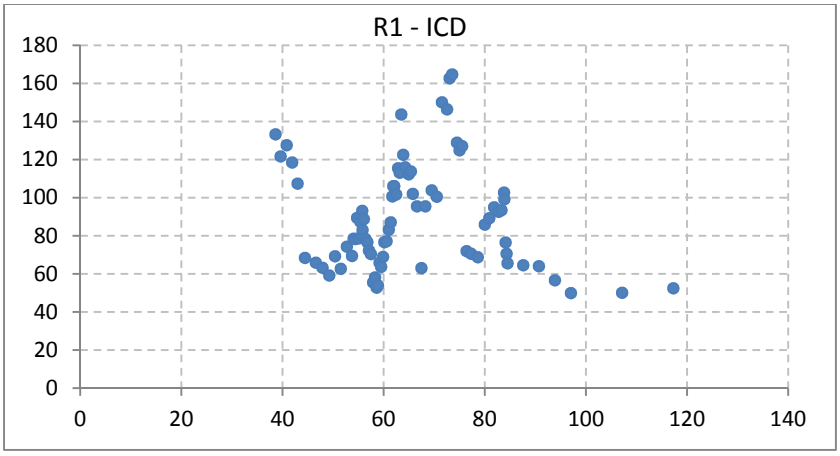

Figure 5.48 Plotting entry path radius R1 against inscribed circle diameter ICD. All of the 87 sampled legs were considered

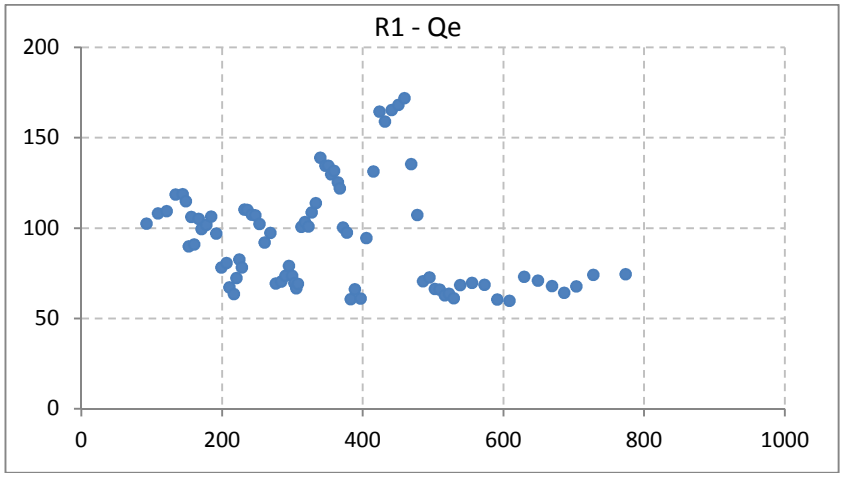

Figure 5.49 Entry path radius of legs plotted against inscribed circle diameter of the related roundabout. All of the 87 sampled legs were considered

By plotting COs against entry path radius, no relation can be traced. This confirms outputs of MLR model carried out for single vehicle run-off where the dependent variable was the number of COs. In these regressions, no significant correlation with geometric features was detected. Separating between low and medium-high Qe leads nowhere too (**Figure 5.50**).

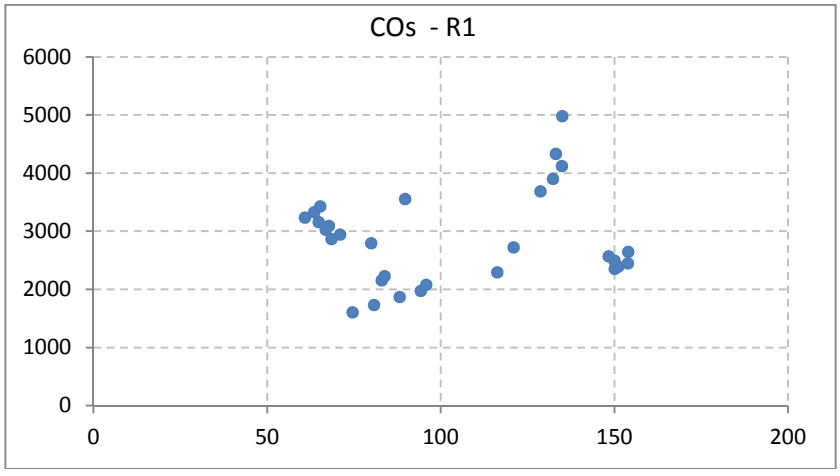

Figure 5.50 Preliminary measures for testing the convenience of factor analysis for uncover concealed information from collected data

Correlation between R1 and crash frequency showed by Figure 5.51 corroborates exploratory analyses and, in particular, indications provided by correlation coefficients and the Cohen's effect size f^2.

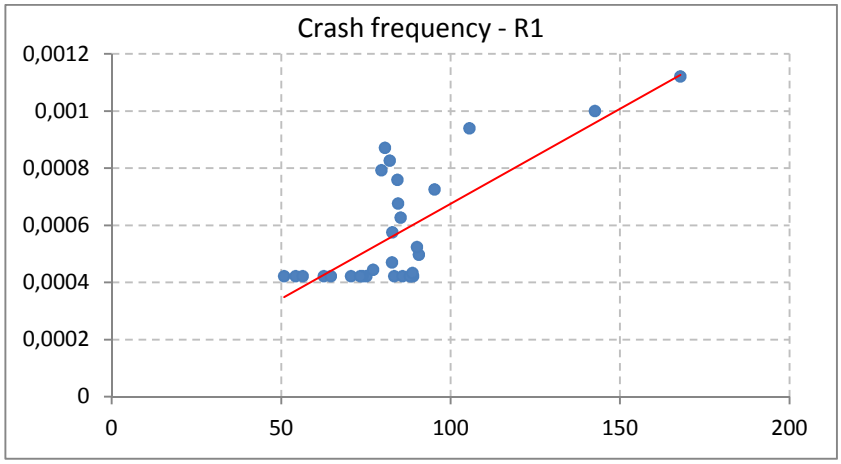

Figure 5.51 Crash frequency of roundabout legs plotted against their entry path radius

Figure 5.46 depicts the calibration curve obtained for single vehicle run-off crashes. It clearly suggests that restrained entry path radii ensure better safety performance for this type of collision. After all, crash-to-conflict ratios are derived by the ratio between crash frequency and CO frequency. While the number conflict opportunities shows no relationship with entry path radius, crash frequency rises as R1 reaches higher values. The trend of this calibration curve seems to be rational and consistent with findings of road safety studies and is confirmed by Bootstrap estimate (**Figure 5.53**):

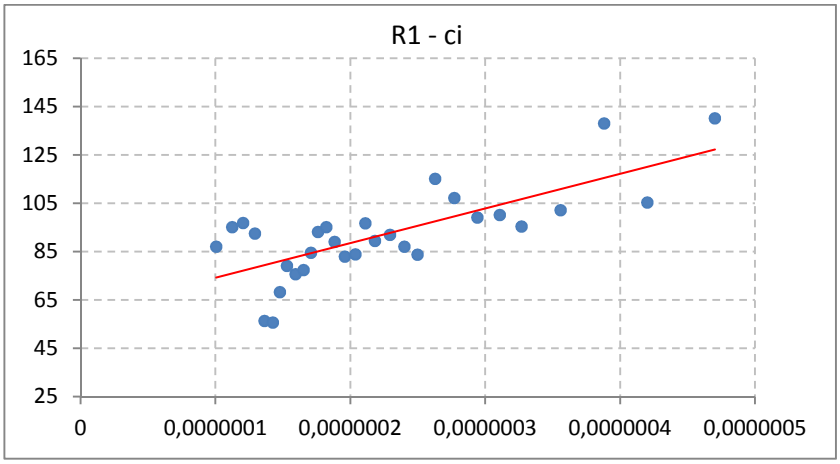

Figure 5.52 Calibration curve for single vehicle run-off crashes

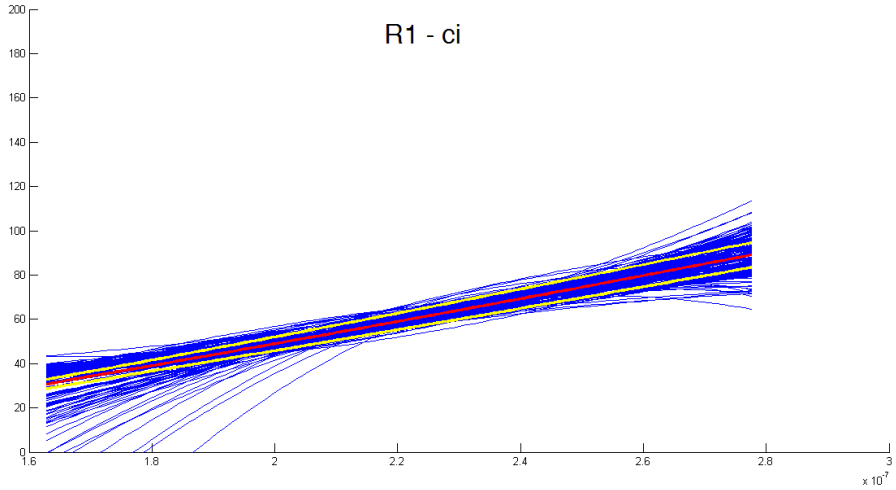

Figure 5.53 Calibration curve. Bootstrap estimation

5.4 Rear-end collision at the entry

5.4.1 Factor analysis

Various factors analyses have been performed for the 33 roundabout legs involved in crash type *Rear-end collision at the entry* at least one time in their operational life. Various attempt were performed, and it was found that the following set of covariates allows reaching the best results.

- ICD;
- Deviation angle;
- R1;
- Visibility angle;
- Entry angle;

There are two preliminary steps to be conducted in order to assess whether factor analysis may be actually useful for better understanding the collected sample. The first one consists in verifying that variables are uncorrelated. If this hypothesis cannot be rejected, there is no reason to do a principal component analysis and consequently a factor one since the variables have nothing in common. **Table 5.45** clearly shows that the null hypothesis can be rejected: there are certain degree of correlation between considered variables. The measure of *Kaiser-Meyer-Olkin* (KMO) statistic predicts if collected data are likely to factor well, based on correlation and partial correlation. KMO index is substantially higher than the conventional threshold value of 0.6. Therefore, even this step gave positive outcomes.

Table 5.45 Preliminary measures for testing the convenience of factor analysis for uncover concealed information from collected data

KMO Measure of sampling	0.677
Bartlett's test of sphericity (Sig.)	<0.001

Taken together, Bartlett's test and KMO measure of sampling adequacy provide a minimum standard which should be passed before a factor analysis should be conducted. Given that both test are positive, PCA technique is then applied to the collected data in order to find the linear combinations of them that account for as much of the total variable as possible.

Among them, the first principal component is the new unveiled variable that explain the maximum amount of the original variable. (**Table 5.46**).

The amount of variance accounted for by each component is shown by the eigenvalue, which is equal to the sum of the squared loadings for a given component. The higher the eigenvalue, the higher the importance of this

component and the probability it will be retained as a factor. The proportion of variance explained by a single component can be determined by the ration between the corresponding eigenvalue and the overall variance. **Table 5.46** also illustrates the cumulative percentage of variance accounted for by the current and preceding factors.

Table 5.46 Eigenvalues of each component and their contribution in explaining the total variance

Component	Eigenvalues	% of variance	% cumulative
1	2.533	50.659	50.659
2	1.361	27.226	77.884
3	0.519	10.370	88.254
4	0.408	8.151	96.405
5	0.180	3.595	100.000

For this crash type, the first two components were retained as factors, since together they explain more than 70 per cent of the entire variance.

Table 5.47 reports loadings of the two retained factors.

Table 5.47 Component matrix showing loadings of each variable

Manifest variables	*Extracted factors*	
	1	**2**
ICD	-0.835	-0.111
Deviation Angle	-0.456	0.723
R1	0.454	-0.726
Visibility Angle	0.773	0.515
Entry Angle	0.908	0.186

Table 5.48 shows the communalities of each manifest variable for the two extracted factors, that is the proportion of each variables' variance explained by the retained factors.

Table 5.48 Factor matrix showing loadings of each variable after Varimax rotation

	Initial	*After extraction*
ICD	1.000	0.709
Deviation Angle	1.000	0.730
R1	1.000	0.733
Visibility Angle	1.000	0.862
Entry Angle	1.000	0.860

By analysing signs and values of factors (**Table 5.47**), their underlying and latent meaning may be realised.

The first factor seems to bring out entries with high design speeds with a fast circulating traffic. High angles of visibility are associated to high entry angles, as already specified in Chapter 4. This layout tends to increase vehicle speeds, as confirmed by the negative sign of deviation angle. The loading related to the entry radius of the left approach seems to be important too. As matter of fact, if vehicles coming from the left moves at higher speeds, the likelihood of *collision due to failure to yield starting from a stopped position* will inevitably increase.

The second factor appears to be essentially focused on the trajectory followed by vehicles being about to enter the ring. In fact, loading factors of entry path radius and deviation angle are predominant and have opposite signs. A large entry path radius along with a restricted deviation angle does not discourage drivers from approaching to the ring with no adequately reduced vehicular speeds.

For the sake of an easier interpretation of manifest meanings of the factors, an orthogonal rotation factor was then applied by following the Varimax criterion where the aim is to reduce for each factor the number of loadings significantly different from zero (**Table 5.49** and **Figure 5.54**).

Table 5.49 *Factor matrix showing loadings of each variable after Varimax rotation*

Manifest variables	*Extracted factors*	
	1	**2**
ICD	-0.801	0.260
Deviation Angle	-0.100	0.849
R1	0.097	-0.851
Visibility Angle	0.919	0.132
Entry Angle	0.900	-0.223

In this situation, Varimax rotation effectively simplified the interpretation of factors. Previous considerations are confirmed. As regard the first factor, angle of visibility and entry angle have the greatest weights, while the rotated second factor

now gives even more importance to deviation angle and entry path radius (**Figure 5.54**).

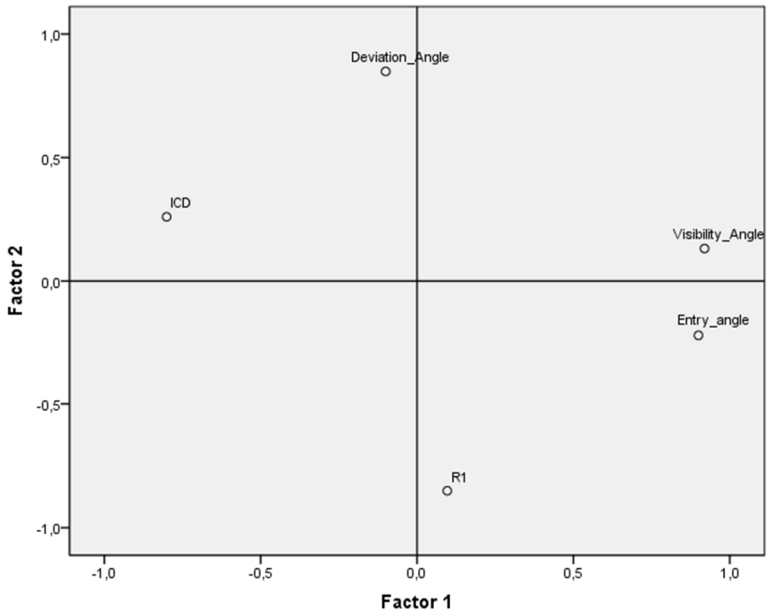

Figure 5.54 *Factor plot in rotated factor space.*

As already explained, the reproduced matrix correlation based on the extracted factors can be obtained from the matrix loadings (**Table 5.50**). It is desirable that corresponding values of the two variables are as close as possible, that is that residuals are close to zero. Correlation matrix estimated by Factor analysis proved to approximate well the original one, with only three residuals greater than the threshold value of 0.05.

Table 5.50 In the top part of the table there are the reproduced correlations, while the bottom part contains the residuals obtained by the difference with the sample correlation matrix.

		ICD	Deviation angle	R1	Visibility Angle	Entry Angle
Reproduced Correlation	ICD	0.709	0.301	-0.299	-0.702	-0.779
	Deviation Angle	0.301	0.730	-0.732	0.020	-0.280
	R1	-0.299	-0.732	0.733[a]	-0.023	0.277
	Visibility Angle	-0.702	0.020	-0.023	0.862[a]	0.798
	Entry Angle	-0.779	-0.280	0.277	0.798	0.860
Residuals[b]	ICD		-0.039	0.039	0.129	0.119
	Deviation Angle	-0.039		0.250	-0.036	0.005
	R1	0.039	0.250		0.034	-0.001
	Visibility Angle	0.129	-0.036	0.034		-0.033
	Entry Angle	0.119	0.005	-0.001	-0.033	

Residuals are computed between observed and reproduced correlations. There are 3 (30.0%) non redundant residuals with absolute values greater than 0.05.

Table 5.51 provides the Matrix Score, that is the coefficient values related to the manifest variables linearly combined in order to obtain the factor score. However, the presence of uniqueness makes it unfeasible reaching an exact solutions, and approximation methods must be applied.

Table 5.51 Matrix score

	ICD	Deviation angle	R1	Visibility Angle	Entry Angle
F1	-0.332	0.066	-0.068	0.438	0.382
F2	0.069	0.557	-0.558	0.210	-0.031

5.4.2 Discriminant analysis

There are 5 initial geometric parameters identified by FA and 33 legs which has been assigned to one of three groups defined on the base of their crash frequency magnitude. Table 5.52 offers an overview about collected data.

Table 5.52 Group statistics

Class frequency		Mean	Std. deviation	Valid cases
1	ICD	81,2978	30,5897	18
	Deviation Angle	62,2222	26,9848	18
	R1	65,0556	23,7696	18

	Visibility Angle	77,4550	43,7530	18
	Entry Angle	48,9444	10,7892	18
2	*ICD*	66,8711	12,3759	9
	Deviation Angle	54,4444	21,4482	9
	R1	56,2222	9,7439	9
	Visibility Angle	74,9944	59,3274	9
	Entry Angle	47,4444	4,7726	9
3	*ICD*	58,3017	22,7327	6
	Deviation Angle	30,1667	39,7462	6
	R1	63,5000	27,3989	6
	Visibility Angle	191,7650	131,0201	6
	Entry Angle	58,1667	27,5566	6
Total	*ICD*	73,1821	26,5690	33
	Deviation Angle	54,2727	29,8865	33
	R1	62,3636	21,3568	33
	Visibility Angle	97,5676	81,3248	33
	Entry Angle	50,2121	14,1813	33

Table 5.53 shows the Within-groups correlation matrix. It corresponds to a correlation matrix of data points obtained by subtracting to them the barycentre of the group they belong to. Multicollinearity should not represent a possible concern for discriminant analysis given that no value is greater than 0.8.

Table 5.53 Within-groups correlation matrix.

	ICD	*Deviation angle*	*R1*	*Visibility Angle*	*Entry Angle*
ICD	1.000	0.154	-0.662	-0.175	-0.666
Deviation Angle	0.154	1.000	-0.030	-0.444	-0.200
R1	-0.662	-0.030	1.000	-0.008	0.792
Visibility Angle	-0.175	-0.444	-0.008	1.000	0.186
Entry Angle	-0.666	-0.200	0.792	0.186	1.000

First of all, significant differences between groups on each of the independent variables are to be examined. If there were not significant differences between

groups, it would not be meaningful proceeding any further with the analysis. **Table 5.54** shows two tests which can be used to evaluate the potential of the considered manifest variables in discriminating the three groups before the DA is performed. In particular, the significance of differences in group means for each variable is tested. The quantity *(1 - Wilks' Lambda)* is the proportion of variance in the dependent variable that can be explained by the considered predictor. Therefore, a relatively small Wilks' Lambda value indicates that the analysed covariate has a potential in discriminating groups. The other columns of **Table 5.54** refer to an F-test performed in a one-way analysis of variance (ANOVA). The null hypothesis is that all population means are equal in regard to a particular variable; the alternative hypothesis is that at least one mean is different.

As can be seen by **Table 5.54**, the Wilk's lambda test presents similar results for the variables, while the ANOVA seem to suggest that only Visibility Angle and to a lesser extent the deviation angle may discriminate the three sub-populations.

Table 5.54 Test of equality of group means table

	Wilks' Lambda	**F**	**df1**	**df2**	**p-value**
ICD	0.873	2.185	2	30	0.130
Deviation Angle	0.838	2.895	2	30	0.071
R1	0.967	0.507	2	30	0.607
Visibility Angle	0.692	6.665	2	30	0.004
Entry Angle	0.926	1.202	2	30	0.315

After this preliminary insight into potential of each manifest variable in separating sub-populations characterised by different crash frequency, discriminant functions can now be sought. The maximum number of discriminant functions produced is equal to the number of groups minus 1. As a result, in this example, there are only two directions of interest; their eigenvalues and their contribution in explaining original variance are shown in **Table 5.55**. The canonical correlation is the multiple correlation between two sets of variables. The first is constituted by the manifest variables, while the second refers to the dummy variables used for coding the three considered groups of different crash frequency. A high canonical correlation indicates a function that discriminates well.

Table 5.55 Eigenvalues table

Function	**Eigenvalue**	**% of variance**	**% cumulative**	**Canonical correlation**
1	0.572	68.1	68.1	0.603
2	0.268	31.9	100.0	0.460

The canonical correlation is then exploited in the statistical methods devoted to ascertain the significance of the acquired discriminant functions.

If canonical correlation of discriminant functions were be equal to zero, no relationship between the set of independent variables and the discriminant scores (i.e. the dependent variable) would be found. The discriminant functions would be worthless because the means of the discriminant scores would be the same in the considered groups.

This is exactly the null hypothesis of the Willk's lambda statistical test, by means of which it is possible to establish the significance of the discriminant functions. Wilks' lambda is the proportion of the total variance lying in the discriminant scores not explained by differences among the groups. It is calculated as the product of the values of *1-canonical correlation*^{2}. Therefore, smaller values of Wilks' lambda are desirable. In this example, canonical correlations are 0.704 and 0.355, so the Wilks' Lambda testing both canonical correlations is $(1-0.603^2)*(1-0.460^2) = 0.502$, and the Wilks' Lambda testing the second canonical correlation is $(1-0.425^2) = 0.789$.

The Chi-square statistic tests whether the canonical correlation of discriminant functions is equal to zero, which implies a unitary Wilk's lambda. This is exactly the null hypothesis, a situation characterised by a negligible contribution offered by discriminant functions in explaining the total variance of the independent variables.

Table 5.56 represents the output of Willk's lambda statistical test carried out on the two discriminant functions obtained for this example. The first test presented in this table tests both canonical correlations ("1 through 2") and the second test presented tests the second canonical correlation alone.

Table 5.56 Wilk's lambda table

Function	Wilks' Lambda	Chi-square	df	p-value
1 through 2	0.502	19.320	10	0.036
2	0.789	6.646	4	0.156

From **Table 5.56**, it can be stated that there is at least one statistically significant function. If the probability for this test had been larger than 0.05, the definitive conclusion would have been that concluded that there are no discriminant functions to separate the groups of the dependent variable.

Discriminant analysis would have been concluded here.

The second line of the Wilks' Lambda table tests the null hypothesis that the mean discriminant scores for the second possible discriminant function are equal in the subgroups of the dependent variable. Since the probability of the chi-square statistic for this test is greater than 0.05, the null hypothesis cannot be rejected. In conclusion, there is only one discriminant function to separate the groups of the dependent variable.

In **Table 5.57**, the standardised coefficients are provided for the two discriminant functions. Their interpretation enable unveiling the latent aspect they

represent, in a similar way to the identification of the meaning embraced by factors adopted in factor analysis. The sign indicates the direction of the relationship, while the magnitudes define how strongly the discriminating variables effect the score.

As pertaining to the first function, the only one that actually separates the three groups, R1, deviation angle and visibility angle have the preponderant coefficients. Entry angle and Angle of visibility score were less successful as predictors, while ICD score is insignificant.

Table 5.57 Standardised canonical discriminant function coefficients table

	Functions	
	1	**2**
ICD	0.606	1.072
Deviation Angle	0.192	0.131
R1	0.762	0.959
Visibility Angle	-0.539	0.748
Entry Angle	-0.378	0.133

There is an alternative way of specifying the relative importance of the predictors. The structure matrix table (**Table 5.58**) provides the correlations of each independent variable with the discriminant functions. These correlations serve as factor loading in factor analysis. By identifying the largest loadings, the researcher gains an insight into how to correctly interpret the discriminant function.

Table 5.58 Structure matrix table

	Functions	
	1	**2**
ICD	-0.806	0.519
Deviation Angle	0.577	-0.091
R1	0.477	0,238
Visibility Angle	-0.317	0.291
Entry Angle	0.060	0,344

Pooled within-groups correlations between discriminating variables and standardised canonical discriminant functions. Variables ordered by absolute size of correlation within function.

Loadings of ICD, R1 and deviation angle stand out as predictor strongly influencing the allocation of legs to the three groups characterised by different

frequency values for the analysed crash type. Structure matrix table confirms the vision obtained from standardised canonical distribution function coefficients.

Discriminant functions are eventually created by unstandardized coefficients, which are reported in **Table 5.59**. Non-standardised values of manifest variables will give the score for the discriminant functions. The greatest coefficients are referred to entry and exit path radius again.

Table 5.59 Canonical discriminant function coefficients table. Unstandardized coefficients

	Functions	
	1	**2**
ICD	0.024	0.042
Deviation Angle	0.007	0.005
R1	0.035	0.044
Visibility Angle	-0.008	0.011
Entry Angle	-0.027	0.009
(Constant)	-2.189	-7.583

A further way of interpreting the DA results is insert the average discriminant score (unstandardised) in the three groups (**Table 5.60**). In detail, the discriminant score for each group when the variable means (rather than individual values for each case) are entered into the discriminant equation. These group means are called centroids.

Table 5.60 Functions at group centroids table

	Functions	
Class frequency	**1**	**2**
1,00	0.529	0.268
2,00	-0.115	-0.802
3,00	-1.415	0.399

Unstandardized canonical discriminant functions evaluated at group means

SPSS also provides a graphical representation of DA output (**Figure 5.55**).

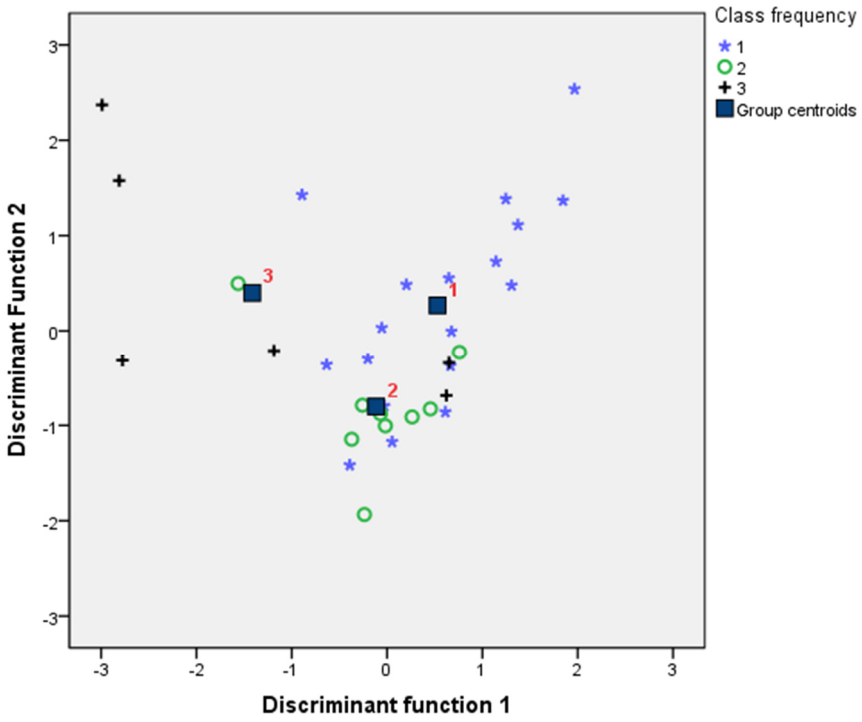

Figure 5.55 Graph of roundabout legs on the discriminant dimensions

The output of discriminant analysis is the classification table, whose rows are the observed categories of the dependent variable while the columns are the predicted categories. When prediction is perfect all cases lie on the diagonal. The percentage of cases on the diagonal is the percentage of correct classifications. The cross validated set of data is a more authentic representation of the outcome achieved by discriminant function. The cross validation is often termed a 'jack-knife' classification, given that successively classifies all cases but one to develop a discriminant function and then categorizes the case that was left out. This process is repeated with each case left out in turn. This cross validation produces a more reliable function. The ratio is that one should not use the case the researcher is trying to predict as part of the categorization process. The classification results for the crash type reveal that 60.6% of legs were classified correctly into the three categories of crash frequency. The third group suffers from the least accuracy.

This overall predictive accuracy of the discriminant functions is called the *hit ratio*. Via a random classification of the collected legs, there would be a 33.3% probability of correctly collocating the 32 subjects into the three categories.

Accordingly to a conventional approach, acceptable hit ratios must be greater than this probability increased by 25%, which gives a threshold value equal to 41.63%. The output of discriminant analysis is substantially up to standard.

Table 5.61 Classification results table. 66.7% of original grouped cases correctly classified. 60.6% of cross validated grouped cases correctly classified.

			Predicted group membership			
		Class frequency	**1.00**	**2.00**	**3.00**	**Total**
Original	Count	1.00	11	6	1	18
		2.00	1	7	1	9
		3.00	1	1	4	6
	%	1.00	61.16	33.34	5.67	100.00
		2.00	11.14	77.81	11.13	100.00
		3.00	16.42	16.65	66.74	100.00
Cross-validated [a]	Count	1.00	11	6	1	18
		2.00	1	7	1	9
		3.00	1	3	2	6
	%	1.00	61.17	33.34	5.62	100.00
		2.00	11.14	77.86	11.11	100.00
		3.00	16.72	50.01	33.30	100.00

a. Cross validation is done only for those cases in the analysis. In cross validation, each case is classified by the functions derived from all cases other than that case.

A discriminant analysis was then conducted to predict the categorical variable *crash frequency* for analysed roundabout legs. Predictor variables were *inscribed circle diameter, deviation angle, entry path radius, visibility angle and entry angle*. These are the same geometric features previously identified via the factorial analysis.

Significant mean differences were observed for the *angle of visibility*. Only one of the two discriminate functions was found to be statistically significant, that is able to effectively separate legs of different crash frequency category. By analysing the standardised coefficients of the discriminant function and the pooled within-groups correlations of the structure table matrix, conclusion can be drawn that *inscribed circle diameter, entry path radius* and *visibility angle* are the only predictors able to explain safety performances of roundabout legs in regard to the rear-end collisions at the entry.

5.4.3 Regression analyses

Multiple linear regression models whit crash frequency as a continuous dependent variable may allow understanding the portion of variance affecting crash frequency explained by the single geometric parameters. From FA and DA, a set of geometric features apparently related to crash frequency was found and then investigated in MLR models. Stepwise regression procedures were applied by exploiting the F-test in order to establish which of these four models should be preferred for analysing the investigated phenomenon.

- *Model 1.* Predictors: Constant, Entry Angle, R1, ICD;
- *Model 2.* Predictors: Constant, Entry Angle, R1, ICD, Visibility Angle;
- *Model 3.* Predictors: Constant, Entry Angle, Deviation Angle, R1, ICD, Visibility Angle;

It is then desired to ascertain whether the full model contributes additional information about the association between Y and the predictors. The null hypothesis is that the additional covariates are not significant, and their related coefficients are therefore equal to zero. If the difference between error sum of squares for the reduced model (i.e. SSE_R) and the error sum of squares for the complete model (i.e. SSE_C) reaches high values, the null hypothesis is likely to be rejected because this would mean that the additional parameters significantly improve the model's fit to the data. Output of F-test for the four tested models are reported in **Table 4.22**, which shows that the independent variables statistically significantly predict the dependent variable for all of tested models.

Table 5.62 F-test carried out for testing statistical significance of various models.

Model		Sum of squares	df	Mean squares	F	Sig.
1	*Regression*	< 0.001	5	< 0.001	4.535	0.004
	Residual	< 0.001	27	< 0.001		
	Total	< 0.001	32			
2	*Regression*	< 0.001	4	< 0.001	5.825	0.002
	Residual	< 0.001	28	< 0.001		
	Total	< 0.001	32			
3	*Regression*	< 0.001	3	< 0.001	7.473	0.001
	Residual	< 0.001	29	< 0.001		

	Total	< 0.001	32

In order to definitively decide on which model focusing the attention, measures of model adequacy were calculated, with particular emphasis to adjusted R square, since it increases only when significant terms are added to the model (**Table 4.23**). By analysing R-square coefficients, in particular adjusted r-square, the full model was then selected.

Table 5.63 Measure of adequacy for the various MLR models.

Model	R	R-square	Adjusted R square	Standard error of the estimate
1	.676	.456	.356	.0004
2	.674	.454	.376	.0004
3	.660	.436	.378	.0004

Unstandardized coefficients indicate the increase experienced by the dependent variable for a unitary increment of the independent variable when all other independent variables are held constant (**Table 4.24**).

The same table reports the outputs of tests pertaining to the statistical significance of each of the independent variables. The null hypothesis is that the related coefficient of the investigated predictor is equal to zero. If p-value < 0.05, the null hypothesis can be rejected, and it can be stated that coefficients are statistically significantly different to zero, which is the case for *entry path radius* and *angle of visibility*.

Table 5.64 Calculating regression coefficients and testing statistical significance of the independent variables.

Model		Unstandardized coefficients		Standardised Coefficients		
		β	*Std. Error*	*β̂*	*t*	*Sig.*
1	*Constant*	0.002	0.001		3.299	0.003
	ICD	-7.197E-6	<0.001	-0.404	-2.071	0.048
	Deviation Angle	-9.314E-7	<0.001	-0.059	-.336	0.739
	R1	2.934E-6	<0.001	0.504	2.807	0.009
	Visibility Angle	-4.732E-6	<0.001	-0.213	-0.875	0.389
	Entry Angle	-1.143E-5	<0.001	-0.342	-1.295	0.206

The variance inflation factor (VIF) quantifies the severity of multicollinearity in MLR models with OLS estimates for the regression coefficients. It provides an index that measures how much the variance of an estimated regression coefficient is increased because of multicollinearity. Given that VIF factor is substantially lower than 2.0 for each predictor, there is not a severe reciprocal correlations between independent variables, with the exception of *entry* and *visibility angle*, whose VIF factors overly exceeds the threshold (**Table 4.25**). Caution is then required for estimations pertaining this parameter and its coefficients, given that is quite likely influenced by other covariates.

Various concerns persist about the reliability of standardised regression coefficients as a measure of actual relationships between each predictor and the dependent variable. As a matter of fact, $\hat{\beta}^*$coefficients can dramatically change in numerical value, and even in sign, as new variables are introduced or as old variables are removed. They simply reflect the amount of credit given to the related predictors. It can be said that they are context-specific to a given model characterised by a specific set of covariates. The problem is that the true model is rarely, if ever, known.

In addition, $\hat{\beta}^*$ coefficients are still sensitive to multicollinearity, and their values may be affected by the amount of Y variance shared with the other predictors. As a result, it can happen that a predictor explaining a consistent part of Y variance may have a near-zero $\hat{\beta}^*$ because another predictor is receiving the credit for the explained variance.

Other techniques are then required for correctly evaluating the importance of single predictors in explaining the analysed phenomenon. There is the need for estimating the relationship between a predictor variable and the outcome variable after controlling for the effects of other predictors in the equation.

Partial correlation represents the correlation between the dependent variable Y and a predictor after common variance with other predictors has been removed from both Y and the predictor of interest.

The squared *semipartial correlations* represent the unique variance of that predictor shared with the dependent variable. This means that the squared semipartial correlation for a variable denotes the decrease in coefficient of determination R^2 if that variable is removed from the regression equation (**Table 4.25**).

Table 5.65 Verifying the presence of severe multicollinearity and calculation of correlation coefficients

	Correlation coefficients			**Collinearity**	
	Zero-order	*Partial*	*Semipartial*	*Toll*	*VIF*
ICD	-0.216	-0.065	-0.048	0.530	1.887
Deviation Angle	-0.345	-0.370	-0.294	0.659	1.517

R1	0.546	0.475	0.398	0.625	1.599
Visibility Angle	-0.238	-0.166	-0.124	0.338	2.955
Entry Angle	-0.072	-0.242	-0.184	0.289	3.464

A squared structure coefficient denotes the amount of variance estimated by the model that the predictor is able to explain. This is equivalent to say that a squared structure coefficient denotes the amount of variance related to R^2 that the predictor is able to explain.

Structure coefficients definitely clarify the contribution of each predictor in explaining the phenomenon described via a multiple linear regression, and they provide support in trying to identify multicollinearity effects. Structure coefficients confirm previous analyses of partial and semipartial correlations.

Crash frequency variance seems to be basically explained by ICD and R1.

The magnitude of these relationships may be directly and synthetically measured by the so-called *Cohen's f^2 effect size*, which is focused on the strength of the association between the predictor of interest and the dependent variable.

Its outcome is a measure of practical significance in terms of the magnitude of the effect exerted by the single predictor. It is independent of the sample size and is appropriate for calculating the effect size within a multiple regression model in which the independent variable of interest and the dependent variable are both continuous. The effect size corroborates previous results: *deviation angle* and *entry path radius* appear to have a remarkable relationship with crash frequency as compared to other 21 investigated geometric factors (**Table 4.26**). This output is partially consistent with the findings of discriminant analysis, which identified the inscribed circle diameter too as a significant geometric factor for safety performance of roundabout as pertaining to rear-end crashes at entry. However, correlation coefficients and the effect size point out its restricted contribution in explaining crash frequency.

Eventually, exploratory analyses reach the conclusion that these aspects should deserve the maximum attention in order to design safer roundabouts from collisions due to failure to yield starting from a stopped position.

Table 5.66 Calculation of structure coefficients and effect size f^2

	Structure coefficient	**Effect size f^2**
ICD	0.1108	0.075
Deviation Angle	0.2900	0.151
R1	0.5733	0.327
Visibility Angle	0.1378	0.103
Entry Angle	0.0127	0.037

The most intuitive way for testing normality of residuals consists in trying to graph a histogram by plotting obtained residuals and placing them in regularly spaced cells. The histogram should approximate a normal distribution of residuals. However, with small sample sizes, which is the case of various crash type here in this study, this is not be the best choice for judging the distribution of residuals (**Figure 4.16**).

A more affordable way is proposed by the $normal\ probability\ plot$ (also called P-P plot). It is obtained by sorting the standardised residuals into ascending order and then calculating the cumulative probability of each residual.

Eventually, the so calculated P values are then plotted versus the normalised cumulative frequency distribution of residuals themselves, that is $(\varepsilon_i - \mu)/\sigma)$, where μ and α are approximated via the mean and standard deviation of residuals respectively. The normal probability plot seems to be able to produce an approximately straight line, which means that residuals may come from a normal distribution (**Figure 4.17**).

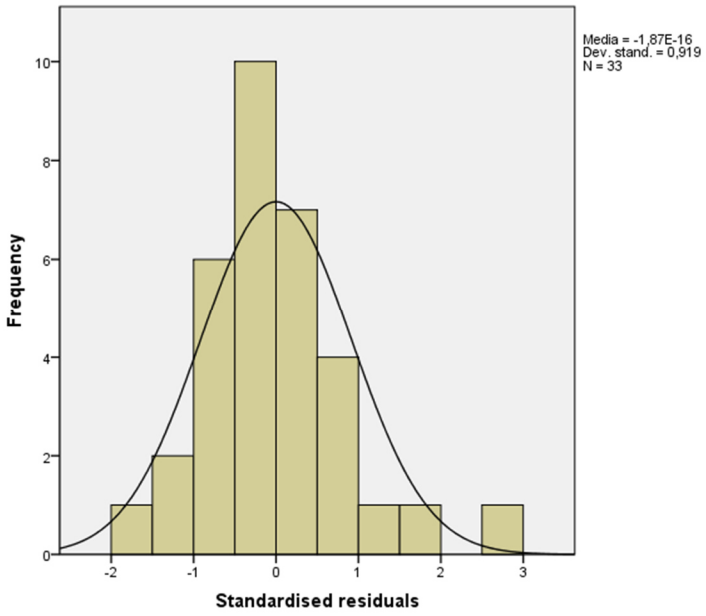

Figure 5.56 Testing normality distribution of residuals. Histogram

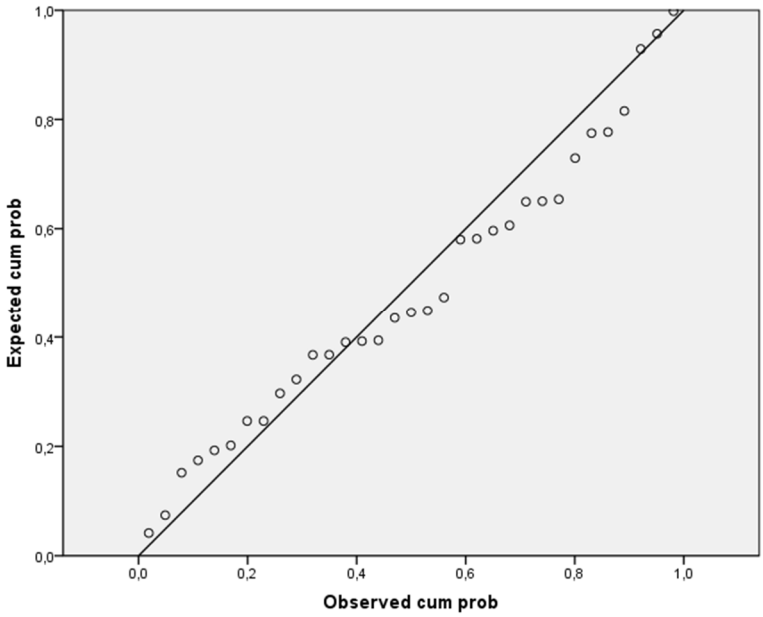

Figure 5.57 Testing normality distribution of residuals. Normal probability plot

There are instead serious concerns about the homoscedastic nature of residuals, which should have a constant variance σ^2. Homoscedastic assumption can be checked by visual examination of a plot of the standardized residuals (the errors) by the regression standardized predicted value. Residuals are not evenly scattered around the line and a certain trend can be recognised (Figure 4.18). This means that homoscedastic assumption is not verified. However, as already said, this cannot compromise results obtained with correlation coefficients and the effect size, which gave substantial results also consistent with previous exploratory analyses.

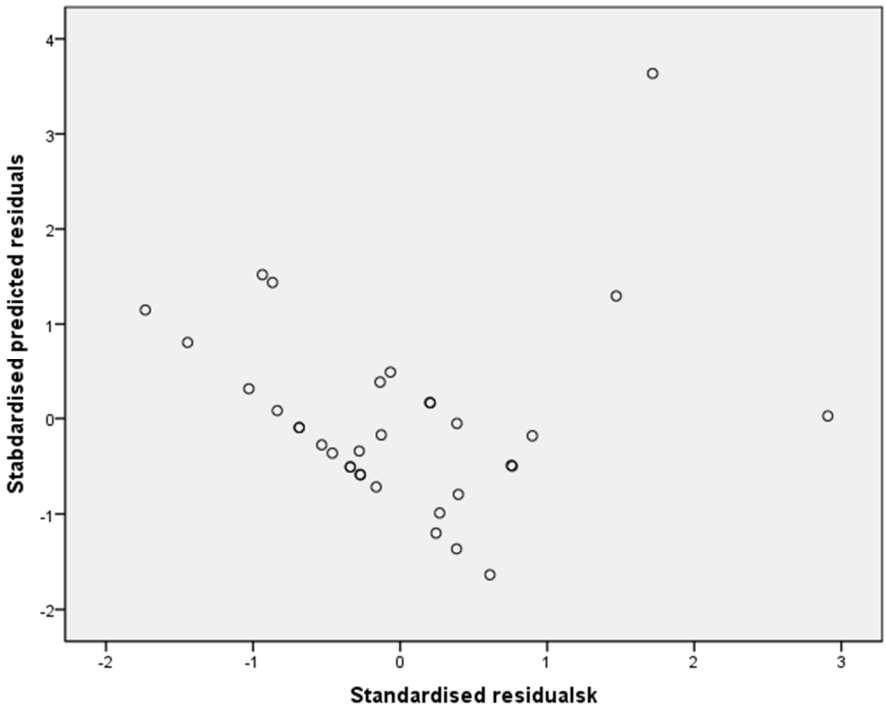

Figure 5.58 Scatter plot for detecting homoscedasticity of residuals

Even if a certain degree of homoscedasticity was revealed affecting the residuals, correlation coefficients and the effect sizes cannot be neglected, given that they clearly identified deviation angle and R1 as predominant factors in explaining crash frequency as compared to the other geometric features.

5.4.4 Estimating the calibration curves

Exploratory analyses identified deviation angle and angle of visibility as the geometric features mot correlated to frequency of crashes due to failure to yield when starting from a stopped position. Conversely, no geometric parameters were found to be correlated to the potential crash frequency.

$$N_3 = Q_e * (1 - P(0))$$

where

- $1 - P(0) = \rho = \frac{Q_e}{C}$

For this type of crash, theoretical trend of COs related to the analysed leg and calculated for each hour of the day shows a peculiar monotone increase, that is COs increase as traffic flows increase (**Figure 5.59**). This trend also emerges by considering the average daily traffic flow entering a roundabout and passing through the analysed specific leg (**Figure 5.60**).

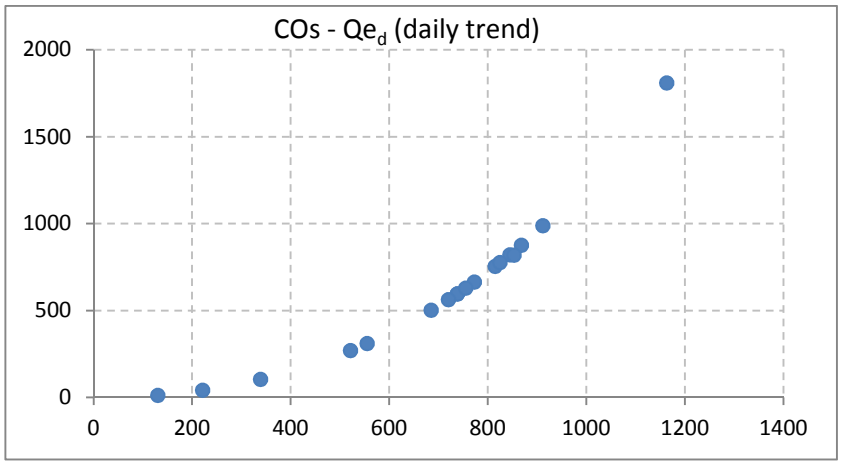

Figure 5.59 Daily evolution of Conflict Opportunities plotted against entering traffic flows measured on an hourly basis for a single roundabout leg

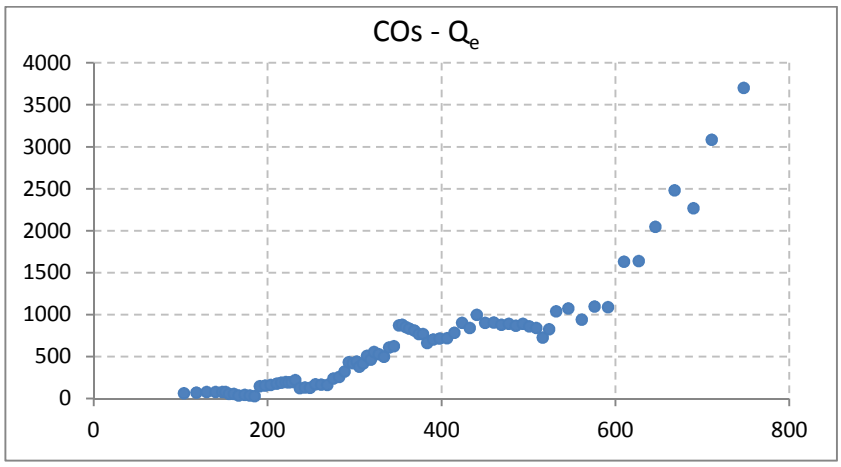

Figure 5.60 Conflict Opportunities plotted against average daily traffic flows entering roundabouts. Each point represent a different leg. All of the 87 legs analysed in this study was considered.

5.4.4.1 Entry path radius

Entry path radius appears not to be correlated to the inscribed circle diameter of the related roundabout and to the average daily traffic flow passing through the leg for entering the ring (**Figure 5.61**, **Figure 5.62**).

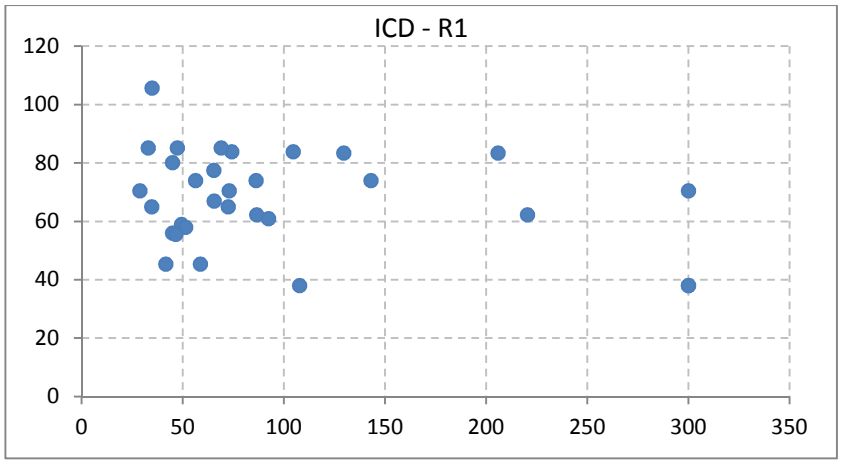

Figure 5.61 Entry path radius of legs plotted against inscribed circle diameter of the related roundabout

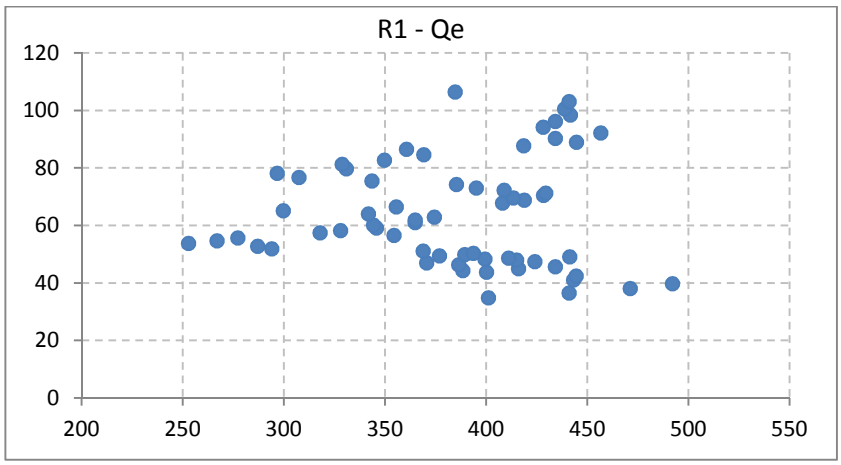

Figure 5.62 Entry path radius of roundabout legs plotted against the average daily traffic flows passing through them for entering the roundabout

COs associated to rear-end collisions denote a clear decline as R1 arises (**Figure 5.63**). This seems to be consistent with the fact that COs are proportional to the ratio ρ of entering flows to the capacity of the leg, and legs with small capacity values have generally reduced entry path radii.

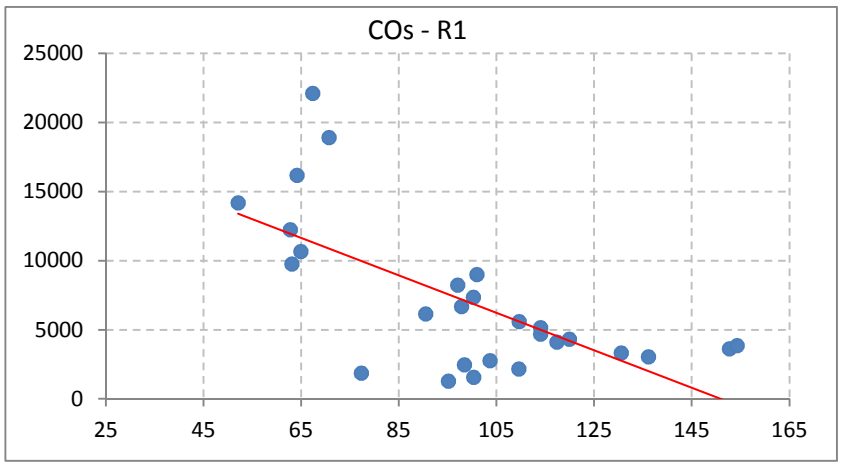

Figure 5.63 Conflict opportunities for rear-end collision at the entry plotted against the entry path radius of the same approach (simple moving average)

Conversely, crash frequency increases with the entry path radius, without significant differences between legs affected by low Qe and those affected by medium-high Qe (**Figure 5.64**).

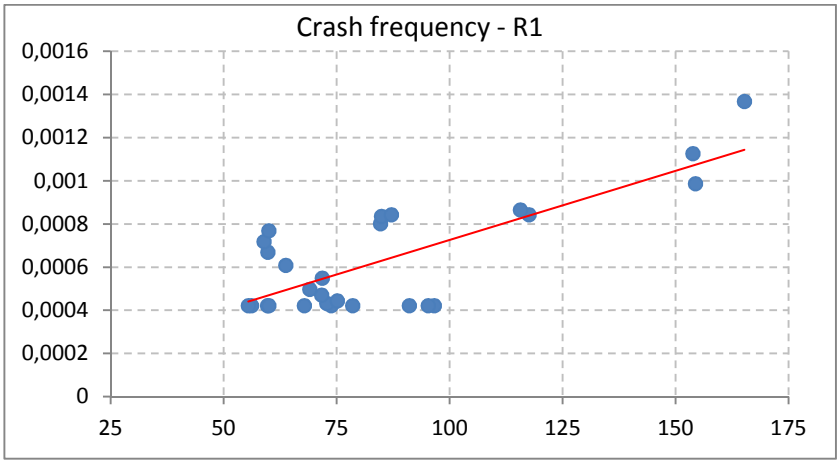

Figure 5.64 Deviation angle plotted against COs for legs experiencing low traffic flows. A simple moving average was applied

The significant increase of crash-to-conflict ratio as R1 arises is the result of the growth recorded for crash frequency and the contemporary reduction shown by conflict opportunities (**Figure 5.65**). The trend of the calibration curve is confirmed by the Bootstrap estimate (**Figure 5.66**).

Therefore, according to the model, great entry path radii are associated with high probabilities of rear-entry collisions. Effectively, these geometric layouts do not induce drivers to reduce their speeds, with consequent safety concerns. At the same time, the highest R1 values have been recorded for legs where ratio ρ between entering traffic flow and the capacity of the leg reaches highest values, a situation where rear-end crashes are more likely to occur.

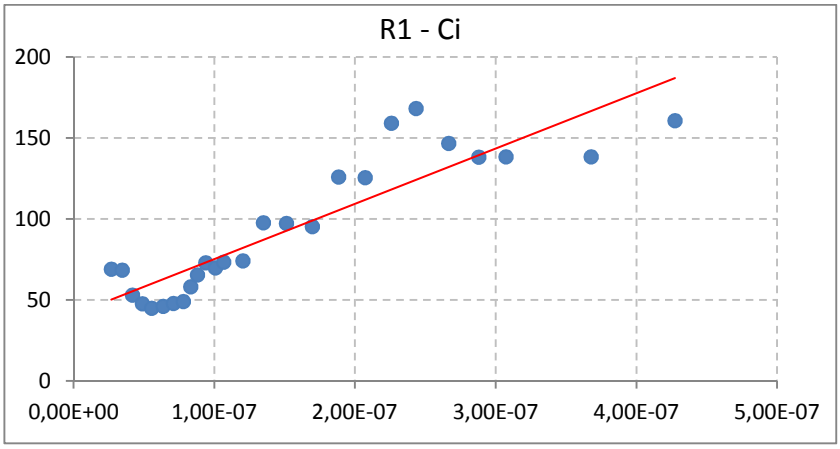

Figure 5.65 Crash frequency plotted against deviation angle

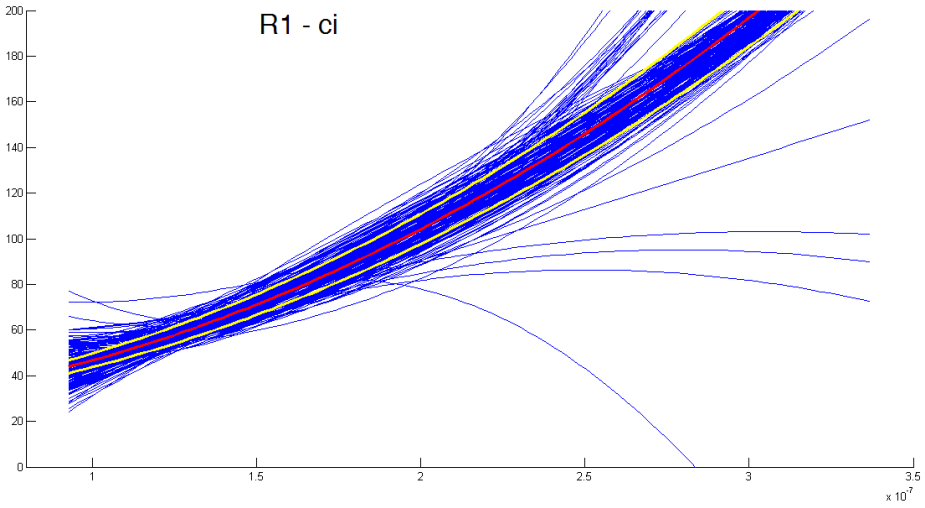

Figure 5.66 Calibration curve. Bootstrap estimation

5.4.4.2 Deviation angle

Neither inscribed circle diameter nor average daily traffic flow entering the roundabouts are correlated to the deviation angle of roundabout legs (**Figure 5.67**, **Figure 5.68**).

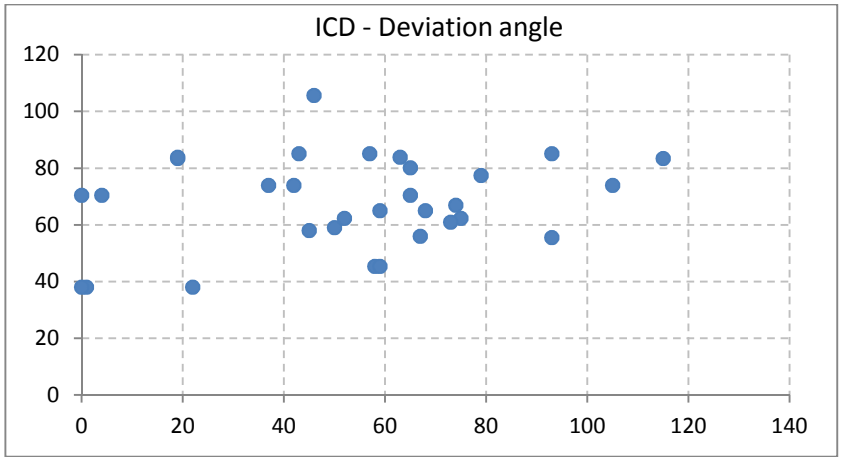

Figure 5.67 Deviation angle of roundabout legs plotted against inscribed circle diameter of the same roundabout

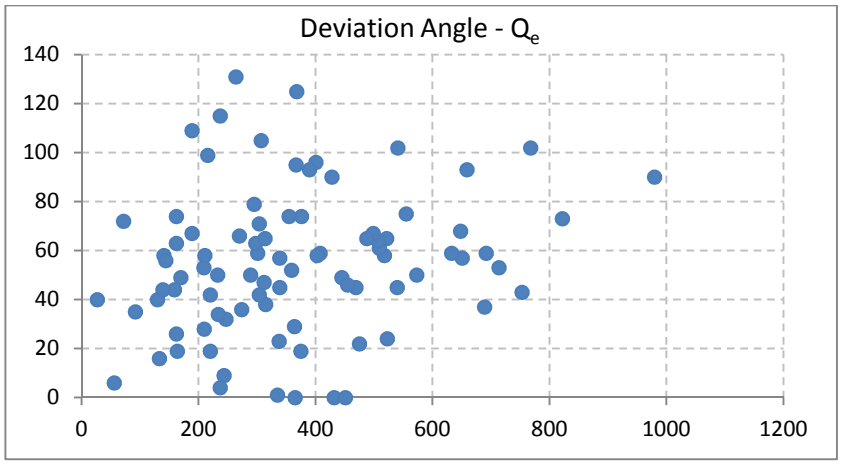

Figure 5.68 Deviation angle of roundabout legs plotted against average daily traffic flow passing through the leg itself for entering the roundabout

A pronounced positive trend comes out between the deviation angle of roundabout legs and conflict opportunities calculated for rear-end crashes (**Figure 5.69**). COs are proportional to the ratio of entering traffic flows Qe to the capacity

of the leg. This means that legs with great deviation angles are generally affected by high traffic flow in relation to their capacity, an operational pattern that makes rear-end crashes more likely to occur.

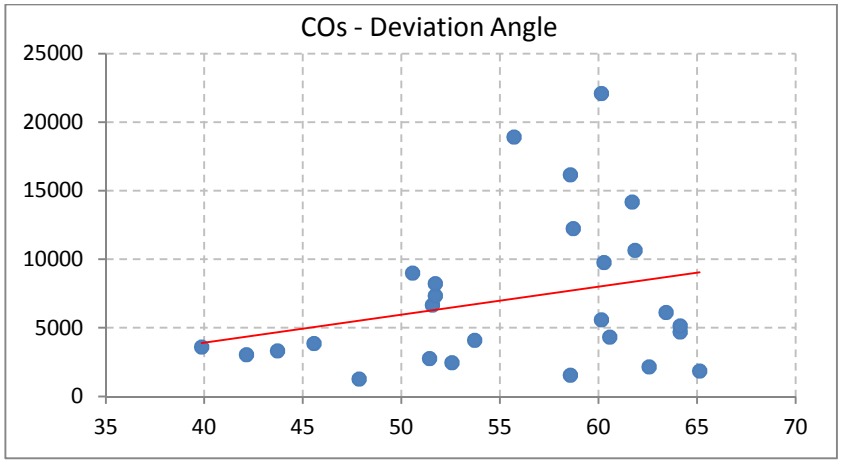

Figure 5.69 Conflict opportunities related to rear-end crashes at a certain leg plotted against the deviation angle of the same leg

Crash frequency presents an expected decline with accentuated deviation angles which force drivers to slow down when approaching and manoeuvring through the roundabout (**Figure 5.70**).

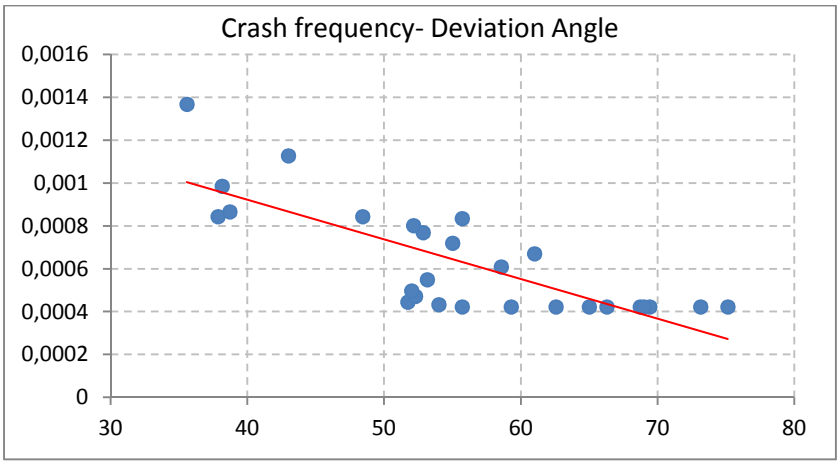

Figure 5.70 Crash frequency of rear-end collisions recorded at a certain leg plotted against the deviation angle of the same leg

The greater the deviation angle is, the smaller the crash-to-conflict ratio is. This is the consequence of deviation angle' trend with COs and crash frequency (**Figure 5.71**). Reliability of these statements is enhanced by the consistency with Bootstrap estimates (**Figure 5.72**).

Ultimately, given the same COs number, that is the same traffic flows, there are less rear-end crashes at legs provided with adequate deviation angles.

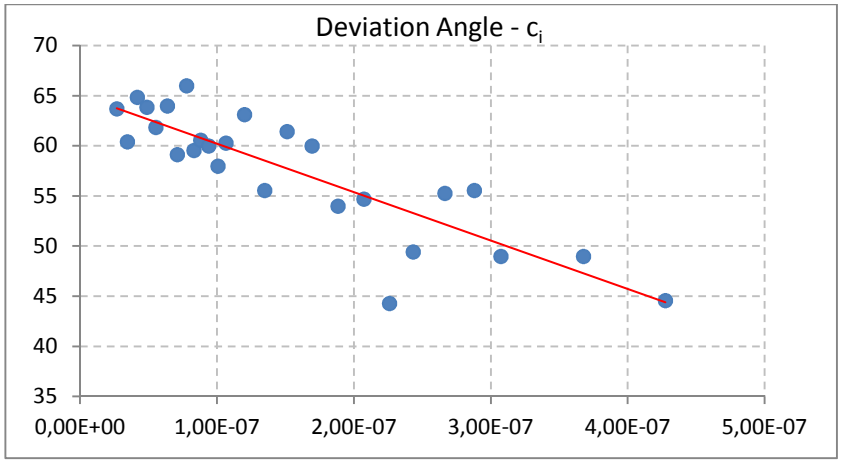

Figure 5.71 Calibration curve, deviation angle plotted against crash-to-conflict ratios

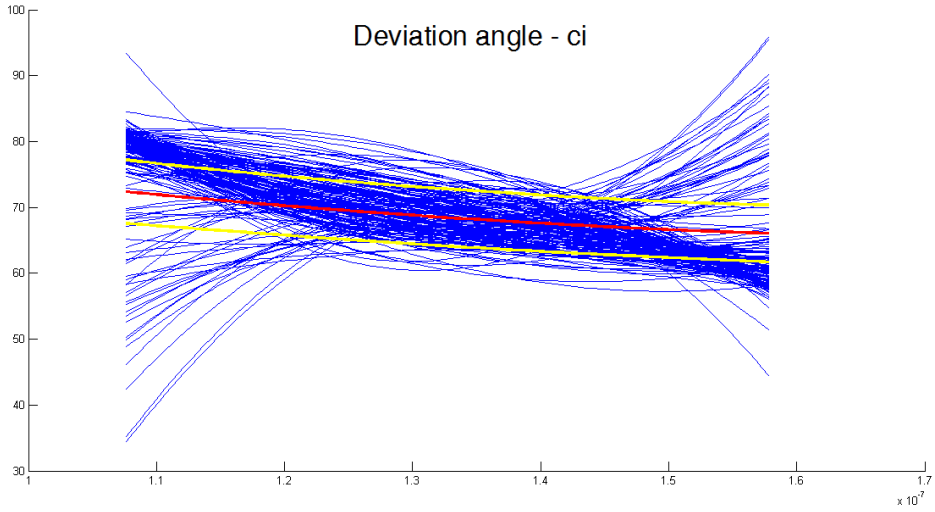

Figure 5.72 Calibration curve, Bootstrap estimation

5.5 Circulating exiting collision

5.5.1 Factor analysis

Various factors analyses have been performed for the 17 roundabout legs involved in crash type *circulating exiting collisions* at least one time in their operational life. The following set of covariates allows reaching the most satisfactory outcome.

- ICD;
- Circulating path radius R2;
- Exit path radius R3;
- Right turn path radius R5.

Only multilane roadway circulatory roundabouts can be the location of circulating exiting crashes. This explain the restricted sample size as compared to the other collisions.

There are two preliminary steps to be conducted in order to assess whether factor analysis may be actually useful for better understanding the collected sample. The first one consists in verifying that variables are uncorrelated. If this hypothesis cannot be rejected, there is no reason to do a principal component analysis and consequently a factor one since the variables have nothing in common. **Table 5.67** clearly shows that the null hypothesis can be rejected: there are certain degree of correlation between considered variables. The measure of *Kaiser-Meyer-Olkin* (KMO) statistic predicts if collected data are likely to factor well, based on correlation and partial correlation. KMO index is substantially higher than the conventional threshold value of 0.6. Therefore, even this step gave positive outcomes.

Table 5.67 Preliminary measures for testing the convenience of factor analysis for uncover concealed information from collected data

KMO Measure of sampling	0.686
Bartlett's test of sphericity (Sig.)	0.111

Taken together, Bartlett's test and KMO measure of sampling adequacy provide a minimum standard which should be passed before a factor analysis should be conducted. Bartlett' test is not positive. The null hypothesis concerning the fact that covariates are reciprocally uncorrelated cannot be rejected. This constitutes a serious concern for reliability of outputs provided by factor analysis. However, the exploratory technique was carried out in order discover whether significant result and information can be obtained despite this serious inadequacy

of available data. After all, as already noted, the general correlation matrix involving all of the 87 roundabout legs clearly show that a correlation exists between *ICD, R2, R3, R5*. The failure of Bartlett' test may be provoked by the shortage of available data compared to other crash types.

PCA technique is then applied to the collected data in order to find the linear combinations of them accounting for as much of the total variable as possible. Among them, the first principal component is the new unveiled variable that explain the maximum amount of the original variable (**Table 5.68**).

The amount of variance accounted for by each component is shown by the eigenvalue, which is equal to the sum of the squared loadings for a given component. The higher the eigenvalue, the higher the importance of this component and the probability it will be retained as a factor. The proportion of variance explained by a single component can be determined by the ration between the corresponding eigenvalue and the overall variance. **Table 5.68** also shows the cumulative percentage of variance accounted for by the current and preceding factors.

Table 5.68 Eigenvalues of each component and their contribution in explaining the total variance

Component	Eigenvalues	% of variance	% cumulative
1	2.199	50.675	50.7
2	1.005	25.132	75.8
3	0.528	13.194	89.0
4	0.440	10.999	100.0

For this crash type, the first two components were retained as factors, since together they explain more than 70 per cent of the entire variance and the knee of the scree plot graphing the magnitude of eigenvalues seems to occur nearby the second factor (**Figure 5.73**).

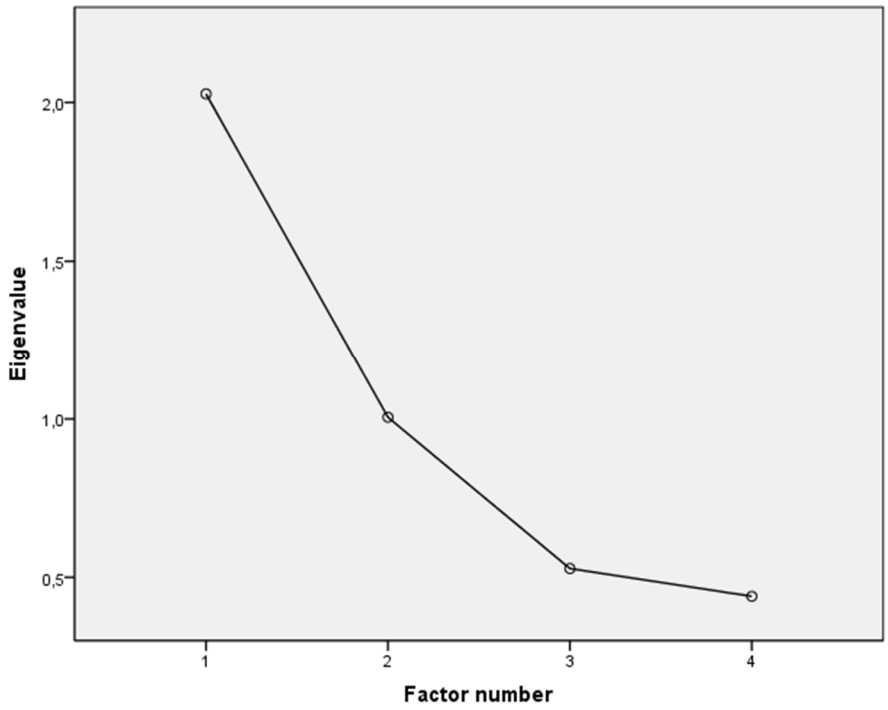

Figure 5.73 *Scatter plot graphing the eigenvalues related to each component*

Table 5.69 reports loadings of the two retained factors.

Table 5.69 Component matrix showing loadings of each variable

Manifest variables	*Extracted factors*	
	1	**2**
ICD	0.845	0.031
R2	0.817	0.026
R3	0.039	0.996
R5	0.803	-0.107

Table 5.70 shows the communalities of each manifest variable for the two extracted factors, that is the proportion of each variables' variance explained by the retained factors.

Table 5.70 *Factor matrix showing loadings of each variable after Varimax rotation*

	Initial	*After extraction*
ICD	1.000	0.715
R2	1.000	0.668
R3	1.000	0.994
R5	1.000	0.656

By analysing signs and values of factors (**Table 5.70**), their underlying and latent meaning may be realised.

The first factor seems to bring out legs of large-sized roundabouts with high design speeds when exiting the ring. Effectively, roundabouts with great inscribed circle diameter and high exit radii may be conducive to circulating-exiting collisions, and this issue may be accentuated if the intersection is travelled at high speeds for the other manoeuvres too, as the great loading associated to R2 seems to suggest.

The second factor may be interpreted under this perspective, given that only the exit path radius R3 has a loading significantly different from zero. The factor is not directly focused on the exit radius of the same considered leg, but it shifts the attention on the 180 degree turns associated with high design speed. Therefore, FA analysis may indicate that circulating exiting collisions can be avoided by designing roundabouts able to achieve an overall vehicular speed reduction.

For the sake of an easier interpretation of manifest meanings of the factors, an orthogonal rotation factor was then applied by following the Varimax criterion where the aim is to reduce for each factor the number of loadings significantly different from zero (**Table 5.71** and **Figure 5.74**).

Table 5.71 *Factor matrix showing loadings of each variable after Varimax rotation*

Manifest variables	*Extracted factors*	
	1	**2**
ICD	0.844	0.056
R2	0.816	0.050
R3	0.009	0.997
R5	0.806	-0.083

In this situation, Varimax rotation was ineffective. Loadings are practically unaltered, and **Figure 5.74** clearly shows that interpretation of the factors is identical to the previous conceived one. Probably, the restricted sample size does not allow the Varimax rotation to furtherly simplify the previous pattern.

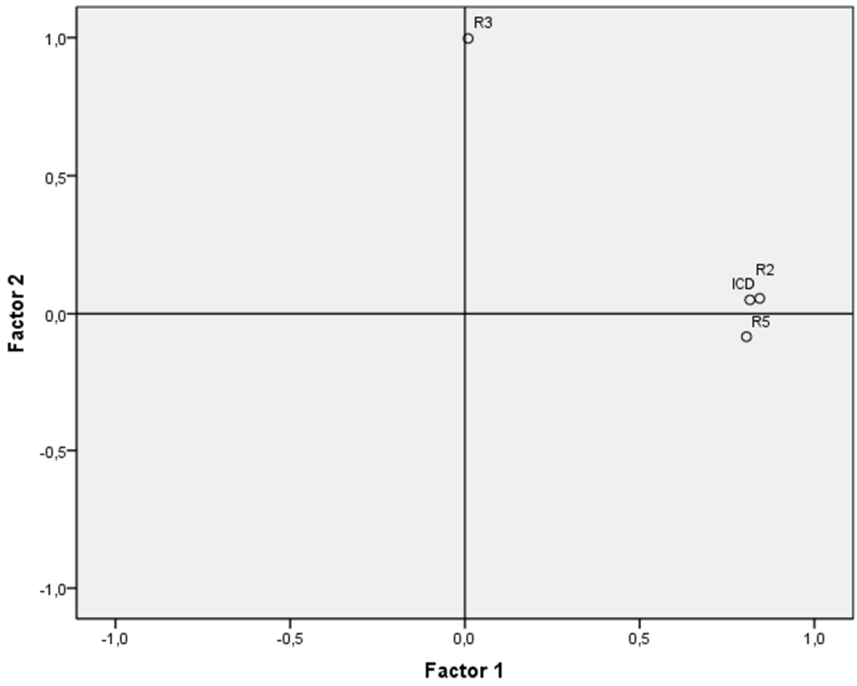

Figure 5.74 *Factor plot in rotated factor space.*

As already explained, the reproduced matrix correlation based on the extracted factors can be obtained from the matrix loadings (**Table 5.72**). It is desirable that corresponding values of the two variables are as close as possible, that is that residuals are close to zero. Correlation matrix estimated by Factor analysis proved to approximate well the original one, with only three residuals greater than the threshold value of 0.05.

Table 5.72 In the top part of the table there are the reproduced correlations, while the bottom part contains the residuals obtained by the difference with the sample correlation matrix.

		ICD	*R2*	*R3*	*R5*
Reproduced Correlation	*ICD*	0.715	0.691	0.063	0.675
	R2	0.691	0.668	0.058	0.653
	R3	0.063	0.058	0.994	-0.075
	R5	0.675	0.653	-0.075	0.656
Residuals	*ICD*		-0.145	-0.021	-0.151
	R2	-0.145		-0.024	-0.184
	R3	-0.021	-0.024		0.046
	R5	-0.151	-0.184	0.046	

Residuals are computed between observed and reproduced correlations. There are 3 (50.0%) non redundant residuals with absolute values greater than 0.05.

Table 5.73 provides the Matrix Score, that is the coefficient values related to the manifest variables linearly combined in order to obtain the factor score. However, the presence of uniqueness makes it unfeasible reaching an exact solutions, and approximation methods must be applied.

Table 5.73 Component matrix showing loadings of each variable

	ICD	*R2*	*R3*	*R5*
F1	0.416	0.402	-0.010	-0.399
F2	0.043	0.038	0.991	-0.095

On the whole, FA gives importance to the vehicular speed attained by drivers through the entire roundabout when trying to identify the geometric features behind circulating-exiting crashes. It is worth recalling that the Bartlett's test failed. Despite this, interesting results were obtained, which will be the starting point for successive exploratory analyses.

5.5.2 Discriminant analysis

There are 4 initial geometric parameters identified by FA, but only 17 legs. The restricted sample side suggested to limit the discriminant analysis to only two groups. Table 5.74 offers an overview about data collected.

Table 5.74 Group statistics

Class frequency	*Mean*	*Std. deviation*	*Valid cases*

1	ICD	62.7375	12.3274	12
	R2	32.9331	15.6546	12
	R3	64.4283	42.4181	12
	R5	92.8292	101.8470	12
2	ICD	72.6920	12.9254	5
	R2	33.8640	8.7399	5
	R3	64.8440	16.2422	5
	R5	76.9460	86.7865	5
Total	ICD	65.6653	12.9654	17
	R2	33.2069	13.7030	17
	R3	64.5506	36.0972	17
	R5	88.1576	95.2367	17

Table 5.75 shows the Within-groups correlation matrix. It corresponds to a correlation matrix of data points obtained by subtracting to them the barycentre of the group they belong. Multicollinearity should not represent a possible concern for discriminant analysis given that no value is greater than 0.8.

Table 5.75 Within-groups correlation matrix.

	ICD	*R2*	*R3*	*R5*
ICD	1.000	0.573	0.043	0.594
R2	0.573	1.000	0.034	0.473
R3	0.043	0.034	1.000	-0.029
R5	0.594	0.473	-0.029	1.000

First of all, significant differences between groups on each of the independent variables are to be examined. If there were not significant differences between groups, it would not be meaningful proceeding any further with the analysis. **Table 5.76** shows two tests that can be used to evaluate the potential of the considered manifest variables in discriminating the three groups before the model is created. In particular, the significance of differences in group means for each variable is tested. The quantity *(1 - Wilks' Lambda)* is the proportion of variance in the dependent variable that can be explained by the considered predictor. Therefore, a relatively small Wilks' Lambda value indicates that the analysed covariate has a potential in discriminating groups. The other columns of **Table 5.76** refers to an F-test performed in a one-way analysis of variance (ANOVA). The null hypothesis is

that all population means are equal in regard to a particular variable; the alternative hypothesis is that at least one mean is different.

As can be seen by **Table 5.76**, the Wilk's lambda test presents similar results for the variables, while the ANOVA seem to suggest that no covariate is able to bring out difference between the two groups.

Table 5.76 Test of equality of group means table

	Wilks' Lambda	F	df1	df2	p-value
ICD	0.870	2.242	1	15	0.155
R2	0.999	0.015	1	15	0.903
R3	1.000	0.000	1	15	0.984
R5	0.994	0.093	1	15	0.765

After this preliminary insight into potential of each manifest variable in separating sub-populations characterised by different crash frequency, discriminant functions can now be sought. The maximum number of discriminant functions produced is equal to the number of groups minus 1. As a result, in this example, there is only one direction of interest; its eigenvalue and its contribution in explaining original variance are shown in **Table 5.77**. The canonical correlation is the multiple correlation between two sets of variables. The first is constituted by the manifest variables, while the second refers to the dummy variables used for coding the three considered groups of different crash frequency. A high canonical correlation indicates a function that discriminates well.

Table 5.77 Eigenvalues table

Function	Eigenvalue	% of variance	% cumulative	Canonical correlation
1	0.322	100.0	100.0	0.493

The canonical correlation is then exploited in the statistical methods devoted to ascertain the significance of the acquired discriminant functions.

If canonical correlation of discriminant functions were equal to zero, no relationship between the set of independent variables and the discriminant scores (i.e. the dependent variable) would be found. The discriminant functions would be worthless because the means of the discriminant scores would be the same in the considered groups.

This is exactly the null hypothesis of the Willk's lambda statistical test, by means of which it is possible to establish the significance of the discriminant functions. Wilks' lambda is the proportion of the total variance lying in the discriminant scores not explained by differences among the groups. It is calculated

as the product of the values of *1-canonical correlation*^{2}. Therefore, smaller values of Wilks' lambda are desirable. In this situation, canonical correlations is equal to 0.493 , so the Wilks' Lambda is (1- 0.493^2) = 0.757.

The Chi-square statistic tests whether the canonical correlation of discriminant function is equal to zero, which implies a unitary Wilk's lambda. This is exactly the null hypothesis, a situation characterised by a negligible contribution offered by discriminant function in explaining the total variance of the independent variables.

Table 5.78 represents the output of Willk's lambda statistical test carried out on the obtained discriminant function. The first test presented in this table tests both canonical correlations ("1 through 2") and the second test presented tests the second canonical correlation alone.

Table 5.78 Wilk's lambda table

Function	Wilks' Lambda	Chi-square	df	p-value
1	0.757	3.628	4	0.45

Table 5.78 warns that the null hypothesis cannot be rejected for the discriminant function. In other words, this function is not able to effectively separate the two groups. This means that DA does not offer reliable outputs. A rigorous application of this statistical method would require the immediate interruption, However, the analysis was carried out, given that the aim of these exploratory analyses is to unveil possible interesting information concerning geometric features related to crash frequency. There is no interest in searching for perfect analytical form able to offer exact predictions.

In **Table 5.79**, the standardised coefficients are provided for the discriminant function. Its interpretation enable unveiling the latent aspect it represents, in a similar way to the identification of the meaning embraced by factors adopted in factor analysis. The sign indicates the direction of the relationship, while the magnitudes define how strongly the discriminating variables effect the score.

Inscribed circle diameter and right turn path radius achieve the greatest scores. The discriminate function tends to separate large-sized roundabouts from those with small diameter and high R3 and R5.

Table 5.79 Standardised canonical discriminant function coefficients table

	Function
	1
ICD	1.340
R2	-0.343
R3	-0.059
R5	-0.773

There is an alternative way of specifying the relative importance of the predictors. The structure matrix table (**Table 5.80**) provides the correlations of each independent variable with the discriminant functions. These correlations serve as loadings in factor analysis. By identifying the largest loadings, the researcher gains an insight into how to correctly interpret the discriminant function. The importance of ICD is confirmed, why the role played by R3 and R5 is nullified.

Table 5.80 Structure matrix table

	Functions
	1
ICD	0.681
R2	-0.138
R3	0.056
R5	0.010

The discriminant function is eventually created by unstandardized coefficients, which are reported in **Table 5.81**. Non standardised values of manifest variables will give the score for the discriminant function. The greatest coefficient is referred to ICD again.

Table 5.81 Canonical discriminant function coefficients table. Unstandardized coefficients

	Functions
	1
ICD	0.107
R2	-0.024
R3	-0.002
R5	-0.008
(Constant)	-5.440

A further way of interpreting the DA results is insert the average discriminant score (unstandardized) in the two groups (**Table 5.82**). In detail, this is the discriminant score for each group obtained by entering the variable means, rather than the individual values for each case, into the discriminant function

These group means are called centroids, and they appear to be effectively distanced from each other.

Table 5.82 Functions at group centroids table

	Functions
Class frequency	**1**
1.00	-0.344
2.00	0.826

The output of discriminant analysis is the classification table, whose rows are the observed categories of the dependent variable while the columns are the predicted categories. When prediction is perfect all cases lie on the diagonal. The percentage of cases on the diagonal is the percentage of correct classifications. The cross validated set of data is a more authentic representation of the outcome achieved by discriminant function. The cross validation is often termed a 'jack-knife' classification, given that successively classifies all cases but one to develop a discriminant function and then categorizes the case that was left out. This process is repeated with each case left out in turn. This cross validation produces a more reliable function. The ratio is that one should not use the case the researcher is trying to predict as part of the categorization process. The classification results for the crash type reveal that 62.5% of legs were classified correctly into the three categories of crash frequency (**Table 5.83**).

This overall predictive accuracy of the discriminant functions is called the *hit ratio*. Via a random classification of the collected legs, there would be a 33.3% probability of correctly collocating the 32 subjects into the three categories.
Accordingly to a conventional approach, acceptable hit ratios must be greater than this probability increased by 25%, which gives a threshold value equal to 41.63%. The output of discriminant analysis is substantially up to standard.

Table 5.83 Classification results table. 64.7% of original grouped cases correctly classified. 47.1% of cross-validated grouped cases correctly classified.

			Predicted group membership			
		Class frequency	**1.00**	**2.00**	**3.00**	**Total**
Original	Count	1.00	8	4	12	8
		2.00	2	3	5	2
	%	1.00	66.7	33.3	100.0	66.7
		2.00	40.0	60.0	100.0	40.0
Cross-validated [a]	Count	1.00	6	6	12	6
		2.00	3	2	5	3
	%	1.00	50.0	50.0	100.0	50.0
		2.00	60.0	40.0	100.0	60.0

a. Cross validation is done only for those cases in the analysis. In cross validation, each case is classified by the functions derived from all cases other than that case.

A discriminant analysis was then conducted to predict the categorical variable *crash frequency* for analysed roundabout legs. Predictor variables were *inscribed circle diameter, circulating path radius R2, exiting path radius R3 and right turn path radius R5.*

These are the same geometric features previously identified via the factorial analysis. Significant mean differences were observed for the *inscribed circle* diameter and *right turn path radius*. The only one discriminate function considered in this analysis failed in proving its statistical significance. However, classification table shows acceptable results in correctly classifying roundabout legs in the appropriate crash frequency group. In particular, by analysing the standardised coefficients of the discriminant function and the pooled within-groups correlations of the structure table matrix, the *inscribed circle diameter* revealed itself to be the only geometric feature able to explain differences in historic crash frequency of roundabout legs.

5.5.3 Regression analyses

Multiple linear regression models whit crash frequency as a continuous dependent variable may allow understanding the portion of variance affecting crash frequency explained by the single geometric parameters. From FA and DA, a set of geometric features apparently related to crash frequency was found and then investigated in MLR models. Stepwise regression procedures were applied by exploiting the F-test in order to establish which of these four models should be preferred for analysing the investigated phenomenon.

- Model 1. Predictors: Constant, R5, ICD;
- Model 2. Predictors: Constant, R5, R3, ICD;
- Model 3. Predictors: Constant, R5, R3, R2, ICD.

It is then desired to ascertain whether the full model contributes additional information about the association between Y and the predictors. The null hypothesis is that the additional covariates are not significant, and their related coefficients are therefore equal to zero. If the difference between error sum of squares for the reduced model (i.e. SSE_R) and the error sum of squares for the complete model (i.e. SSE_C) reaches high values, the null hypothesis is likely to be rejected because this would mean that the additional $k-h$ parameters significantly improve the model's fit to the data. Output of F-test for the four tested models are reported in **Table 5.84**, which shows that the independent variables statistically significantly predict the dependent variable for all of tested models.

Table 5.84 F-test carried out for testing statistical significance of various models

Model		Sum of squares	df	Mean squares	F	Sig.
1	*Regression*	0.003	2	0.001	4.099	0.040
	Residual	0.005	14	<0.001		
	Total	0.008	16			
2	*Regression*	0.003	3	0.001	2.614	0.096
	Residual	0.005	13	<0.001		
	Total	0.008	16			
3	*Regression*	0.003	4	0.001	1.811	0.191
	Residual	0.005	12	0.000		
	Total	0.008	16			

In order to definitively decide on which model focusing the attention, measures of model adequacy were calculated, with particular emphasis to adjusted R square, since it increases only when significant terms are added to the model (**Table 5.85**). The model having only R5 and ICD as covariates proved to offer best performances, and this corroborates DA analysis which defines ICD as the decisive geometric feature for circulating-exiting crashes. However, the full multiple linear model was investigated in order to capture the degree of correlation between each of them and crash frequency and confirm or not these evidences.

Table 5.85 Measures of adequacy for the considered multiple linear models

Model	R	R-square	Adjusted R square	Standard error of the estimate
1	0.608	0.369	0.279	0.018
2	0.613	0.376	0.232	0.020
3	0.614	0.376	0.169	0.019

Unstandardized coefficients indicate the increase experienced by the dependent variable for a unitary increment of the independent variable when all other independent variables are held constant (**Table 5.86**). The same table also provides the standardised coefficients, which allow taking into account the differences among the unit of measurements of the various predictors.

The same table reports the outputs of tests pertaining to the statistical significance of each of the independent variables. According to the null hypothesis, the regression coefficient of the investigated predictor is equal to zero. If the p-value < 0.05, the null hypothesis can be rejected, and it can be stated that coefficients are statistically significantly different to zero. This seems to be true only for the inscribed circle diameter.

Table 5.86 Calculating regression coefficients and testing statistical significance of the independent variables.

Model		Unstandardized Coefficients		Standardised Coefficients		
		β	*Std. Error*	$\hat{\beta}$	*t*	*Sig.*
1	*Constant*	-0.010	0.028		-0.358	0.726
	ICD	0.001	<0.001	0.692	2.368	0.036
	R2	3.146E-5	<0.001	0.020	0.070	0.945
	R3	-5.036E-5	<0.001	-0.084	-0.366	0.721
	R5	<-0.001E-5	<0.001	-0.518	-1.866	0.087

The variance inflation factor (VIF) quantifies the severity of multicollinearity in MLR models with OLS estimates for the regression coefficients. It provides an index that measures how much the variance of an estimated regression coefficient is increased because of multicollinearity. Given that VIF factor is substantially lower than 2.0 for each predictor, there is not a severe reciprocal correlation between independent variables (**Table 5.87**).

Various concerns persist about the reliability of standardised regression coefficients as a measure of actual relationships between each predictor and the

dependent variable. As a matter of fact, $\hat{\beta}^*$coefficients can dramatically change in numerical value, and even in sign, as new variables are introduced or as old variables are removed. They simply reflect the amount of credit given to the related predictors. It can be said that they are context-specific to a given model characterised by a specific set of covariates. The problem is that the true model is rarely, if ever, known.

In addition, $\hat{\beta}^*$ coefficients are still sensitive to multicollinearity, and their values may be affected by the amount of Y variance shared with the other predictors. As a result, it can happen that a predictor explaining a consistent part of *Y* variance may have a near-zero $\hat{\beta}^*$ because another predictor is receiving the credit for the explained variance.

Other techniques are then required for correctly evaluating the importance of single predictors in explaining the analysed phenomenon. There is the need for estimating the relationship between a predictor variable and the outcome variable after controlling for the effects of other predictors in the equation.

Partial correlation represents the correlation between the dependent variable *Y* and a predictor after common variance with other predictors has been removed from both *Y* and the predictor of interest.

The squared *semipartial correlations* represent the unique variance of that predictor shared with the dependent variable. This means that the squared semipartial correlation for a variable denotes the decrease in coefficient of determination R^2 occurring if that variable is removed from the regression equation.

From **Table 5.87**, ICD and R5 have the highest associations with dependent variable *Y*.

Table 5.87 Verifying the presence of severe multicollinearity and calculation of correlation coefficients

	Correlation coefficients			**Collinearity**	
	Zero-order	*Partial*	*Semipartial*	*Toll*	*VIF*
ICD	0.428	0.564	0.540	0.609	1.642
R2	0.151	0.020	0.016	0.656	1.525
R3	-0.039	-0.105	-0.083	0.994	1.006
R5	-0.144	-0.474	-0.425	0.675	1.482

A squared structure coefficient denotes the amount of variance estimated by the model that the predictor is able to explain. This is equivalent to say that a squared structure coefficient denotes the amount of variance related to R^2 that the predictor is able to explain.

Structure coefficients definitely clarify the contribution of each predictor in explaining the phenomenon described via a multiple linear regression, and they provide support in trying to identify multicollinearity effects. Structure coefficients

confirm previous analyses of partial and semipartial correlations. Crash frequency variance seems to be basically explained by ICD only.

The magnitude of these relationships may be directly and synthetically measured by the so-called *Cohen's f^2 effect size*, which is focused on the strength of the association between the predictor of interest and the dependent variable (**Table 5.88**). Its outcome is a measure of practical significance in terms of the magnitude of the effect exerted by the single predictor. It is independent of the sample size and is appropriate for calculating the effect size within a multiple regression model in which the independent variable of interest and the dependent variable are both continuous.

The effect size corroborates indications provided by structure coefficients: ICD appears to have a marked relationship with crash frequency as compared to other 17 investigated geometric factors.

Eventually, exploratory analyses reach the conclusion that ICD is the only geometric feature with a significant correlation with crash frequency of circulating-exiting collisions. According to this result, the size of the roundabout is the only decisive factor.

Table 5.88 Calculation of structure coefficients and effect size f^2

	Structure coefficient	**Effect size f^2**
ICD	0.490	0.534
R2	0.019	0.004
R3	0.023	0.005
R5	0.064	0.147

The most intuitive way for testing normality of residuals consists in trying to graph a histogram by plotting obtained residuals and placing them in regularly spaced cells. The histogram should approximate a normal distribution of residuals. However, with small sample sizes, which is the case of various crash type here in this study, this is not be the best choice for judging the distribution of residuals (**Figure 5.75**).

A more affordable way is proposed by the $normal\ probability\ plot$ (also called P-P plot). It is obtained by sorting the standardised residuals into ascending order and then calculating the cumulative probability of each residual.

Eventually, the so calculated P values are then plotted versus the normalised cumulative frequency distribution of residuals themselves, that is $(\varepsilon_i - \mu)/\sigma)$, where μ and α are approximated via the mean and standard deviation of residuals respectively. The normal probability plot seems to be able to produce an approximately straight line, which means that residuals may come from a normal distribution (**Figure 5.76**).

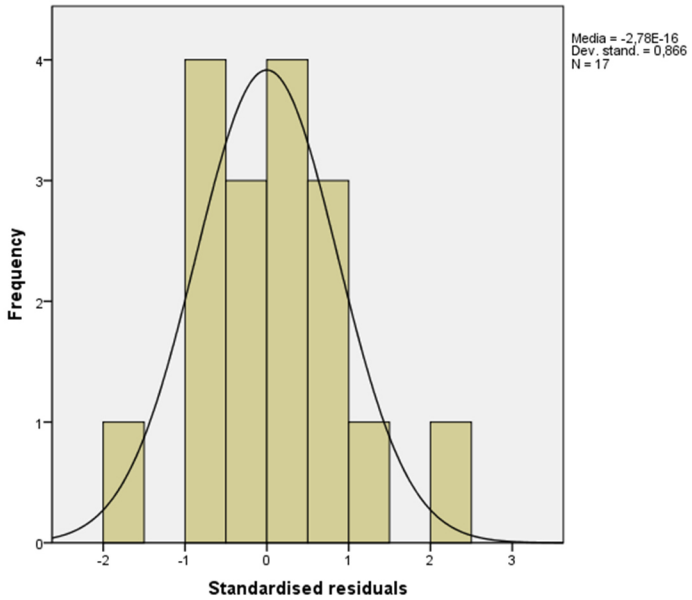

Figure 5.75 Testing normality distribution of residuals. Histogram

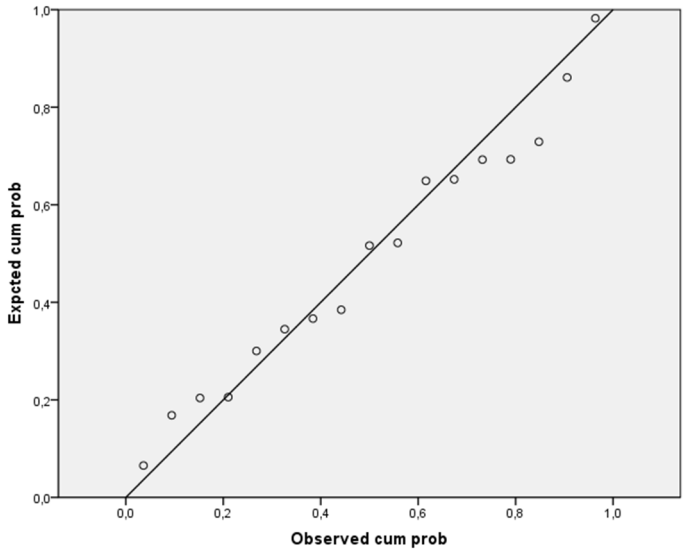

Figure 5.76 Testing normality distribution of residuals. Normal probability plot

There are instead serious concerns about the homoscedastic nature of residuals, which should have a constant variance σ^2. Homoscedastic assumption can be checked by visual examination of a plot of the standardized residuals (the

errors) by the regression standardized predicted value. Residuals are not evenly scattered around the line and a certain trend can be recognised (**Figure 5.77**). This means that homoscedastic assumption is not verified. However, as already said, this cannot compromise results obtained with correlation coefficients and the effect size, which gave substantial results also consistent with previous exploratory analyses.

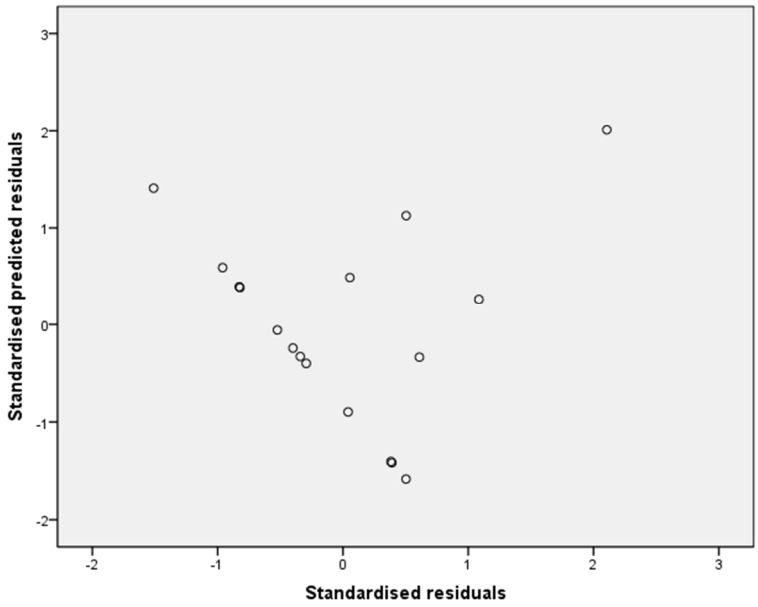

Figure 5.77 Scatter plot for detecting homoscedasticity of residuals

5.5.4 Estimating the calibration curves

Exploratory analyses identified inscribed circle diameter as the geometric features most correlated to crash frequency of circulating exiting collisions. Conversely, no geometric parameter was found to be correlated to the frequency of conflict opportunities. COs for circulating-exiting collisions are calculated by this formula (Chapter 3):

$$N_4 = Q_{out,int} * P(t < t_{coll})$$

where:

- t_{coll}: time of collision fixed at 2s.

For this type of crash, theoretical trend of COs over hourly changes of traffic flows passing through a given roundabout leg shows a peculiar monotone increase. More directly, COs increase as traffic flows increase (**Figure 5.78**). This trend also

emerges by considering the average daily traffic flow passing through the leg for entering the roundabout (**Figure 5.79**).

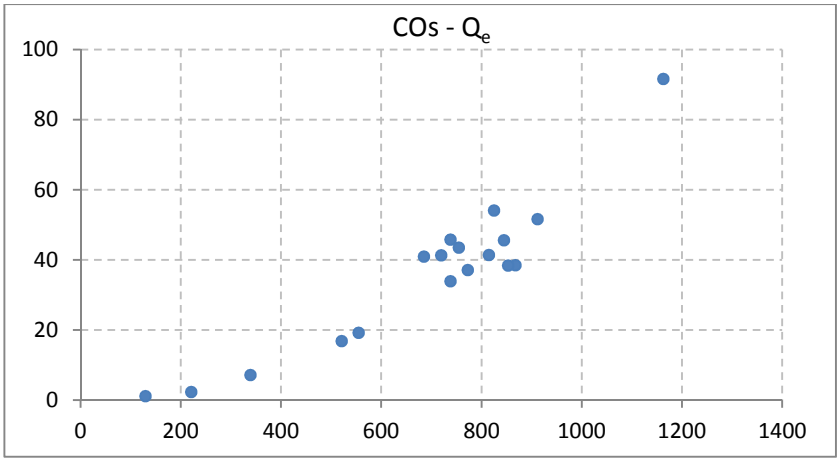

Figure 5.78 Daily evolution of Conflict Opportunities plotted against entering traffic flows measured on an hourly basis for a single roundabout leg

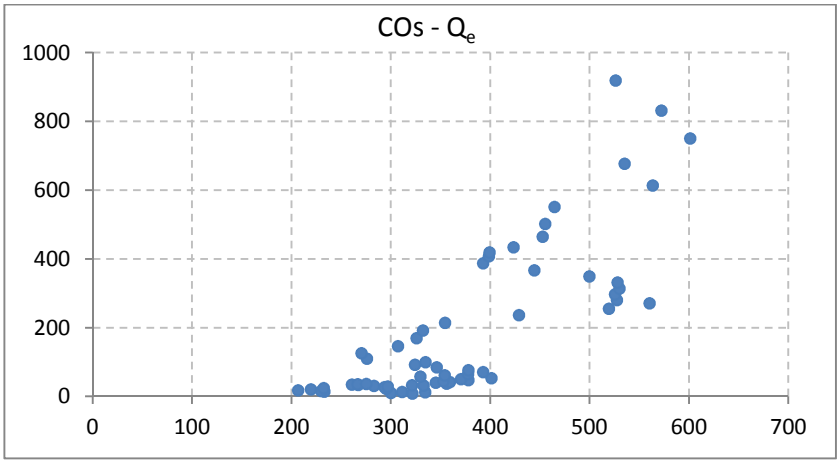

Figure 5.79 Conflict Opportunities plotted against average daily traffic flows entering roundabouts. Each point represent a different leg. All of the 87 legs analysed in this study were considered.

5.5.4.1 Inscribed circle diameter

Conflict opportunities of circulating-exiting collisions rise as inscribed circle

diameter increases, and this is true for both legs with small traffic and legs subjected to medium-high traffic flows (**Figure 5.80**).

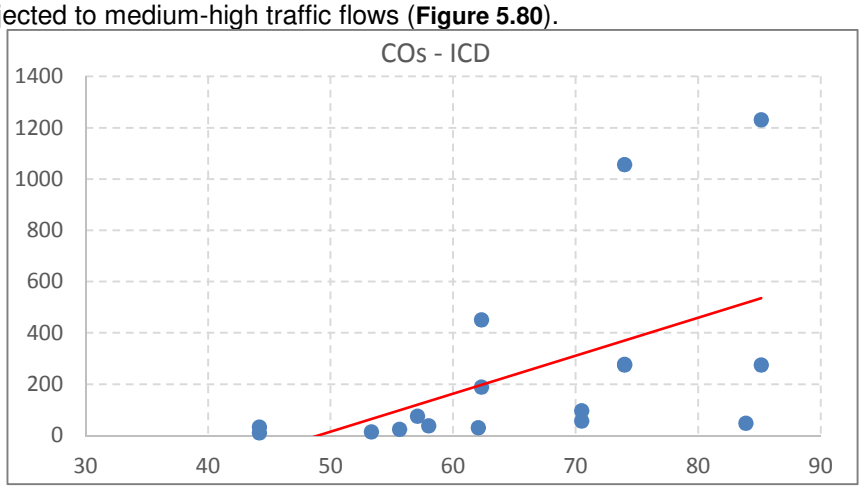

Figure 5.80 Entering traffic flows measured on an hourly basis plotted against inscribed circle diameter (Simple Moving Average)

Figure 5.81 shows an upward trend between crash frequency and the geometric parameter of interest, without significant differences between small and medium-high Qe passing through the roundabout legs.

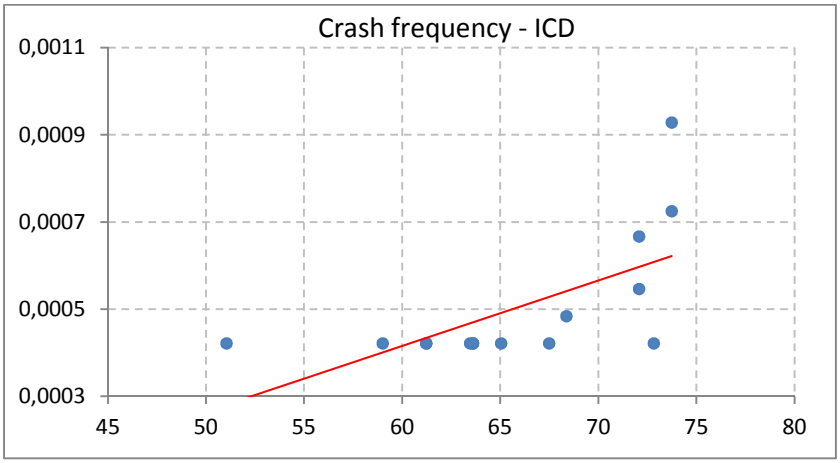

Figure 5.81 Inscribed circle diameters plotted against deviation angles for legs with low traffic flows

The roundabouts with the greatest ICD are associated with the lowest crash-to-conflict ratio (**Figure 5.82**). There is, in fact, a negative relationship between the coefficients of the model and the geometric feature of interest, with the result that large-size roundabouts seems to be less exposed to circulating exiting collisions, which is a contradiction with previous considerations and outputs of exploratory analyses. Bootstrap estimate of the calibration curve supports this analysis (**Figure 5.83**).

This unrealistic outcome is probably due to the greater increase of crash frequency as compared to COs as ICD reaches higher values. Overly restricted sample size may explain the failure of the model in implementing this kind of crash. More available roundabouts would probably allow achieving consistent results.

Despite issues pertaining to the reliability of the model, it is worth noting that crash frequency effectively decrease for small roundabouts, which is a confirmation of the output of exploratory analyses.

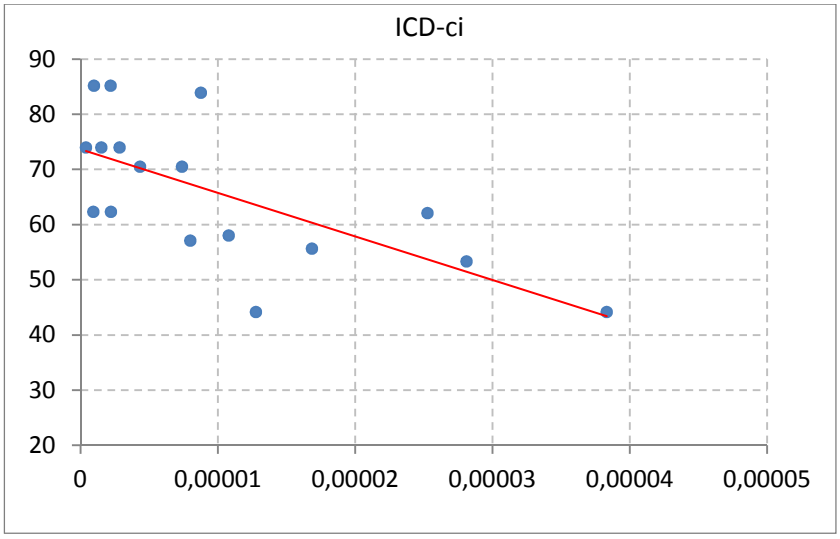

Figure 5.82 Inscribed circle diameters plotted against deviation angles for legs with high traffic flows

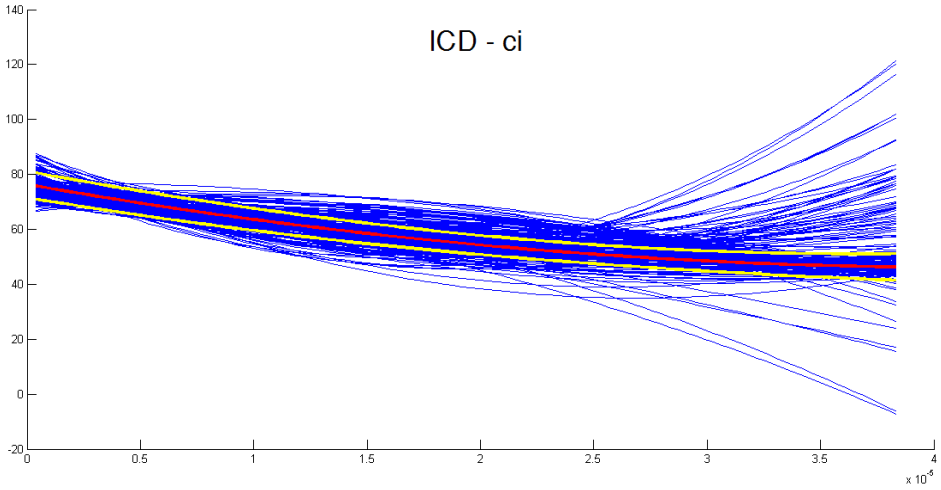

Figure 5.83 Calibration curve, Bootstrap estimation

5.6 Comparing the outputs of crash prediction model based on CO technique with findings of Scientific Literature and empirical evidences

Previous analyses identified the following geometric features as the most correlated ones to the crash frequency recorded for investigated sites:

- *Collision due to failure to yield starting from a stopped position*
  Deviation Angle and Visibility Angle;
- *Collision due to failure to yield without stopping*
  Entry path radius of the left approach R1sx;
- *Single vehicle run-off*
  Entry path radius R1;
- *Rear-end collision at entry*
  Entry path radius R1 and Deviation Angle;
- *Circulating-exiting collision*
  Inscribed circle diameter.

In the followings, a comparison is proposed between outputs of the model developed in this study with findings of road safety researches.

Among researchers, there is a wide consensus that speed management is a key factor for safety performances of roundabouts. Relative speed between conflicting traffic flows is a recurrent subject in road safety studies.

The actual profile speed of drivers when manoeuvring through the roundabout was not available among collected data. Design speeds were considered by implementing as covariates the critical radii of various paths. This means that drivers were supposed to behave in the same manner. As a result, the actual influence of geometric features of roundabouts on drivers' attained speeds could not be taken into account, as well as the safety repercussions of drivers' behaviour.

Entry path radius proved to be significantly correlated to various crash typologies, while the other critical radii showed negligible association with historic crash frequency.

5.6.1 Collision due to failure to yield starting from a stopped position

The users' wrong evaluation of the time interval available between vehicles circulating in the ring is the cause of this crash type. Extended lags do not constitute a threat and neither do the small ones since they would certainly be rejected. Conversely, if available lags are close to critical intermediate values, dangerous situations may arise (Mauro & Cattani, 2004) (Pecchini, et al., 2014). In particular, the user of the entering vehicle may misjudge the intentions of the other vehicles coming from his left which appear to be about to exit the roundabout while instead continuing to advance along the ring. An adequate separation between entry and exit of the same leg may help entering driver avoid these mistakes. Even analytical formulae conceived for calculating capacity of roundabout legs recognise the separation between entry and previous exit as a decisive factor for reaching better operational condition (Ministero delle Infrastrutture dei Trasporti, 2001) (SETRA, 1998). At the other extreme, excessive separation between the entry and exit of the adjacent leg increases the probability of merging conflicts involving the entry and circulating vehicular paths, with an increased risk for multiplane roundabout (NCHRP, 2010).

To sum up, the spacing of entries and exits is recognised as particularly important for this kind of crash. However, the model here proposed does not implement these factors given that exploratory analyses showed no correlation between them and historic frequency for this type of crash.

Instead, deviation and visibility angle emerged as decisive geometric features. It is worth noting that designing legs provided with pronounced deviation angles implies a certain degree of entry curvature. The latter, if sufficiently high, allows drivers to quickly access to the ring, without the need for turning at the yielding line and, at the same time, checking for available lags. In fact, with a similar geometric layout, they deviate their path by following the entry curvature, so that they do not have to move the steering wheel at the yield line. As a result, they can focus exclusively on circulating traffic flow, and the likelihood of mistaking traffic lags is reduced. Alongside this aspect, an adequate angle of visibility gives to the

approaching driver a complete vision of oncoming traffic flow (NCHRP, 2010). Evaluation of legs within circulating traffic flow and comprehension of drivers' intensions surely benefit from correctly designed deviation and visibility angles.

Calibration curves providing crash-to-conflict ratios offer a realistic pattern as pertaining the safety repercussions of these two geometric features. A reduction of expected crash frequency is in fact expected as deviation and visibility angles increase. The output is then consistent with International guidelines and findings of road safety studies.

It is worth recalling that distance between entries and exits did not reveal itself as decisive factors for preventing crashes due to failure to yield starting from a stopped position. This is not a failure of the model. Simply, exploratory analyses found no correlation between these distances and crash frequency within sampled roundabouts. Probably other data sets collected in different geographical areas may have provided different results, but for Province of Mantua, distances between entries and exits are not relevant for the investigated crash typology.

5.6.2 Collision due to failure to yield without stopping

Accordingly to various National guidelines and road safety studies (Department of Transport and Main Roads, 2014) (Arndt, 1998) (Arndt & Troutbeck, 1995) (Austroads, 2011) (Kennedy, 2007), the spread between vehicular speeds attained by entering and circulating traffic flows is the predominant cause for this crash type. In this perspective, successful geometric layout should tend to reduce these differences, such as, for example, decreasing R1 for each approach, increasing the diameter of the inner island and enhancing deviation of trajectories followed by vehicles (Maycock & Hall, 1984) (Montella, 2011). Excessive entry path radius of the left approach R1sx has detrimental effects too on vehicles coming from the analysed leg, which should interact with a circulating traffic flow approaching at high speed. At the same time, entries should not be designed tangentially to the roundabout, since entering drivers could wrongly think to have the right-of-way. The worst possible situation occurs when entries and exit are tangent to the central island, a geometric layout which allows drivers to pass through the roundabout without the need for deviating their trajectory and slow down.

Other studies enlighten the importance entry width, with particular emphasis to the number of entry lanes. It is demonstrated that multilane entries enhance the likelihood of this type of crash because they have a greater number of conflict points (and COs) as compared to single-lane entries (Montella, et al., 2012). Another reason is that multilane entries experience high vehicular speeds since deviation of trajectories and entry path radius are inevitably small (NCHRP, 2010).

From this wide set of geometric features supposed to condition likelihood of this type of crash, the entry path radius of the left approach R1sx emerged as the only geometric factor able to explain a significant amount of variance related to the historic crash frequency of sampled roundabouts. Calibration curves correctly

predict an effective prevention of these crashes by designing reduced entry path radii. It is interesting that R1 was not found to be remarkably correlated to crash frequency. This suggests that speed attained by circulating traffic flow is more important than speeds of entering vehicles.

In short, International research outlined that numerous parameters condition the occurrence probability of crashes due to failure to yield without stopping, but accordingly to exploratory analyses carried out on sampled roundabouts in the Province of Mantua, only R1sx is significantly correlated to historic crash data.

5.6.3 Single vehicle run-off

The most important factor is obviously the profile speed achieved by drivers when manoeuvring through the roundabout, with particular emphasis to the entry speed when approaching to the ring (Arndt & Troutbeck, 1995) (Mauro & Cattani, 2004) (Kennedy, 2007) (Department of Transport and Main Roads, 2014). In order to make drivers slow down and then reduce occurrence probability for this type of crash, various National guidelines propose to arrange the approaches by designing a series of reverse curves and avoid entries implemented tangentially to the central island (Arndt & Troutbeck, 1995) (NCHRP, 2010) (Department of Transport and Main Roads, 2014). Entry path radius has a great impact too on occurrence probability of this type of crash (Montella, et al., 2012). Moderate approaching speed actually protect drivers from incurring in run-off crashes. Multilane entries raise additional problems. They require greater entry path radius than single-lane entries; in addition, when no vehicle stands at the yield line waiting for entering the ring, approaching drivers may exploit the wider carriageway and follow a straight path without adequate speed reduction (NCHRP, 2010).

As far as the sampled roundabouts located in the Province of Mantua, from the framework provided by exploratory analyses, R1 comes up as the decisive factor, given its high correlation with historic crash records. The solution of arranging reverse curves before the entry was not applied at investigated roundabouts.

Other geometric features revealed themselves not to be able to explain variance of crash records. Calibration curve has a rational trend, with high crash probabilities for great entry path radius.

5.6.4 Rear-end collision at entry

This type of crash is more likely to occur at roundabouts affected by high traffic flows during the peak hours, as well as roundabouts with tangential entries and reduced visibility (Guichet, 1993). There is a wide consensus that approaching

speed is a determinant factor (Arndt & Troutbeck, 1995) (Kennedy, 2007) (NCHRP, 2010) (Montella, et al., 2012). As a result, horizontal curvature 1/R0 preceding the entry, entry path radius and number of entry lanes are the factors deserving the highest importance at the design phase in order to limit to the minimum extent rear-end crashes. Entry angle should be carefully evaluated too, since overly high angles may provoke a sudden braking posing the condition for rear-end collisions (Highway Agency, 2007) (NCHRP, 2010).

Exploratory analyses detected entry path radius and deviation angle as decisive factors. It is worth recalling that *R0* and *R1* are highly correlated for collected data, so it was not possible discerning their specific contribute in explaining variance of crash frequency. The presence of deviation angle among decisive geometric features is probably due to its influence on entry vehicular speed, as already noted for collisions due to failure to yield.

Calibration curves clearly denote that high deviation angles along with small entry path radius significantly reduce the risk rear-end crashes may happen.

5.6.5 Circulating-exiting collision

This is the only typology of crash for which the model proposed in this study proved to be entirely unreliable. Exploratory analyses found that inscribed circle diameter is able to explain a significant amount of variance related to historic crash data. All of the other features were not able to offer any significant contribute.

However, road safety studies offer a more articulated framework where numerous factors are to be analysed in order to prevent these crashes.

The most important factor is the degree of the relative speed between exiting and circulating traffic flows (Arndt & Troutbeck, 1995) (Kennedy, 2007). Remarkable differences, which are typical at large-size roundabouts, make these crashes more likely to occur. Speed management through the entire roundabout is of primary importance for preventing high speeds attained by circulating vehicles. Again, a small entry path radius for all of the approaches has beneficial safety consequences, which can be increased via a trajectory deviation imposed by the central island to vehicular paths and by preferring single-lane entries to multilane ones (Highway Agency, 2007) (Department of Transport and Main Roads, 2014). Overlap of conflicting trajectories is another issue that should be taking into account. Excessive separation between the entry and exit of adjacent legs increase the probability of merging conflicts involving the circulating and exiting vehicular paths (NCHRP, 2010).

Furthermore, it is a fact that roundabouts provided with great inscribed circle diameters experience high vehicular speeds and then high frequency crashes, which can reach even greater values if there are wide circulatory carriageways (Spacek, 2004) (NCHRP, 2007) (Kennedy, 2007).

As already anticipated, only ICD came up as a decisive factor from exploratory analyses. In addition, related calibration curve indicates that the small ICD is, the

greater is the crash frequency, which is the opposite of literature knowledge. The bootstrap analysis too confirms this trend.

Probably, unreliability of the model for this type of crash is due to the shortage of collected data in relation to other situations. After all, exiting collision crashes can occur only at multilane roundabouts with multilane carriageways. In addition, the inscribed circle diameter refers to the roundabout as a whole. No indication about appropriate design of legs can be achieved by simply considering the inscribed circle diameter. Even if calibration curve of the model had been consistent with scientific studies, stating that ICD should be kept to a minimum would not enhance the quality of geometric design of roundabouts, given that ICD is practically the result of previous choices pertaining geometric and operational issues.

Increasing the sample size of roundabouts affected by circulating-exiting collisions may allow capturing more realistic pattern about actual influence of geometric layout of roundabout on these crashes.

References

Arndt, O.K. *Relationship between Roundabout Geometry and Accident Rates - Final Report.* Report Number ETD02, Brisbane, Australia: Queensland Department of Main Roads, 1998.

Arndt, O.K., and R. Troutbeck. "Relationship between roundabout geometry and accident rates." *Proceedings of the International Symposium on Highway Geometric Design Practices.* Boston, MA: Transportation Research Board of National Academies, 1995.

Austroads. "Guide to Road Design, Part 4B Roundabouts. Report AGRD08/11." Sydney, NSW, Australia, 2011.

Department of Transport and Main Roads. *Road Planning and design manual - 2nd edition.* Quuensalnd Government, 2014, Volume 3: Guide to Road Design, part 4B: Roundabouts.

Guichet, B. "Typologie des accidents dans les giratoires urbains." *Seminaire Giratoires 92.* Bagneux, France: Service d'Etudes Techniques des Routes et Autorutes (SETRA), Centre d'Etudes des Transport Urbains, 1993. 145-151.

Highway Agency. «Geometric Design of Roundabouts. Design Manual of Roads and Bridges - TD 16/07.» London, United Kingdom, 2007.

Kennedy, Janet. *International Comparison of Roundabout Design Guidelines - Report PPR206.* Workingham, United Kingdom: Transport Research Laboratory, 2007.

Mauro, R., and M. Cattani. "Model to evaluate potential accident rate at roundabouts." *ASCE Journal of Tranportation Engineering* 130, no. 5 (2004): 602-609.

Maycock, G., and R. Hall. *Accidents at 4-Arm Roundabouts.* Crowthorne: Transportation and Road Research Laboratory, 1984.

Ministero delle Infrastrutture dei Trasporti. "Geometrical and functional standards for the design of road intersections." Italian prenormative document approved by road commission of Centro Nazionale Ricerche, Rome, Italy, 2001.

Montella, A. «Identifying crash contributory factors at urban roundabouts and using association rules to explore their relationships to different crash types.» *Accident Analysis and Prevention* 43, n. 4 (2011): 1451-63.

Montella, A., S. Turner, S. Chiaradonna, and D. Aldridge. "Proposals for Improvement of the Italian Roundabout Geometric Design Standard." *Procedia - Social and Behavioral Sciences* 53 (2012): 189-202.

NCHRP. *Report 572: Roundabouts in the United States.* Washnigton D.C.: National Cooperative Highway Research Program (NCHRP), Transportation Research Board (TRB) of National Academies, 2007.

NCHRP. "Roundabouts: An Informational Guide - Second Edition." National Cooperative Highway Reserach Program (NCHRP), Tranportation Research Board of the National Academies (TRB), Washington D.C., 2010.

Pecchini, D., R. Mauro, e F. Giuliani. «Model of Potential Crash Rates of Rural Roundabouts with Geometrical Features.» *ASCE Journal of Tranposrtation Engineering* 140, n. 11 (2014): 04014055.

SETRA. "Aménagement des carrefours interurbains sur les routes principales. Carrefours plans - Guide technique." Service d'Etude Technqiues des Routes and Autoroutes (SETRA),Centre d'etudes et d'expertise sur le risques, l'environment, la mobilitè et l'amenagement (CEREMA), Ministere de l'éecologie et de développement durable at de l'énergie, Paris, France, 1998.

Spacek, P. "Basis of the Swiss Design Standard for Roundabout." *Transportation Research Record* (Transportation Reserach Board (TRB) of National Academies) 1881 (2004): 27-35.

Conclusions

Exploratory analyses allowed achieving a drastic reduction of variables to take into account. This greatly simplified implementation of geometric design in the model, when correlations were searched for between the coefficients of the model (i.e. crash-to-conflict ratios) and geometric factors found to be significant for safety issues. Calibration functions specific to each type of crash were then obtained.

Starting from numerous covariates, only the vehicle trajectory deflection, the entry path radius and visibility measures revealed to significantly condition crash rates. The output of explorative data analyses and trends of achieved calibration curves seem reasonable and consistent with other studies, except for circulating exiting crashes, for which the only important parameter is the inscribed circle diameter. No regard for vehicle path radii of roundabouts and differences in speed between circulating and exiting flows, which instead are established as decisive factors for this kind of crash. The same trend of the calibration curve is not consistent with findings of technical literature.

These controversial results are probably due to the few available data for this kind of crash. More extended records would probably allow achieving better results. These considerations may be extended to the other four typologies of vehicle collisions, although, in these cases, results appear to be more reliable. All of the crashes associated with injuries and deaths occurred in the Province of Mantua were considered. More accurate calibration functions could be attained by increasing the size of dataset and extending data collection to the near Provinces. This should be the priority for enhancing the proposed crash prediction model. Another aspect susceptible to improvements regards the speed of vehicles at roundabouts. In this work, they were estimated as the equilibrium-speeds of turning path radii, in accordance to procedures proposed by various national guidelines for verifying speed consistency at the ring. However, distribution of vehicular speeds at roundabouts is a complex topic, which would deserve specific analyses. Drivers are certainly influenced by roundabout design, but each of them may apply different strategies for crossing roundabouts, with inevitable dispersion of trajectories and speeds. Given that turning path radii resulted to be decisive parameters in influencing safety performances of roundabouts, quite different and more realistic outcomes are expected.

Final aspects worth of special consideration are the assumptions made for behavioural characteristics of drivers, such as, for instance, accepted gap when entering the ring. These parameters, which directly influence calculations of Conflict Opportunities, were assumed to be equal to the values proposed by scientific literature. However, drivers' behaviour significantly changes from one Country to another, and no statistical variability of these factors can be assessed.

Great benefits could be obtained by recurring to traffic microsimulation software. These stochastic models simulate the single vehicle as a unique entity with its own goals and behavioural characteristics. Via calibration procedure, realistic estimations of actual behavioural parameters could be obtained, and aforementioned limits would be overcome. Calculation of Conflict Opportunities would be more realistic, and the influence could be ascertained of a specific behavioural parameter on estimates of crash rates provided by the model.

Ringraziamenti

Dedico l'intera e sofferta tesi a tutti quanti mi hanno sostenuto e sopportato in questi ulteriori anni di studio, senza l'apporto dei quali non sarebbe potuto compiersi il perseguimento di tale traguardo. Sono grato ai miei genitori per la libertà garantitami nel decidere quale strada percorrere e su quali esperienze tendere. Ringrazio il Prof. Giuliani per avermi fornito la possibilità di sperimentare la dimensione accademica e di aver potuto affrontare molteplici e diversificate tematiche. La mia più sentita devozione al Prof. Mauro per la sua completa disponibilità nell'avermi sostenuto ed efficacemente indirizzato per l'intero sviluppo della tesi. Grazie di cuore ad Alice per tutto l'aiuto ed il supporto incondizionato dimostrati in questi anni. Sono in grande obbligo pure verso Benedetta e Valeria, per le quali non posso che desiderare il meglio possibile per il loro futuro. Un immenso grazie ad Emanuele, che tanto mi ha dato per crescere come persona. Ringrazio, al contempo, Ana e tutti i dottorati del Dipartimento a cui rivolgo i migliori auguri possibili.
Ringrazio l'Ing. Cadei per la pazienza mostrata a suo tempo nell'introdurmi allo studio dell'incidentalità stradale. Un sentito grazie pure agli studenti che ho seguito durante lo svolgimento delle loro tesi di Laurea, che mi hanno arricchito sia dal punto di vista conoscitivo che umano. Tra questi, non posso non menzionare Stefano, Christian e Davide, se non altro per aver sopportato infinite sedute di rilievi di traffico oltre che ad avermi fornito un notevole contributo per la mia tesi medesima.
Ringrazio infine Luca e Marco per la loro amicizia, oltre che gli ex-compagni di studio all'Università con cui è sempre un piacere incontrarsi di tanto in tanto.